

# YEAR END TECHNICAL REPORT

September 29, 2022, to September 28, 2023

## Waste and D&D Engineering and Technology Development

**Date submitted:**

December 8, 2023

**Principal Investigator:**

Leonel E. Lagos, Ph.D., PMP®

**Florida International University Collaborators:**

Leonel E. Lagos, Ph.D., PMP® (Project Manager)

Himanshu Upadhyay, Ph.D., PMP®

Joseph Sinicrope, M.S., MBA

Walter Quintero, M.S.

Santosh Josh, M.S.

Jayesh Soni, Ph.D.

Clint Miller, MCSE+Security

Mellissa Komninakis, B.S.

DOE Fellows

**Submitted to:**

U.S. Department of Energy

Office of Environmental Management

Under Cooperative Agreement No. DE-EM0005213



**Applied Research Center**

FLORIDA INTERNATIONAL UNIVERSITY

Addendum:

This document represents one (1) of five (5) reports that comprise the Year End Reports for the period of September 29, 2022 to September 28, 2023 prepared by the Applied Research Center at Florida International University for the U.S. Department of Energy Office of Environmental Management (DOE-EM) under Cooperative Agreement No. DE-EM0005213.

The complete set of FIU's Year End Reports for this reporting period includes the following documents:

Project 1: Chemical Process Alternatives for Radioactive Waste  
Document number: FIU-ARC-2022-800012997-04b-007

Project 2: Environmental Remediation Science and Technology  
Document number: FIU-ARC-2022-800013918-04b-006

Project 3: Waste and D&D Engineering and Technology Development  
Document number: FIU-ARC-2022-800013919-04b-007

Project 4: DOE-FIU Science & Technology Workforce Development Initiative  
Document number: FIU-ARC-2022-800013920-04b-011

Project 5: Long-Term Stewardship of Environmental Remedies: Contaminated Soils and Water and STEM Workforce Development  
Document number: FIU-ARC-2022-800013922-04b-005

Each document will be submitted to OSTI separately under the respective project title and document number as shown above. In addition, the documents are available at the DOE Research website for the Cooperative Agreement between the U.S. Department of Energy Office of Environmental Management and the Applied Research Center at Florida International University: <https://doeresearch.fiu.edu>

### **DISCLAIMER**

This report was prepared as an account of work sponsored by an agency of the United States government. Neither the United States government nor any agency thereof, nor any of their employees, nor any of its contractors, subcontractors, nor their employees makes any warranty, express or implied, or assumes any legal liability or responsibility for the accuracy, completeness, or usefulness of any information, apparatus, product, or process disclosed, or represents that its use would not infringe upon privately owned rights. Reference herein to any specific commercial product, process, or service by trade name, trademark, manufacturer, or otherwise does not necessarily constitute or imply its endorsement, recommendation, or favoring by the United States government or any other agency thereof. The views and opinions of authors expressed herein do not necessarily state or reflect those of the United States government or any agency thereof.

# TABLE OF CONTENTS

---

TABLE OF CONTENTS..... i

LIST OF FIGURES ..... vi

LIST OF TABLES..... xii

PROJECT 3 EXECUTIVE SUMMARY.....1

MAJOR TECHNICAL ACCOMPLISHMENTS.....4

TASK 1: WASTE INFORMATION MANAGEMENT SYSTEM (WIMS) (HQ) .....7

Subtask 1.1 WIMS System Administration - Database Management, Application  
Maintenance & Performance Tuning .....8

Subtask 1.1: Introduction ..... 8

Subtask 1.1: Objectives..... 8

Subtask 1.1: Methodology ..... 9

Subtask 1.1: Results and Discussion..... 13

Subtask 1.1: Conclusions ..... 13

Subtask 1.1: References ..... 13

Subtask 1.2: Waste Stream Annual Data Integration .....13

Subtask 1.2: Introduction ..... 13

Subtask 1.2: Objectives..... 13

Subtask 1.2: Methodology ..... 13

Subtask 1.2: Results and Discussion..... 16

Subtask 1.2: Conclusions ..... 21

Subtask 1.2: References ..... 22

Subtask 1.5: Cyber Security of WIMS Infrastructure .....22

Subtask 1.5: Introduction ..... 22

Subtask 1.5: Objectives..... 22

Subtask 1.5: Methodology ..... 22

Subtask 1.5: Results and Discussion..... 23

Subtask 1.5: Conclusions ..... 23

Subtask 1.5: References ..... 24

TASK 2: D&D SUPPORT TO DOE EM FOR TECHNOLOGY INNOVATION,  
DEVELOPMENT, EVALUATION AND DEPLOYMENT .....25

Subtask 2.1: Development of Uniform Testing Protocols and Standard  
Specifications for Fixative Technologies in Support of Complex-wide D&D  
Activities.....25

Subtask 2.1: Introduction ..... 25

Subtask 2.1: Objectives..... 25



Subtask 2.1: Methodology ..... 25

Subtask 2.1: Results and Discussion..... 25

Subtask 2.1: Conclusions ..... 26

Subtask 2.1: References ..... 26

Subtask 2.2: Test and Evaluation of Down-selected Intumescent Foams/Foam  
 Plug Technologies to Mitigate Contaminant Release during Nuclear Pipe  
 Dismantling in Support of a Hot Demo at F/H Labs .....27

Subtask 2.2: Introduction ..... 27

Subtask 2.2: Objectives..... 28

Subtask 2.2: Methodology ..... 29

Subtask 2.2: Results and Discussion..... 33

Subtask 2.2: Conclusions ..... 40

Subtask 2.2: References ..... 40

Subtask 2.3: Certifying Fixative Technology Performance when Exposed to  
 Impact Stressors as Postulated in Contingency Scenarios Highlighted in  
 Safety Basis Documents .....41

Subtask 2.3: Introduction ..... 41

Subtask 2.3: Objectives..... 42

Subtask 2.3: Methodology ..... 42

Subtask 2.3: Results and Discussion..... 45

Subtask 2.3: Conclusions ..... 47

Subtask 2.3: References ..... 47

Subtask 2.4: Multi-functional 3D Polymer Framework for Mercury Abatement .....49

Subtask 2.4: Introduction ..... 49

Subtask 2.4: Objectives..... 49

Subtask 2.4: Methodology ..... 50

Subtask 2.4: Results and Discussion..... 51

Subtask 2.4: Conclusions ..... 57

Subtask 2.4: References ..... 57

**TASK 3: KNOWLEDGE MANAGEMENT INFORMATION TOOL (KM-IT)**  
**(HQ, SRNL, INL, ANL).....60**

Subtask 3.4: Content Management.....60

Subtask 3.4: Introduction ..... 60

Subtask 3.4: Objectives..... 60

Subtask 3.4: Methodology ..... 60

Subtask 3.4: Results and Discussion..... 60

Subtask 3.4: References ..... 71

Subtask 3.5: Marketing and Outreach .....71

    Subtask 3.5: Introduction ..... 71

    Subtask 3.5: Objectives..... 72

    Subtask 3.5: Methodology ..... 72

    Subtask 3.5: Results and Discussion..... 73

    Subtask 3.5: Conclusions ..... 78

    Subtask 3.5: References ..... 79

Subtask 3.6: D&D KM-IT System Administration .....79

    Subtask 3.6: Introduction ..... 79

    Subtask 3.6: Objectives..... 79

    Subtask 3.6: Methodology ..... 79

    Subtask 3.6: Results and Discussion..... 79

    Subtask 3.6: Conclusions ..... 83

    Subtask 3.6: References ..... 83

Subtask 3.7: Cyber Security of D&D KM-IT Infrastructure.....83

    Subtask 3.7: Introduction ..... 83

    Subtask 3.7: Objectives..... 83

    Subtask 3.7: Methodology ..... 83

    Subtask 3.7: Results and Discussion..... 85

    Subtask 3.7: References ..... 85

Subtask 3.8: KM-IT Tech Talks .....85

    Subtask 3.8: Introduction ..... 85

    Subtask 3.8: Objectives..... 86

    Subtask 3.8: Methodology ..... 86

    Subtask 3.8: Results and Discussion..... 86

    Subtask 3.8: Conclusions ..... 94

    Subtask 3.8: References ..... 94

**TASK 7: AI FOR EM PROBLEM SET (SOIL AND GROUNDWATER) -  
EXPLORATORY DATA ANALYSIS AND MACHINE LEARNING MODEL  
FOR HEXAVALENT CHROMIUM [CR (VI)] CONCENTRATION IN 100-H  
AREA (PNNL).....95**

    Subtask 7.3: Algorithm development for spatiotemporal relationship  
    identification.....95

    Subtask 7.3: Introduction ..... 95

    Subtask 7.3: Objectives..... 96

Subtask 7.3: Methodology ..... 96

Subtask 7.3: Results and Discussion..... 99

Subtask 7.3: Conclusions ..... 108

Subtask 7.3: References ..... 108

Subtask 7.4: Publishing AI/ML models on AAML System.....109

Subtask 7.4: Introduction ..... 109

Subtask 7.4: Objectives..... 109

Subtask 7.4: Methodology ..... 109

Subtask 7.4: Results and Discussion..... 109

Subtask 7.4: Conclusions ..... 110

Subtask 7.4: References ..... 110

**TASK 8 AI FOR EM PROBLEM SET (SOIL AND GROUNDWATER) - DATA ANALYSIS AND VISUALIZATION OF SENSOR DATA FROM THE WELLS AT THE SRS F-AREA USING MACHINE LEARNING (LBNL, SRNL) .....111**

Subtask 8.6: Subtask 8.6: Publishing AI/ML models on AAML System .....111

Subtask 8.6: Introduction ..... 111

Subtask 8.6: Objectives..... 111

Subtask 8.6: Methodology ..... 112

Subtask 8.6: Results and Discussion..... 121

Subtask 8.6: Conclusions ..... 128

Subtask 8.6: References ..... 128

**Task 9: AI FOR EM PROBLEM SET (WASTE PROCESSING) - NUCLEAR WASTE IDENTIFICATION AND CLASSIFICATION USING DEEP LEARNING .....129**

Subtask 9.1: Algorithm and Model Development to Identify and Classify Nuclear Waste .....129

Subtask 9.1: Introduction ..... 129

Subtask 9.1: Objectives..... 129

Subtask 9.1: Methodology ..... 129

Subtask 9.1: Results and Discussion..... 134

Subtask 9.1: Conclusions ..... 137

Subtask 9.1: References ..... 138

Subtask 9.2: Transition Previously Trained Deep Learning Models to Advance Automated Machine Learning System (AAMLS) .....139

Subtask 9.2: Introduction ..... 139

Subtask 9.2: Objectives..... 139

Subtask 9.2: Methodology ..... 139

Subtask 9.2: Results and Discussion..... 142

Subtask 9.2: Conclusions ..... 144

Subtask 9.2: References ..... 144

CONFERENCE PARTICIPATION, PUBLICATIONS, AWARDS &  
ACADEMIC MILESTONES .....145

ACKNOWLEDGEMENTS .....145

APPENDIX.....146

## LIST OF FIGURES

---

Figure 1. WIMS poster for WM2023 titled “Waste Information Management System with 2022-23 Waste Streams” undergoing final review. .... 7

Figure 2. FIU-DOE team presenting WIMS poster at WM2023. From left to right, Walter Quintero, Himanshu Upadhyay and Douglas Tonkay (DOE HQ). .... 8

Figure 3. Snapshot report from Google PageSpeed Insights for emwims.org. .... 9

Figure 4. Accessibility tool ANDI applied on the homepage of the WIMS application. .... 11

Figure 5. Accessibility tool ANDI applied on the Forecast Data module on the WIMS application. .... 12

Figure 6. WIMS reporting module showing waste stream data starting from 2023 from "All Sites" to "Waste Control Specialists". .... 15

Figure 7. WIMS Disposition Map module with legend for waste streams from “All Sites” to “Clean Harbors” starting in 2023 for all materials. .... 16

Figure 8. WIMS Forecast Data module showing waste data forecast from All Sites to Waste Control Specialist. .... 17

Figure 9. WIMS Disposition Map module with data from “Kansas City Plant” to “All Facilities”. .... 17

Figure 10. WIMS GIS Map module with data from “All Sites” to “Waste Control Specialist”. .. 18

Figure 11. WIMS Transportation module with data from “Naval Reactor Facility” to “All Facilities”. .... 18

Figure 12. WIMS Report module (Waste Stream Report) with data from “All Sites” to “Remote Waste Disposition Project”. .... 19

Figure 13. WIMS Report module showing proper report height with website footer. .... 20

Figure 14. Buried pipe removal site at F/H Labs. .... 27

Figure 15. Operational concept for employing foam technology. .... 28

Figure 16. Depiction of FOAMBAG™ technology, which holds the resin foam in place as it expands. At full expansion, some of the foam seeps through the semi-porous panels of the bag to form an adhesive seal with the pipe. .... 29

Figure 17. Plug strength test schematic (left) and plug strength testing for pipe samples using the “plunger – bucket” method on an MTS testing device (right). .... 30

Figure 18. Pipe with thermocouples at varying depths. .... 31

Figure 19. Extech equipment and FLIR E53 thermal imaging camera. .... 31

Figure 20. Horizontal flame test per IEC 60695-11-10. .... 32

Figure 21. Vertical flame test per IEC 60695-11-10. .... 33

Figure 22. Hilti foam curing temperature profile graphs in Hastelloy C-22 pipes. .... 36

Figure 23. External temperature profiles for C22-1 (top), C22-9 (middle), and C22-10 (bottom) Hilti samples. .... 37

Figure 24. FoamBag™ curing temperature profile..... 38

Figure 25. External temperature profile of FoamBag™ in Hastelloy C-22 pipes..... 38

Figure 26. Hilti Foam flammability testing. .... 39

Figure 27. FoamBag™ flammability comparison with (top sample) and without (bottom sample) the Exolit AP-750 additive..... 39

Figure 28. Stippled contaminant solution on 304-SS coupon (left) and after solvent evaporation (right). .... 43

Figure 29. BYK-Gardner PF-5546 Extra Heavy-Duty Impact Tester..... 44

Figure 30. Impact tester with acrylic impact housing and Flite 3 901-3011 air sampler setup. ... 44

Figure 31. Collection and analysis process..... 45

Figure 32. ICP-MS Cesium calibration curve..... 45

Figure 33. DOE-HDBK-3010 ARF coefficients for various contaminant forms under impact stress. Initial data indicates a fixative state with an ARF less than a liquid contaminant. .... 47

Figure 34. The mPDMS-MRs before (left) and after (right) thermal oxidation..... 52

Figure 35. The magnetic field responsiveness of unheated mPDMS-MRs (left) and heated mPDMS-MRs (right). .... 53

Figure 36. The mPDMS-MRs that were thermally oxidized at 370°C for 24h..... 55

Figure 37. A) Synthesized mPDMS-MRs. B) Thermally oxidized mPDMS-MRs. C and D) The thermally oxidized mPDMS-MRs with surface functionalized using MPTMS. .... 55

Figure 38. The mercury adsorption results using mPDMS-MRs. The concentrations of mercury remaining in the solutions were normalized to the original mercury concentration in the control sample. .... 57

Figure 39. Technology LaserBlast™ Cleaning System 100 Watts on the D&D KM-IT from vendor Allied Scientific Pro. .... 62

Figure 40. News article on the D&D KM-IT title “Waste Treatment Plant Prepares to Receive Sodium Hydroxide”. .... 65

Figure 41. News article on the D&D KM-IT titled “First Shipment of Downblended Plutonium for Disposal Departs New SRS Location”. .... 65

Figure 42. News article posted to D&D KM-IT titled “” DOE Fellows Help Demonstrate Robotic Monitoring of EM Waste Site”. .... 66

Figure 43. Waste Management Symposia 2023 event entry on the D&D KM-IT. .... 66

Figure 44. D&D facility training course on the Training module of the D&D KM-IT..... 67

Figure 45. Event added to the D&D KM-IT titled “2023 RadWaste Summit 2.0” to be held in Las Vegas next month. .... 67

Figure 46. D&D KM-IT video and picture library showing a legacy video converted to mp4 and uploaded to YouTube..... 68

Figure 47. Converted legacy video (DeWalt Reciprocating Saw- DW309) uploaded to YouTube and updated on the D&D KM-IT website..... 69

Figure 48. Raw RSS feed from Content Management System (CMS) that published the D&D KM-IT news..... 69

Figure 49. D&D KM-IT RSS Feeds page..... 70

Figure 50. Number of vendors, technologies, users, and SMS as of September 2023. .... 70

Figure 51. KM-IT web analytics infographic presented during the Year End review with DOE HQ ..... 71

Figure 52. .... 73

Figure 53. KM-IT poster presented at WM2023 in Phoenix, AZ on March 1, 2023. .... 73

Figure 54. Dr. Himanshu Upadhyay (FIU), Nancy Bushman (DOE) and Walter Quintero (FIU) in front of the D&D KM-IT poster at WM2023. .... 74

Figure 55. Newsletter sent to registered users of the KM-IT to remind recipients to join the January Tech Talk. .... 74

Figure 56. Newsletter prepared to promote the Tech Talk and sent to D&D KM-IT users prior to the event. .... 75

Figure 57. Newsletter prepared to promote the July Tech Talk and sent to D&D KM-IT users prior to the event. .... 75

Figure 58. D&D KM-IT Newsletter to be sent in June..... 76

Figure 59. D&D KM-IT Newsletter to be sent in October 2023. .... 77

Figure 60. Promotional graphic for announcing FIU participation at WM2023 on social media. 78

Figure 61. Snapshot report from Google PageSpeed Insights for dndkm.org. .... 80

Figure 62. D&D KM-IT Google Analytic (GA) old tracking code activity. .... 81

Figure 63. D&D KM-IT Google Analytic 4 (GA4) new tracking code activity. .... 82

Figure 64. Number of users visiting the D&D KM-IT during Jul – Sep, 2023..... 82

Figure 65. Tech Talk registration form using Microsoft Forms. .... 87

Figure 66. October Tech Talk event webpage. .... 88

Figure 67. Webpage for Tech Talk hosted on January 24 titled “International Perspective on Decommissioning with focus on 3D hazard aware digital and robotics technology-based transformation”. .... 89

Figure 68. Organizations that attended the Tech Talk on January 24, 2023. .... 89

Figure 69. D&D KM-IT Tech Talk banner for the next event on April 25, 2023..... 90

Figure 70. Tech Talk flyer for April 2023. .... 90

Figure 71. D&D KM-IT Tech Talk event webpage hosted on April 25, 2023..... 91

Figure 72. KM-IT Tech Talk webpage conducted on July 18, 2023 titled “AI/ML Research support for Advance Long-Term Environmental Monitoring Systems (ALTEMIS)”. .... 92

Figure 73. Tech Talk recording from February uploaded to the YouTube platform..... 93

Figure 74. Tech Talk recording uploaded to YouTube and embedded on the KM-IT website.... 94

Figure 75. LSTM/CNN model architectures (modeling with 26 wells). ..... 98

Figure 76. Analysis workflow for Subtask 7.3. .... 98

Figure 77. Feature importance bar plot for target groundwater well 199-D8-55. The most influential well in the decision-making process here was 199-D8-72..... 99

Figure 78. Regression prediction performance of the AdaBoost model predicted chromium concentration values vs actual concentration values for 199-D4-39 for all angles and 1,000-meter radius. MAE was 1.1434..... 99

Figure 79. Overall feature importance versus distance plot for target well 199-D8-55. MAE error wise, the best performing models were Random Forest and ExtraTrees. Correlation wise, all the algorithms suggest that the relationship between the feature importance score and the distance is negatively correlated. .... 100

Figure 80. Wells exhibiting the biggest contribution change according to target well 199-D4-98. .... 101

Figure 81. Spatial plots of 199-D4-98 contributions on (a) 2019-12-06, (b) 2019-03-11, and (c) 2019-08-05..... 102

Figure 82. Instantaneous contribution explanations on prediction. (a) Target well 199-D5-127 had its change in concentration on October 30<sup>th</sup> largely due to wells 199-D4-95, 199-D4-85, and 199-D4-99. (b) Target well 199-D4-39 had its change in concentration on August 18<sup>th</sup> largely due to wells 199-D4-38, 199-D4-95, and 199-D8-68. (c) Target well 199-D5-92 had its change in concentration on November 14<sup>th</sup> largely due to wells 199-D8-53, 199-D2-11, and 199-D5-127. .... 105

Figure 83. Base prediction results using established modeling on contaminant concentration versus prediction results using extra sensor data and PCA..... 106

Figure 84. The amount of explained variance from each principal component. .... 107

Figure 85. Correlations principal component with the highest explained variance it has with original features. .... 107

Figure 86. The absolute mean contribution of original features on the last sequence gathered from correlation coefficient approximation..... 108

Figure 87. Deployment of LSTM-DENSE algorithm within AAMLS: (a) has the default hyper parameters to use when building the model; (b) shows LSTM-DENSE as a selectable algorithm in the model building page of AAMLS; and (c) shows how results would look when predicting with the model built using LSTM-DENSE..... 110

Figure 88. Spatial map of SRS F-Area with individual test prediction errors are shown as a colormap, ..... 112

Figure 89. FSB138D tritium prediction using all 4 input variables at all 22 wells. .... 113

Figure 90. Comparison of the powerset of inputs on prediction..... 114

Figure 91. Tritium prediction using previous architecture (relu activation)..... 115

Figure 92. Added feature to the input of the LSTM model. .... 116

Figure 93. Linear regression model for pH..... 117



Figure 94. Linear regression model for specific conductivity. .... 117

Figure 95. Linear regression model for depth to water. .... 118

Figure 96. Screenshot of command line that runs the python script. .... 119

Figure 97. Screenshot of SQL stored procedure for efficiently accessing and filtering the data in the SQL database. .... 120

Figure 98. Screenshot of the code for the function `remove_unwanted_zeros_and_spaces`. .... 120

Figure 99. Sample time series for "Depth to Water". .... 121

Figure 100. Sample time series for "Specific Conductance". .... 121

Figure 101. LSTM model's performance for Specific Conductivity. .... 123

Figure 102. LSTM model's performance for DepthToWater. .... 123

Figure 103. Time Series of Specific Conductivity with LSTM Predictions and Outlier Detection. .... 124

Figure 104. Time Series of DepthToWater with LSTM Predictions and Outlier Detection. .... 124

Figure 105. LSTM Model Prediction with Pre-Processing. .... 125

Figure 106. WaterLevel data for each well. .... 126

Figure 107. AAML model development for water contamination dataset ..... 126

Figure 108. AAML model validation results for water contamination dataset ..... 127

Figure 109. AAML Prediction development for water contamination dataset ..... 127

Figure 110. AAML Prediction results for water contamination dataset ..... 128

Figure 111. Example of an image in the COCO dataset and its corresponding pixel masks. .... 130

Figure 112. Example of an image in WISDOM dataset and its corresponding disparity image. 130

Figure 113. Example of an image in the custom dataset from the robotics team. .... 131

Figure 114. Example of augmentations applied to the dataset like mosaic, rotations, cropping, etc. .... 131

Figure 115. YOLOv7 architecture. .... 132

Figure 116. STEGO architecture. .... 132

Figure 117. Mask R-CNN architecture. .... 133

Figure 118. OWL-ViT Architecture for zero-shot object detection where the text transformers were replaces with vision transformers for one shot object detection. .... 133

Figure 119. Example of the best results from the instance segmentation YOLOv7 model. .... 134

Figure 120. Example of the results from STEGO where blue pixels are convex polygons and red pixels are the holes within the convex polygons. .... 135

Figure 121. Example of the results from SD Mask R-CNN. .... 136

Figure 122. Example of simulated images that resemble real disparity images. .... 136

Figure 123. Example of the results from OWL-ViT where the boxes are too large for the object it is encompassing. .... 137

Figure 124. Image of the robotic arm which uses the computer vision models to determine what objects to collect and how to collect them (from their shape). .... 138

Figure 125. VGG16 architecture..... 140

Figure 126. ResNet50 architecture. .... 140

Figure 127. InceptionNet architecture. .... 140

Figure 128. Autoencoder architecture..... 141

Figure 129. YOLOv3 architecture ..... 141

Figure 130. Image Classification page at AAMLS..... 142

Figure 131. Image Classification Validation Results page at AAMLS. .... 142

Figure 132. Anomaly Detection page at AAMLS. .... 143

Figure 133. .... 143

Figure 134. Example of object detection pages..... 144

## LIST OF TABLES

---

Table 1. Summary of Results.....	33
Table 2. Baseline Plug Strength for Hilti under Normal Operating Conditions.....	34
Table 3. Baseline Plug Strength for FoamBag™ under Normal Operating Conditions.....	34
Table 4. ICP-MS Analysis and the Associated Airborne Release Fractions for Baseline Powder Contamination under Impact Stress .....	46
Table 5. Average Airborne Release Fractions for FD Coating under Impact Stress .....	46
Table 6. Average Airborne Release Fractions for BPBS Coating under Impact Stress .....	46
Table 7. Coverage Density of Iron Oxide Particles at PDMS-MRs Surfaces .....	51
Table 8. Methods for mPDMS-MRs Synthesis .....	53
Table 9. Results of mPDMS-MRs Synthesis at an Increased Scale under Different Synthesis Conditions .....	54
Table 10. Conditions of mPDMS-MRs Thermal Oxidation.....	54
Table 11. Sample Information of Mercury Adsorption Tests using mPDMS-MRs.....	56

## PROJECT 3 EXECUTIVE SUMMARY

---

The Waste and D&D Engineering and Technology Development Project (Project 3) focuses on delivering solutions under the waste, D&D and IT/data science areas for the DOE Office of Environmental Management. This work directly supports D&D activities being conducted across the DOE EM complex to include Oak Ridge, Savannah River, Hanford.

During FIU Year 3, the following DOE Fellows directly supported this project: Aurelien Meray (graduate, Ph.D., Computer Science), Rohan Shanbhag (graduate, Computer Science), Alejandro De-La-Noval (graduate, Computer Science), Aris Duani Rojas (graduate, Ph.D., Computer Science), Fabiola Rivera-Noriega (undergraduate, Computer Science), and Nicholas Espinal (undergraduate, Mechanical Engineering).

The following ARC researchers are supporting this project and mentoring the DOE-EM Fellows: Himanshu Upadhyay (Ph.D., Engineering/Management, Task 1, 3, 7, 8 & 9, Associate Professor, Electrical and Computer Engineering), Walter Quintero (M.S., Computer Engineering, Task 1 & 3, Research Scientist/IT Team Lead), Santosh Joshi (M.S., Engineering Management, Task 7, 8 & 9, Research Specialist II / AI Team Lead), Clint Miller (MCSA, MCSE, CompTIA Security +, C|EH, Cyber Systems Engineer), Masudur Siddiquee (Ph.D., Electrical and Computer Engineering, Task 7, Postdoctoral Associate), Jayesh Soni (Ph.D., Computer Science & Engineering, Task 8, Postdoctoral Associate), Joseph Sinicrope (M.S., Technology Leadership/MBA, Task 2, Research Scientist), Mellissa Komninakis (B.S., Biological Eng./Materials Science & Engineering, Task 2, Research Analyst), Kexin Jiao (Ph.D., Material Science & Nanotechnology, Task 2, Postdoctoral Associate), Jose Rivera (B.S., Civil Engineering, Research Analyst), Leonel Lagos (Ph.D., PMP®, Mechanical Eng./Civil/Env. Engineering, PI).

This project included the following tasks during the September 29, 2022, to September 28, 2023, period of performance:

### **Task 1: Waste Information Management System (WIMS) (HQ)**

This task provides direct support to DOE EM for the management, development, and maintenance of a Waste Information Management System (WIMS). WIMS was developed to receive and organize the DOE waste forecast data from across the DOE complex and to automatically generate waste forecast data tables, disposition maps, GIS maps, transportation details, and other custom reports. WIMS is successfully deployed and can be accessed from the web address <https://emwims.org/>. The waste forecast information is updated annually. WIMS has been designed to be extremely flexible for future additions and is being enhanced on a regular basis.

### **Task 2: D&D Support to DOE EM for Technology Innovation, Development, Evaluation and Deployment**

This task provides direct support to DOE EM for D&D technology innovation, development, evaluation, and deployment. Based on high priority operational requirements expressed by DOE EM HQ, the national labs, and site personnel, FIU expanded its research in technology test and evaluation in the following key areas by: 1) Confirming the experimental designs intended to certify fixative technology performance when exposed to impact stressors that are postulated in contingency scenarios in DOE EM-wide Safety Basis Documents; 2) Investigating the application of a down-selected intumescent foam technology to mitigate contaminate release in support of F/H

Labs pipe decommissioning project and other D&D activities; 3) Collaborating with ASTM to continue development of standards and testing protocols in support of D&D technologies; and 4) Investigating the potential for multi-functional fixatives intended for mercury abatement during D&D Activities (This activity was discontinued mid-year due to personnel departure). FIU will further support the EM D&D program by participating in D&D workshops, conferences, and serving as subject matter experts.

### **Task 3: Knowledge Management Information Tool (KM-IT) (HQ, SRNL, INL, ANL)**

The Knowledge Management Information Tool (KM-IT) is a web-based system developed to maintain and preserve the EM knowledge base. The system was developed by Florida International University's Applied Research Center with the support of the D&D community, including DOE-EM, the former DOE ALARA centers, and with the active collaboration and support of the DOE's Energy Facility Contractors Group (EFCOG). The KM-IT is a community driven system tailored to serve the technical issues faced by the workforce across the DOE Complex. The KM-IT can be accessed from web address <http://www.dndkm.org>.

### **Task 7: AI for EM Problem Set (Soil and Groundwater) - Exploratory data analysis and machine learning model for Hexavalent Chromium [Cr (VI)] concentration in 100-H Area (PNNL)**

Identification of the spatiotemporal relationships in Cr (VI) content between groundwater wells and how groundwater wells impact each other as they change in behavior according to natural factors throughout the year, were explained and visualized in spatial plots with the help of feature importance/contribution extraction from the utilized models. Those models include Adaboost, LSTM (Long Short-Term Memory), and CNN (1-Dimensional Convolutional Neural Network), with the LSTM model being the most capable in providing the best comparative prediction performance and interpretive insight via contribution extraction. The use of PCA (Principal Component Analysis) and coefficient calculation using correlation loadings allows for the approximation of contributions of well features beyond just hexavalent chromium, additionally resulting in better prediction performance.

### **Task 8: AI for EM Problem Set (Soil and Groundwater) – Data analysis and visualization of sensor data from the wells at the SRS F-Area using machine learning (LBNL, SRNL)**

Task 8 is focused on creating a data interface module for the AI system. This kind of module assists in ingesting the time-series data from the sensors that the ALTEMIS project has deployed. Prior to the raw data from the sensors being used by the AI system, this module comprises of submodules like data exploration, visualization, and anomaly detection. The SRS area will serve as the initial development location for the AI system for pattern identification, prediction, and anomaly detection. SRS is the target site for sensor deployment under the ALTEMIS project. The AI system is fine-tuned and put through its tests using the time-series (Aqua TROLL 500 sensors) datasets made available by the recently deployed sensors. Regarding anomaly identification and time-series analysis, FIU will investigate Recurrent Neural Network - Long Short-Term Memory (RNN-LSTM) and Auto Encoder. Other DOE sites with comparable sensor and AI system implementations can use the trained AI system. Lastly, these trained models are then transitioned to the Advanced Automated Machine Learning (AAML) System.

### **Task 9: AI for EM Problem Set (Waste Processing) - Nuclear Waste Identification and Classification using Deep Learning**

The objective of this task is to research applications of computer vision and artificial intelligence algorithms to develop solutions that can identify and classify low level nuclear waste under different constraints. Some of these constraints include limitations on available raw data, available labeled data, computer power at inference time, frequency of new low-level waste, types of input images, etc. This task also focused on extending existing deep learning models for computer vision beyond the datasets they were trained on. This includes creating end-to-end pipelines that allow for data preprocessing, data augmentation, model building with optimization, and model prediction on any image dataset that can arise within the DOE complex. The models developed will be given to the FIU-DOE robotic team, so part of this task includes the development of scripts that allow for model predictions that can be integrated with ROS2 and utilized for the Robotic arm for the Waste Segregation.

## MAJOR TECHNICAL ACCOMPLISHMENTS

---

### Task 1: Waste Information Management System (WIMS) (HQ)

- FIU continued to successfully ensure a consistent high level of performance of the WIMS application through day-to-day maintenance and administration tasks. The team continued to use tools like Google Analytics and Google Search Console to monitor the performance of the application.
- FIU received the revised waste forecast data from DOE HQ and incorporated the data on the system. FIU completed integration of 2023 waste forecast and transportation data into WIMS system (Milestone 2022-P3-D5). The production system was updated with the 2023 Forecast Waste stream information (6 waste types, 708 waste streams, 36 reporting sites and 36 disposition facilities). DOE was notified on May 5, 2023.
- The team used multiple tools to monitor the site performance, accessibility and Search Engine Optimization (SEO). These tools offer insight into the website's overall performance and can help identify potential issues before they become a problem.
- The team also updated the script for the Google Map API which supports the GIS module to ensure it was compliant with the new version of the API.
- A sandbox was created for the WIMS application and the reporting server for the team to test new patches and OS updates before they are released to the production server.
- FIU successfully ensured the WIMS application remained secure and reliable by consistently engaging with the external FIU security team to do independent testing and with the DOE Fellows to do internal testing.
- A poster based on the WIMS application was presented at the Waste Management Symposia 2023 (WM2023) and a new abstract was submitted and accepted for WM2024.

### Task 2: D&D Support to DOE EM for Technology Innovation, Development, Evaluation and Deployment

- A Technical Progress Report titled, “*Test and Evaluation of a Selected Polyurethane Foam Technologies for Mitigating Risk During Nuclear Pipe Decommissioning*”, document number FIU-ARC-2022-800013919-04C-005, was completed and will be published on OSTI.
- A Technical Progress Report titled, “*Certifying Fixative Technologies under Impact: Powder Contamination*”, document number FIU-ARC-2022-800013919-04C-006, was completed and will be published on OSTI.
- A peer-reviewed manuscript, “*Determination of Airborne Release Fractions from Loose Powder Contamination under Impact Stress*”, ref: MS#NT23-148R1, was accepted for publication in the journal, *Nuclear Technology*.
- FIU continued to chair the ASTM International E10.03 Subcommittee and led the formal 5-year reapproval and promulgation for 2 international standards in support of the D&D community: a) E3104-22, *Standard Specification for Strippable & Removable Coatings to Mitigate Spread of Radioactive Contamination*; and b) E3105-22, *Standard Specification for Permanent Coatings to Mitigate Spread of Radioactive Contamination*, for renewal and balloting.
- The commercial-off-the-shelf foam technology, FoamBag™, passed all Phase II test objectives outlined by stakeholders involved in the F/H Lab Decommissioning Project and

has advanced to the next level of testing for Year 4. Initial planning and coordination will be pursued with SRNL representatives to conduct a hot demo of the technology in FY'25.

### **Task 3: Knowledge Management Information Tool (KM-IT) (HQ, SRNL, INL, ANL)**

- FIU published 11 technologies and 44 news articles, updated vendor information, and posted 8 events on the KM-IT platform. In addition, the team kept the content fresh with relevant resources for the community, such as D&D-related training, conferences, and workshops. The content management efforts continue to keep the website current and informative for the D&D community.
- FIU attended the 2023 Waste Management Symposia where the team hosted a booth to display and demo its research and presented a poster titled “*D&D KM-IT 2023 Updates*” during the professional poster session on Wednesday, March 1, 2023.
- Eight (8) newsletters for mass communication via email were developed to keep users informed of new system features and other related activities. Newsletters were also sent to the registered users of the KM-IT and to the participants of the Waste Management Symposia with news articles and upcoming events.
- Four (4) Tech Talks were hosted during this period of performance (in October 2022, and January, April, and July 2023). This involved collaboration with Washington River Protection Solutions (WRPS), Institute for Energy Technology in Norway, Savannah River National Laboratory (SRNL), and Florida International University's Applied Research Center (FIU-ARC) research team to present topics relevant to the DOE EM Complex.
- The team has successfully kept the D&D KM-IT application and production environment running with optimal performance. In addition, the team continued to test, maintain, secure and administer the KM-IT system to keep it secured and up to date with industry standards by updating the Secure Socket Layer (SSL), updating the production environment with updates/patches, replacing hardware for optimum performance, and testing the application on a secure network using cyber security tools.

### **Task 7: AI for EM Problem Set (Soil and Groundwater) – Exploratory data analysis and machine learning model for Hexavalent Chromium [Cr (VI)] concentration in 100-H Area (PNNL)**

- FIU researched and developed algorithms for the forecasting of hexavalent chromium within target wells by utilization of surrounding wells in 100 H area.
- Algorithms are implemented to extract the feature contribution to perform prediction using recurrent neural networks, which are used to visualize and explain impacts of surrounding wells on the target and their dynamics throughout time.
- An algorithm was implemented for the incorporation of additional well sensor data beyond hexavalent chromium concentration.

### **Task 8: AI for EM Problem Set (Soil and Groundwater) - Data analysis and visualization of sensor data from the wells at the SRS F-Area using machine learning (LBNL, SRNL)**

- FIU worked on modifying the hyper parameters of the Deep learning models for predicting contaminant concentrations.
- Input parameters were modified and passed to the Deep learning models. Previously, developed models relied on all 6 input parameters (pH, specific conductance, water temperature, water table, precipitation, and air temperature) to make predictions.



- The FIU research team successfully completed the deliverable 2022-P3-D6 for deployment of an AI/ML model on the AAML system.

### **Task 9: AI for EM Problem Set (Waste Processing) - Nuclear Waste Identification and Classification using Deep Learning**

- FIU researched and developed algorithms for the detection of low-level nuclear waste. These algorithms are: YOLOv7, STEGO, SD Mask R-CNN, and OWL-ViT. Each of these algorithms addresses different needs relating to the frequency of new low level nuclear waste, and for each new low level nuclear waste, how much raw data and labeled data are available, the limitations on compute power, types of images within the data, etc.
- FIU deployed multiple algorithms for computer vision classification, anomaly detection and object detection within the Advanced Automated Machine Learning System (AAMLS). These algorithms include VGG16, ResNet50, InceptionNetv3, and EfficientNetv2 for image classification. It also includes Convolutional Autoencoder for anomaly detection and YOLOv3 for object detection. DOE personnel can apply these algorithms on their image datasets to support solutions to their problems.

# TASK 1: WASTE INFORMATION MANAGEMENT SYSTEM (WIMS) (HQ)

The Waste Information Management System (WIMS) was developed to receive and organize the DOE waste forecast data from across the DOE complex and to automatically generate waste forecast data tables, disposition maps, GIS maps, transportation details, and other custom reports. WIMS is successfully deployed and can be accessed from the web address <http://www.emwims.org>.

During this period, the team developed a poster titled “*Waste Information Management System with 2022-23 Waste Streams*” which was presented at the WM2023 conference in Phoenix on February 28, 2023. The image below shows the final version of the poster.



Figure 1. WIMS poster for WM2023 titled “Waste Information Management System with 2022-23 Waste Streams” undergoing final review.

The picture below shows the FIU and DOE team presenting the poster (pictured from left to right, Walter Quintero, Dr. Himanshu Upadhyay, and Douglas Tonkay (FIU’s WIMS point of contact at DOE HQ)).



Figure 2. FIU-DOE team presenting WIMS poster at WM2023. From left to right, Walter Quintero, Himanshu Upadhyay and Douglas Tonkay (DOE HQ).

## Subtask 1.1 WIMS System Administration - Database Management, Application Maintenance & Performance Tuning

### Subtask 1.1: Introduction

This subtask includes the day-to-day maintenance and administration of the application and the database servers. FIU maintains the WIMS application system to ensure a consistent high level of performance. In addition, the database administrators perform routine maintenance in order to keep the WIMS database and server in a stable condition. The WIMS application is also maintained on the web server by the Web Server Administrator. This administrator monitors the network and server traffic and performs changes necessary to optimize the application performance. In addition, as part of this subtask, FIU will provide application and database security, as well as Help Desk support to DOE site waste managers, HQ managers and other users who need assistance in using WIMS.

### Subtask 1.1: Objectives

The goal of this assignment is to uphold the maintenance of the WIMS application, ensuring it operates according to its design. This requires ongoing commitment from the team to regularly update both the software and hardware, safeguarding the application's resilience. Given the escalating frequency of cyber threats, the FIU team actively maintains the application's security through timely updates. This proactive approach not only mitigates the risk of cyber breaches but also enhances the user experience, enabling the application to run optimally.

### Subtask 1.1: Methodology

FIU continues to perform day-to-day maintenance and administration of the application and the database servers to ensure a consistent high level of performance of the WIMS application system. In addition, FIU constantly executes certain security tasks, including antivirus engine and definitions updates on both the web and database servers. Other maintenance tasks included Windows OS updates and patches that were applied to the servers running the emwims.org application. This routine maintenance is necessary in order to keep the WIMS database and server in a stable condition and to monitor the network and server traffic to optimize the application’s performance.

The team used multiple tools to monitor the site performance, accessibility, and Search Engine Optimization (SEO). These tools offer insight into the website's overall performance and can help identify potential issues before they become a problem. The image below (Figure 3-1) shows a snapshot of the website after running a report which not only shows that the site is performing at an optimal level, but also points out that there are some accessibility issues that need to be addressed. The team used this information to prioritize if something needs attention on the site. For instance, in this report, it is recommended that some images have alternative text, some cache capability be added to the site, and that a viewport be set up to help with mobile devices and modern browsers.

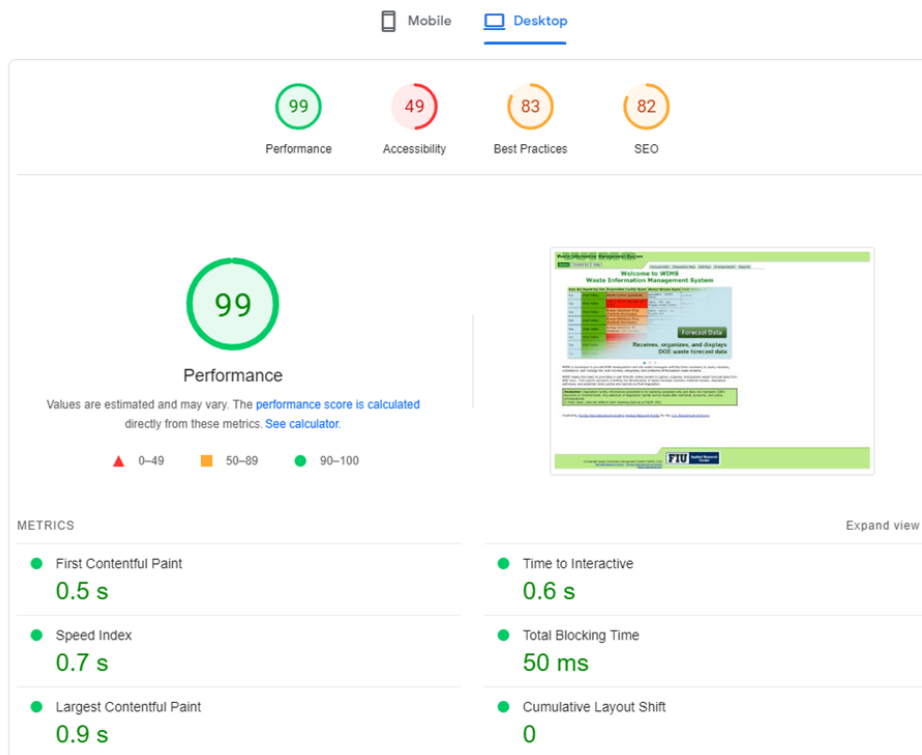


Figure 3. Snapshot report from Google PageSpeed Insights for emwims.org.

Moreover, the team addressed some recommendations by the Google Search Console tools to add alternative text to some images and modified the code to help with some modern browsers that required a viewport setting in the heading section. These changes helped the page to be compatible with search engines which helps with Search Engine Optimization (SEO).

Also, the team created a sandbox for the WIMS application on the malware lab. This version of the WIMS application is the exact replica of the production environment that is used by the team to test security vulnerabilities. If the team does not find any issues with the application after an update or patch, the solutions/patches/updates are replicated on the production environment. The reason for doing this on a sandbox is so that there is no interruption of the WIMS application on the production environment.

The team updated the production application reporting service module. It created a webpage to accommodate future reports. This page contains a report viewer control that is used to display a particular report based on the report URL parameter (ReportPath & ReportServerURL). This page was created in the production environment because this is where the reporting server is running to avoid any issues with authentication.

The team also verified that the Google Map API key was working properly after a recent update by testing the GIS module. This API key frequently updates, and the team has to update the configuration of the script with the updated key.

One major effort included the team setting up a development environment to perform Task 1.2. This new environment was a backup of the current production environment and was used to work on Task 1.2 in parallel to the production environment. This way, the WIMS application was able to remain online without any interruption. The specific efforts included creating a virtual machine for development, installing appropriate software (MS SQL and Visual Studio), backing up the application files and the SQL database from production, setting up a remote connection for the team to work on the virtual machine and updating of the firewall rules to interact with the applications, such as the Google Map API.

After the team completed the 2022-P3-D5 deliverable, the team created a development and staging environment for the application. The development environment was used to import the new waste stream data and to work on the application in parallel to the production application. In addition, the team created a staging environment to share the progress with DOE HQ and allow them to provide feedback on the development. After DOE completed the review, the team moved the application to production (<https://emwims.org/>) which completed the deliverable. The team then proceeded to clean up the development and staging environment.

The team also ran some tests on the WIMS application focusing on accessibility to make sure the site is 508 compliant. The team used the Accessible Name & Description Inspector (ANDI) tool developed by the Social Security Administration. ANDI is a free open-source tool that does not require installation. It is basically a plugin for modern browsers that can be added as a bookmark. To use it, the team simply visited the desired URL (<https://emwims.org/>) and then clicked on the ANDI bookmark. This showed a ribbon that highlighted the elements on the page that needed to be addressed. The team proceeded to address the issues by making changes to the HTML code of the application. The following two images show the ANDI tool being applied to the home page of the WIMS application and the Forecast Data module. On each instance, the tools highlighted the element on the page while providing a list of all the elements that needed to be addressed on the top section.

**ANDI** focusable elements tab order

Element: <a>  
 Accessibility Components: 0  
 No accessibility markup found for this Element.  
 ANDI Output:  
 Link has no accessible name, innerText, or [title].

Focusable Elements Found: 16  
 Accessibility Alerts: 1  
 Elements with No Accessible Name: (1)  
 1. Link has no accessible name, innerText, or [title].

**Waste Information Management System**

Home Contact Us Help Forecast Data Disposition Map GIS Map Transportation Reports

**Welcome to WIMS**  
**Waste Information Management System**

Waste Type	Physical Form	Volume	Class A/Status	Treatment	Disposition
U.S. G	Solids	1,993.20 m <sup>3</sup>	Yes		200 Area 2 (1000 m <sup>3</sup> )
Waste	Department of Energy, Office	1,361.20 m <sup>3</sup>	No		
180.16					
2.3					
14					
2483.7					
2					
23.66					
13741.08					
35692.1					
3978.69					
40					

**Disposition Map**  
 Automatically generates DOE waste disposition maps

WIMS is developed to provide DOE Headquarters and site waste managers with the tools necessary to easily visualize, understand, and manage the vast volumes, categories, and problems of forecasted waste streams.

WIMS meets this need by providing a user-friendly online system to gather, organize, and present waste forecast data from DOE sites. This system provides a method for identification of waste forecast volumes, material classes, disposition pathways, and potential choke points and barriers to final disposition.

**Disclaimer:** Disposition facility information presented is for planning purposes only and does not represent DOE's decisions or commitments. Any selection of disposition facility will be made after technical, economic, and policy considerations.  
 In most cases, data set reflects sites' planning data as of 4Q FY 2022.

Created by Florida International University's Applied Research Center for the U.S. Department of Energy

© Copyright Waste Information Management System (WIMS) 2023  
 Applied Research Center Florida International University  
<https://wimswmi.org>

**FIU** Applied Research Center

Figure 4. Accessibility tool ANDI applied on the homepage of the WIMS application.



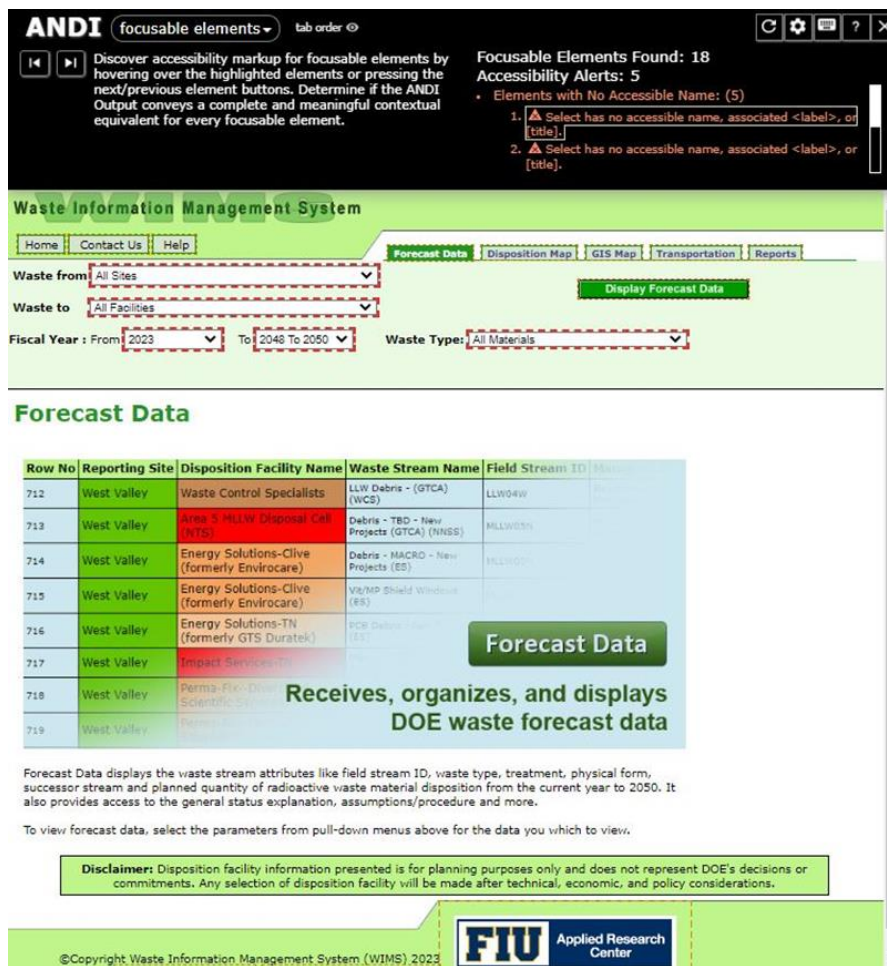


Figure 5. Accessibility tool ANDI applied on the Forecast Data module on the WIMS application.

Other maintenance tasks included updating the HTML footer of the website to prevent the content of the footer from getting trimmed. The issue was resolved and tested across multiple browsers. In addition, hardware maintenance was conducted by replacing several hard drives on the backup server. The FIU team closely monitors all the hardware that supports the application and keeps track of performance issues and lifetime of the hardware. Any hardware that starts to underperform or is close to its recommended life cycle is replaced to avoid failures.

A copy of the reporting server was also made and moved to another server to test new features without disturbing the current production version. Microsoft sends updates and patches to their operating system on a regular basis. On some occasions, these updates interfere with custom configurations that have been made to the server and cause performance issues. This mirror of the production server was created to test updates and patches before they are deployed to the production server. This allows the developer to ensure that the server and application will not have any issues following the installation of one of these updates/patches. This is similar to the sandbox created for the WIMS web application but focusing on the reporting server.

Finally, an abstract was submitted to the Waste Management Symposia 2024 (WM2024) titled “Waste Information Management System with 2023-24 Waste Streams”. WM is held every year

in Phoenix, AZ during the month of March. If the abstract was accepted, the team will submit a full paper and poster to present at the conference.

### **Subtask 1.1: Results and Discussion**

FIU continued to perform day-to-day maintenance and administration of the application and the database servers to ensure a consistent high level of performance of the WIMS application system. FIU continued to execute certain security tasks, including antivirus engine and definitions updates on both the web and database servers. Other maintenance tasks included Windows OS updates and patches that were applied to the servers running the emwims.org application. This routine maintenance is necessary to keep the WIMS database and server in a stable condition and to monitor the network and server traffic to optimize the application's performance.

### **Subtask 1.1: Conclusions**

The culmination of these efforts is a robust and secure WIMS web application that consistently performs at its best. By proactively addressing maintenance needs, the team ensures the application's resilience against cyber threats. This not only reduces the likelihood of security breaches but also contributes to an enhanced user experience. The result is a reliable and optimized WIMS application that aligns with its intended design, providing users with a secure and seamless digital experience.

### **Subtask 1.1: References**

*Waste Information Management System (WIMS)*, <https://emwims.org/>, Applied Research Center, Florida International University.

## **Subtask 1.2: Waste Stream Annual Data Integration**

### **Subtask 1.2: Introduction**

Under this subtask, FIU receives revised waste forecast data as well as transportation data as formatted data files on an annual basis. To incorporate these new files, FIU built a data interface to allow the files to be received by the WIMS application and imported into SQL Server. SQL server is the database server where the actual WIMS data is maintained. This data is typically received from DOE in the April/May timeframe.

### **Subtask 1.2: Objectives**

The objective of this subtask is to consolidate waste forecast information from separate DOE sites and build forecast data tables, disposition maps, and GIS maps on the web. An integrated system was needed to receive and consolidate waste forecast information from all DOE sites and facilities and to make this information available to all stakeholders and the public. As there was no off-the-shelf computer application or solution available for creating disposition maps and forecast data, FIU built a DOE complex-wide, high performance, n-tier web-based system for generating waste forecast information, disposition maps, GIS Maps, successor stream relationships, summary information and custom reports based on DOE requirements.

### **Subtask 1.2: Methodology**

Under this subtask, FIU receives and incorporates the revised waste forecast data files into the system on a yearly basis. The new waste data replaces the existing waste data and becomes fully



viewable and operational in WIMS. During March timeframe, FIU received revised waste forecast data from DOE-HQ as formatted data files. To incorporate these new files, FIU built a data interface to allow these specific files to be formatted for the WIMS application and imported into SQL Server. This data was imported and mapped to the 2023 waste stream structure which then updated the Forecast Data, Disposition map, Successor stream map, Transportation and Reports.

The team started by backing up the existing production database and application to move to a development environment. The team proceeded to test the development environment to get it ready for the data import.

FIU received the 2023 waste forecast data from DOE HQ at the end of March. The team inspected the data to make sure it included all the sites and facilities, waste stream types and forecasted dates required for import. The team normalized the data by updating column headings to match the current database schema. The data was imported and reviewed/matched to the original source data sent by DOE HQ. Once this verification process was completed, the team started the development process to make sure each module was able to access the new data. DOE Fellows helped with testing the application modules to make sure everything was working, while the staff continued to address any development issues and make sure the application was running smoothly before moving it back to the production server.

Next, the team began working on validating the data, making sure all the site and facility information match current data. The team normalized the data to get it ready to import to the SQL server. The data was imported successfully to the SQL server and work began on the actual development of the application to consume the new data. The team worked on the development environment so that the production application will not experience any interruptions. The first module the team worked on was the reporting module. This module was updated to accommodate the new data year range, material and waste type. Once multiple reports were finished, the team started to generate reports to compare their output with the original Excel data received from DOE HQ. The DOE Fellows assisted in this Quality Assurance (QA) process to make sure the results matched the original data provided exactly. The image below shows a sample WIMS report showing waste stream data starting from 2023 from "All Sites" to "Waste Control Specialists". While the DOE Fellows continued to work on this process, the team proceeded to work on the other modules (Forecast Data, Disposition Map, GIS Map and Transportation).

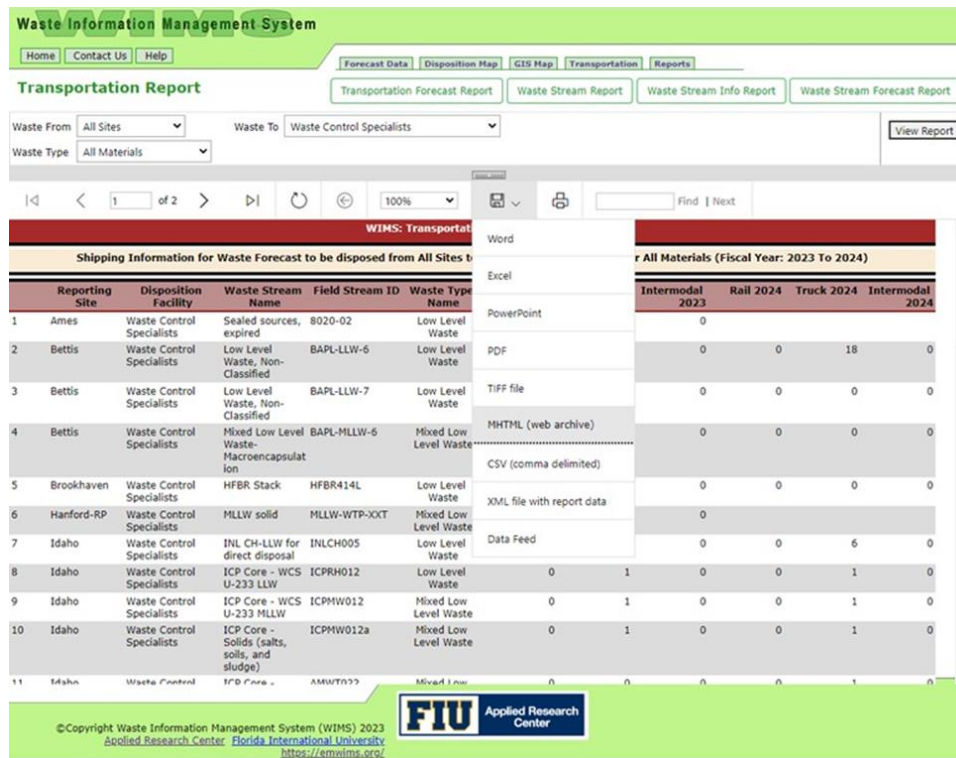


**Figure 6. WIMS reporting module showing waste stream data starting from 2023 from "All Sites" to "Waste Control Specialists".**

In addition to the development updates to each of the modules, DOE requested enhancements to certain modules such as a legend to include the waste streams status and treatment codes. The image below shows the new legend under the disposition map for waste streams from “All Sites” to “Clean Harbors” starting in 2023 for all materials.

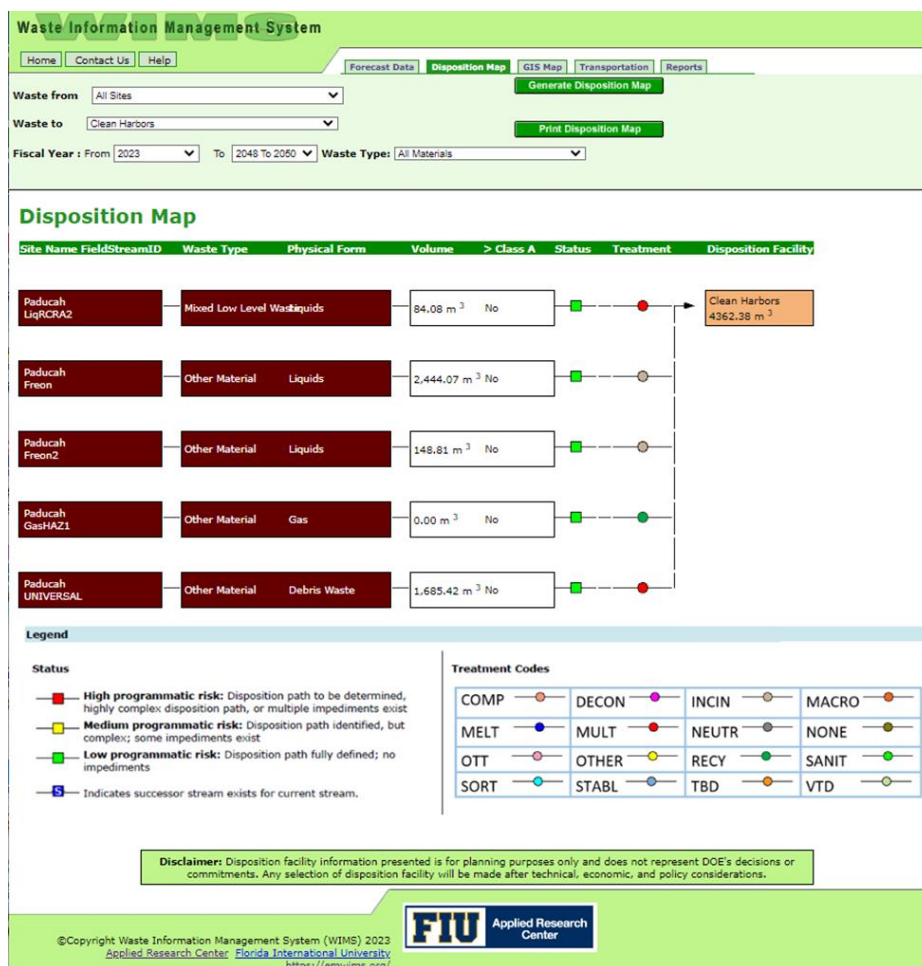


Figure 7. WIMS Disposition Map module with legend for waste streams from “All Sites” to “Clean Harbors” starting in 2023 for all materials.

By the end of April, the team completed the input of the data, development, and enhancement of each of the modules on the development environment. FIU provided DOE HQ with a URL on the staging server for them to review the progress, test the application and provide additional feedback and comments. The DOE Fellows continues to perform data validation on each of the modules.

### Subtask 1.2: Results and Discussion

During the month of May, the team completed the development and enhancement of each of the modules after performing an internal review. FIU provided DOE HQ with a URL on the staging server for them to review the progress, test the application and provide additional feedback and comments. FIU addressed the feedback provided from DOE HQ and moved the application to the production server making the new data and application live at <http://emwims.org>. DOE HQ was notified about the completion of this deliverable (2022-P3-D5 due on May 27, 2023) on May 5, 2023. The following screenshots show the WIMS application running live on the production server. The modules shown are Forecast Data, Disposition Map, GIS Map, Transportation and Reports.

The image below shows the Forecast Data module with data from “All Sites” to “Waste Control Specialist” from year “2023” to “2048 to 2050” for all material waste types.

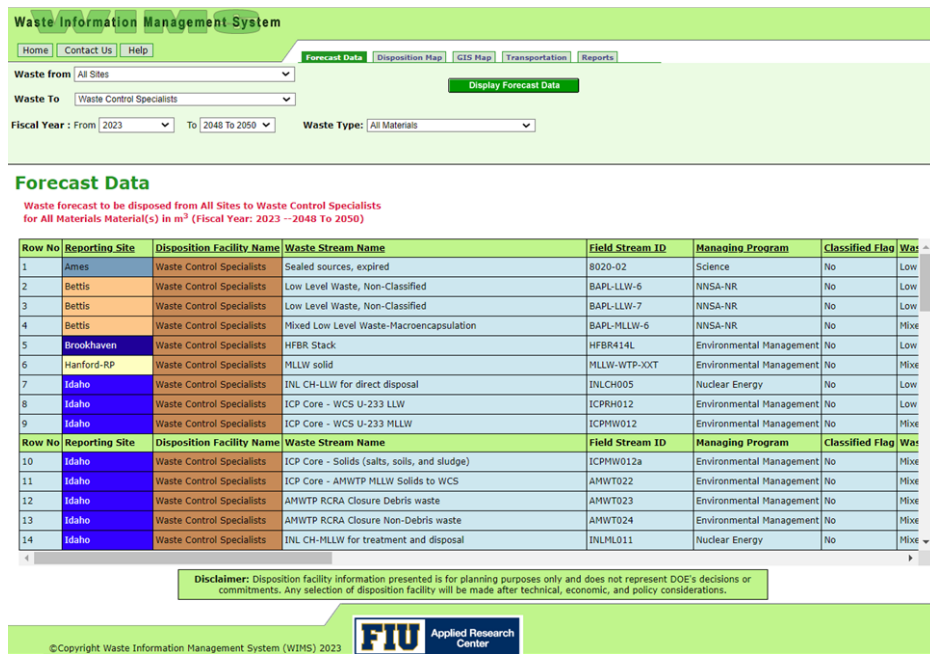


Figure 8. WIMS Forecast Data module showing waste data forecast from All Sites to Waste Control Specialist.

The image below shows the Disposition Map module with data from “Kansas City Plant” to “All Facilities” from year “2023” to “2048 to 2050” for all material waste types. Notice that total waste is grouped by disposition facilities.

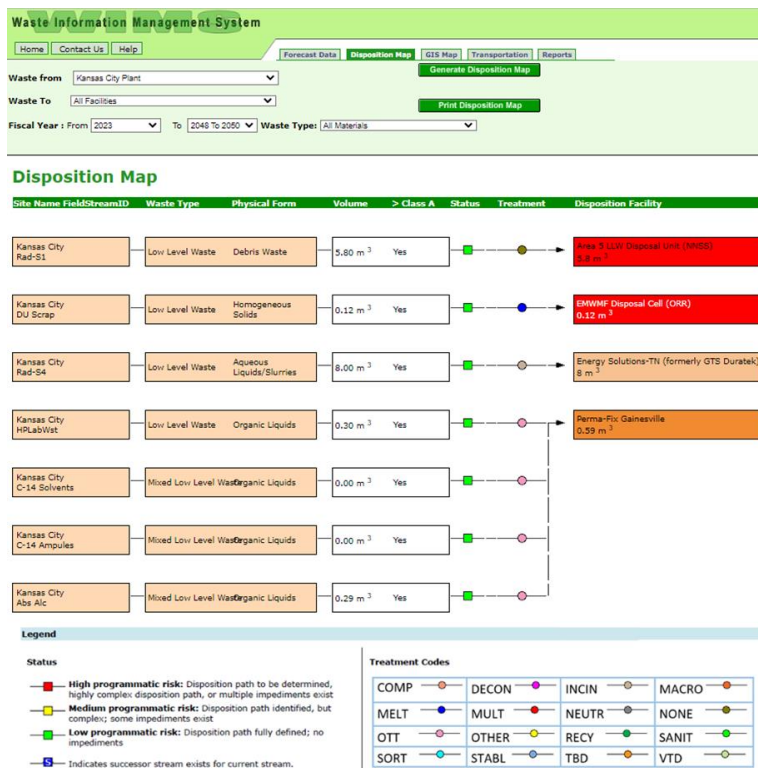


Figure 9. WIMS Disposition Map module with data from “Kansas City Plant” to “All Facilities”.

The following image below shows the GIS Map module with data from “All Sites” to “Waste Control Specialist” from year “2023” to “2048 to 2050” for all material waste types. The GIS map shows the multiple disposition locations across the country with the total volume. The list of disposition locations is also shown on the left side banner which can be used to filter the data on the map.

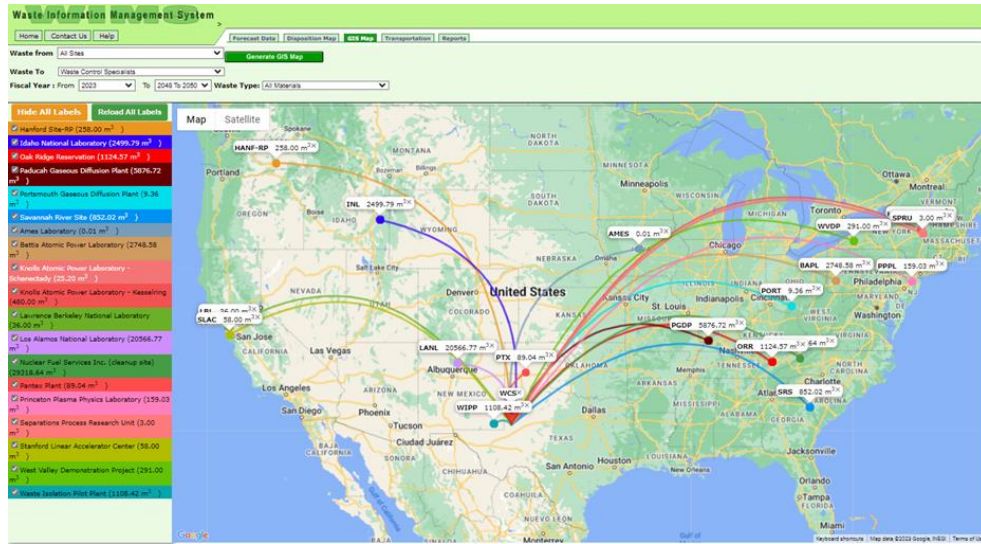


Figure 10. WIMS GIS Map module with data from “All Sites” to “Waste Control Specialist”.

This next image shows the Transportation module with data from “Naval Reactor Facility” to “All Facilities” from year “2023” to “2048 to 2050” for all material waste types. This module lists the mode of transportation to be used (Rail, Truck, Intermodal) for the next few years (2023, 2024).

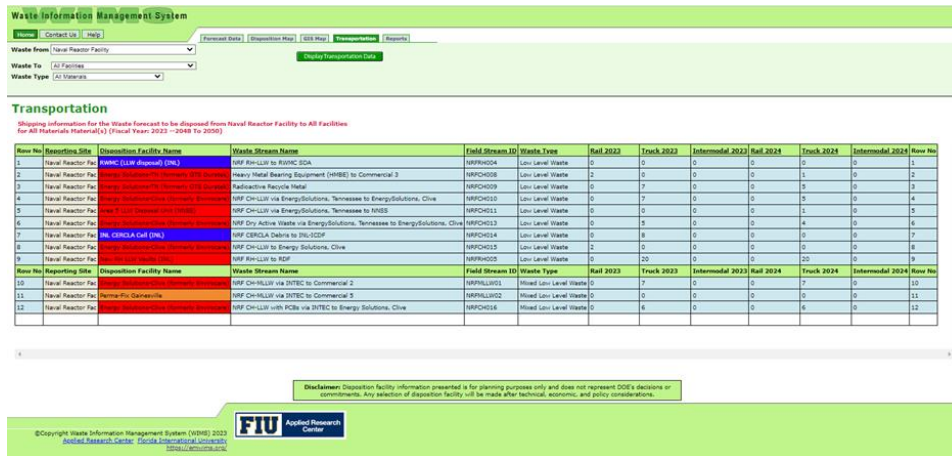
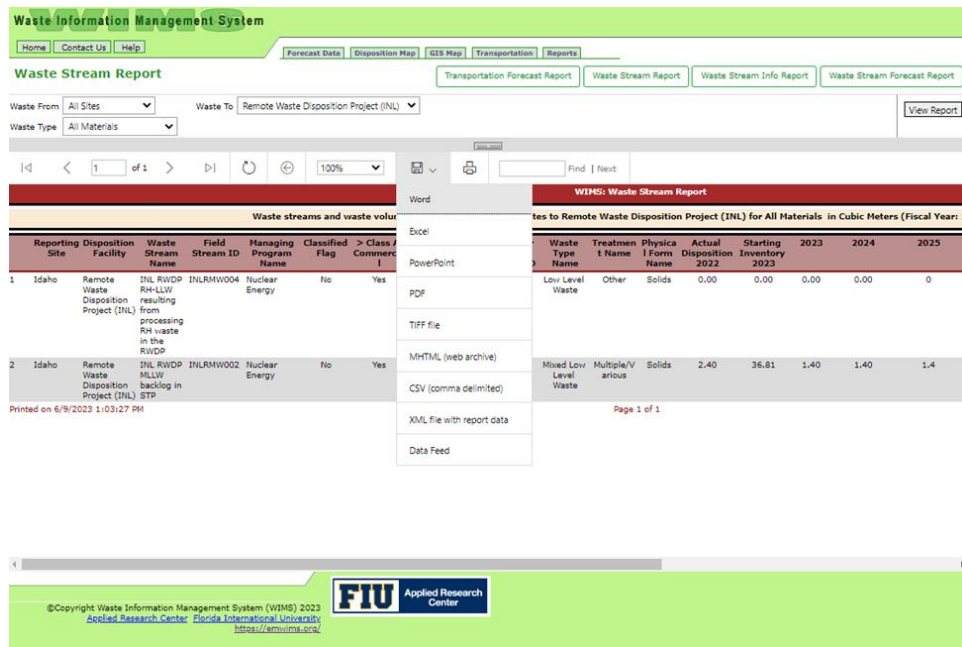


Figure 11. WIMS Transportation module with data from “Naval Reactor Facility” to “All Facilities”.

Finally, the image below shows the Report module (Waste Stream Report) with data from “All Sites” to “Remote Waste Disposition Project” for all material waste types. Note that the report module supports export of any report to multiple formats (Word, Excel, PowerPoint, PDF and more).





**Figure 12. WIMS Report module (Waste Stream Report) with data from “All Sites” to “Remote Waste Disposition Project”.**

After publishing the updated 2023 waste stream data from DOE to the production server, the team has continued to monitor the performance of the website modules and reports and has since made minor tweaks to address display issues (updating HTML and CSS code). The team will continue to monitor the site and will address any other issues that may arise. The team also performed administrative and security tasks. Specifically, during this period, the team configured a DOE firewall that required creating new zones, NAT policies, new user groups, VPN policies and web policies for emwims.org. Finally, the team completed backing up the staging and development environment after publishing the latest version of the application to production.

After publishing the application to the production server, the team has continued to monitor the performance of the website modules and reports and made minor tweaks to address display issues (updating HTML and CSS code). One issue involved the height of the container which resulted in the reports not being displayed correctly on some browsers. This type of update is an ongoing process where the team continues to monitor the site and addresses any issues that may arise. To identify performance issues, the team uses server log reports and Google Search Console reports. The image below shows a screenshot of the WIMS report module correctly displayed (i.e., filling up the complete height of the webpage including the footer).

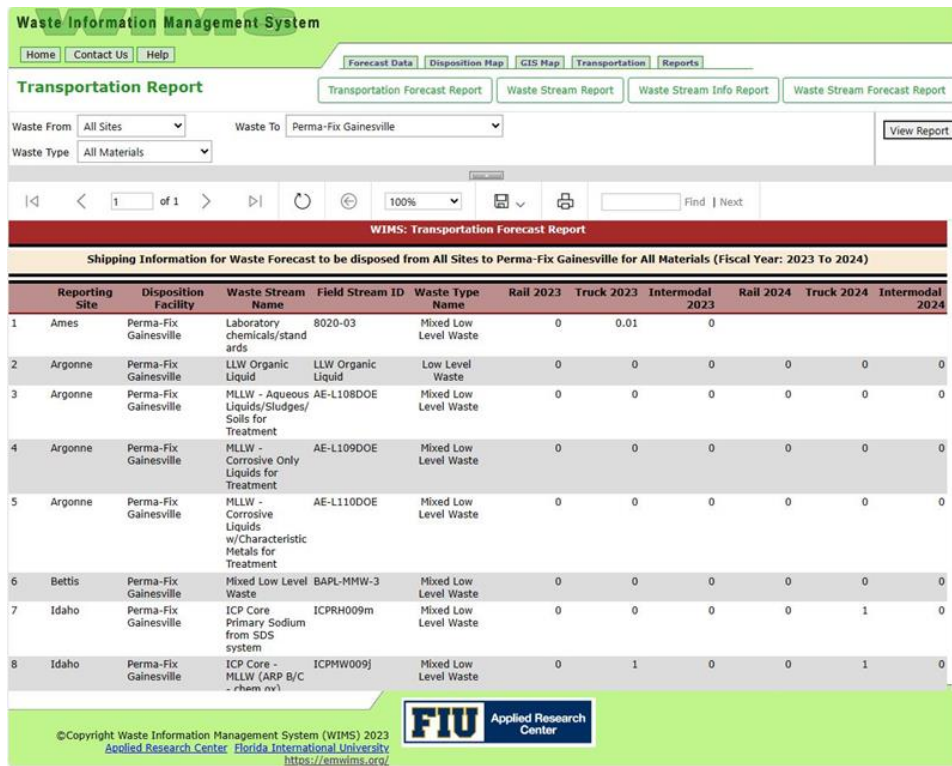


Figure 13. WIMS Report module showing proper report height with website footer.

Below is the list of the 36 supported sites on WIMS.

- |   |   |
|---|---|
| <ul style="list-style-type: none"> <li>• Ames Laboratory</li> <li>• Argonne National Laboratory</li> <li>• Bettis Atomic Power Laboratory</li> <li>• Brookhaven National Laboratory</li> <li>• Energy Technology Engineering Center</li> <li>• Fermi National Accelerator Laboratory</li> <li>• Hanford Site-RL</li> <li>• Hanford Site-RP</li> <li>• Idaho National Laboratory</li> <li>• Kansas City Plant</li> <li>• Knolls Atomic Power Laboratory – Kesselring</li> <li>• Knolls Atomic Power Laboratory – Schenectady</li> <li>• Lawrence Berkeley National Laboratory</li> </ul> | <ul style="list-style-type: none"> <li>• Norfolk Naval Shipyard</li> <li>• Nuclear Fuel Services, Inc. (cleanup site)</li> <li>• Oak Ridge Reservation</li> <li>• Paducah Gaseous Diffusion Plant</li> <li>• Pantex Plant</li> <li>• Pearl Harbor Naval Shipyard</li> <li>• Pacific Northwest National Laboratory</li> <li>• Portsmouth Gaseous Diffusion Plant</li> <li>• Portsmouth Naval Shipyard</li> <li>• Princeton Plasma Physics Laboratory</li> <li>• Puget Sound Naval Shipyard</li> <li>• Sandia National Laboratories – NM</li> <li>• Savannah River Site</li> <li>• Stanford Linear Accelerator Center</li> <li>• Separations Process Research Unit</li> <li>• Thomas Jefferson National Accelerator Facility</li> </ul> |
|---|---|

<ul style="list-style-type: none"> <li>• Lawrence Livermore National Laboratory</li> <li>• Los Alamos National Laboratory</li> <li>• Naval Reactor Facility</li> <li>• Nevada National Security Site</li> <li>• NG Newport News</li> </ul>	<ul style="list-style-type: none"> <li>• Waste Isolation Pilot Plant</li> <li>• West Valley Demonstration Project</li> </ul>
--	--

Below is the list of the 36 supported facilities on WIMS.

<ul style="list-style-type: none"> <li>• 200 Area Burial Ground (HANF)</li> <li>• 746-U Landfill(Paducah)</li> <li>• Area 5 LLW Disposal Unit (NTS)</li> <li>• Area 5 MLLW Disposal Cell (NTS)</li> <li>• Area G (LLW disposal) (LANL) (New)</li> <li>• Clean Harbors</li> <li>• Commercial TBD</li> <li>• E-Area Disposal (SRS)</li> <li>• EMWMF Disposal Cell (ORR)</li> <li>• Energy Solutions-Clive (formerly Envirocare)</li> <li>• Energy Solutions-TN (formerly GTS Duratek)</li> <li>• ERDF (HANF)</li> <li>• Heritage Liverpool (Ohio) (New)</li> <li>• Impact Services-TN</li> <li>• INL CERCLA Cell (INL)</li> <li>• Integrated Disposal Facility (HANF)</li> <li>• New RH LLW Vaults (INL)</li> <li>• Omega Waste Logistics</li> </ul>	<ul style="list-style-type: none"> <li>• OSWDF(Portsmouth)</li> <li>• Paducah CERCLA</li> <li>• Perma-Fix Gainesville</li> <li>• Perma-Fix--Diversified Scientific Services, Inc.</li> <li>• Perma-Fix--Northwest (formerly PEcoS)</li> <li>• Perma-Fix/Materials &amp; Energy Corp</li> <li>• Remote Waste Disposition Project (INLS)</li> <li>• River Metals</li> <li>• RMW Trenches (MLLW/LLW) (HANF)</li> <li>• RMW Trenches/IDF (HANF) • RWMC (LLW disposal) (INL)</li> <li>• Siemens</li> <li>• Smokey Mountain Solutions</li> <li>• To Be Determined</li> <li>• Unitech</li> <li>• US Ecology-Idaho</li> <li>• Veolia</li> <li>• Waste Control Specialists</li> </ul>
--	--

**Subtask 1.2: Conclusions**

WIMS continues to successfully accomplish the goals and objectives set forth by DOE. WIMS has replaced the historic process of each DOE site gathering, organizing, and reporting their waste forecast information utilizing different database and display technologies. In addition, WIMS meets DOE’s objective to have the complex-wide waste forecast information available to all stakeholders and the public in one easy-to-navigate system. The data includes low-level and mixed low-level radioactive waste forecast data supplied by all DOE programs in addition to transportation information. After a final review, the FIU team published the 2023 stream data (6



waste types, 708 waste streams, 36 reporting sites and 36 disposition facilities) and application to the production server running live at <https://emwims.org/>. DOE HQ was notified about the completion of this deliverable (2022-P3-D5 due on May 27, 2023) on May 5, 2023.

### **Subtask 1.2: References**

*Office of Environmental Management (DOE-EM), <https://www.energy.gov/em/office-environmental-management>, U.S. Department of Energy.*

*Waste Information Management System (WIMS), <https://emwims.org/>, Applied Research Center, Florida International University.*

## **Subtask 1.5: Cyber Security of WIMS Infrastructure**

### **Subtask 1.5: Introduction**

The cyber security of WIMS Infrastructure involves securing the network not only by system administration tasks mentioned above, but also by conducting routine cyber security tasks to test the network's vulnerability. This involves coordination between the FIU security team and DOE Fellows who also learn cybersecurity skills while assisting staff do penetration testing and other tasks to test the overall security of the system at the application, database, and infrastructure levels.

### **Subtask 1.5: Objectives**

The objective of this task is to focus on specific cyber security threats that could affect the WIMS application and framework. The team achieves this by implementing the latest industry security standards on the application and network to protect the WIMS application from malicious attacks.

### **Subtask 1.5: Methodology**

Cyber security of WIMS involves securing the network infrastructure that is deployed, secured and maintained in the FIU facility. This includes administration tasks described in Subtask 1.1, but also includes conducting routine cyber security tasks to test the network's vulnerability. This involves coordination between the FIU security team and DOE Fellows who learn cyber security skills while assisting staff do penetration testing and other tasks to test the overall security of the system at the application, database and infrastructure levels. This is a continuous effort as the team actively monitors cyber security activity to ensure that the network remains safe.

The team started the first quarter of this period by updating the machines in the cybersecurity lab. They finished updating all the machines in the lab to the latest version of their operating system. Currently the lab is composed of both Microsoft Windows and Linux machines. All the necessary updates were performed including updates to the security software used for research such as Kali Linux.

During the second quarter, the team began experimenting with the updated security tools installed in the lab using the WIMS application sandbox copied from the production environment. These tools are used to perform penetration testing and other security testing on a replica of the WIMS application. Typically, the team replicates known security issues currently affecting other websites. If any vulnerability is found, the team proceeds to patch or make the necessary updates to the application to fix the issue and prevent any security breaches or degraded application performance.

In addition, there were cyber security efforts closely related to support Subtask 1.2. When the team created the development environment, there were cyber security tasks performed so that the development environment remained secure during the development process. This involved updating the virtual machine used for development with the latest security patches, antivirus, and firewall rules and creating user accounts to access this environment. Also, this development server was created behind a firewall to secure it from current security threats.

During the third quarter, the cyber security efforts revolved around supporting Subtask 1.2. As mentioned in Subtask 1.1, a new staging environment was created to allow DOE HQ to test the application. This staging environment was designed to be exactly as the production environment with the same security settings and policies to test the application performance. After the team created the environment on Subtask 1.1, it was secured and tested carefully before providing the URL link to DOE HQ to make sure it worked properly and that there were no issues with integration in this new environment. The team also closely monitored the application during the time on the staging server to make sure there were no security breaches. This is one of the reasons the staging environment inherited the security settings from the production environment, so that no new vulnerabilities were introduced.

The team completed the deliverable from Subtask 1.2 and proceeded to reset the development environment used to develop this task. The team also secured the staging environment, by applying identical security settings from the production environment, while DOE HQ reviewed the application and provided feedback. After DOE finished their review, the team proceeded to dismantle the staging and development server so that no security vulnerability footprint remained. This included:

- Removing access to the staging environment.
- Removing the virtual directory used by DOE to access the application.
- Removing user access for testing the application.
- Resetting developer access to the development and staging server.

Finally, the security policies previously implemented (firewall rule updates, NAT policies and user groups) continued to be monitored. An intermediate issue was also fixed that occurred with certain browsers that had an SSL configuration. This issue was resolved by reinstalling the certificate on the webserver. This process involved requesting a new SSL certificate key from the provider (GoDaddy), installing the new SSL certificate on the web server, and configuring the website on IIS to use the updated SSL certificate. The certification process is repeated every year unless it needs to be reconfigured for other reasons.

### **Subtask 1.5: Results and Discussion**

The teams continued to secure the application on a constant basis. This effort needs to be performed regularly as new security threads are developed daily. The team has engaged with the external FIU security team to do independent testing and engaged the DOE Fellows to do internal testing. As a result, the WIMS application has remained secure and reliable.

### **Subtask 1.5: Conclusions**

As mentioned above, this is a continuous task in which multiple teams work together to achieve the goal of securing the WIMS application. The team has been successful in keeping the application secure and is always looking for new tools to test the application security. As new

threats are identified on the internet, the team tests the application against those threats and quickly applies the appropriate patches and software updates to minimize the system vulnerability.

### **Subtask 1.5: References**

*Waste Information Management System (WIMS)*, <https://emwims.org/>, Applied Research Center, Florida International University.

## **TASK 2: D&D SUPPORT TO DOE EM FOR TECHNOLOGY INNOVATION, DEVELOPMENT, EVALUATION AND DEPLOYMENT**

---

### **Subtask 2.1: Development of Uniform Testing Protocols and Standard Specifications for Fixative Technologies in Support of Complex-wide D&D Activities**

#### **Subtask 2.1: Introduction**

The U.S. Department of Energy's Office of Environmental Management (DOE EM) has taken a leading role in investing in the research and development (R&D) of critical technologies to support the safe and efficient decommissioning of legacy nuclear facilities. To facilitate the complex-wide deployment and adoption of those technologies from the laboratory to end users, and to maximize return on investment of government-sponsored R&D projects, DOE EM proactively solicits and evaluates initiatives intended to enhance achievement of these goals. Given that standards-based testing and evaluation is a critical enabler to the successful transition and deployment of D&D technologies from the lab to the end user, FIU continued to actively participate in ASTM International's E10 and E10.03 Committees to develop and promulgate uniform performance metrics and testing protocols for D&D technologies.

#### **Subtask 2.1: Objectives**

Under this task, FIU ARC continues to actively participate in ASTM International's E10 and E10.03 Committees to develop and promulgate uniform performance metrics and testing protocols for D&D technologies, with a particular emphasis on fixatives and foams. This activity directly supports the planned operational deployment of those technologies on site, as well as establishes the groundwork for updating the DOE-HDBK-3010. Providing a uniform certification methodology for fixative technologies has been deemed an essential goal under this activity.

#### **Subtask 2.1: Methodology**

Leveraging the fixatives research and development activities being led by Savannah River National Laboratory (SRNL) and Florida International University's Applied Research Center (FIU ARC) on behalf of DOE EM's Office of Infrastructure and D&D, a collaboration with ASTM International's E10 Committee and E10.03 Subcommittee has been established to develop, codify, and promulgate consensus-based standard specifications and uniform testing practices. This initiative captures the advancements made in experimental design formulation for fixative technologies during the test and evaluation phases of designated activities across the DOE EM complex. An FIU researcher serves as the Chair and a SRNL researcher serves as the Vice-Chair, with other national lab representatives joining as voting members. As testing protocols for various fixative technologies (e.g.: permanent, foam, decon gels, etc.) are developed and proven, they are subsequently introduced to the E10.03 Subcommittee for review, balloting, approval, and promulgation as an international standard.

#### **Subtask 2.1: Results and Discussion**

As highlighted above in the achievements section, two benchmark standard specifications for fixative technologies were updated and reapproved over this reporting period. Specifically, E3104-

22, Standard Specification for Removable Coatings and Decon Gels, and E3105-22, Standard Specification for Permanent Coating Fixatives were successfully balloted after a comprehensive review and update by the D&D community. These standards outline the performance parameters for fixatives and are now valid through 2027.

The E10.03 Subcommittee's Fixative Working Group will now begin working on ASTM E3191 on Permanent Foam Fixatives since it is up for its 5-year renewal starting in 2024. This standard is important as it is being used to guide the testing and evaluation of foam fixatives being considered for potential use in support of an F/H lab decommissioning project. This standard specification has served as a guiding document for the testing and evaluation of the foam technologies being investigated as potential plugs in support of the F/H lab decommissioning project of the piping in the courtyard. Additional performance requirements identified during this project will be incorporated into the updated standard specification by the E10.03 Fixatives Working Group. Once completed, the revised ballot will be submitted into the ASTM balloting process, with a goal of having the revised standard formally approved and promulgated by September 2024. It will be used to assist in the evaluation of the hot demo of the foam technology at F/H labs tentatively scheduled in 2025.

### **Subtask 2.1: Conclusions**

The ASTM International E10.03 Subcommittee will continue pursuing further testing protocol and standards development for fixatives and other technology categories associated with D&D, creating consensus-based standards for D&D technologies that are not only aligned with technical specifications, but also account for the safety, regulatory, and operational requirements encountered during D&D activities. Addressing existing shortfalls through standards will provide credibility, yield a significant return on investment, and allow all types of D&D technologies (robotics, fixatives, characterization, decontamination, demolition, etc.) to be developed, tested, evaluated, and compared to a set of uniformly accepted metrics.

International standards and testing protocol development plays a critical role in successful technology development and deployment programs. These standards lay the groundwork for setting the necessary conditions to successfully test, evaluate, compare, transition, and employ technologies in support of D&D activities in the highly regulated, safety conscience, risk adverse industry in which work is done. Universally accepted standards are essential in building the bridge to full field deployment of new technologies. This is particularly relevant when working at the higher ends of the TRL readiness scale and addresses many concerns on the part of all stakeholders – from researchers and developers to end users, regulatory agencies, and the public.

### **Subtask 2.1: References**

ASTM International. (2017). *E3104-22 Standard Specification for Strippable & Removable Coatings to Mitigate Spread of Radioactive Contamination*. Retrieved from <https://doi.org/10.1520/E3104-17>

ASTM International. (2017). *E3105-22 Standard Specification for Permanent Coatings Used to Mitigate Spread of Radioactive Contamination*. Retrieved from <https://doi.org/10.1520/E3105-17>

ASTM International. (2018). *E3191-18 Standard Specification for Permanent Foaming Fixatives Used to Mitigate Spread of Radioactive Contamination*. Retrieved from <https://doi.org/10.1520/E3191-18>

ASTM International. (2019). *E3190-19 Standard Practice for Preparation of Fixed Radiological/Surrogate Contamination on Porous Test Coupon Surfaces for Evaluation of Decontamination Techniques*. Retrieved from <https://doi.org/10.1520/E3190-19>

ASTM International. (2021). *E3283-21 Standard Practice for Preparation of Loose Radiological/Surrogate Contamination on Nonporous Test Coupon Surfaces for Evaluation of Decontamination Techniques*. Retrieved from <https://doi.org/10.1520/E3283-21>

## Subtask 2.2: Test and Evaluation of Down-selected Intumescent Foams/Foam Plug Technologies to Mitigate Contaminate Release during Nuclear Pipe Dismantling in Support of a Hot Demo at F/H Labs

### Subtask 2.2: Introduction

FIU, in collaboration with SRNL, continued investigating COTS technologies that could be used to immobilize or isolate, or both, dispersible contamination deposited within 3-dimensional void spaces of various volumes that would be difficult to otherwise coat with conventional 2-dimensional fixatives. The suitable technology must support the dismantling of pipework during decommissioning activities at F/H labs. By FY '27, the F/H Laboratory Deactivation Project Team plans to remove all the buried, shown in Figure 14. The piping length to be removed is about 250 feet and will be cut to 5' lengths so it may be disposed to B-25. The site team is interested in investigating whether the application of certain down-selected foam technologies could enhance engineering controls to mitigate the risk of contaminate release and reduce costs.

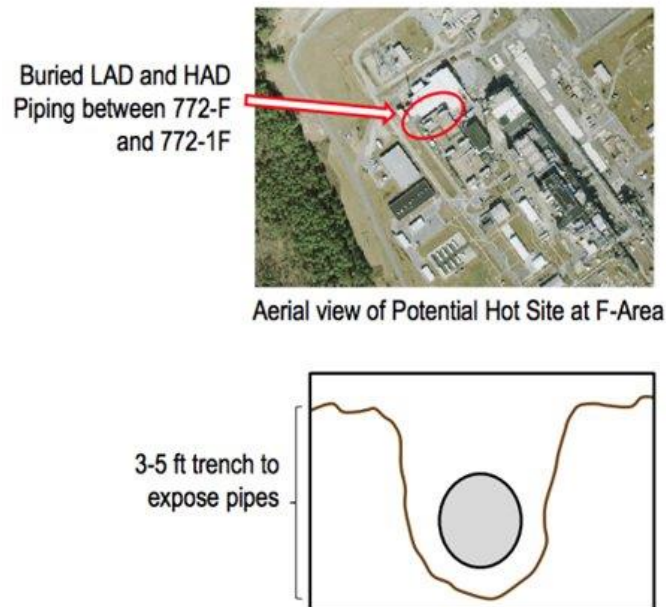


**Figure 14. Buried pipe removal site at F/H Labs.**

The basic premise in employing the selected technology is to create an air and watertight, lightweight foam plug using an expandable foam that can be applied via established hot tap

procedures prior to the actual dismantling of the pipes, thereby allowing workers to cut into sealed pipes rather than open pipes, as depicted in Figure 15. The foam plugs can be placed at 5' increments to mirror the planned packaging and transportation procedures and serve as an added engineering control to isolate gross / residual contamination within the pipe segment. The foam technology would be applied during the normal course of the hot tap process.

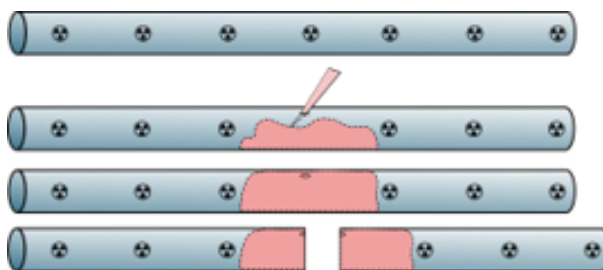


**Figure 15. Operational concept for employing foam technology.**

During this performance year, the Radiation Hardened Foam Cold Demo Test Plan: Phase II was developed and executed. This document outlined the Phase-II test objectives and implementation plan for a downselected foam fixative technology intended to facilitate activities in support of the Savannah River Site (SRS) F/H labs' D&D efforts. It is a collaborative effort between SRNL, FIU, and the SRS F/H labs' team intended to test and evaluate the potential of a polyurethane foam in mitigating the release of contamination during dismantling operations on radioactively contaminated piping in legacy facilities. The cold demo test plan addresses specific requirements highlighted by site and safety personnel and will be executed in FIU's Outdoor Test and Evaluation Facility using a mock-up that replicates the operational conditions at the proposed hot test location at the F/H labs. Results from the cold test plan will inform the hot test at the F/H labs, which will use the foam fixative to confine and/or isolate residual contamination within a 3-dimensional void space of Hastelloy C-22 piping designated for removal from the site and transported to a proper disposal facility.

### **Subtask 2.2: Objectives**

Phase II of the cold demo test plan outlined the following objectives:

1. Evaluate the adhesion and bonding properties of the foam plug to Hastelloy C-22 piping.
2. Evaluate the adhesion and bonding properties of the foam plug to Hastelloy C-22 piping under various moisture conditions.
3. Determine the heat profile of the foam during curing in Hastelloy C-22 piping.
4. Determine the internal pipe pressure after foam deployment and curing.
5. Determine the effectiveness of the foam plug using a standard leak test.
6. Evaluate off-gas formed during foam curing.
7. Evaluate the impacts of temperature and humidity on the foam plug's stability during environmental chamber testing.

Test objectives 1-5 were conducted at FIU, with objectives 6-7 being conducted at SRNL. Over the course of the past year, FIU and SRNL have hosted several periodic updates with the F/H Labs Decommissioning Team and DOE EM HQ.

## Subtask 2.2: Methodology

The COTS foam selected for evaluation in Phase II is the FoamBag™ technology. FoamBag™ has been in use in the UK in gloveboxes at Sellafield and meets the UK gas industry technical standard T/SP/E/59. The FoamBag™ holds resin foam in place as it expands. At full expansion, the foam seeps through the semi-porous panels of the bag to form an adhesive seal with the pipe.

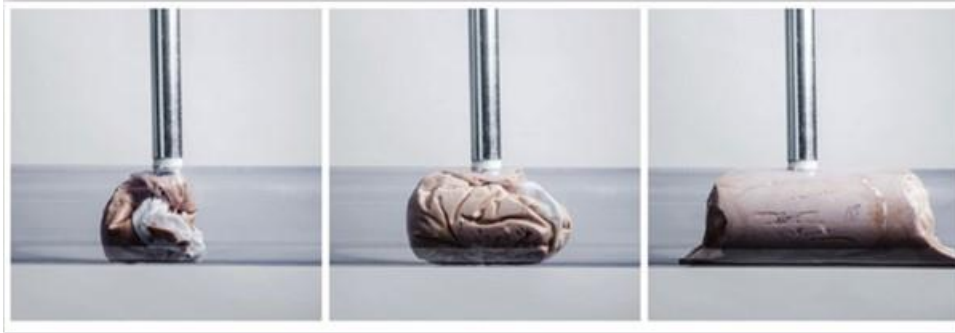


**Figure 16. Depiction of FOAMBAG™ technology, which holds the resin foam in place as it expands. At full expansion, some of the foam seeps through the semi-porous panels of the bag to form an adhesive seal with the pipe.**

### *Evaluation of the adhesion and bonding properties of the foam plug to Hastelloy C-22 piping*

Adhesion capabilities of the foam to Hastelloy C-22 piping will ultimately decide whether a foam fixative plug can confine and immobilize residual contamination in piping prior to transportation and disposition. The adhesion test will assess if any potential incidental impact could cause the FoamBag™ foam to delaminate from Hastelloy C-22 piping, causing the release of contamination. The tensile adhesion, compressive and shear properties of the foam itself have been baselined by FIU and SRNL in accordance with ASTM D1623: *Test method for tensile adhesion properties of rigid cellular plastics*, ASTM D1621: *Standard Test Method for Compressive Properties of Rigid Cellular Plastics*, and ASTM D3574E: *Foam Tension Testing*. Furthermore, FIU and SRNL previously developed a series of testing practices specifically designed to evaluate the foam's ability to perform and function as a permanent plug in a pipe under normal operating conditions and when exposed to a variety of environmental and impact stressors. Using the MTS Criterion series 43 Tensile Tester with compression plates, shown in Figure 17, the amount of force required to push a foam plug out of a 3" D x 14" L pipe segment was determined. This test will be used on foam plugs in Hastelloy C-22 pipes, and the data will be compared with that obtained from the 304-stainless steel pipes to ascertain any differences in adhesion and bonding properties between the two pipe materials.



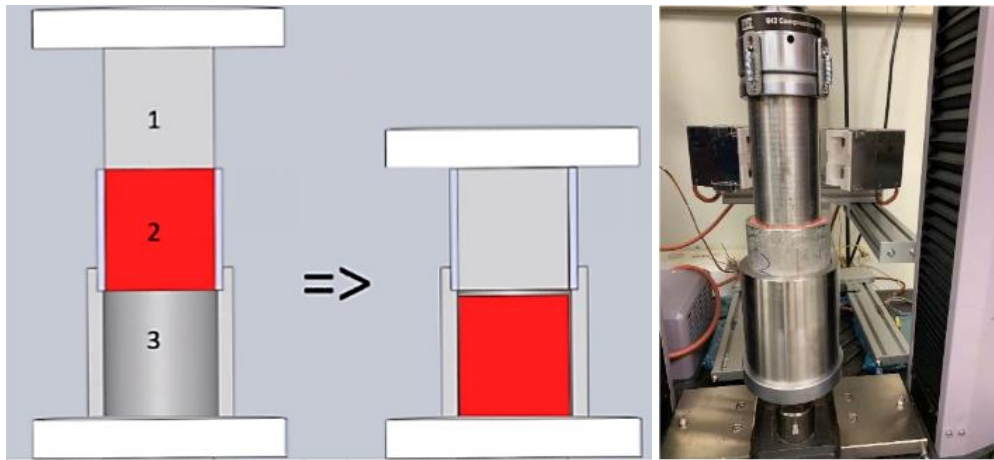


**Figure 17. Plug strength test schematic (left) and plug strength testing for pipe samples using the “plunger – bucket” method on an MTS testing device (right).**

### ***Determination of the heat profile of the foam during curing in Hastelloy C-22 piping***

Section 7.10 of *ASTM E3191-18: Standard specification for permanent foaming fixatives used to mitigate spread of radioactive contamination* states that “the foaming fixative shall not generate heat sufficient to compromise any of the components within the enclosure to which it is applied”. Site personnel also expressed an interest in documenting the external pipe temperature profile during the curing process to further ensure worker safety during handling.

Determining the heat profile inside the pipe during the foam curing process involved inserting four Extech TP870 Type K thermocouples at varying depths into the Hastelloy C-22 pipes (Figure 18) and connecting them to an Extech SDL200 datalogger for 24 hours to determine the internal temperature of the foam while curing (Figure 19). Simultaneously, to measure the external pipe temperatures during the curing process, the FLIR E53 thermal imaging camera was employed to achieve this objective. The FLIR E53 has the capacity to measure object temperatures up to 1200°F, has a thermal sensitivity of < 0.07°F (40 mK), and a measurement accuracy of ± 2%. The supplemental FLIR software provides insight in terms of temperature data analysis. The multi-spectral Dynamic imaging (MSX) mode was used for all image analysis. MSX mode overlays both the thermal and digital images together and provides a more detailed thermal image for the external pipes.



Figure 18. Pipe with thermocouples at varying depths.



Figure 19. Extech equipment and FLIR E53 thermal imaging camera.

***Evaluation of resistance to thermal stressors***

The purpose of this test is to evaluate the resistance of FoamBag™ in sustaining exposure to extreme thermal stressors that may be present during the pipe cutting evolution at F/H Labs, especially if a torch is selected as the preferred method. ***This testing is still ongoing, but some of the initial findings are highlighted below.***

Though not specifically developed to test and evaluate polyurethane foams and their resistance to thermal stressors, the IEC 60695-11-10 Flammability Standard has been identified as a potential “near fit / best fit” standard after extensive discussions between FIU and SRNL researchers. The standard specifies small-scale laboratory test procedures intended to compare the burning behavior of plastics and foams when vertically or horizontally oriented test bar specimens are exposed to a

flame ignition source, displayed in Figure 20 and Figure 21. The objectives of the Phase II thermal stressor test are to conduct a modified version of the IEC 60695-11-10 Flammability Test (both horizontal and vertical methods), a 30-minute direct exposure test of the FoamBag™ to a 2000°F propane flame, and a mass loss test through exposure to incremental temperatures in a muffle furnace.

Two test methods are described. Method A is a horizontal burning test and is intended to determine the linear burning rate of materials under specific test conditions. Method B is a vertical burning test and is intended to determine whether materials self-extinguish under specific test conditions.

#### 1. Method A - Horizontal Test

- **Step 1:** Original length of sample is recorded.
- **Step 2:** The sample is supported in a horizontal position.
- **Step 3:** A flame is applied to the end of the specimen for 30 seconds then removed. Time of flame application will be recorded.
- **Step 4:** Once sample is cooled, new length of sample will be recorded.
- **Step 5:** Repeat this test for all six samples.

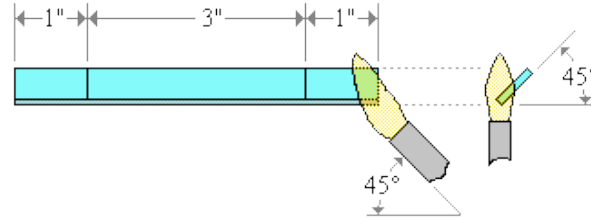


**Figure 20. Horizontal flame test per IEC 60695-11-10.**

#### 2. Method B - Vertical Test

- **Step 1:** Support the sample in a vertical position.
- **Step 2:** Apply the flame to the bottom of the specimen for 10 seconds and then remove it until the flaming stops and record time.
- **Step 3:** Reapply the flame for another ten seconds, remove, and record time until the flame extinguishes.
- **Step 4:** Repeat this test for all six samples.

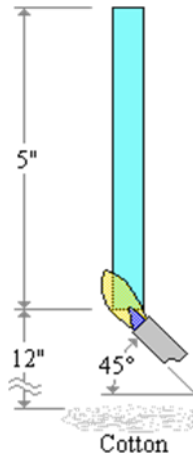


Figure 21. Vertical flame test per IEC 60695-11-10.

### Subtask 2.2: Results and Discussion

Table 1 below provides a summary of the test and evaluation results to date. A detailed analysis of each test objective is provided in subsequent sections. Note that these results are in direct response to the specific testing parameters identified by the site for their pipe decommissioning and removal project. *It is not intended to be viewed as an all-encompassing test and evaluation of the technologies for other potential applications where they may very well be perfectly suited.* A strategic take away throughout this process is that COTS foam technologies are exceptionally versatile and warrant further investigation for their potential applicability to other D&D problem sets.

Table 1. Summary of Results

Foam Technology	Curing Time	Max Curing Temp.	Average Plug Strength	Adhesion to Wetted Surface	Fire Retardant	Environmental Chamber	Headspace	Hot Tap Compatible
Hilti	1-3 mins	276°F	7733 lbf	888 lbf	YES	PASS	PASS	No
FoamBag	15-45 mins	277°F	9684 lbf	4741 lbf	YES* With Exolit AP750 Additive	In progress (SRNL)	In progress (SRNL)	Yes

***Evaluation of the adhesion and bonding properties of the foam plug to Hastelloy C-22 piping***

**Plug Strength Results (Dry Surface Application)**

As highlighted in Table 2 and Table 3 below, both technologies displayed excellent adhesion and bonding characteristics when applied to dry surfaces of both Hastelloy C-22 and 304-stainless steel pipes. Even the results for the sample segments that produced the lowest failure load measurements (i.e., 5431.38 lbf in the case of FoamBag™ sample 3), the plug strength was considered more than adequate. The difference in pipe material seems to have little to no effect on the plug strength of the foam when applied to dry surfaces. This observation remained consistent regardless of the time lapse associated with the testing, as there was no notable difference in plug strength data whether tested 24 hours or 96 hours after curing. For the Hilti CP-620, the average failure load was 7,733 lbf with a standard deviation of ±1,213, and none of the data points were statistical outliers. The results for the 304-stainless steel pipes were similar for the Hilti at 7,447 ± 1,110 lbf. For the FoamBag™, the average failure load was slightly better than Hilti when applied to dry Hastelloy C-22 pipe segments, registering at an average of 9683.61 ± 3104.29 lbf.

**Table 2. Baseline Plug Strength for Hilti under Normal Operating Conditions**

<b>Hilti – Baseline Plug Strength</b>		
<b>Sample</b>	<b>Load (lbf)</b>	<b>Stress (psi)</b>
1	7250.07	54.95
2	6940.50	52.60
3	9983.59	75.66
4	6963.39	52.77
5	6988.26	52.96
6	8273.61	62.70
<b>AVERAGE</b>	<b>7733.24</b>	<b>58.61</b>
Standard Deviation	1213.72	9.20

**Table 3. Baseline Plug Strength for FoamBag™ under Normal Operating Conditions**

<b>FoamBag™ – Baseline Plug Strength</b>		
<b>Sample</b>	<b>Load (lbf)</b>	<b>Stress (psi)</b>
1	12364.49	93.71
2	9072.84	68.76
3	5431.38	41.16
4	10116.45	76.67
5	14163.98	107.34
6	10341.36	78.37

7	6294.74	47.71
<b>AVERAGE</b>	<b>9683.61</b>	<b>73.39</b>
Standard Deviation	3104.29	23.53

Plug Strength Results (Wetted Surface Application)

The piping system within F/H labs was previously used for the transport of radioactive waste-bearing liquids. Residual moisture may be present within the Hastelloy C-22 piping when the FoamBag™ and/or Hilti foam is being injected into the pipes. Based on discussions with site personnel, the requirement to understand the impact that residual moisture will have on the adhesion of the foam technologies to the inner wall of the Hastelloy C-22 pipes was deemed essential. FIU evenly coated 3mL of sprayed water onto the internal pipe surfaces of 14” segments of 3” diameter Hastelloy C-22 pipes. The respective foam technology was injected into the pipe immediately after wetting and allowed to cure over 24-96 hours. The adhesion test was conducted in the same manner as the adhesion testing in Section 4.1 using the MTS Criterion series 43 Tensile Tester with compression plates.

The plug strength results for the Hilti foam technology showed an average failure load of 888 lbf, which is significantly less than the 7,733 lbf average baseline plug strength observed when applied to dry surfaces. These results indicate a severe degradation in the bonding / adhesion characteristics of the Hilti CP-620 when applied to wet surfaces, and it increases the potential for delamination from the pipe during removal and transport. However, the results for the FoamBag™ were more promising. The average failure load was significantly better than Hilti when applied to wet Hastelloy C-22 pipe segments, registering at an average of 4741.61 lbf with a standard deviation of ± 2012.95 lbf. Although this value is lower than when applied to dry surfaces, it is still considered adequate as a temporary engineering control during cutting and removal of the pipes.

***Determination of the heat profile of the foam during curing in Hastelloy C-22 piping***

A comparison of the internal curing temperature profiles indicates little variance between the two technologies. In the case of Hilti, the average maximum internal temperature of the foam during curing was 261.5°F, with a standard deviation of ±1.9°F. It reached its peak temperature within 5 minutes of application and decreased to 70°F within 2.5 hours, shown in Figure 22. The maximum external pipe temperature during that period was approximately 75°F, shown in Figure 23. It is important to note that all testing was conducted on Hastelloy C-22 Schedule 40 pipes. The pipes being decommissioned at the F/H Lab courtyard are expected to be Schedule 80, so barring impacts that may be encountered from degraded pipes, the external temperature could be even lower. Internal curing temperatures for the FoamBag™ were similar, reaching a peak temperature of 276.8°F (136°C). This peak temperature occurred within 12 minutes of application (expected since the foam technology cures slightly slower, thereby increasing working time) and began to steadily decrease 3 minutes after, depicted in Figure 24. The external temperatures were slightly higher, reaching a peak temperature of 108°F in the Schedule 40 pipes, shown in Figure 25, but it dissipated quickly.

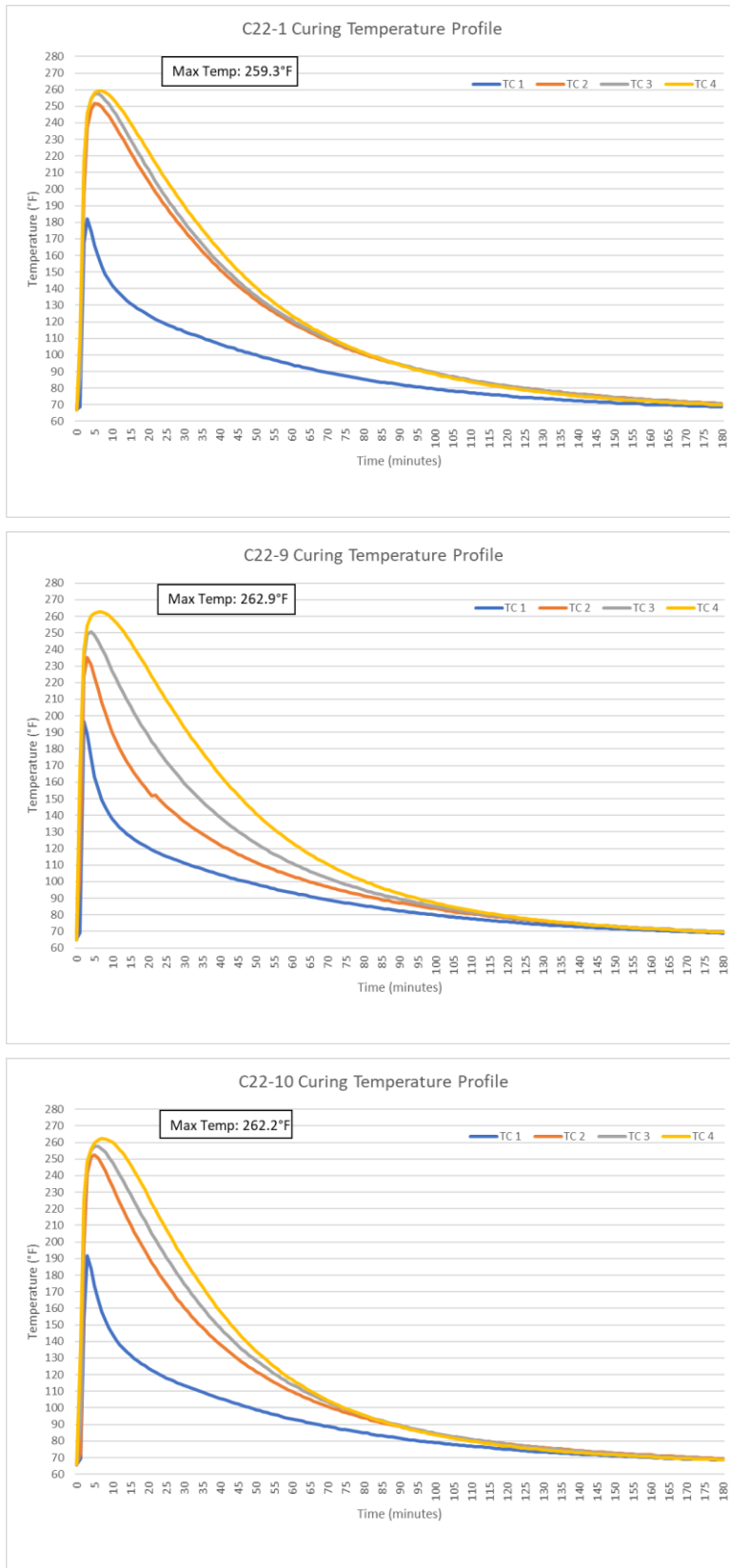


Figure 22. Hilti foam curing temperature profile graphs in Hastelloy C-22 pipes.



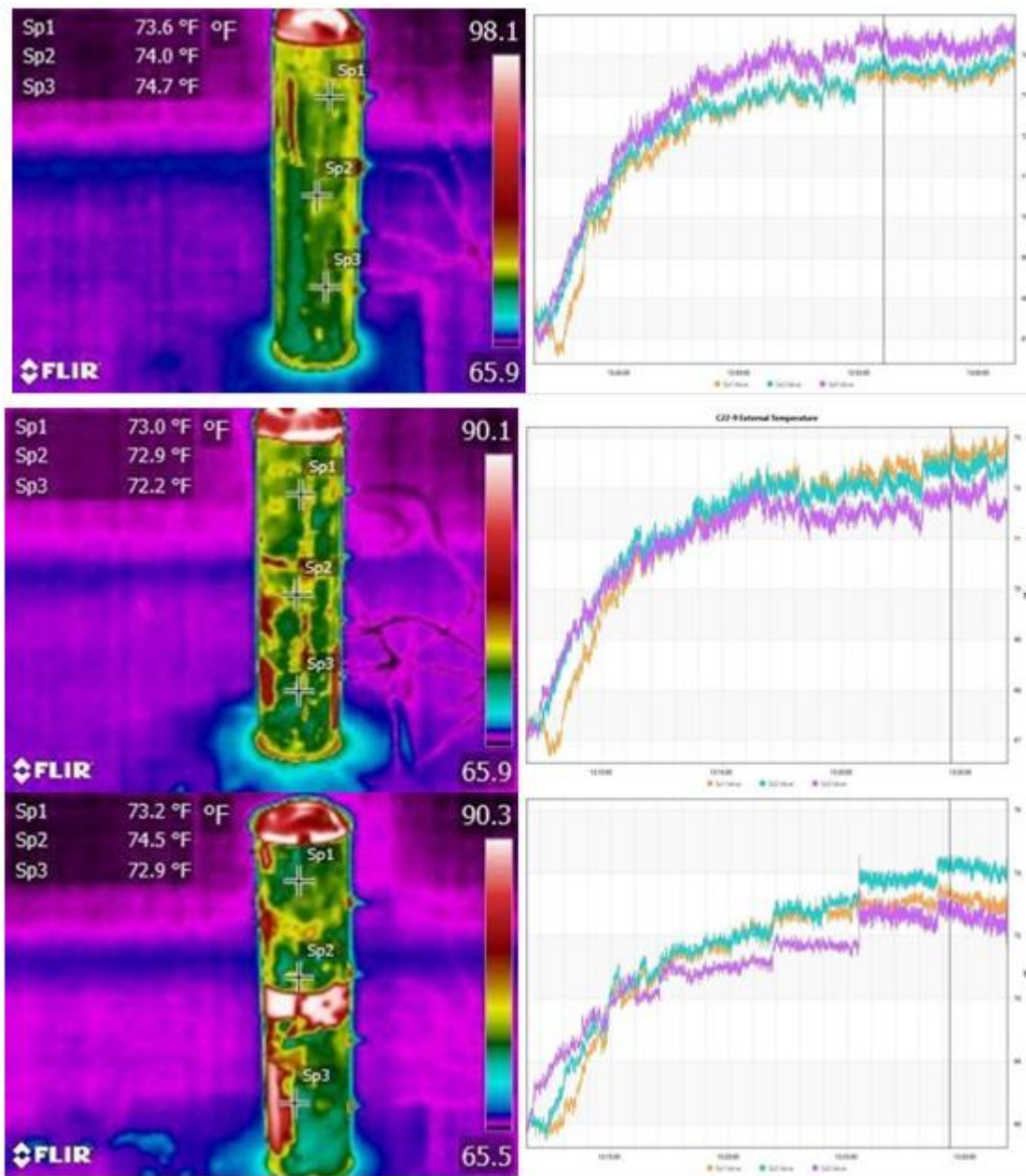


Figure 23. External temperature profiles for C22-1 (top), C22-9 (middle), and C22-10 (bottom) Hilti samples.



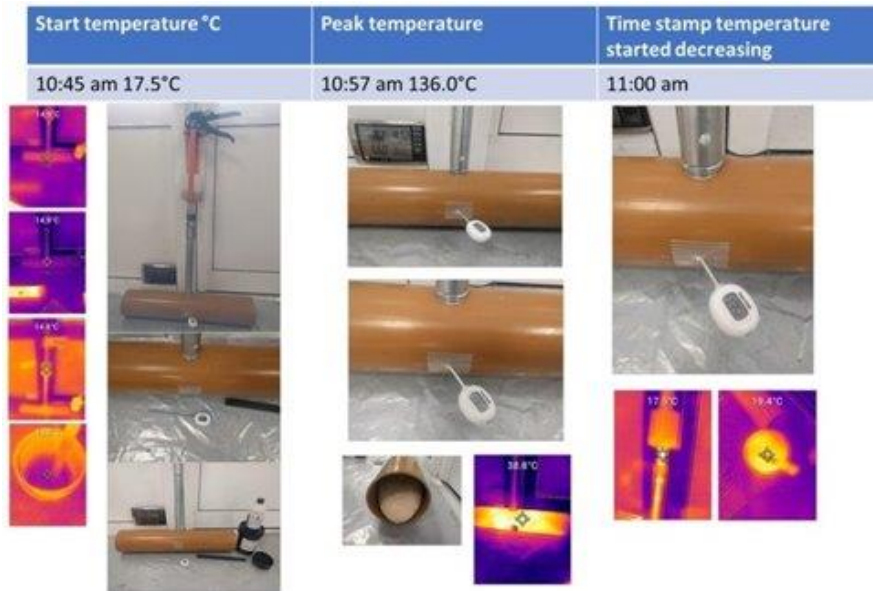


Figure 24. FoamBag™ curing temperature profile.

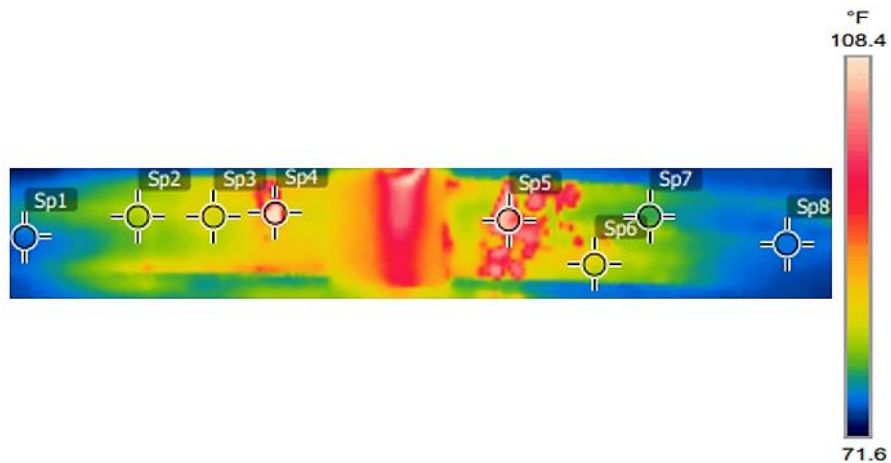
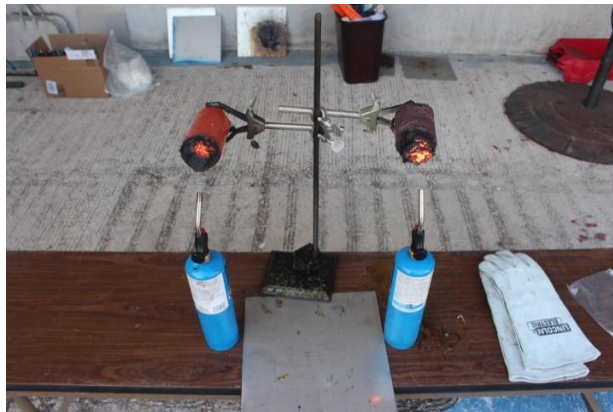


Figure 25. External temperature profile of FoamBag™ in Hastelloy C-22 pipes.

***Evaluation of resistance to thermal stressors***

As expected, being classified as an intumescent technology, the Hilti CP-620 performed exceptionally well when exposed to thermal stressors. An insulating char immediately formed when exposed to a direct flame, resulting in excellent fire-retardant qualities. There was little to no flame and smoke propagation during the conduct of the tests and the foam self-extinguished as soon as the direct flame source was removed. On its own, the FoamBag™ technology failed both test methods under the IEC 60695-11-10 Flammability Standard used by FIU ARC. As seen in Figure 27, FoamBag™ has no inherent fire-retardant capabilities and, as such, is flammable when exposed to certain thermal stressors such as a direct flame. To address this deficiency, ARC researchers identified a COTS fire-retardant additive called Exolit AP-750. Exolit AP-750 is characterized by the vendor as a non-halogenated flame retardant based on ammonium polyphosphate as its main component, which develops its effectiveness through

phosphorus/nitrogen synergism. It differs in its mode of action from non-phosphorus-based flame retardants by achieving its effect through intumescence. Materials containing Exolit AP 750 will intumesce on exposure to flame. The carbon-rich foam layer so formed will protect the polymer and in many cases the substrate through its heat-insulating effect, reducing further oxygen access and preventing dripping in case of a thermoplastic based formulation. Beyond the primary effects on fire behavior such as reduction of flame propagation rate, rate of heat release, dripping behavior, residual lengths of test specimens after flame tests etc., positive secondary fire effects such as low smoke density, no release of corrosive off-gases, lower formation of toxic smoke gases are also present and of great interest. Again, additional testing is required, but initial results support the hypothesis that the fire-retardant capabilities of FoamBag™ can be significantly enhanced with the addition of the Exolit AP-750. When mixed to a 1:1 ratio, FoamBag™ samples performed similarly to the Hilti intumescent foam technology. An insulating char was formed immediately upon exposure to a direct flame and overall flame and smoke propagation were negligible. A focus for the research activity’s future work is to conduct more comprehensive tests of FoamBag™ and Exolit configuration.



**Figure 26. Hilti Foam flammability testing.**



**Figure 27. FoamBag™ flammability comparison with (top sample) and without (bottom sample) the Exolit AP-750 additive.**

## Subtask 2.2: Conclusions

Based on the specific project parameters associated with the F/H Lab Decommissioning efforts of the Hastelloy C-22 pipes in the courtyard, it was decided that future testing will be focused on the FoamBag™ technology only. It has the greatest potential to meet the operational requirements for the F/H Lab Decommissioning Project, and discussions have commenced to set it on a trajectory that results in a hot demo at the SRNL Test Bed in Aiken, S.C. The focus of effort for this research activity over the next two years is outlined below. All stakeholders will continue to collaborate closely, and modifications will be made, as required, depending on additional requirements and/or the results of testing.

1. Conduct containment and leak testing of the FoamBag™ on intact and fire-stressed plugs in Hastelloy C-22 piping using hydrostatic and pneumatic pressure testing protocols (2024). As highlighted in the figures below, the initial results have been generally positive.
2. Determine the optimal ratio of Exolit AP-750 fire retardant additive to FoamBag™ that balances resistance to thermal stressors with adhesion and bonding properties of the foam plugs to Hastelloy C-22 piping under dry and wet surface conditions (2024).
3. Confirm application procedures for installation of foam plugs are hot tap compatible under operating conditions expected during dismantling (2024).
4. Identify potential cutting technologies for the Hastelloy C-22 Schedule 80 pipes and conduct cold demo at FIU ARC under operating conditions (2025).
5. Conduct hot demo onsite at SRNL Test Bed, to include planning, coordination, safety approval, work plan development and execution (2024-2025).

## Subtask 2.2: References

- A. Materials, "C1892: Nominal Joint Strength of End-Plug Joints in Advanced Ceramic Tubes at Ambient and Elevated Temperatures".
- ASTM International. (2016). *D1621-16 Standard Test Method for Compressive Properties of Rigid Cellular Plastics*. Retrieved from <https://doi.org/10.1520/D1621-16>
- ASTM International. (2017). *D1623-17 Standard Test Method for Tensile and Tensile Adhesion Properties of Rigid Cellular Plastics*. Retrieved from <https://doi.org/10.1520/D1623-17>
- ASTM International. (2018). *E3191-18 Standard Specification for Permanent Foaming Fixatives Used to Mitigate Spread of Radioactive Contamination*. Retrieved from <https://doi.org/10.1520/E3191-18>
- Extech Instruments. (2016). *Product Datasheet SDL200*. Retrieved from Extech: [http://www.extech.com/resources/SDL200\\_DS-en.pdf](http://www.extech.com/resources/SDL200_DS-en.pdf)
- Fabricatore, E.D., Moore, P.M., Sinicrope, J., McDonald, F.S., Walker, R., Wohlwend, J.L. Permanent Foam Fixatives for Radioactive Contamination Control: Environmental Chamber Testing (SRNL-STI-2022-00004), February 2022. <https://doi.org/10.2172/1846768>.
- FLIR. (2019). *Electrical/Mechanical Applications FLIR EXX-Series*. Retrieved from [https://www.flir.com/globalassets/imported-assets/document/17-3307-ins-e53-\\_-exx-series-datasheet-mfg-web.pdf](https://www.flir.com/globalassets/imported-assets/document/17-3307-ins-e53-_-exx-series-datasheet-mfg-web.pdf)
- Hilti. (2015). *Hilti CP 620 Instruction for use*. Retrieved from Hilti: [https://www.hilti.com/medias/sys\\_master/documents/h4a/9158089048094/Instruction-for-use-INT-CP-620-Instruction-for-use-PUB-5188045-000.pdf](https://www.hilti.com/medias/sys_master/documents/h4a/9158089048094/Instruction-for-use-INT-CP-620-Instruction-for-use-PUB-5188045-000.pdf)

- Hilti. (2016). *Hilti Firestop Foam solid CFS-F SOL; CP 620 Safety information for 2-Component-Products*. Retrieved from Hilti: [https://www.hilti.com/medias/sys\\_master/documents/hfc/9178915405854/Documentation-ASSET-DOC-APPROVAL-0564.pdf](https://www.hilti.com/medias/sys_master/documents/hfc/9178915405854/Documentation-ASSET-DOC-APPROVAL-0564.pdf)
- Lagos, L., Sinicrope, J., Shoffner, P., Komninakis, M., Simoes-Ponce, T., Nuñez, J., & Rendon, J. (2019). *Testing and Evaluating Intumescent Foams in Operational Scenarios - Test Plan*. Miami: Applied Research Center - Florida International University.
- Lagos, L., Sinicrope, J., Shoffner, P., Viera, J., Simoes-Ponce, T., & Nuñez, J. (2018). *Testing and Evaluating Radiological Shielding Foams Resistance to Thermal Stressors - Test Plan*. Miami: Applied Research Center - Florida International University.
- Klempner, D., & Sendjarevic, V. "Polymeric foams and foam technology," Hanser, 2004.
- MTS Criterion® Series 40. (2014). Retrieved from Product Information: <https://engineering.jhu.edu/labs/wp-content/uploads/sites/76/2016/04/MTS-Criterion-40-Product-User-Manual.pdf>
- Mahmood, N. "Investigations on the adhesion and interfacial properties of polyurethane foam/thermoplastic materials," 2007. [Online]. Available: [https://www.academia.edu/6047100/Investigations\\_on\\_the\\_adhesion\\_and\\_interfacial\\_properties\\_of\\_polyurethane\\_foam\\_thermoplastic\\_materials](https://www.academia.edu/6047100/Investigations_on_the_adhesion_and_interfacial_properties_of_polyurethane_foam_thermoplastic_materials).
- Marinzuli, G., Surace, R., & Ludovico, A. "A preliminary study on adhesion on steel cylinder filled with aluminum foam," 213.
- Nicholson, D., Peters, B., Washington, D., & Wilson, J. (2016). *Fabrication and Evaluation of Radiation Hardened Polyurethane Foams for D&D Activities (SRNL-L3100-2016-00231)*. Savannah River National Laboratory.

## **Subtask 2.3: Certifying Fixative Technology Performance when Exposed to Impact Stressors as Postulated in Contingency Scenarios Highlighted in Safety Basis Documents**

### **Subtask 2.3: Introduction**

Department of Energy (DOE) facilities undergoing decontamination and decommissioning (D&D) activities struggle with safety concerns of residual radioactive contamination leftover after gross decontamination efforts have concluded. Regulations, such as the DOE-HDBK-3010, "Airborne Release Fractions/Rates and Respirable Fractions for Nonreactor Nuclear Facilities", provide some direction on appropriate factors for dealing with the residual contamination. However, this directive has not been updated since 1994, with much of the data originating from studies performed in the 1970s and does not account for new technological advances. As such, overly conservative or lenient airborne release fractions (ARFs) in the Source Term Formula are applied that either require the implementation of challenging operational restrictions and costly nuclear safety controls or pose serious safety concerns to the public and environment.

The Source Term Formula is a linear equation used to calculate the amount of radioactive material, in grams or curies, that could be released<sup>1</sup>. This equation is mainly used for safety and environmental analyses and considerations. Some of the major challenges include: (1) inaccurate

Source Term calculations; (2) inaccurate safety controls; and (3) failure to provide new data to corroborate results from over 30 years ago. This concern was also identified in recent studies published by Hubbard et. al., where ARFs from nuclear fires were reevaluated for surrogate liquid and solid contaminants.

The handbook provides the postulated ARF coefficients based on the contaminant form and accident scenario. Specifically, the ARF coefficient is defined as an approximation of radioactive material suspended in air that can be transported as a result of physical stresses from an accident. Airborne particles are specified as having an aerodynamic equivalent diameter (AED) greater than 10  $\mu\text{m}$ . Many stressors of interest are outlined in both the DOE-HDBK-3010 and the Basis of Interim Operations (BIO), where impact scenarios are highlighted in many nuclear facilities. Impact accidents can be as minor as an item dropping in a hot cell or as significant as a natural disaster that causes larger falling debris. For instance, in the event of a seismic release, powder contamination may experience a free-fall spill, vibration-shock, air turbulence from impact, and/or resuspension.

Under this subtask, FIU focused on the development of a standardized experimental design for impact stress with modern equipment and the process of reevaluating historical data for powder contamination under this specific stress. Additionally, fixative performance was evaluated when exposed to impact stressors associated with safety basis analysis in response to high priority requirements identified across the DOE complex. This research effort has the added benefit of potentially providing essential data points on the positive effects of fixative technologies on mitigating airborne release fractions, respirable fractions, and resuspension rates used in safety basis calculations and the Source Term Formula outlined in DOE-HDBK-3010.

### **Subtask 2.3: Objectives**

- 1. Develop and validate experimental design for the quantification of contamination release during impact stress.**

This objective focuses on the experimental methodology for impact stress and includes four main aspects: surrogate contaminant, impact test chamber, collection of released particulates, and analysis.

- 2. Reevaluate ARF coefficients for powder contaminants under impact stress.**

This approach will either confirm or dispute the original ARFs for powder contamination as determined in the DOE-HDBK-3010. Since there have been new technological advances in analytical techniques, it is possible that the coefficients in the present version of the handbook are outdated and do not accurately reflect the airborne release.

- 3. Determine ARF coefficients for fixative materials under impact stress.**

This objective focuses on investigating the ARFs for fixatives applied over powder contamination under impact. Initially, two polymer fixatives will be used as a starting point to provide data to substantiate the Fixative State for this stressor. Based on previous research conducted, the use of fixatives will produce much lower ARFs.

### **Subtask 2.3: Methodology**

Throughout numerous DOE nuclear facilities, there are many different types of substrates to which the fixatives may be applied. However, these initial experiments only consider non-porous substrates (stainless steel coupons). All testing is performed on: (1) coupons without a fixative as

a baseline and to confirm the original data for ARFs for powder contaminants under impact, and (2) two fixatives (FD and PBS) as a starting point to provide data to substantiate the fixative/polymer state under impact. There are four main aspects to this experimental methodology: surrogate contaminant, impact test chamber, collection of released particulates, and analysis.

### ***Surrogate Contaminant and Controlled Contamination of Test Coupons***

Cesium chloride (CsCl) is the surrogate contaminant used as it is a non-radioactive soluble powder and contains a unique chemical element that will be detectable in the analysis component. It is essential that the coupons are weighed before and after contaminant application in order to quantify the initial amount of contamination prior to any stressor for proper release measurements. Another main aspect is to be able to uniformly contaminate the test coupons for all experiments. Previous work and existing standards, such as ASTM E3283-21 “*Standard Practice for Preparation of Loose Radiological/Surrogate Contamination on Nonporous Test Coupon Surfaces for Evaluation of Decontamination Techniques*”, are being leveraged for this design.

A small known quantity of CsCl was used to create a solution in deionized (DI) water. The contaminant solution was mixed homogeneously and then applied to 304-stainless steel coupons at different points. 10  $\mu\text{L}$  drops of contaminant solution were stippled in a pattern towards the center of the coupon, per ASTM E3283, which created a uniform distribution and reduced the risk of run-off at the edge of the coupon. The coupons were undisturbed while the solvent was allowed to evaporate, shown in Figure 28. After evaporation, the coupons were weighed to initially quantify the amount of contaminant present. The fixative could then be applied and cured to the manufacturer’s requirements. The coating thickness was confirmed using the Defelsko PosiTector 6000. The Defelsko PosiTector LPD pin-hole detector is used, where appropriate, to confirm that there are no small cracks/holes in the coating application before all testing.

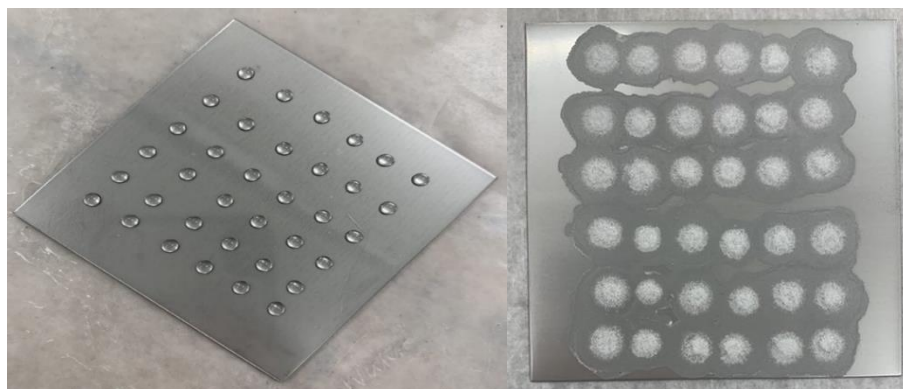


**Figure 28. Stippled contaminant solution on 304-SS coupon (left) and after solvent evaporation (right).**

### ***Impact Stressor***

BYK-Gardner PF-5546 Extra Heavy-Duty Impact Tester, shown in Figure 29, has a maximum force of 320 in-lb and is used to evaluate impact resistance and determine the exact point of failure and/or establish pass/fail specifications. It specifically complies with ASTM D2794, “*Standard Test Method for Resistance of Organic Coatings to the Effects of Impact*”. While this method was not originally designed to test for contamination release, it establishes a standard method to test a coating’s response to rapid deformation. The coupons are required to have the following dimensions: 3.0” length, 3.0” height; and 0.024” width. Additionally, an acrylic housing assembly



was placed around the device which will allow for artificially contaminated coupons to be tested for release fractions.



**Figure 29. BYK-Gardner PF-5546 Extra Heavy-Duty Impact Tester.**

***Contamination Release Collection***

In order to quantify a total release, effective collection methods must be used to ensure accuracy of the data. Collection of released contamination includes airborne and any particulates that may have resettled on the stressor apparatus or test chamber surfaces. Mixed cellulose ester (MCE) filter cassettes and an air-sampling pump were used to collect any suspended airborne particulates. Any contamination that has settled on the walls of the test chamber or stress apparatus can be collected using sampling wipes. Then the filters and wipes are dissolved in an acidic medium for the analysis process. The experimental setup is displayed in Figure 30.

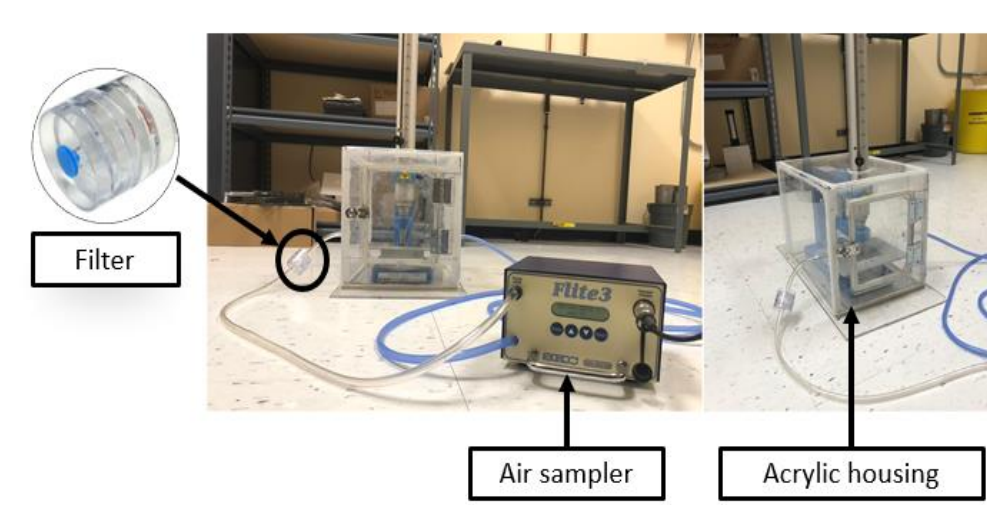


**Figure 30. Impact tester with acrylic impact housing and Flite 3 901-3011 air sampler setup.**

***Analysis***

After collection of the released contaminant, it can be analyzed using mass spectrometry. The surrogate contamination has a unique signature that can be detected using ICP-MS. Mass spectroscopy detects charged particle impacts following a deflection by a magnetic field that separates ions by mass/charge ratios. Carefully tracked dilutions or dissolutions are required to correctly determine the amount of collected contaminant. These analysis methods will detect only

the specified element in the surrogate (Cesium), which is imperative in certifying and quantifying fixative performance.

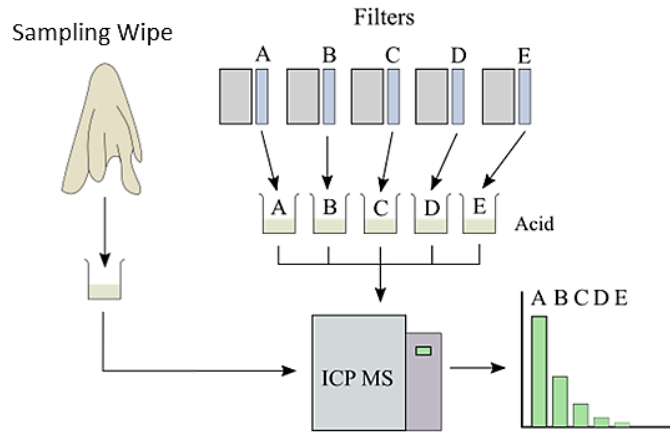


Figure 31. Collection and analysis process.

**Subtask 2.3: Results and Discussion**

A calibration curve of cesium was obtained from the ICP-MS prior to the analysis, shown in Figure 32. This indicated very good accuracy for the subsequent analyses.

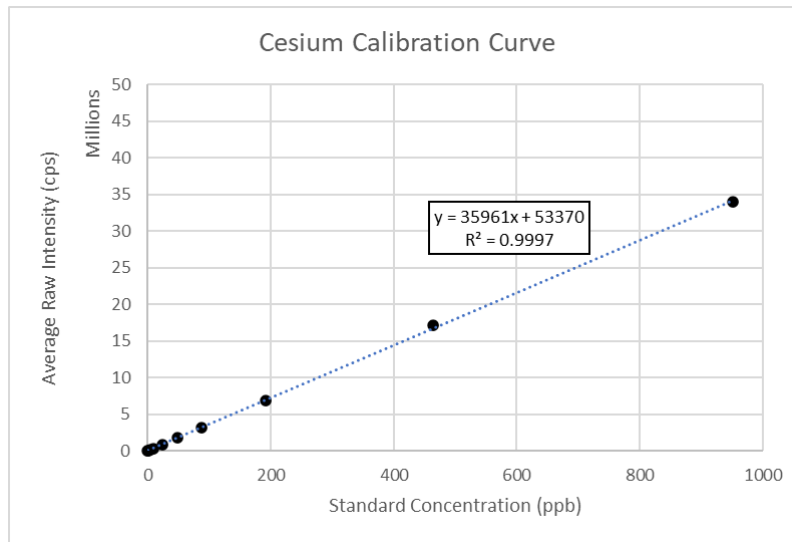


Figure 32. ICP-MS Cesium calibration curve.

Varying force levels were tested with the surrogate powder contamination to encompass a sufficient range. Control samples with the same sample preparation but experienced no impact were included in the analysis. A minimum of six coupon samples were used for each force level to account for any outliers that may arise during testing. The respective averages for each impact force tested up to maximum is shown in Table 4.



**Table 4. ICP-MS Analysis and the Associated Airborne Release Fractions for Baseline Powder Contamination under Impact Stress**

	<b>Impact Force (in-lb) / (kg-cm)</b>	<b>Average Airborne Release Fraction</b>
Powder	320 / 368	2.27E-04
	240 / 276	1.08E-04
	200 / 230	1.05E-05
	160 / 184	6.32E-07
<b>Total Average</b>		<b>3.47E-04</b>

In addition, testing proceeded on contaminated coupons with fixatives to determine its impact on ARFs. The impact forces used are at varying intervals from 160 in-lb to 320 in-lb (maximum). ICP-MS testing was completed on impact samples for FD coating. The results, displayed in Table 5, show a significant reduction in the ARFs for powder contaminants. This data provides evidence that supports that there is a different ARF coefficient that should be implemented for fixatives in the DOE-HDBK-3010.

**Table 5. Average Airborne Release Fractions for FD Coating under Impact Stress**

	<b>Impact Force (in-lb) / (kg-cm)</b>	<b>Average Airborne Release Fraction</b>
FD	320 / 368	5.55E-07
	240 / 276	6.78E-07
	200 / 230	8.34E-07
	160 / 184	3.33E-08
<b>Total Average</b>		<b>5.25E-07</b>

Similarly, FIU performed ICP-MS testing on the additional BPBS-coated samples. The results are shown in Table 6. The average airborne release fraction (ARF) for BBPS was similar to the results from the FD-coated samples, 4.96e-7 and 5.25e-7 respectively. Overall, this lower ARF for fixative coatings further confirms the idea of a “fixative/polymer state”, which should be included in the DOE-HDBK-3010 so that this reduction can be credited in safety basis calculations.

**Table 6. Average Airborne Release Fractions for BPBS Coating under Impact Stress**

	<b>Impact Force (in-lb) / (kg-cm)</b>	<b>Average Airborne Release Fraction</b>
BPBS	320 / 368	5.55E-07
	240 / 276	6.78E-07
	200 / 230	8.34E-07
	160 / 184	3.33E-08
<b>Total Average</b>		<b>5.25E-07</b>

### Subtask 2.3: Conclusions

As the number of nuclear facilities undergoing demolition and D&D activities increases, there is an overwhelming need for additional safety measures. However, the guiding documents for safety basis analyses are outdated and do not accurately reflect advancements in new materials and technologies. The data collected during this performance year regarding the ARFs for surrogate powder contamination under impact were characterized and reevaluated. Most of the work previously performed lacked sufficient detail to completely replicate the experiments and there was a considerable amount of uncertainty in the measurements and the impacts applied may not have been comparable to a real-world scenario. Therefore, to address the need for repeatability, a standardized process for applying impact stress was developed using an ASTM-rated impact tester. MCE filters and an air sampler were utilized to capture any airborne release, with 80 cycles to ensure sufficient collection of particulates. The filters were then leached and/or dissolved in nitric acid and diluted, if necessary, for ICP-MS analysis. Based on the analysis presented, the ARF for powder contamination under impact produced an average ARF of  $3.47 \times 10^{-4}$ , which reconfirmed the validity of the value presented in the DOE-HDBK-3010,  $4 \times 10^{-4}$ . These initial results for fixatives establish an ARF that is less than that of a liquid contaminant, as shown in Figure 33, which supports the idea of a fixative/polymer state.

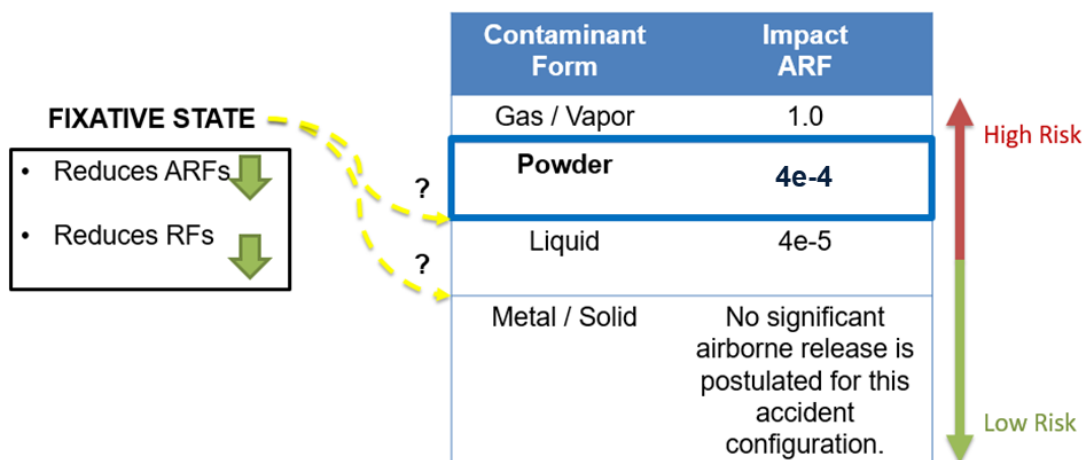


**Figure 33. DOE-HDBK-3010 ARF coefficients for various contaminant forms under impact stress. Initial data indicates a fixative state with an ARF less than a liquid contaminant.**

FIU will continue collaboration with SRNL and other sites to leverage ASTM practices and principles to further define operational parameters. FIU will proceed with any additional testing required to quantify release and the performance of fixative technologies to support and update the DOE-HDBK-3010. Various substrate types and/or thicknesses will be considered for future testing.

### Subtask 2.3: References

U.S. Department of Energy, "Airborne Release Fractions/Rates and Respirable Fractions for Nonreactor Nuclear Facilities (DOE-HDBK-3010-94)," December 1994. [Online]. Available: <https://www.nrc.gov/docs/ML1307/ML13078A031.pdf>.

ASTM International, "E3283-21 Standard Practice for Preparation of Loose Radiological/Surrogate Contamination on Nonporous Test Coupon Surfaces for

- Evaluation of Decontamination Techniques," 2021. Available: <https://doi.org/10.1520/E3283-21>.
- SKC Inc., "Flite 3 High Flow Air Sampler Product Data Sheet," [Online]. Available: <https://www.skcinc.com/catalog/pdf/instructions/1806.pdf>.
- ASTM International, "D522/D522M-17 Standard Test Methods for Mandrel Bend Test of Attached Organic Coatings," 2017. Available: [https://doi.org/10.1520/D0522\\_D0522M-17](https://doi.org/10.1520/D0522_D0522M-17).
- ASTM International, "D2794-93(2019) Standard Test Method for Resistance of Organic Coatings to the Effects of Rapid Deformation (Impact)," 2019. Available: <https://doi.org/10.1520/D2794-93R19>.
- 3M, "3M Fire Protection Products 3M™ FireDam™ Spray 200". Available: <https://multimedia.3m.com/mws/media/373702O/3m-firedam-spray-200-flyer.pdf>.
- 3M, "3M™ FireDam™ Spray 200 Product Data Sheet". Available: <https://multimedia.3m.com/mws/media/373703O/3m-firedam-spray-200-flyer-technical-data-sheet.pdf>.
- BHI Energy, "Specialty Coatings". Available: <https://www.bhienergy.com/services/power-services/technologies/specialty-coatings/>.
- Bartlett Nuclear, Inc. , "Product Data Sheet Polymeric Barrier System (PBS)". Available: <https://www.dndkm.org/DOEKMDocuments/GetMedia/Technology/1620-PBS%20Data%20Sheet.pdf>.
- BHI Energy, "Material Safety Data Sheet Polymeric Barrier System (PBS)". Available: <http://www.bhienergy.com/assets/PBS-MSDS-2015Revised-3-15.pdf>.
- 3M, "Safety Data Sheet 3M FireDam Spray 200 - Red," 13 April 2020. Available: [https://multimedia.3m.com/mws/mediawebserver?mwsId=SSSSSuUn\\_zu8l00xM82vn8tUOv70k17zHvu9lxtD7SSSSSS--](https://multimedia.3m.com/mws/mediawebserver?mwsId=SSSSSuUn_zu8l00xM82vn8tUOv70k17zHvu9lxtD7SSSSSS--).
- R. Demmer, D. Fox, S. Reese, A. Banford and J. Dodds, "Fixatives Used for Decommissioning and Maintenance of Radiological Facilities – 17537," in *Waste Management Symposia*, Phoenix, AZ, 2017.
- J. Hubbard, T. Boyle, E. Zepper, A. Brown and T. Settecerci, "Airborne Release Fractions from Surrogate Nuclear Waste Fires Containing Lanthanide Nitrates and Depleted Uranium Nitrate in 30% Tributyl Phosphate in Kerosene," *Nuclear Technology*, vol. 207, no. 1, pp. 103-118, 2020.
- ASTM International, "D7091-13 Standard Practice for Nondestructive Measurement of Dry Film Thickness of Nonmagnetic Coatings Applied to Ferrous Metals and Nonmagnetic, Nonconductive Coatings Applied to Non-Ferrous Metals," 2013. Available: <https://doi.org/10.1520/D7091-13>.

ASTM International, "E3190-19 Standard Practice for Preparation of Fixed Radiological/Surrogate Contamination on Porous Test Coupon Surfaces for Evaluation of Decontamination Techniques," 2019. Available: <https://doi.org/10.1520/E3190-19>.

Sinicrope, J., Komninakis, M., Gabaldon, D., Moore, P., Lagos, L., Nicholson, J.C., Wohlwend, J.L. Certifying Fixatives - Impact Technical Progress Report (FIU-ARC-2020-800013919-04c-006), September 2021.

## **Subtask 2.4: Multi-functional 3D Polymer Framework for Mercury Abatement**

### **Subtask 2.4: Introduction**

The development of innovative, new generation mercury abatement technologies containing high fixative efficiency, low environmental toxicity, high selectivity, low cost, and high recyclability is of great interest to DOE-EM. During Year 1, FIU investigated the feasibility of using a 3D polymeric filtration/absorption matrix containing self-assembled and functionalized polymer micro-ribbons (MRs) for Hg(II) abatement in aqueous systems. In Year 2, FIU designed, synthesized, and functionalized polydimethylsiloxane micro-ribbons (PDMS-MRs) and tested the mercury removal ability of the functionalized PDMS-MRs under different experimental conditions. During Year 3, FIU focused on PDMS-MRs' optimization to expand its application to different types of mercury contaminant species adsorption, on improving the stability of mPDMS-MRs under different environments and applying mPDMS-MRs in mercury adsorption.

Under this subtask, FIU will explore the feasibility of using a 3D polymeric filtration/absorption matrix containing self-assembled and functionalized polymer MRs for Hg(II) abatement in aqueous systems. The benefits of this strategy include:

- The self-supported 3D polymeric matrix does not require additional supporting foundation during Hg filtration.
- The backbones of the polymer MRs are composed of siloxanes, which are environmentally friendly and non-hazardous to human beings.
- The surfaces of the polymer MRs are rich in silanol groups which enable versatile functionalization at their surfaces for selective heavy metal removal.
- The 3D polymeric matrix forms a self-assembled network which can be easily recycled and regenerated.

### **Subtask 2.4: Objectives**

For FIU Performance Year 3, FIU focused on the following objectives:

- Test the abilities of surface functionalized PDMS-MRs in adsorbing organic mercury (i.e., CH<sub>3</sub>Hg) and natural organic matter-mercury complexes (NOMs-Hg). Specifically, the PDMS-MRs will be tested for cleaning CH<sub>3</sub>Hg and NOMs-Hg solutions with varying concentrations for different cleaning variations. The adsorbing rate, removal efficiency, and adsorbing capacity will be investigated.

- Test the stability of mPDMS-MRs under different conditions (i.e., solvent types). Determine the adsorption power of mPDMS-MRs for inorganic mercury primarily, and then for organic mercury and NOMs-Hg.
- Design and conduct a large-scale demo of using mPDMS-MRs for mercury abatement. After noticing that a sufficient number of mPDMS-MRs will be produced following the current fabrication procedure for the lab, an industrial-scale fabrication method for PDMS-MRs will be continuously explored in the subsequent years.

## Subtask 2.4: Methodology

### *PDMS-MR Fabrication*

In a typical fabrication route, the PDMS-MRs were synthesized by spin-coating a mixture composed of PDMS Part A and B with a ratio of 10:1 on a clean glass slide followed by curing at 100 °C for 15 min. The glass slide with cured PDMS film was heated above 400°C in the furnace for a few minutes followed by natural cooling in the air. The synthesis procedure was varied to find the optimal conditions for PDMS-MR formation.

### *PDMS-MR Surface Functionalization*

The PDMS-MRs were post-heated at 330 °C for ~ 3 h followed by filtration using ethanol through a stainless-steel mesh with 50 µm pores twice. The filtered and cleaned PDMS-MRs were added into 0.05 M MPTMS ethanol solution. For 0.5g PDMS-MRs, about 20 mL solution was needed. The solution containing PDMS-MRs was placed for 30 min on a stirrer. For the 20 mL solution, ~ 1-2 drops of acetic acid was added while stirring. The solution was stirred for another 30 min followed by rinsing of the PDMS-MRs using copious amounts of ethanol to remove the excess MPTMS at the PDMS-MR surfaces. The rinsed PDMS-MRs were placed in a glass container and heated to 80°C to complete the polymerization of MPTMS.

### *Magnetic PDMS-MRs (mPDMS-MRs)*

#### Glue solution preparation

PDMS Parts A and B were mixed in a ratio of 10:1 by weight. The mixture was added into acetone to make the glue solution.

#### Iron oxide micro-particles stability at mPDMS-MRs surfaces

The stability of iron oxide micro-particles at mPDMS-MRs surfaces were tested by sonicating the mPDMS-MRs in ethanol for 15 min, followed by determining the particle concentration in the elution.

#### Surface coverage of iron oxide micro-particles

Given the average diameter and density of iron oxide particles being ~5 µm and 5.17g/cm<sup>3</sup>, the surface area and the weight of a typical PDMS-MR are 2.1×10<sup>6</sup> µm<sup>2</sup> and 9.65×10<sup>-6</sup> g, respectively. The coverage of iron oxide micro-particles at mPDMS-MRs surfaces ( $f_c$ ) was estimated using the following equation:

$$f_c = \frac{\left( \frac{m_1 - m_0}{\rho_p V_p} \right)}{\left( \frac{m_0}{\rho_r V_r} \right) S_r}$$

Where  $m_1$  and  $m_0$  are the weight of PDMS-MRs before and after magnetization,  $\rho_p$  and  $I$  represent the densities of iron oxide particles and PDMS-MRs, respectively,  $V_p$  and  $V_r$  are the volume of single iron oxide particles and single PDMS-MR, respectively, and  $S_p$  represents the superficial surface area of a single PDMS-MR.

Responsiveness to an external magnetic field

A neodymium-iron-boron alloy magnet with a dimension of 1” × 1” × 0.5” was used to test the mPDMS-MRs. The magnet was slowly moved towards vials each containing 0.2 g of mPDMS-MRs to determine the maximum distance between the magnet and the vial that allows mPDMS-MRs to respond to the magnetic field.

**Mercury-contaminated Water Sample Preparation**

The inorganic mercury-contaminated water samples were prepared by diluting the original 1,000 ppm to 1 ppm stock solution using distilled water. During the test, 0.5 mL stock solution was added to 9.5 mL distilled water to make a 0.05 ppm Hg<sup>2+</sup> solution.

The organic mercury-contaminated water samples were prepared by diluting the original 1M methylmercury hydroxide solution to 1 ppm stock solution. During the test, 0.5 mL stock solution was added to 9.5 mL distilled water to make a 0.05 ppm Hg<sup>2+</sup> solution.

**Mercury Abatement Test**

For inorganic mercury abatement and organic mercury abatement tests, 10 μm of PDMS-MRs was added to each 10 mL inorganic or organic mercury-contaminated water sample respectively. The mixture was sealed and then shaken on an orbital shaker for different durations. About 1 mL of cleaning solution was transferred to a new vial for further tests from the original mixture using a syringe. Transfer of the PDMS-MRs was carefully avoided.

**Subtask 2.4: Results and Discussion**

**Magnetic PDMS-MRs (mPDMS-MRs)**

Increased  $f_c$  was observed at higher glue concentrations. However, a theoretical single-layer full coverage of iron-oxide micro-particles at PDMS-MRs surfaces is ~ 2,500/mm<sup>2</sup> given an average particle diameter of 5 μm. That suggested a potential stacking of iron oxide microparticles at PDMS-MRs surfaces when the glue concentration was higher than 15%. The stacking of micro-particles at PDMS-MRs surface may disturb the self-entanglement of mPDMS-MRs in water and may affect the interactions between the mPDMS-MRs and consequently the mercury removal efficiency due to the hindrance of the aggregated micro-particle clusters. FIU selected  $C_{glue} = 8\%$  as the optimized glue concentration for all the mPDMS-MRs syntheses.

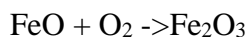
**Table 7. Coverage Density of Iron Oxide Particles at PDMS-MRs Surfaces**

$C_{glue}$ (v/v)	2%	4%	8%	15%
$f_c$ (particle/mm <sup>2</sup> )	103	322	1815	3249

FIU evaluated the effects of the particle-MRs weight ratio on the stability and magnetic responsiveness of the mPDMS-MRs. Methods of activating the surface mPDMS-MRs to enable surface functionalization with MPTMS were investigated. Thermal oxidation of mPDMS-MRs

was employed to partially oxidize their surfaces. The oxidized mPDMS-MRs contain a higher density of hydroxyl groups which may allow surface silanization with MPTMS.

The mPDMS-MRs with a weight ratio (Iron Oxide/PDMS-MRs) of 0.25 was synthesized following the procedure outlined previously. About 0.5g of the synthesized mPDMS-MRs were contained in a glass vial and heated at 320°C for 2 h. The magnetic field responsiveness of the activated mPDMS-MRs was then tested using magnets. The color of thermally oxidized mPDMS-MRs changed from the original black to brown (Figure 34). This is due to the oxidation of Iron Oxide magnetic microparticles. The chemical reaction is:



No significant weight loss or shape change was observed on the heated mPDMS-MRs. This indicates the integrity of PDMS-MRs and the stability of the binding between the PDMS-MRs and the Iron Oxide microparticles on the surface.

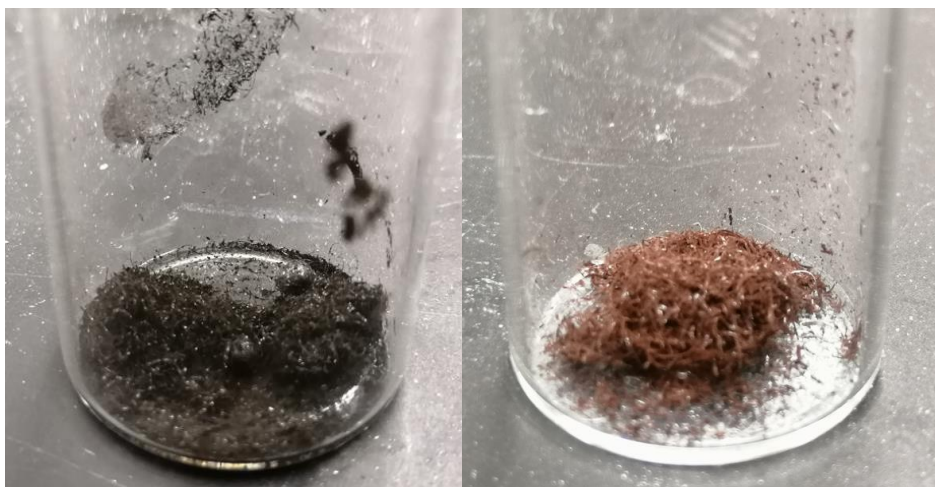


**Figure 34. The mPDMS-MRs before (left) and after (right) thermal oxidation.**

The magnetic responsiveness of the unheated and heated mPDMS-MRs was tested and compared (Figure 35). Both the unheated and heated mPDMS-MRs showed strong responsiveness to an external magnetic field (the magnet). This result suggested that the heated mPDMS-MRs retained the magnetism and can be applied for magnetic field-driven removal.



**Figure 35. The magnetic field responsiveness of unheated mPDMS-MRs (left) and heated mPDMS-MRs (right).**

### *PDMS-MRs Optimization*

FIU explored and optimized the procedure for larger scale production of mPDMS-MRs, described in Table 8.

**Table 8. Methods for mPDMS-MRs Synthesis**

Method	PDMS-MRs	Iron Oxide Powder	PDMS glue	Solvent/Medium
A	0.1 g	0.1 g	0.025 g/mL	Acetone
B	0.1 g	0.1 g	0.025 g/mL	Hexane
C	0.1 g	0.1 g	0.025 g/mL	Hexane + Dry

When increased by a factor of 20 (PDMS-MRs 2g, Iron Oxide Powder 2g), Method A failed by forming large mPDMS-MRs aggregations. The bulk aggregated mPDMS-MRs were not able to become hydrophilic at their surfaces after thermal heating in air at 350°C for 24h. This was attributed to the low solubility of the PDMS glue in acetone, which may cause PDMS emulsions to disperse in acetone. During the mixing step for PDMS-MRs and Iron Oxide powders, those emulsions will glue multiple PDMS-MRs and greater numbers of Iron Oxide powders together and form an aggregated mPDMS-coating at the surfaces of mPDMS-MRs aggregations which may inhibit the thermal oxidation at mPDMS-MRs surfaces.

In Method B, acetone was replaced with hexane in which PDMS is soluble. This solved the aggregation issue seen in Method A. However, the high solubility of PDMS in hexane reduced the amount of glue at PDMS-MRs-Iron Oxide powder interfaces during the rinsing step, after the mixing of PDMS-MRs and Iron Oxide powders. This led to a significantly reduced number of Iron Oxide powders and consequently, a reduced magnetic field responsiveness of mPDMS-MRs.

After consideration of the challenges faced in the previous methods, Method C was produced as a potential solution. The PDMS-MRs were intensively mixed with Iron Oxide powders in the hexane-glue solution. The excess glue solution was removed to leave a moist paste mixture or glue-coated PDMS-MRs and Iron Oxide powders. The mixture was sonicated for 2 minutes to ensure a thorough contact between MRs and powders. The mixture was then heated to 100°C for 15 minutes to polymerize the PDMS glue. After heating, the mixture was rinsed using ethanol three times. The mPDMS-MRs synthesized following Method C also have customizable hydrophobicity at their surfaces. After being heated at 350°C for 24h, the mPDMS-MRs



synthesized following Method C showed good wettability in water and therefore can be used for surface functionalization of MPTMS.

FIU continued to synthesize mPDMS-MRs following the Method C procedures. It was concluded that when the synthesis scale is larger than 0.5 g of PDMS-MRs, the aggregation of PDMS-MRs and Iron Oxide micro-powders became severe due to the increased density of the MRs and micro-powders. This aggregation may result in unequal and inefficient attachment of the micro-powders to PDMS-MRs surfaces. This problem was solved by increasing the volume of the glue solution and introducing mechanical stirring, as shown in Table 9. The synthesized mPDMS-MRs were thermally oxidized at different temperatures to activate their surfaces for silanization. The conditions are shown Table 10.

**Table 9. Results of mPDMS-MRs Synthesis at an Increased Scale under Different Synthesis Conditions**

PDMS-MRs (g)	Glue solution volume (mL)	Mixing method	Aggregation of PDMS-MRs and Iron Oxide powder
0.5	20	sonication	severe aggregation
0.5	50	sonication	severe aggregation
0.5	100	sonication	some aggregation
0.5	100	magnetic stirring	all aggregated to the magnetic stir
0.5	100	mechanical stirring	no significant aggregation

**Table 10. Conditions of mPDMS-MRs Thermal Oxidation**

Trial	Temperature (°C)	Time (h)	mPDMS-MRs surface
1	340	3	hydrophobic
2	350	3	hydrophobic
3	350	24	hydrophobic
4	360	24	partially hydrophilic
5	370	24	partially hydrophilic

Unlike the original PDMS-MRs, which can be temporarily thermally oxidized at 330°C for 3h, the mPDMS-MRs cannot be thoroughly oxidized even after being heated at 370°C for 24h. The reason that mPDMS-MRs exhibit this high resistance to thermal oxidation is still unclear. It is hypothesized that the iron oxide micro-powders densely attach to the PDMS-MRs surface which inhibits the surface oxidation at the mPDMS-MRs surface by reacting to the oxygen in the furnace. This is evident by the color change seen in the iron oxide micro-powders, from black to red after heating, shown in Figure 36. The reaction is as follows:

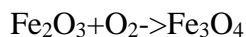




**Figure 36. The mPDMS-MRs that were thermally oxidized at 370°C for 24h.**

Surface oxidation is essential for introducing enough hydroxyl groups at mPDMS-MRs surfaces for silanization. The mPDMS-MRs were heated at 370°C overnight to partially thermally oxidize their surfaces. The oxidized mPDMS-MRs surfaces are activated and ready for MPTMS functionalization. Figure 37A and B show the mPDMS-MRs before and after thermal oxidation respectively. The surface functionalization at mPDMS-MRs surfaces involved 100  $\mu$ L of MPTMS solution added to 10 mL ethanol dropwise while stirring. About 0.2 g of mPDMS-MRs was added into the MPTMS-ethanol solution while stirring. The mixture was stirred for at least 30 min to allow the MPTMS molecules to evenly coat the mPDMS-MRs surfaces. The immersed mPDMS-MRs were transferred to ~10 mL clean ethanol while stirring to remove the excess MPTMS molecules coated at the mPDMS-MRs surfaces. This cleaning process was repeated twice. The MPTMS functionalized mPDMS-MRs are shown in Figure 37C and D.

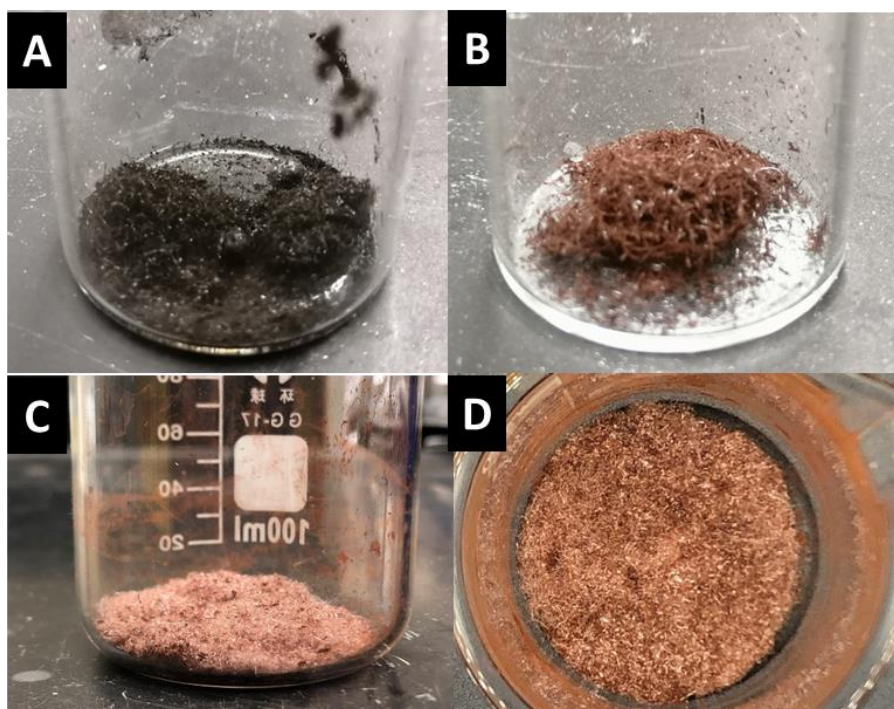


**Figure 37. A) Synthesized mPDMS-MRs. B) Thermally oxidized mPDMS-MRs. C and D) The thermally oxidized mPDMS-MRs with surface functionalized using MPTMS.**

To activate the covalent bonding between the MPTMS and mPDMS-MRs surfaces, acid or base solution needs to be added to the initial solution to accelerate the hydrolysis of the anchor group

of MPTMS in ethanol. Therefore, after cleaning, the mPDMS-MRs were transferred to another 10 mL ethanol. About 150 mL HCl solution was added into the mixture solution while stirring. Stirring continued for another 30 min until the reaction was completed. The mPDMS-MRs were then cleaned twice using ethanol again followed by heating at 100°C for 15 min to polymerize the neighboring MPTMS molecules at mPDMS-MRs surfaces. After that, a pinhole-free monolayer of MPTMS should be synthesized at the mPDMS-MRs surfaces.

A successful SAMs functionalization using MPTMS requires a –OH-rich surface. However, according to the surface wettability test, the mPDMS-MRs surface is hydrophobic which indicates the lack of –OH at its surface. The hydrophobic mPDMS-MRs surface would result in an inefficient surface functionalization using MPTMS. The inefficient functionalization with MPTMS may cause a decreased mercury abatement efficiency.

FIU identified the following as potential solutions to resolve this issue:

1. Reheating the mPDMS-MRs under 380°C for 24h was found to allow sufficient thermal oxidation which resulted in an increased hydrophilicity at the mPDMS-MRs surface. The reheated mPDMS-MRs showed excellent wettability in water. In the future, FIU will functionalize the reheated mPDMS-MRs using MPTMS to ensure successful surface coating.
2. Perform a mercury abatement test for the functionalized mPDMS-MRs and unfunctionalized mPDMS-MRs as a control. FIU plans to do this for two goals: (1) to investigate the mercury-adsorbing ability of clean mPDMS-MRs and; (2) to determine if the surface functionalization at mPDMS-MRs was successful.

Furthermore, FIU tested the mercury-adsorbing ability of mPDMS-MRs with and without surface functionalization to determine if there are any effects from the porous structure of the non-functionalized mPDMS-MRs. The mPDMS-MRs were synthesized using the method discussed in the previous reporting period. 10 mg of mPDMS-MRs were added to glass vials containing 10 mL mercury samples, each containing 0.5 ppm of  $\text{Hg}(\text{NO}_3)_2$ . The mercury samples containing mPDMS-MRs were shaken for different time periods, shown in Table 11, after which they were transferred to new vials using syringes to remove the mPDMS-MRs. The mercury concentrations in the transferred samples were determined using DMA.

**Table 11. Sample Information of Mercury Adsorption Tests using mPDMS-MRs**

Sample name	mPDMS-MRs (mg)	$\text{C}_{\text{Hg}^{2+}}$ (ppm)	Total Volume (mL)	Shaking Time (min)
A	10	0.5	10	5
B	10	0.5	10	15
C	10	0.5	10	30
D	10	0.5	10	60
Control	0	0.5	10	0

The results are shown in Figure 38. The concentration of the mercury species left in the solution decreased to about 78.5% of the original mercury concentration after 5 min of shaking. This value slowly decreased as the shaking time increased to about 75.4% after 60 min of shaking. This result indicates that the mercury adsorption at unfunctionalized mPDMS-MRs surfaces and their inner pores is rapid. Without surface functionalization, the mPDMS-MRs have the ability to remove about 24.5% of the mercury in the solution at maximum.

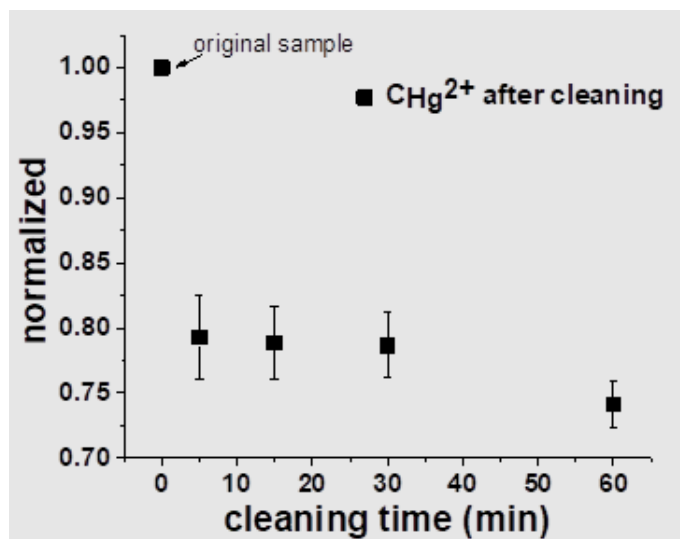


**Figure 38.** The mercury adsorption results using mPDMS-MRs. The concentrations of mercury remaining in the solutions were normalized to the original mercury concentration in the control sample.

According to this preliminary data, the PDMS-MRs (no magnetic particle attached) with surface functionalization using MPTMS can adsorb about 68.5% of the inorganic mercury species after 60 min of shaking. Assuming the iron oxide magnetic microparticles do not significantly affect the mercury-adsorbing ability of PDMS-MRs, it can be concluded that the inner pores of PDMS-MRs contribute about 35-37% of the total mercury removal ability. The mPDMS-MRs used for the mercury adsorbing test were not treated using post-thermal oxidization. The unoxidized mPDMS-MRs were much more hydrophobic than the oxidized ones, which may reduce the contact between the mPDMS-MRs surface and the mercury species in the solution. Further investigation is needed to determine the mercury-adsorbing ability of mPDMS-MRs having surface functionalized using MPTMS in future experiments.

### Subtask 2.4: Conclusions

FIU confirmed that PDMS-MRs are a great candidate for mercury remediation in water due to its unique physical and chemical properties. The superiority of PDMS-MRs in mercury cleaning finds expression in its high adsorbing efficiency, low cost, easy recycling, and environmental friendliness. The PDMS-MR surface can be turned into a silica-like surface via thermal oxidization which embodies enormous potential in different types of contaminant remediation. FIU will continue the investigations into optimizing the PDMS-MRs properties, figuring out the proper working conditions of PDMS-MRs in mercury abatement, improving the performance of PDMS-MRs in mercury remediation, and organizing large-scale tests or on-site demos of mercury remediation using PDMS-MRs to meet the requirements from different stakeholders.

*\*Subtask 2.4 has been discontinued due to personnel departure.*

### Subtask 2.4: References

- Miranda, I. *et al.* Properties and Applications of PDMS for Biomedical Engineering: A Review. *J Funct Biomater* **13**, doi:10.3390/jfb13010002 (2021).
- Yu, J.-G. *et al.* Removal of mercury by adsorption: a review. *Environmental Science and Pollution Research* **23**, 5056-5076, doi:10.1007/s11356-015-5880-x (2016).

- Sams, C. Methylmercury Contamination: Impacts on Aquatic Systems and Terrestrial Species, and Insights for Abatement. (2007).
- Bernhoft, R. A. Mercury Toxicity and Treatment: A Review of the Literature. *Journal of Environmental and Public Health* **2012**, 460508, doi:10.1155/2012/460508 (2012).
- Zhang, D., Yin, Y. & Liu, J. Removal of Hg<sup>2+</sup> and methylmercury in waters by functionalized multi-walled carbon nanotubes: adsorption behavior and the impacts of some environmentally relevant factors. *Chemical Speciation & Bioavailability* **29**, 161-169, doi:10.1080/09542299.2017.1378596 (2017).
- Huang, Y., Gong, Y., Tang, J. & Xia, S. Effective removal of inorganic mercury and methylmercury from aqueous solution using novel thiol-functionalized graphene oxide/Fe-Mn composite. *Journal of Hazardous Materials* **366**, 130-139, doi:<https://doi.org/10.1016/j.jhazmat.2018.11.074> (2019).
- Hua, K. *et al.* Effective Removal of Mercury Ions in Aqueous Solutions: A Review. *Current Nanoscience* **16**, 363-375, doi:<http://dx.doi.org/10.2174/1573413715666190112110659> (2020).
- Liu, Z. *et al.* Mercury Removal Based on Adsorption and Oxidation by Fly Ash: A Review. *Energy & Fuels* **34**, 11840-11866, doi:10.1021/acs.energyfuels.0c02209 (2020).
- Gworek, B., Bemowska-Kalabun, O., Kijeńska, M. & Wrzosek-Jakubowska, J. Mercury in Marine and Oceanic Waters—a Review. *Water, Air, & Soil Pollution* **227**, 371, doi:10.1007/s11270-016-3060-3 (2016).
- Moreau, J. W. *et al.* The Effect of Natural Organic Matter on Mercury Methylation by *Desulfobulbus propionicus* 1pr3. *Frontiers in Microbiology* **6**, doi:10.3389/fmicb.2015.01389 (2015).
- Henneberry, Y. K. *et al.* Removal of inorganic mercury and methylmercury from surface waters following coagulation of dissolved organic matter with metal-based salts. *Sci Total Environ* **409**, 631-637, doi:10.1016/j.scitotenv.2010.10.030 (2011).
- Peterson, M. J. *et al.* Mercury Remediation Technology Development for Lower East Fort Poplar Creek - FY2018 Update. doi:10.2172/1490603 (2018).
- Liu, H. *et al.* A nanozyme-based enhanced system for total removal of organic mercury and SERS sensing. *Journal of Hazardous Materials* **405**, 124642, doi:<https://doi.org/10.1016/j.jhazmat.2020.124642> (2021).
- Dong, W., Liang, L., Brooks, S., Southworth, G. & Gu, B. Roles of dissolved organic matter in the speciation of mercury and methylmercury in a contaminated ecosystem in Oak Ridge, Tennessee. *Environmental Chemistry* **7**, 94-102, doi:<https://doi.org/10.1071/EN09091> (2010).
- Gu, B. *et al.* Mercury reduction and complexation by natural organic matter in anoxic environments. *Proceedings of the National Academy of Sciences* **108**, 1479-1483, doi:10.1073/pnas.1008747108 (2011).
- Pacyna, J. M. *et al.* An Assessment of Costs and Benefits Associated with Mercury Emission Reductions from Major Anthropogenic Sources. *Journal of the Air & Waste Management Association* **60**, 302-315, doi:10.3155/1047-3289.60.3.302 (2010).

- Otto, M. & Bajpai, S. Treatment technologies for mercury in soil, waste, and water. *Remediation Journal* **18**, 21-28, doi:<https://doi.org/10.1002/rem.20150> (2007).
- Gökaltun, A., Kang, Y. B., Yarmush, M. L., Usta, O. B. & Asatekin, A. Simple Surface Modification of Poly(dimethylsiloxane) via Surface Segregating Smart Polymers for Biomicrofluidics. *Scientific Reports* **9**, 7377, doi:10.1038/s41598-019-43625-5 (2019).
- Billinge, S. J. L. *et al.* Mercury Binding Sites in Thiol-Functionalized Mesostructured Silica. *Journal of the American Chemical Society* **127**, 8492-8498, doi:10.1021/ja0506859 (2005).
- Ulman, A. Formation and Structure of Self-Assembled Monolayers. *Chemical Reviews* **96**, 1533-1554, doi:10.1021/cr9502357 (1996).
- Lessel, M. *et al.* Self-assembled silane monolayers: an efficient step-by-step recipe for high-quality, low energy surfaces. *Surface and Interface Analysis* **47**, 557-564, doi:<https://doi.org/10.1002/sia.5729> (2015).

## **TASK 3: KNOWLEDGE MANAGEMENT INFORMATION TOOL (KM-IT) (HQ, SRNL, INL, ANL)**

---

### **Subtask 3.4: Content Management**

#### **Subtask 3.4: Introduction**

Content Management includes publishing D&D technologies and QA/QC of existing content in the system. This is accomplished with the assistance of DOE Fellows who do most of the data mining across the system. Addition of vendors, lessons learned, best practices, D&D news, and conferences are also a part of content management.

#### **Subtask 3.4: Objectives**

The objective of this effort is for FIU to continue to publish additional technologies, vendors, and lessons learned on the KM-IT platform in addition to other relevant resources for the community, such as D&D-related training, conferences, and workshops to maintain fresh and informative content on the website.

#### **Subtask 3.4: Methodology**

FIU used factsheets, conference material (agenda, proceedings, brochures, etc.), vendor website, publications, DOE newsletters, and other sources to continue to publish additional technologies, vendors and lessons learned on the KM-IT platform. In addition, the team used other relevant resources for the community, such as D&D-related training, seminars, and workshops to share information with the D&D community. The team also uses website data analytics on the D&D KM-IT website and looked for anomalies, spikes in traffic, and other information that should be addressed. By using data analytics, the developers and team members can focus on critical issues affecting the website. It can also provide great insight into features that should be enhanced and/or added to the website based on user behavior.

#### **Subtask 3.4: Results and Discussion**

FIU continues to publish additional technologies, vendors, and lessons learned on the KM-IT platform in addition to other relevant resources for the community, such as D&D-related training, conferences, and workshops. There were 11 technologies published on the D&D KM-IT website. Below is the list of technologies published during this period including title, description, and link to technology on the D&D KM-IT website.

1. High Power Diode Pumped Cr:YAG Passively Q-switched Lasers - Tough, reliable laser machining has never been so affordable. These lasers are designed for added-value integration applications within a wide range of applications.  
<https://www.dndkm.org/Technology/TechnologyFactSheet.aspx?TechnologyID=5235>
2. 473nm ASP-SL-Low Noise Blue Laser 1-500mW - All solid state 473nm low noise laser is made of features consisting of ultra-compact, long lifetime and easy operating, which is widely used in fluorescence sensors, Raman spectrum, holography, physics experiment, etc.  
<https://www.dndkm.org/Technology/TechnologyFactSheet.aspx?TechnologyID=5236>

3. 593.5nm ASP-SL- DPSS Green Laser 1-200mW - ASP-SL-DPSS 593nm Yellow Laser. - Power: 1-200mW. - Operating mode: CW. - 1 year Warranty. <https://www.dndkm.org/Technology/TechnologyFactSheet.aspx?TechnologyID=5237>
4. 593.5nm ASP-SL-Lower Noise Green Laser1-100mW - ASP-SL-Lower Noise 593.5nm Laser - Power: 1-100mW - Noise of amplitude (rms)<2% - Operating mode: CW <https://www.dndkm.org/Technology/TechnologyFactSheet.aspx?TechnologyID=5238>
5. QCL Mid-Infrared Spectrometer Compatible with Microscope - LaserScope utilizes a high brightness QCL point source, and the high spectral power density (or high photon flux) results in rapid scanning with good signal to noise ratio (SNR) and high-quality data from miniature samples. The higher SNR results in improved spectral quality at very high spatial resolution. The high spectral power density can make it possible to analyze optically thick, highly diffusive or very small samples. <https://www.dndkm.org/Technology/TechnologyFactSheet.aspx?TechnologyID=5239>
6. QCL, Quantum Cascade Laser - LaserTune is a pulsed mid-infrared (IR), widely tunable laser source based on a next generation Quantum Cascade Laser (QCL). The fully integrated LaserTune system is a single box solution which has the widest tuning range of any mid-IR QCL laser source available. <https://www.dndkm.org/Technology/TechnologyFactSheet.aspx?TechnologyID=5240>
7. SAMpack 120 (RD-120)- Isotope identification backpacks (backpack radiation detectors) for clandestine monitoring of gamma and neutron radiation. Can be customized to specific applications with a variety of detector and networking options. Low power drain allows for many hours of uninterrupted monitoring. Multi-detector algorithms provide directionality to the user, enabling faster localization of nuclear sources. <https://www.dndkm.org/Technology/TechnologyFactSheet.aspx?TechnologyID=5241>
8. 457nm ASP-SL Blue Single Longitudinal Mode Laser - Features of ultra-compact, long lifetime, low cost, and easy operation, which is used in DNA sequencing, flow cytometry, cell sorting, optical instrument, spectrum analysis, interference, measurement, holography, physics experiment, and other field applications. <https://www.dndkm.org/Technology/TechnologyFactSheet.aspx?TechnologyID=5242>
9. 473nm ASP-SL Blue Single Longitude Mode Blue Laser – A solid state single longitudinal mode blue laser at 473nm is made features of ultra-compact, long lifetime, low cost and easy operating, which is used in DNA sequencing, flow cytometry, cell sorting, optical instrument, spectrum analysis, interference, measurement, holography, physics experiment, etc. <https://www.dndkm.org/Technology/TechnologyFactSheet.aspx?TechnologyID=5243>
10. LASER AERO - Offers full control over a wide range of parameters. This system is compact, robust and has a long lifetime with low or no maintenance for years. <https://www.dndkm.org/Technology/TechnologyFactSheet.aspx?TechnologyID=5251>
11. LaserBlast™ Cleaning System 100 Watts - A laser cleaning system. Allows for precise cleaning with the ability to retain patinas. <https://www.dndkm.org/Technology/TechnologyFactSheet.aspx?TechnologyID=5252>



The following image shows the technology LaserBlast™ Cleaning System 100 Watts on the D&D KM-IT website. This technology belongs to the vendor Allied Scientific Pro. When a new technology is added to the KM-IT, a technology page is created to contain the technology description, benefits, comments, and pictures. When the user clicks on the picture, the image of the technology is enlarged as seen in the image below.

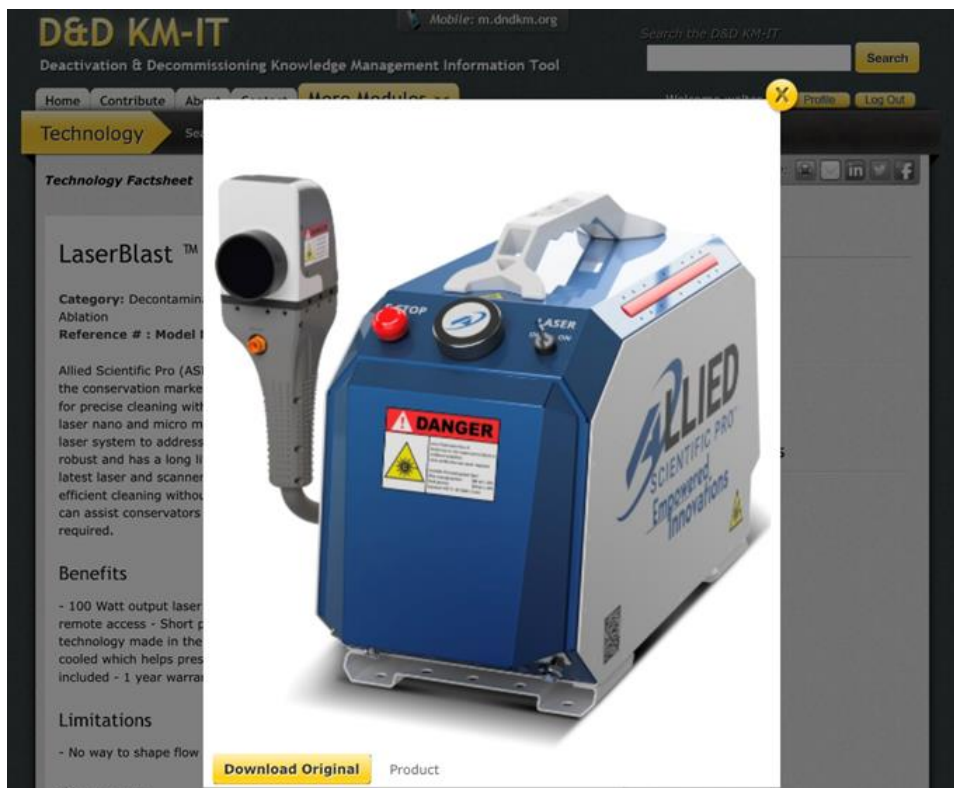


**Figure 39. Technology LaserBlast™ Cleaning System 100 Watts on the D&D KM-IT from vendor Allied Scientific Pro.**

During this period, the team focused on adding news articles and events relevant to the D&D community. The team added 44 articles to the news module of the KM-IT. The source of the articles was mainly from the EM Newsletter. The complete list of news is archived on the KM-IT at the following URL - <https://www.dndkm.org/News/NewsDefault.aspx>. The following articles were added to the website. The link to the article on the D&D KM-IT is also provided.

1. Duo Returns 24 Years Later to Conduct Mapping for EM Nevada Cleanup  
<https://www.dndkm.org/News/NewsDefault.aspx?name=Leak%20in%20Idaho%20Site%20Treatment%20Facility%20Cell%20Results%20in%20Startup%20Delay#Leak+in+Idaho+Site+Treatment+Facility+Cell+Results+in+Startup+Delay>
2. Waste Treatment Plant Prepares to Receive Sodium Hydroxide  
<https://www.dndkm.org/News/NewsItem.aspx?id=373&name=Waste+Treatment+Plant+Prepares+to+Receive+Sodium+Hydroxide>
3. Oak Ridge Prevents Infrastructure Failures Due to Extreme Cold  
<https://www.dndkm.org/News/NewsItem.aspx?id=374&name=Oak+Ridge+Prevents+Infrastructure+Failures+Due+to+Extreme+Cold>

4. Subcontractor Selected to Manage Operations at Key Hanford Site Facilities  
<https://www.dndkm.org/News/NewsItem.aspx?id=375&name=Subcontractor+Selected+to+Manage+Operations+at+Key+Hanford+Site+Facilities>
5. Duo Returns 24 Years Later to Conduct Mapping for EM Nevada Cleanup  
<https://www.dndkm.org/News/NewsItem.aspx?id=376&name=Duo+Returns+24+Years+Later+to+Conduct+Mapping+for+EM+Nevada+Cleanup>
6. First Shipment of Downblended Plutonium for Disposal Departs New SRS Location  
<https://www.dndkm.org/News/NewsItem.aspx?id=377&name=First+Shipment+of+Downblended+Plutonium+for+Disposal+Departs+New+SRS+Location>
7. EM Laboratory Works To Develop Long-Term Groundwater Monitoring  
<https://www.dndkm.org/News/NewsItem.aspx?id=378&name=EM+Laboratory+Works+To+Develop+Long-Term+Groundwater+Monitoring>
8. Hanford Engineers Spark STEM Interest  
<https://www.dndkm.org/News/NewsItem.aspx?id=379&name=Hanford+Engineers+Spark+STEM+Interest>
9. Oak Ridge Team Makes Headway on Mercury Treatment Facility  
<https://www.dndkm.org/News/NewsItem.aspx?id=388>
10. Savannah River Site Preps to Provide Fuel for Advanced Nuclear Reactors  
<https://www.dndkm.org/News/NewsItem.aspx?id=387>
11. Crunch Time: Demolition Crews Continue to Change Hanford Site Landscape  
<https://www.dndkm.org/News/NewsItem.aspx?id=386>
12. West Valley Workers Safely Remove Chemical Process Cell Shield Windows  
<https://www.dndkm.org/News/NewsItem.aspx?id=385>
13. SRS Completes First Transfer in Accelerated Basin De-inventory Mission  
<https://www.dndkm.org/News/NewsItem.aspx?id=384>
14. EM Nevada Removes Insulation Material from Tanks to Prepare Them for Demolition  
<https://www.dndkm.org/News/NewsItem.aspx?id=383>
15. Big Dig Update: WIPP Team Achieves Halfway Mark for Utility Shaft Sinking  
<https://www.dndkm.org/News/NewsItem.aspx?id=382>
16. Hanford Resumes Tank Waste Processing  
<https://www.dndkm.org/News/NewsItem.aspx?id=381>
17. Surface Barrier Contract Awarded for Hanford Tank Farm  
<https://www.dndkm.org/News/NewsItem.aspx?id=380>
18. Investment in Small Businesses at SRS Builds Jobs Locally and Beyond  
<https://www.dndkm.org/News/NewsItem.aspx?id=389>
19. EM Knockdown: Another Reactor Coming Down at Oak Ridge  
<https://www.dndkm.org/News/NewsItem.aspx?id=390>
20. New Advisory Board Members Get Firsthand Look at Oak Ridge Cleanup  
<https://www.dndkm.org/News/NewsItem.aspx?id=391>
21. Hanford Makes Progress Retrieving Tank Waste, Prepares for Future Transfers  
<https://www.dndkm.org/News/NewsItem.aspx?id=392>

22. WIPP Waste Shipment Drivers Surpass 16 Million Safe Miles  
<https://www.dndkm.org/News/NewsItem.aspx?id=393>
23. New Equipment Sets Stage for Future Deactivation at Paducah Site  
<https://www.dndkm.org/News/NewsItem.aspx?id=394>
24. New Security Facility Arrives for Mission to Remove Plutonium From SRS  
<https://www.dndkm.org/News/NewsItem.aspx?id=395>
25. Oak Ridge Makes Former Reactor Safer as It Awaits Demolition  
<https://www.dndkm.org/News/NewsItem.aspx?id=396>
26. Hanford Uses 3D Scanning to Enhance Worker Safety for Demolitions  
<https://www.dndkm.org/News/NewsItem.aspx?id=397>
27. West Valley Workers Dismantle Former Fuel Reprocessing Cell  
<https://www.dndkm.org/News/NewsItem.aspx?id=398>
28. 2<sup>nd</sup> Annual Cleanup Caucus Event Showcases Technology in Use at EM Sites  
<https://www.dndkm.org/News/NewsItem.aspx?id=399>
29. EM Invests \$30 Million in Hanford Tank Waste Research & Development  
<https://www.dndkm.org/News/NewsItem.aspx?id=401>
30. Standing Tall: Hanford Reactor Cocoon Voted Local Project of the Year  
<https://www.dndkm.org/News/NewsItem.aspx?id=401>
31. Highlights of Environmental Cleanup Over Past Five Years at Los Alamos  
<https://www.dndkm.org/News/NewsItem.aspx?id=402>
32. Hanford Makes Progress Preparing Historic Building for Demolition  
<https://www.dndkm.org/News/NewsItem.aspx?id=403>
33. Testing Underway at Renovated Wastewater Load-in Station at Hanford  
<https://www.dndkm.org/News/NewsItem.aspx?id=404>
34. [Idaho Site's Largest Building Progressing Toward Closure](#)
35. [Oak Ridge Sets Pace of Cleanup Nationwide](#)
36. [National Academies Focus on Hanford Cleanup Approaches by SRNL-led Center](#)
37. [The Manhattan Project: EM's Origin Story](#)
38. [DOE Fellows Help Demonstrate Robotic Monitoring of EM Waste Site](#)
39. [Crews Begin Demolition Near Former Hanford Plutonium Processing Facility](#)
40. [Hanford Demolition Paves Way for Cleanup Progress Near Columbia River](#)
41. [Oak Ridge Demolishes Second Reactor at Lab, Delivering EM Priority](#)
42. [Idaho Site Celebrates 7,000 Shipments To Waste Isolation Pilot Plant](#)
43. [SRS Employees Complete 100th Plutonium Downblending for Fiscal Year 2023](#)
44. [First Uranium-Oxide Shipment from Portsmouth Reaches Disposal Destination](#)

The images below are screenshot samples of the articles recently added to the website. The new module on the D&D KM-IT also has an archive or past articles that can be accessed at the following URL: <https://www.dndkm.org/News/NewsDefault.aspx>.

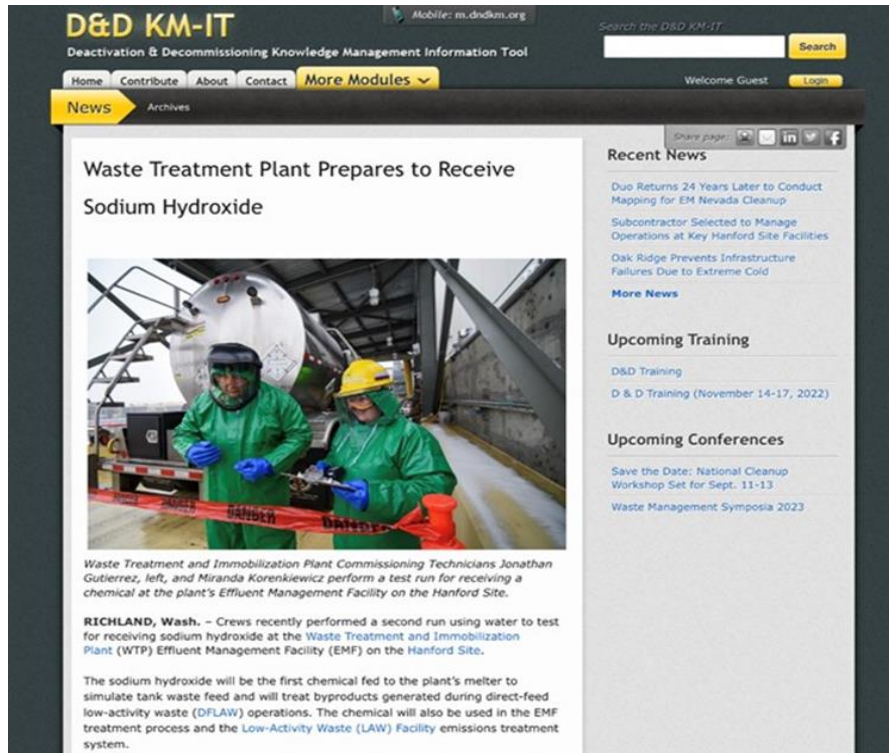


Figure 40. News article on the D&D KM-IT title “Waste Treatment Plant Prepares to Receive Sodium Hydroxide”.

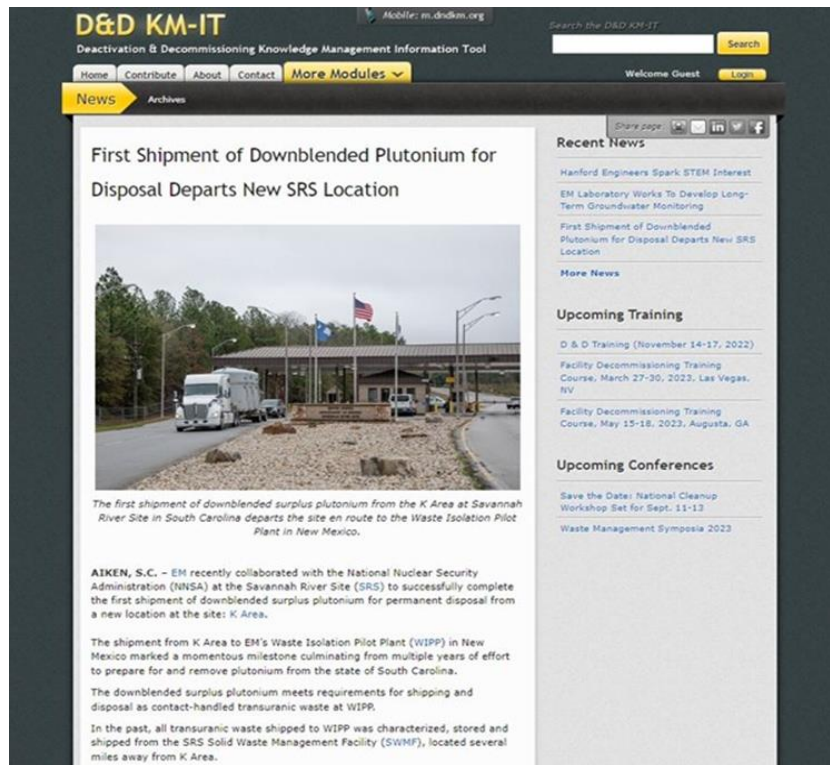


Figure 41. News article on the D&D KM-IT titled “First Shipment of Downblended Plutonium for Disposal Departs New SRS Location”.



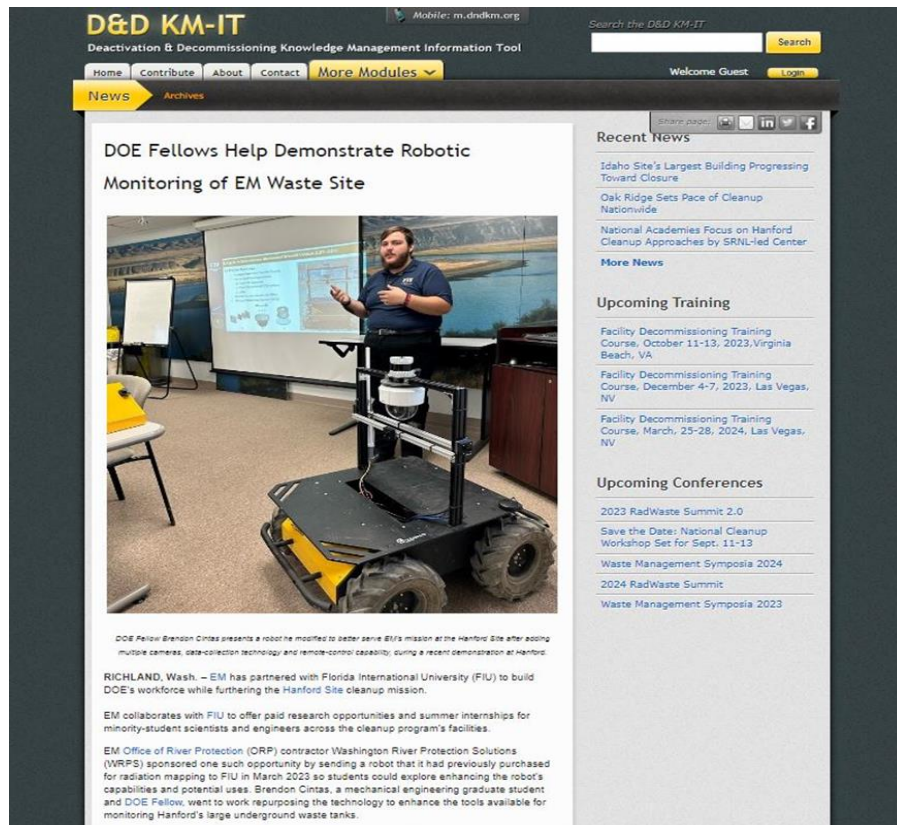


Figure 42. News article posted to D&D KM-IT titled “ DOE Fellows Help Demonstrate Robotic Monitoring of EM Waste Site”.

In addition, the team added events relevant to the community like the Waste Management and D&D facility decommissioning training. All the events added to the KM-IT can be found on the Training module of the website at <https://www.dndkm.org/Training/TrainingDefault.aspx>.

The screenshots below show the sample entries for these events.



Figure 43. Waste Management Symposia 2023 event entry on the D&D KM-IT.

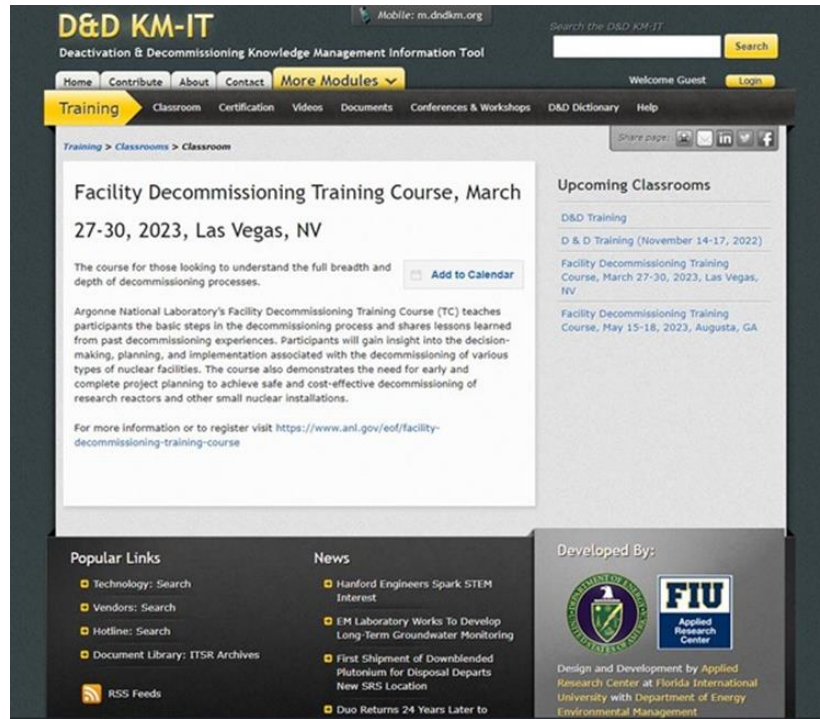


Figure 44. D&D facility training course on the Training module of the D&D KM-IT.

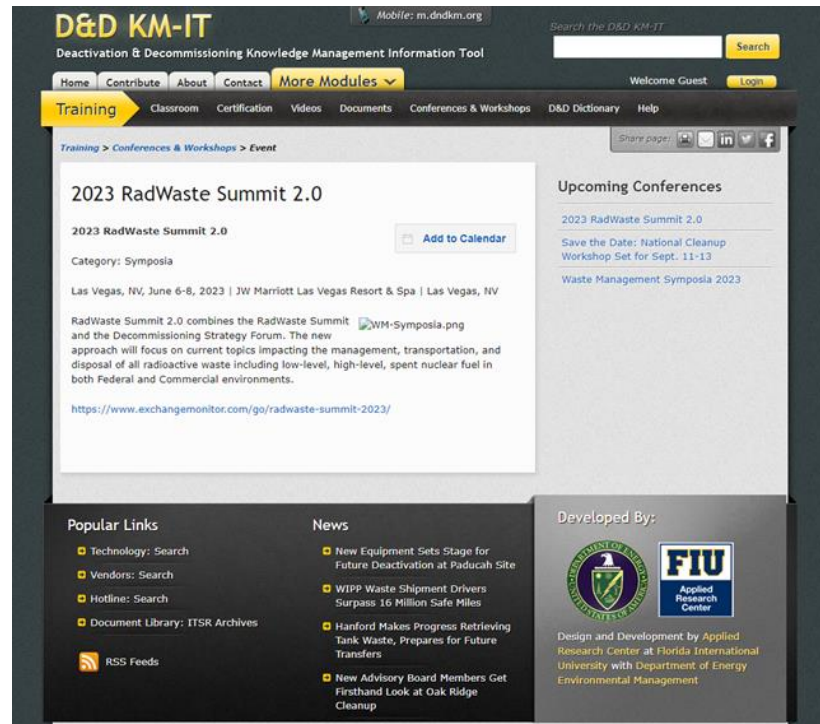


Figure 45. Event added to the D&D KM-IT titled “2023 RadWaste Summit 2.0” to be held in Las Vegas next month.

Finally, the team continued the task of converting legacy videos on the site originally created with Adobe Flash to mp4 so that they can be uploaded to YouTube. Once these videos are uploaded to

YouTube, the video can be easily embedded on the site. Three (3) additional videos (see title and description below) were converted and uploaded to YouTube, after which the KM-IT website was updated so that the new videos could be used. These new videos include:

- *DeWalt Reciprocating Saw - DW309* – The DeWalt reciprocating saw is used for general roughing-in work, nail-embedded wood, and fast cutting of different materials. The video demonstrates the working of the reciprocating saw.
- *E-PERM Electret Ion Chamber* – The E-PERM Alpha Surface Monitor measures alpha surface radiation of radioactive sources as a function of exposure time and alpha contamination levels. The video features the capability and performance of the equipment.
- *FIU-ARC Applied Robotics Technology Development for DOE-EM Facilities and Repositories* – This video features the multiple robotics capabilities at Florida International University's Applied Research Center (FIU-ARC). They include the H-Canyon Repair Wall Crawler, Pipe Crawler equipped with a Lateral Gamma Scanner at Hanford Cold Test Facility Deployment, Miniature Magnetic Rover deployed at the Hanford AP-105 Double Shell Tank, Remote Inspection & Repair Platform, and Nuclear Facilities and Repositories Long-Term Surveillance.

The images below show two of the videos that were completed.

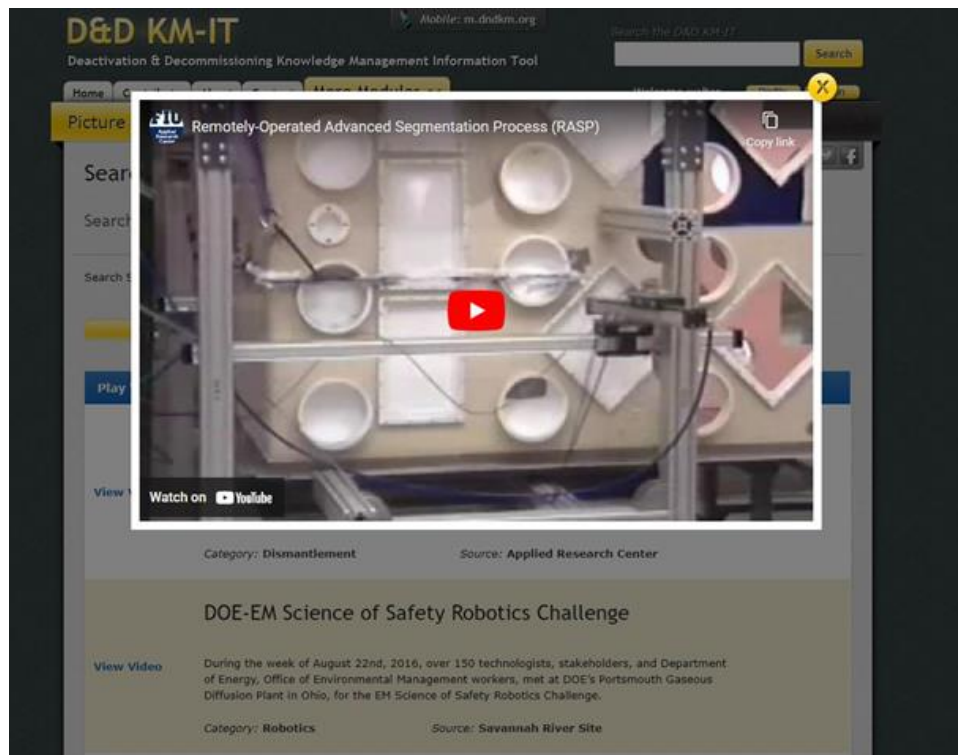


**Figure 46. D&D KM-IT video and picture library showing a legacy video converted to mp4 and uploaded to YouTube.**





**Figure 47. Converted legacy video (DeWalt Reciprocating Saw- DW309) uploaded to YouTube and updated on the D&D KM-IT website.**

Finally, the backend framework that supports the news, events and other modules on the D&D KM-IT runs on the SharePoint Content Management System (CMS). For instance, the news is published by this system to an RSS feed in raw XML format that the KM-IT website consumes and uses to display the news. The team continues to maintain this system as well, and after a recent update, the URL for the RSS feed changed. The team had to update the script that used the URL for the news module on the D&D KM-IT. Below is the updated URL and the screenshot of the raw news being published from the CMS:

[https://collaborationtools.fiu.edu/\\_layouts/listfeed.aspx?List=%7BE189B27C%2DEAA2%2D4C4D%2D81C1%2D6046008D088C%7D&Source=https%3A%2F%2Fcollaborationtools%2Efiu%2Eedu%2FLists%2FDefault%2520News%2FAllItems%2Easpx](https://collaborationtools.fiu.edu/_layouts/listfeed.aspx?List=%7BE189B27C%2DEAA2%2D4C4D%2D81C1%2D6046008D088C%7D&Source=https%3A%2F%2Fcollaborationtools%2Efiu%2Eedu%2FLists%2FDefault%2520News%2FAllItems%2Easpx)

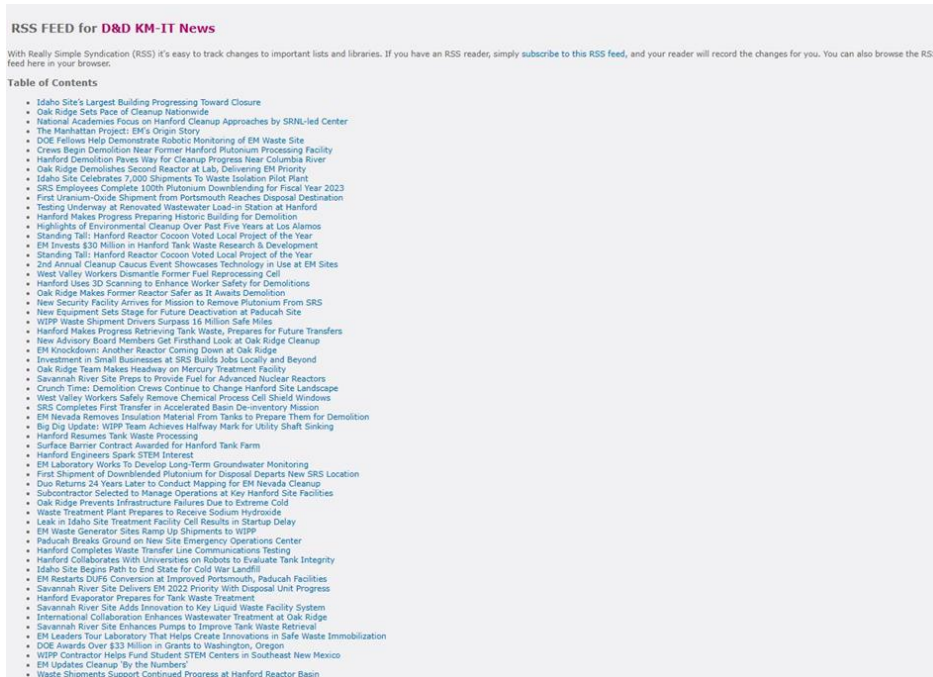


**Figure 48. Raw RSS feed from Content Management System (CMS) that published the D&D KM-IT news.**



The screenshot below shows the multiple RSS feeds available for users to consume.

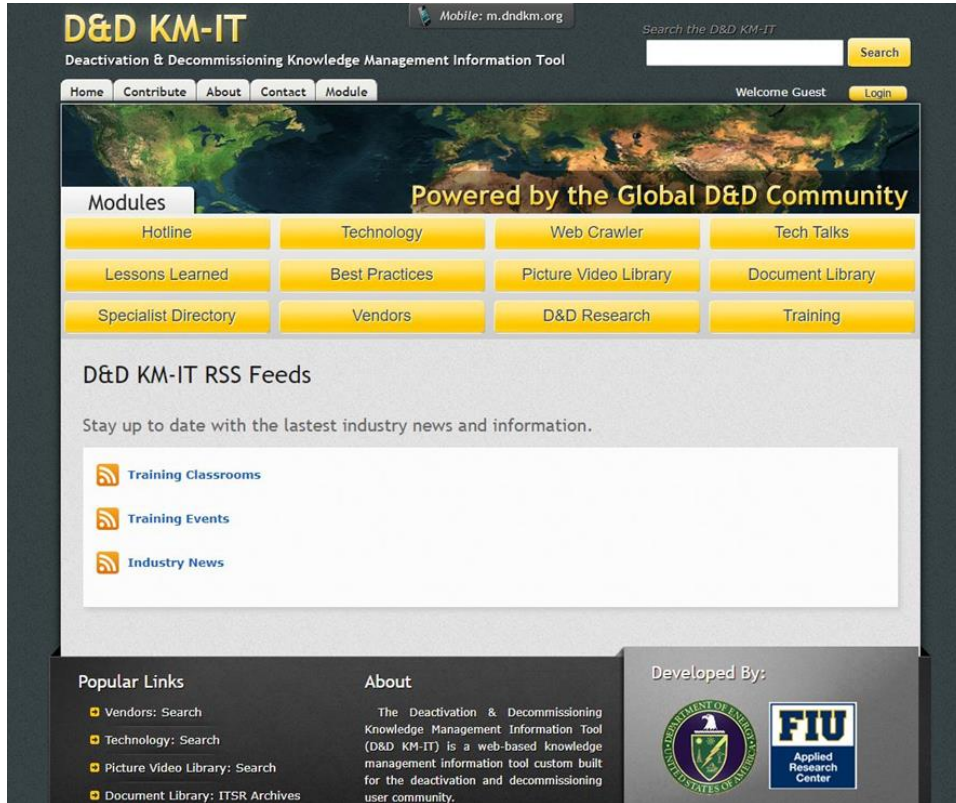


Figure 49. D&D KM-IT RSS Feeds page.

Content management has allowed the D&D KM-IT to increase its content. The graph below (Figure 50) summarizes the growth over the years. As of September 2022, the system had 1,577 D&D technologies, 1,170 registered users, 999 D&D vendors, and 109 subject matter specialists.

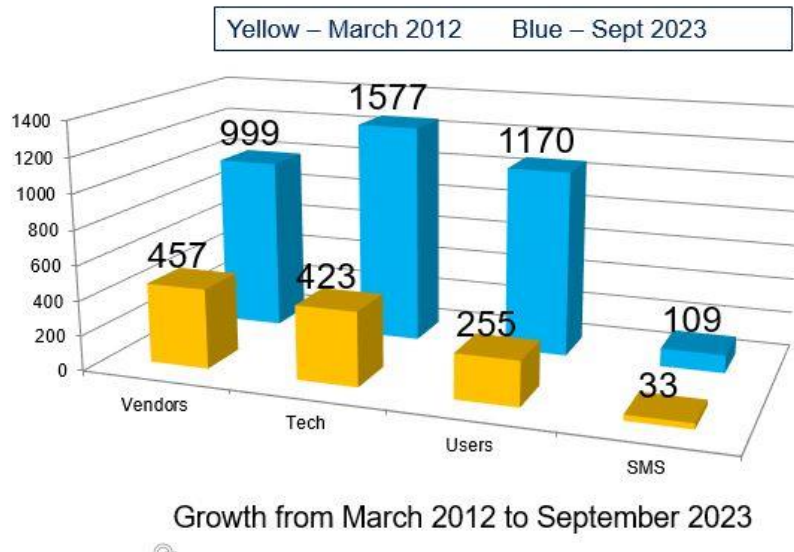
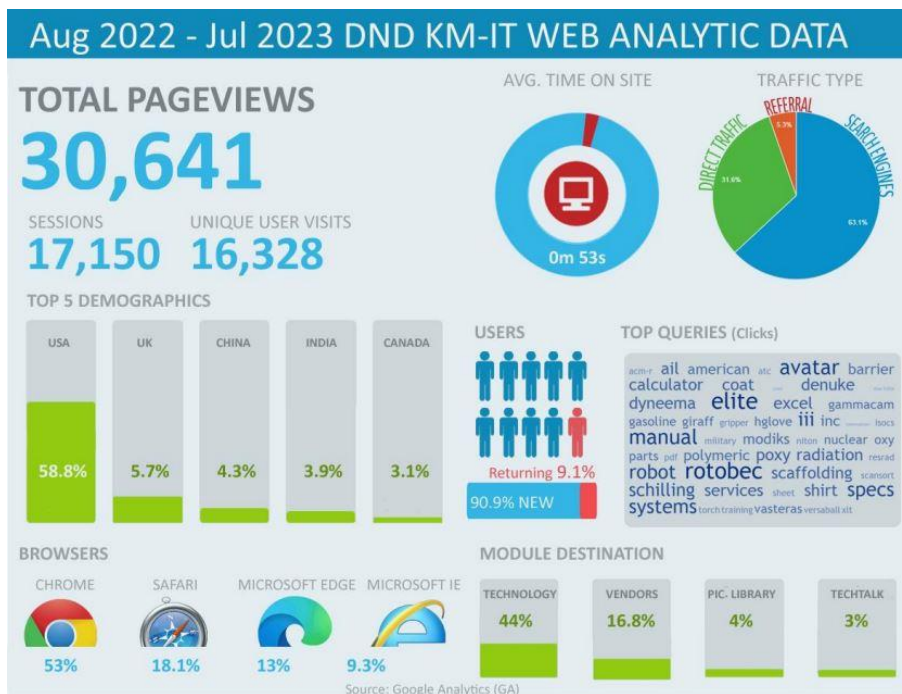


Figure 50. Number of vendors, technologies, users, and SMS as of September 2023.

As part of this task, the team also tracks web activity on the D&D KM-IT website. The following figure (Figure 51) shows an infographic prepared for the Year-End Review presentation for DOE HQ derived from key metrics using Google Analytics (GA). The infographic captures the main information such as pageview, top countries visiting the site, traffic type, browsers used, top queries and popular module destinations.



**Figure 51. KM-IT web analytics infographic presented during the Year End review with DOE HQ**

FIU achieved the abovementioned objectives by publishing 11 technologies, 44 news items and 8 events on the D&D KM-IT website over the past year. In addition, website data analytics captured key metrics that helped the FIU developer focus on specific issues on the website. The legacy videos started to get converted to be compliant with modern browsers. The content management efforts continue to keep the website current and informative for the D&D community.

**Subtask 3.4: References**

*Deactivation & Decommissioning Knowledge Management Information Tool (D&D KM-IT)*, <https://dndkm.org/>, Applied Research Center, Florida International University.

*Google Analytics*, <https://analytics.google.com>, Google Analytics, Google Inc.

*Google Search Console*, <https://search.google.com/search-console/>, Google Search Console, Google Inc.

**Subtask 3.5: Marketing and Outreach**

**Subtask 3.5: Introduction**

This task involves reaching out to sites/national labs to increase KM-IT user involvement as well as presentations at conferences and collaboration with other organization involved in D&D. In addition, the team focused on increasing engagement from DOE sites and national labs on D&D KM-IT by a series of methods such as Tech Talks, public and internal newsletters.

Some specific activities for outreach and marketing of KM-IT included the following:

Newsletters and Mass Communications: Newsletters and online promotions are a great way to bring waves of traffic to the website. By using the registered users as recipients, users were kept up to date on new features and content on the D&D KM-IT.

Conferences and Workshops: Participation and presentations of KM-IT at industry conferences boosts awareness of the website and its capabilities to the target users. FIU presented KM-IT at conferences, such as the Waste Management Symposia, through a combination of oral and poster presentations as well as individual and small-group demonstrations and workshops hosted in the exhibition hall. At these events, the site features can be explained in detail and participants can share their feedback and ideas.

User Support and Ad Hoc Specialized Reports: This task includes supporting KM-IT users with a help desk role to resolve issues on a day-to-day basis, as well as developing specialized reports using the KM-IT system for unforeseen data requests from DOE or the EM community of practice.

### **Subtask 3.5: Objectives**

The objective of this task is to reach the D&D community and educate them on the features available on the D&D KM-IT system. There are many industry leaders who work at various DOE sites and national labs that can benefit greatly from the capabilities that the system has to offer. In many cases, these individuals are not aware of the system, so by doing outreach and marketing, the system usage can be promoted while helping the D&D community meet their knowledge management needs.

Marketing and outreach are critical for the self-sustainability of the system as it introduces the system to subject matter experts who may not be aware of its features and capabilities. This task increased the footprint of the D&D KM-IT in the community by allowing users to discover the capabilities of the D&D KM-IT.

### **Subtask 3.5: Methodology**

This task is an ongoing process that is executed over the course of the year. When new features or content is added to the system, DOE is notified and others in the industry are reached via email to get feedback and comments. This is done not only to communicate with DOE regarding accomplishments and milestones, but also to involve other leaders in the industry in the process of spreading the word about D&D KM-IT. When sending newsletters, FIU uses the D&D KM-IT as its recipients. Currently, there are 1,166 registered users in the system. FIU has also used the public distribution list provided by the Waste Management Symposia (WMS) to make announcements about the D&D KM-IT training workshop typically held at the FIU booth during WMS.

FIU uses a third-party application/service called Mailchimp to send newsletters to a large distribution list. This service supports email stats like opened emails and read emails, and it also tracks clicks. However, for official announcement of milestones and deliverables, FIU uses a typical email system to notify its stakeholders. During the course of this year, several emails were sent to DOE notifying them about new features, such as the development of a sub-module on the KM-IT platform to highlight current EM research efforts and activities in support of D&D. The team also updates flyers, postcards and factsheets to promote the D&D KM-IT.



Figure 52. Multiple marketing and outreach material used to promote the D&D KM-IT (postcards, flyers, factsheets, and newsletters).

### Subtask 3.5: Results and Discussion

The team created a KM-IT poster that was presented at WM2023 in Phoenix, AZ. The title of the poster was “D&D KM-IT 2023 Updates” and focuses on the recent major updates performed on the KM-IT during 2022. This poster was presented during the professional poster session on Wednesday, March 1, 2023. The image below shows the final poster that was presented at the conference. The image after that shows Dr. Himanshu Upadhyay (FIU), Nancy Bushman (DOE) and Walter Quintero (FIU) in front of the D&D KM-IT poster at WM2023 in Phoenix, AZ.



Figure 53. KM-IT poster presented at WM2023 in Phoenix, AZ on March 1, 2023.





**Figure 54. Dr. Himanshu Upadhyay (FIU), Nancy Bushman (DOE) and Walter Quintero (FIU) in front of the D&D KM-IT poster at WM2023.**

In addition, the team prepared newsletters to be sent to the registered users of the KM-IT to promote the Tech Talks as part of the marketing and outreach efforts. The images below show multiple newsletters sent to remind the community of these events.



**Figure 55. Newsletter sent to registered users of the KM-IT to remind recipients to join the January Tech Talk.**

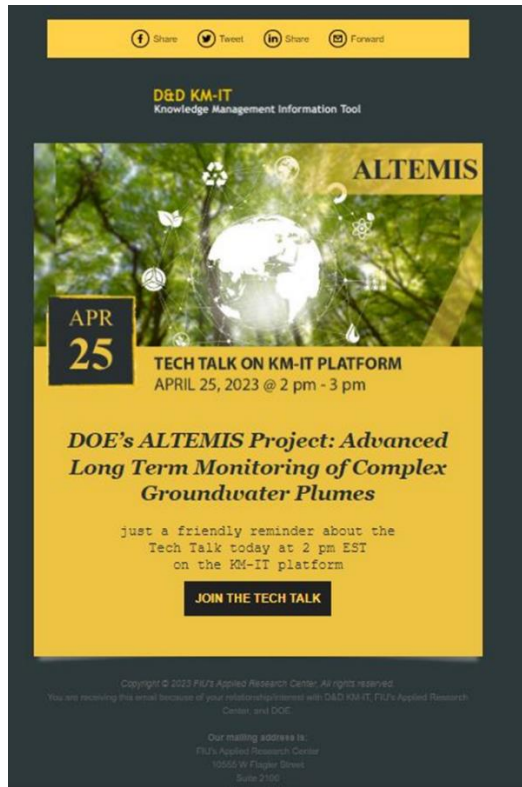


Figure 56. Newsletter prepared to promote the Tech Talk and sent to D&D KM-IT users prior to the event.



Figure 57. Newsletter prepared to promote the July Tech Talk and sent to D&D KM-IT users prior to the event.

During this period, the team sent additional newsletters to keep the community informed about recent news and events. The images below show a screen capture of the newsletter which includes the following topics:

- Virtual D&D Tech Talk on KM-IT Platform - DOE’s ALTEMIS Project: Advanced Long-Term Monitoring of Complex Groundwater Plumes
- FIU-ARC participates at 2<sup>nd</sup> Annual Cleanup Caucus Event Showcasing Technology in Use at EM Sites
- FIU-ARC Lateral Gamma Scanner featured at WRPS FY2022 Accomplishments

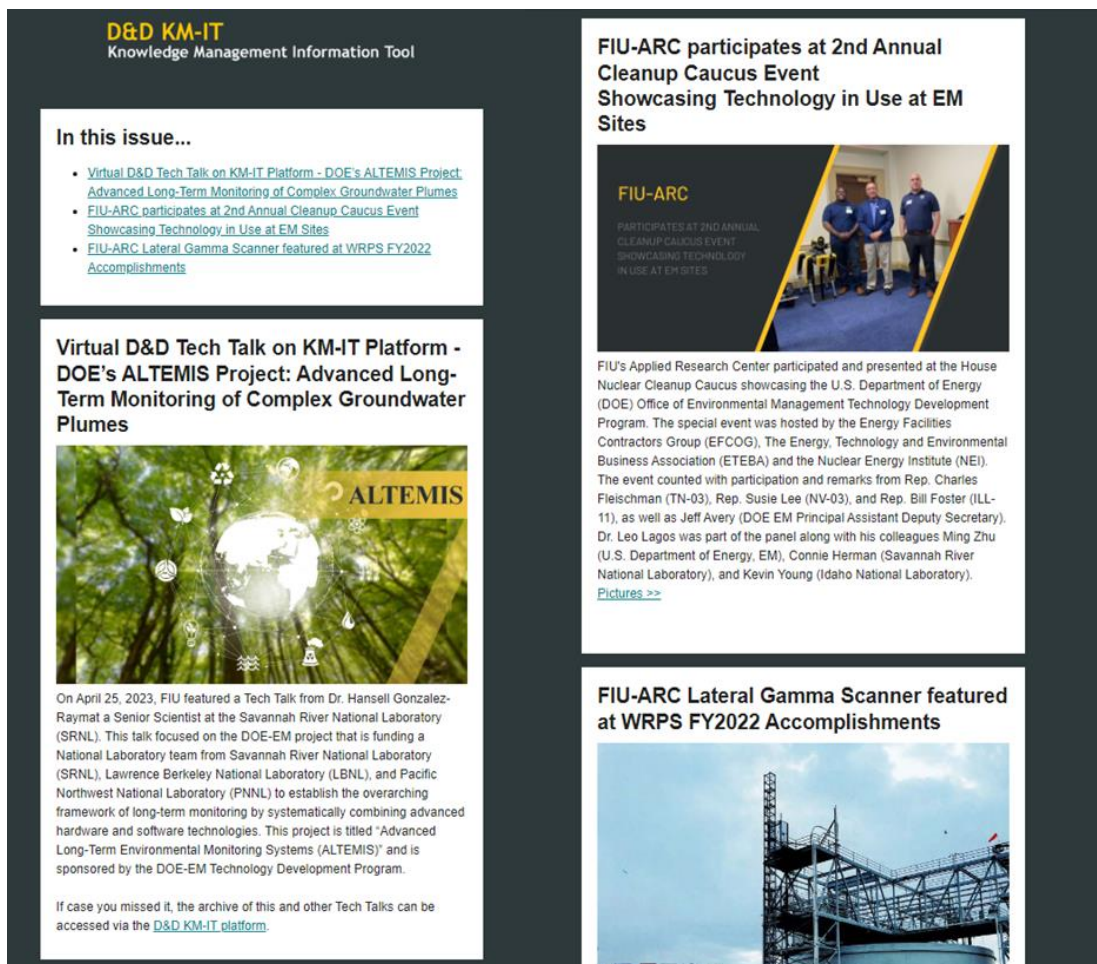


Figure 58. D&D KM-IT Newsletter to be sent in June.

The image below shows a screen capture of another newsletter that was prepared which included the following topics:

- Virtual D&D Tech Talk on KM-IT Platform - AI/ML Research support for Advance Long-Term Environmental Monitoring Systems (ALTEMIS)
- Tech Talks recording available on the D&D KM-IT
- DOE Fellows Help Demonstrate Robotic Monitoring of EM Waste Site



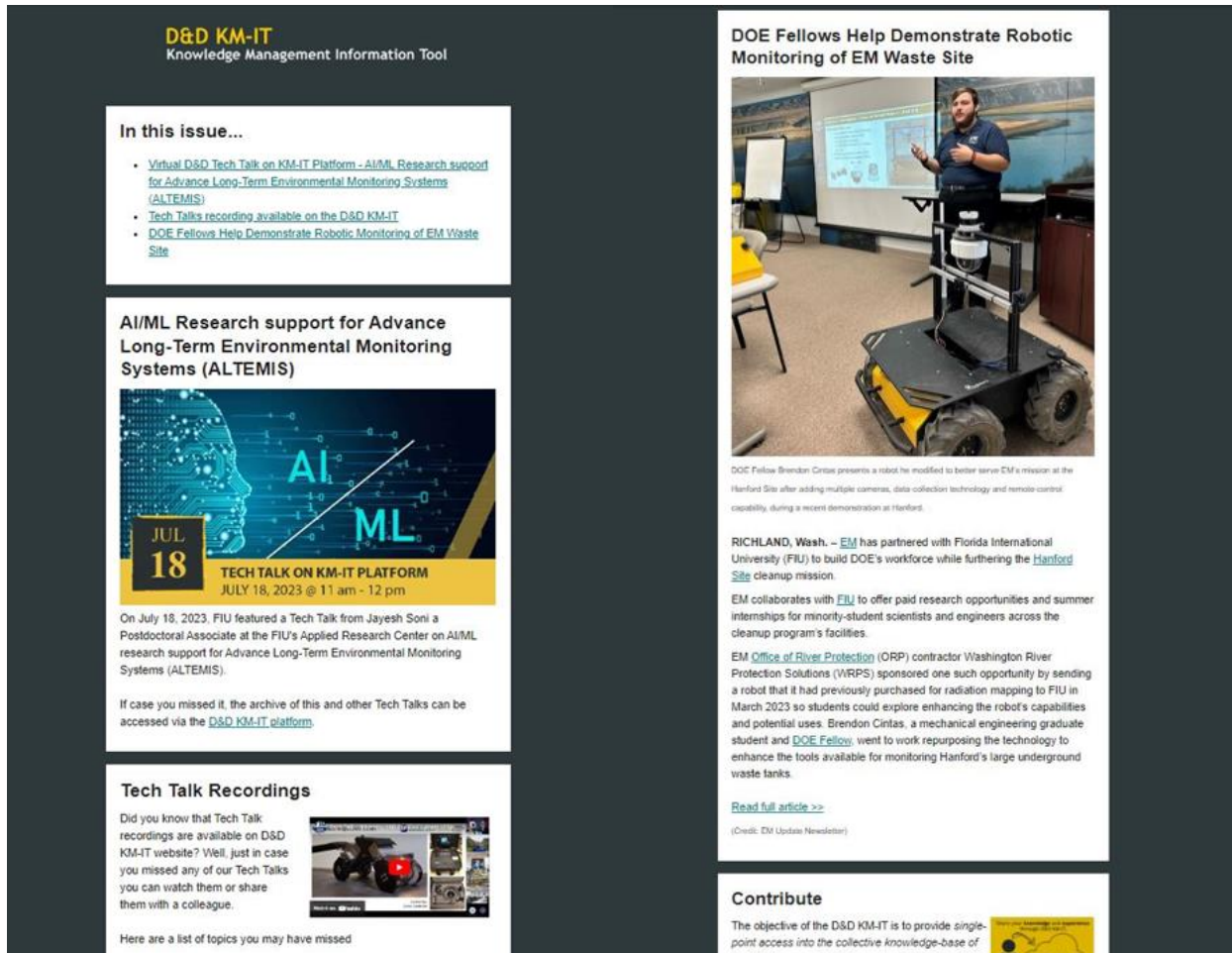


Figure 59. D&D KM-IT Newsletter to be sent in October 2023.

In addition, the team prepared a newsletter and other promotion graphics to announce the FIU presence at Waste Management 2023. The image below shows a sample promotional graphic used on social media to announce the FIU participation at WM2023. This sample post had the booth number and basic information about FIU's participation in the conference. This announcement was posted across FIU's ARC social media outlets (Facebook, LinkedIn and Twitter).





**Figure 60. Promotional graphic for announcing FIU participation at WM2023 on social media.**

In total, the team developed 8 newsletters:

- Four newsletters were targeted to promote Tech Talks.
- Three newsletters were sent to KM-IT users with news articles and events.
- One newsletter was specifically targeted to promote the FIU participation at WM2023.

Finally, the team submitted an abstract to Waste Management 2024 (WM2024) titled “*Artificial Intelligence Based Nuclear Decommissioning Document Summarization*”. WM is held every year in Phoenix, AZ during the month of March. If the abstract is accepted, the team will submit a full paper to be presented. During this conference, the team has the opportunity to demonstrate the capabilities and features of the D&D KM-IT at the FIU booth. This allows the team to get feedback from the D&D community, engage users to register with the system, and become subject matter experts.

### **Subtask 3.5: Conclusions**

Outreach and marketing are critical elements towards the long-term sustainability of this knowledgebase and are essential for the long-term strategic vision of D&D KM-IT. Moving forward, FIU will continue to participate in industry conferences (such as Waste Management Symposia) and other workshops to demonstrate and promote the KM-IT system. This allows for collaboration with other centers, facilities, and DOE sites to increase usage and subject matter specialist participation. In addition, FIU will continue to develop newsletters for mass communication via email to keep users informed of new system features and other related activities.

### **Subtask 3.5: References**

*Deactivation and Decommissioning Knowledge Management Information Tool (D&D KM-IT)*, <https://www.dndkm.org/>, Applied Research Center, Florida International University.

## **Subtask 3.6: D&D KM-IT System Administration**

### **Subtask 3.6: Introduction**

D&D KM-IT system administration is an ongoing task, which involves day-to-day administration of servers that house the KM-IT databases and web applications. This task includes updating patches and OS fixes, updating antivirus engines and definitions, updating drivers and assuring that the network (firewall, routers and switches) is working properly.

### **Subtask 3.6: Objectives**

The KM-IT infrastructure is deployed, secured, and maintained in the FIU facility. The objective of this task is for researchers and DOE Fellows to continue to test, maintain, secure, and administer the KM-IT system to keep it reliable with no down time.

### **Subtask 3.6: Methodology**

The KM-IT system administration encompasses a range of responsibilities focused on maintaining the optimal performance, security, and functionality of the KM-IT. This involves the management of servers, including setup and scaling, overseeing the database with tasks like optimization and backups, monitoring and optimizing performance, implementing robust security measures, managing user access and authentication, creating and executing backup and recovery plans, ensuring timely software updates and patch management, analyzing log files for insights, planning for scalability as the application grows, and addressing compliance with relevant industry regulations. It is an ongoing and multifaceted process that demands a combination of technical expertise and proactive management to sustain the application's reliability and security.

### **Subtask 3.6: Results and Discussion**

During this period, the team performed several tasks. One of them included running a Google PageSpeed Insight report for the D&D KM-IT website shown below (Figure 3-3). This report captured issues that could improve the website's speed, such as eliminating the render-blocking resources by caching or reducing the amount of Cascading Style Sheet (CSS) files or compressing them. Also, the report suggested adding some of these files to cache to speed up performance on the first content paint (this is when the website first loads). After that, the site is cached by the browser and the speed is not an issue.

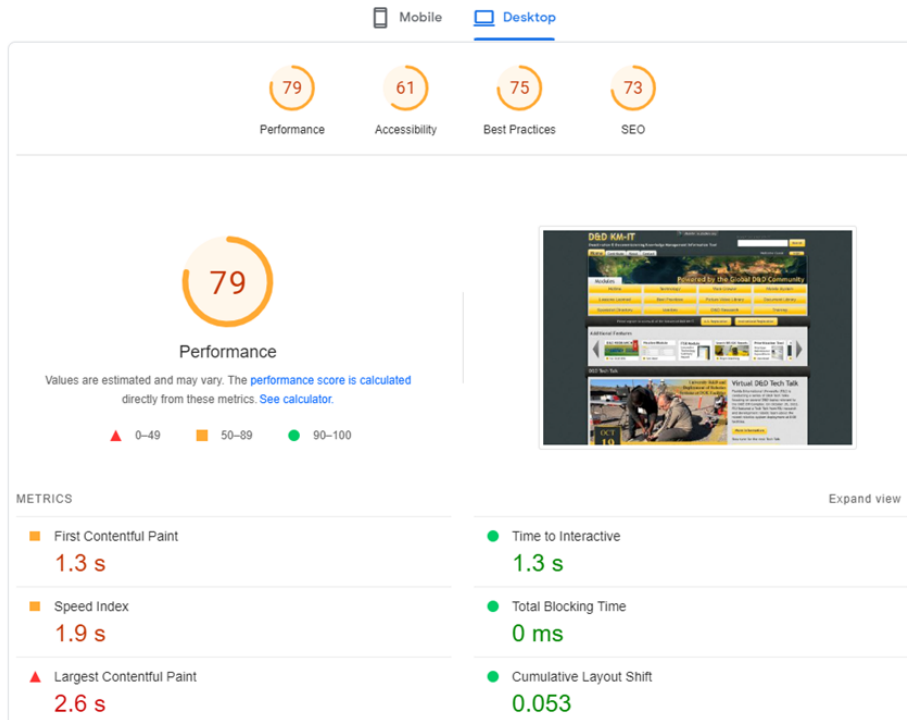


**Figure 61. Snapshot report from Google PageSpeed Insights for dndkm.org.**

The team addressed some recommendations from Google PageSpeed Insight which suggested caching the Cascading Style Sheets (CSS). The KM-IT used multiple CSS files so the team is reviewing them all to see which CSS properties can be merged to reduce the size of the files. The team will then apply a caching functionality to address the recommendation from the report.

Other specific tasks performed during this period included:

- Checking all the DOE server backups – The backups are occasionally checked to make sure they are running properly, that the scripts are completed without errors, that there is space on the backup destination and more. On some occasions, a backup set is restored to verify the backup authenticity.
- Purging of old backup files – the team manually deletes old and outdated files to make room on the backup server for new backups. These old files are typically outdated and occupy valuable storage space and must be purged.
- Updating of backup scripts on the DOE server – The backup scripts have to be updated when there are new directories created/deleted. The scripts must be monitored to make sure they are able to run without issues. If an error occurs, the team addresses the issue by updating the backup scripts.
- Updating of the load balance for better power distribution between servers on the Universal Power Supply (UPS). The team also resolved a power supply issue on the DOE domain controller.
- The team also performed some specific tasks that involved replacing a failing hard drive on the backup server. The KM-IT is backed up on a regular basis (incremental and differential backups).
- Creation of new user accounts for the DOE Fellows on the Linux servers.
- Troubleshooting and resolving of the DOE SQL IP for the DOE Research server.

- DOE Domain Controller – The team troubleshoot and resolved the power supply issue on the DOE Domain Controller. Also, the team installed an array raid controller application to manage the current storage.
- Collaboration Tools updates – The team installed updates on the SQL collaboration tools server. These were operating system updates required to maintain OS performance. The team also installed a new array raid controller application on this server which is running the SharePoint application powering the collaboration tools.
- Hard drive replacement on backup server – The backup server periodically backs up the KM-IT application and database. The team replaced a hard drive that was starting to fail. This server is configured with a RAID controller which allows hard drives to fail without interruption, but the hard drives need to be replaced before the integrity of the system is compromised.
- Created new domain accounts to access critical services running on the domain controller.
- Installed new APC/UPS on the DOE server computer rack.
- Calibrated the other APC/UPS in the DOE Server to balance the load.
- Upgraded the DOE Domain controllers (DNC 1 and DNC 2) to latest software version. Because of this upgrade several configuration settings had to be addressed.

In addition, the team also created a demo script for D&D KM-IT to be used to demo the application. During the process, the team identified some legacy videos that were not working due to the retired Adobe Flash support by modern browsers. So, to keep the application stable, the team started to convert these videos to .mp4 format and upload the videos to YouTube so that they can be embedded back on the website.

The team also updated the index on the DTSearch application. The team updates the index manually to monitor that the index updates successfully. The index is updated regularly to make sure new content added to the site is added to the index. The DTSearch is used on the Global Search module and individual search modules.

During this period, the Google Analytics (GA) tag was updated to the new Google Analytics 4 (GA4) tag. The new tag was implemented on May 16, 2023, and began tracking the website traffic starting on that date. The following image shows the old GA tag activity on the website. Notice that the traffic stops being recorded after May 17, 2023.

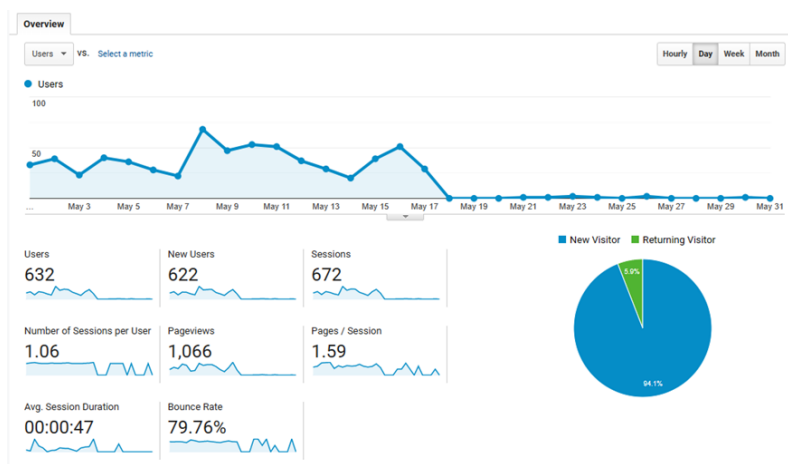
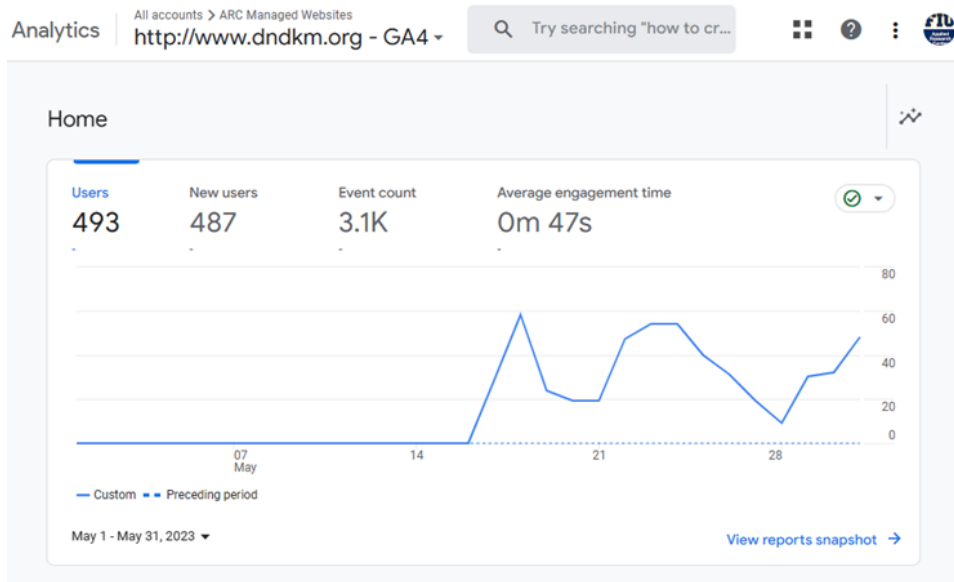


Figure 62. D&D KM-IT Google Analytic (GA) old tracking code activity.

The following image shows the activity on the new Google Analytics 4 (GA4) code on the website. Notice that the activity of this code started on May 16, 2023. The team is learning about the new functionality and features of GA4 and will provide a summary in the next reporting period.



**Figure 63. D&D KM-IT Google Analytic 4 (GA4) new tracking code activity.**

To accomplish this change, the team had to modify the HTML code on the website by replacing the old code with the new code. This required updating the master and master landing templates with the updated script. It also required inspection of the entire site to make sure that the old code was no longer executed to eliminate conflict. The HTML <Head> code on the site’s master page was updated with the new GA4 code. The current code was retired by GA<sub>2</sub>, so the new code has been implemented on the website. GA4 supports new features but there are a lot of configurations that need to take place to properly take advantage of this information. The team is working to understand these new features and is monitoring the updated code to make sure the reporting is consistent. The image below shows a quick snapshot of the Jul – Sep period. This particular graph shows the number of users visiting the site during this period.

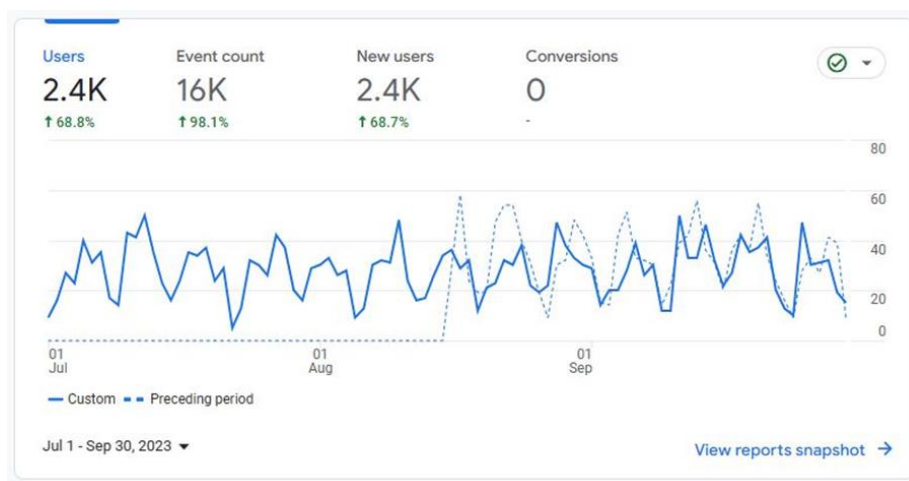


**Figure 64. Number of users visiting the D&D KM-IT during Jul – Sep, 2023.**

Another major effort involved creating a copy of the KM-IT application and database from the production environment. The purpose of this test server is to test security updates before they are rolled out to the production environment. In some instances, the updates and patches released by Microsoft interfere with the custom configuration of the production environment. This test environment will allow the system administrator to verify that the new updates are installed correctly and do not affect the performance of the application.

Finally, the collaboration tools platform (SharePoint) that supports the news and events modules continues to be updated. The team has created a new server with the latest Operating System running Windows Server 2019 and IIS 10.4. This machine is running on a new virtual machine hosted by Generation 10 hardware hypervisor with more resources. This is being done to make sure the application continues to run smoothly and securely. This upgrade will meet the security compliance requirement of the FIU network security department. The team is currently finalizing the configuration of the server and will bring it fully online when all the testing is completed.

### **Subtask 3.6: Conclusions**

The team has successfully kept the D&D KM-IT application and production environment running with optimal performance. After all the hardware and software updates were done, the application did not experience any outages. As a result, the application continues to be more reliable because of the routine maintenance performed on the environment where the application is running.

### **Subtask 3.6: References**

*Deactivation and Decommissioning Knowledge Management Information Tool (D&D KM-IT)*, <https://www.dndkm.org/>, Applied Research Center, Florida International University.

## **Subtask 3.7: Cyber Security of D&D KM-IT Infrastructure**

### **Subtask 3.7: Introduction**

Cyber security of D&D KM-IT involves securing the network infrastructure that is deployed, secured and maintained in the FIU facility. This includes administration tasks described in Subtask 3.6, but also includes conducting routine cyber security tasks to test the network's vulnerability. This involves coordination between the FIU security team and DOE Fellows who learn cyber security skills while assisting staff do penetration testing and other tasks to test the overall security of the system at the application, database, and infrastructure levels.

### **Subtask 3.7: Objectives**

The KM-IT infrastructure is deployed, secured, and maintained in the FIU facility. The objective of this task is for researchers and DOE Fellows to continue to test, maintain, secure, and administer the KM-IT system to keep it secured and up to date with industry standards. This is done to prevent any security breaches on the system and to train DOE Fellows on security tools used in the industry.

### **Subtask 3.7: Methodology**

The KM-IT infrastructure is deployed, secured, and maintained in the FIU facility. This is a repetitive task, as researchers and DOE Fellows continue to test, maintain, secure and administer the KM-IT system. This involves the administration and upkeep of the application server, windows

server and database servers of D&D KM-IT system. Penetration testing tools, malware analysis and reverse malware engineering techniques are used in the DOE Cyber lab to test and secure the KM-IT infrastructure. To keep this infrastructure secure, the team performs various tasks.

Some of the specific tasks performed during this period included:

- Updating the anti-virus application software on the Domain Controllers and the SharePoint server. A RAID controller is a hardware device that manages one or more disk arrays and provides data redundancy, fault tolerance, and improved performance through a technique called RAID (redundant array of independent disks). In the case of a hard drive failure, the team can replace the hard drive without any data loss.
- Updating the DnDKM.org website SSL – this involved purchasing the SSL, configuring the SSL with the provider, installing the SSL on the server.
- Updating the m.DnDKM.org SSL – required for purchase of the SSL, configuration with provider and installing the SSL on the server.
- Installing latest windows server OS and security updates – Upgrading the latest stable version of Windows and downloading known security updates.
- Installing latest group policies – to restrict access to unauthorized users.
- Setting up new users’ profiles – setting up username, password and adding users to proper group policies.
- Updating of the antivirus definition and software on the domain controller server.
- Reorganization of the DOE malware lab (network cables, power supplies, servers).
- Removal of old and updated software from the malware lab.
- Application of security policies to workstations in the malware lab.
- Purchasing of a new Secure Socket Layer (SSL) certificate from DigiCert for the KM-IT web server. This certificate was installed and configured on the server.
- Renewal of the domain for kbem.org.
- Renewal and configuration of the email address used for replies when sending newsletters ([webmaster@dndkm.org](mailto:webmaster@dndkm.org)).
- Monitoring of the security policy changes performed during the last period (NAT policies, VPN policies and web policies of [dndkm.org/collaborationtools.fiu.edu](http://dndkm.org/collaborationtools.fiu.edu)).
- Creation of new users on the newly created DOE VMs. These users were added to the ARC domain which allows users to utilize the same credentials to multiple servers. This allows a more efficient login procedure. It also allows the system administrator to have more control over the security policies implemented across the domain.
- The entire web server is in the process of migration to a new production environment to remain compliant with security policies from the University and to implement the best security practices. This process involves migrating the database and web server to new servers with the latest operating system.
  - The first stage of this process was completed, which included moving the entire production environment.



- The staff is finishing some configuration and testing to ensure that all the modules are working properly. Once the testing is complete, the domain will be redirected to this new environment.
- The team started to perform periodic testing on the KM-IT sandbox application running on the cyber security lab. This effort is conducted a few times a week by our staff. Just like the WIMS application, the KM-IT has a shadow application running locally where the team tests against known threats, so the team uses this application to test new security threats discovered in the industry.
- Finally, related to the security of the application, the team created a copy of the application and database from the production environment after creating a test D&D KM-IT server. The purpose of this test server is to test security updates before they are rolled out to the production environment.

### **Subtask 3.7: Results and Discussion**

Ensuring the D&D KM-IT web application's security is an ongoing commitment, with active cybersecurity administration being integral to its reliability. The absence of detected breaches underscores the effectiveness of implemented security measures, emphasizing the crucial nature of this ongoing subtask. This continuous effort reflects a proactive stance against potential threats, showcasing the adaptability of the cybersecurity framework to address evolving risks. Sustaining this vigilant approach is essential, not only for safeguarding data and user trust but also for acknowledging cybersecurity as an evolving discipline that demands consistent attention. In essence, the absence of breaches is a result of strategic planning and ongoing maintenance, highlighting the ongoing importance of treating cybersecurity as a continual support process for the KM-IT.

### **Subtask 3.7: Conclusions**

Cybersecurity and administration of the D&D KM-IT application are ongoing processes to keep the application secure and reliable. The fact that there was no breach of the system detected can likely be attributed to the cyber security measures implemented, which is an indicator of the significance of this subtask and the need to maintain it as an ongoing support process for the D&D KM-IT application.

### **Subtask 3.7: References**

*Deactivation and Decommissioning Knowledge Management Information Tool (D&D KM-IT)*, <https://www.dndkm.org/>, Applied Research Center, Florida International University.

*Metasploit*, <https://www.metasploit.com/>, Metasploit, Rapid1.

## **Subtask 3.8: KM-IT Tech Talks**

### **Subtask 3.8: Introduction**

The FIU team met with DOE EM prior to the start of the period of performance to discuss opportunities to promote the D&D KM-IT across the DOE sites and facilities. Several topics were discussed, and one was the development of a Tech Talk series where scientists performing D&D-



related work would present their research to the community. Several Tech Talks were conducted during the previous period and due to their success, this task continues to introduce the D&D community with cutting edge research being performed by subject matter experts.

### **Subtask 3.8: Objectives**

The objective of the Tech Talks is to provide a platform for scientists to share their D&D research with the community. By using the KM-IT platform, FIU can promote the KM-IT application through newsletters, flyers and event websites. The goal is to increase the engagement of DOE sites and facilities by participating in the Tech Talks as a presenter or attendees.

### **Subtask 3.8: Methodology**

The FIU team organized D&D-focused Tech Talks every quarter on the D&D KM-IT platform. FIU collaborated with national laboratories and/or DOE sites to identify and present technical topics of interest to the community where scientists can present their research. The Tech Talks were performed virtually using an online meeting platform (Microsoft Teams). The event information, including schedule and archive of previous Tech Talks were hosted on the D&D KM-IT. The team promoted Tech Talks via newsletters, website, emails, and flyers developed by FIU. The Tech Talks were recorded, and the video was uploaded to YouTube and archived on the KM-IT platform supporting the next generation of scientists and engineers.

### **Subtask 3.8: Results and Discussion**

FIU conducted four Tech Talks during this period where the team collaborated with national laboratories and/or DOE sites/facilities to identify and present technical topics of interest to the community. The Tech Talks were conducted virtually using an online meeting platform (Microsoft Teams) which was accessible through the KM-IT platform. The Tech Talks were promoted via newsletters sent to the registered user of the KM-IT and other recipients. The user had to register prior to attending the event using Microsoft Forms (Figure 65).

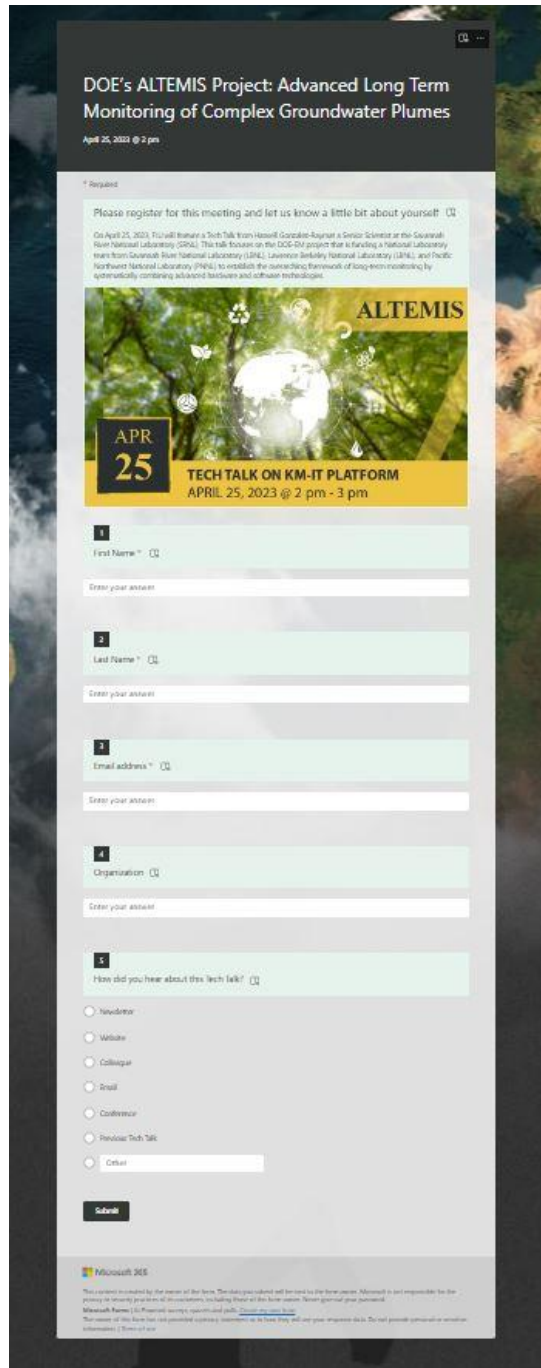
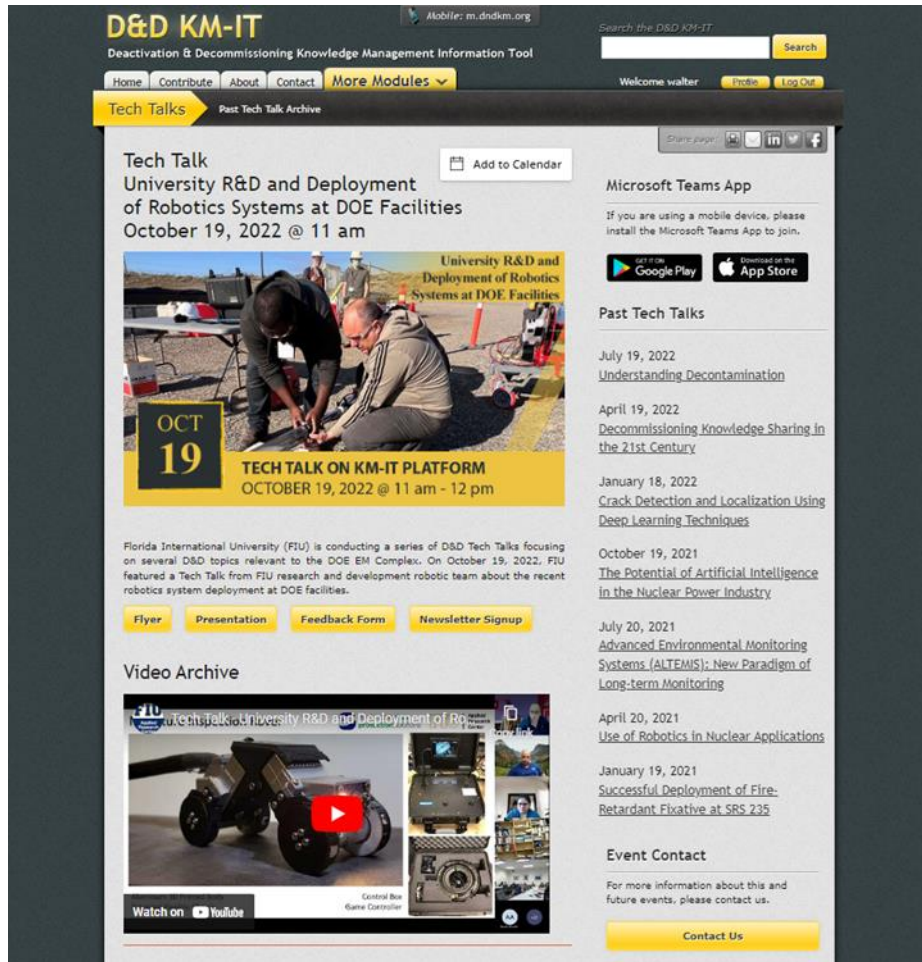


Figure 65. Tech Talk registration form using Microsoft Forms.

The team started this period by hosting a Tech Talk on October 19, 2022, titled “University R&D and Deployment of Robotics Systems at DOE Facilities”. This Tech Talk was conducted by Florida International University’s robotics research team members (Dr. Leonel Lagos and Mr. Anthony Abrahao) and focused on a recent accomplishment which involved the deployment of a robotic system at DOE’s Hanford site. An event webpage was created at <https://www.dndkm.org/TechTalk/> and the video recording of the Tech Talk was published on YouTube and embedded on the website. The image below shows the Tech Talk website.



**Figure 66. October Tech Talk event webpage.**

The second Tech Talk was held on January 24, 2023, titled “*International Perspective on Decommissioning with focus on 3D hazard aware digital and robotics technology-based transformation*”. The guest speaker was Dr. István Szőke from the Institute for Energy and Technology in Norway. Dr. Szőke was the first international speaker featured in the Tech Talk series.

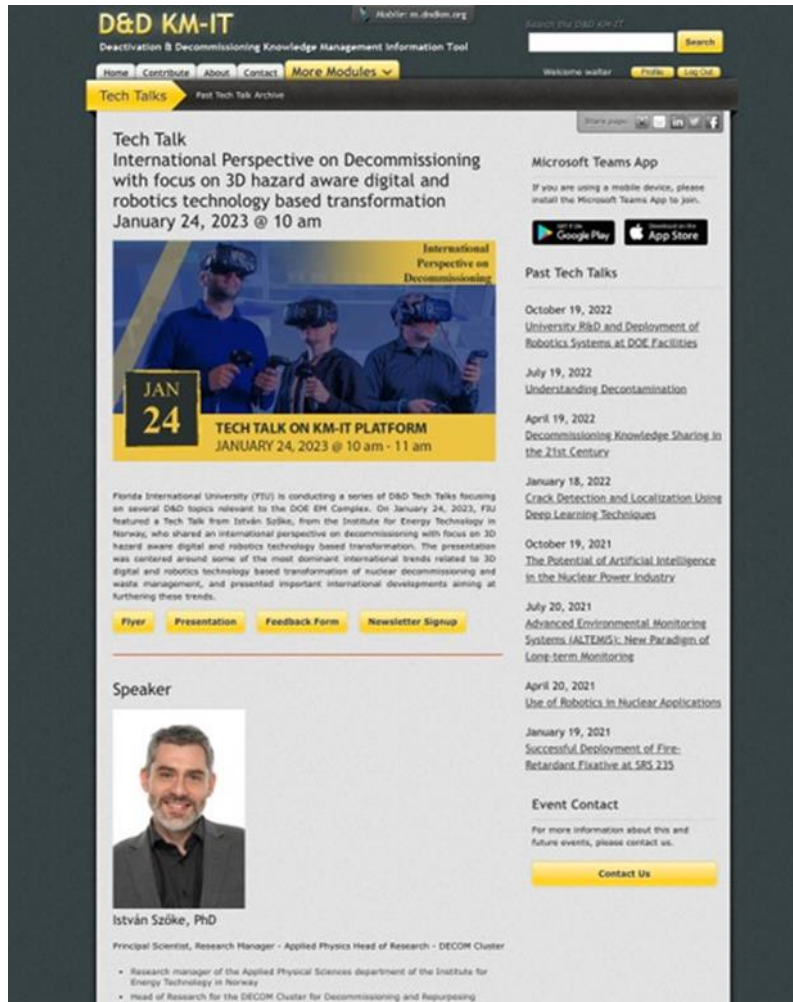


**Figure 67. Webpage for Tech Talk hosted on January 24 titled “International Perspective on Decommissioning with focus on 3D hazard aware digital and robotics technology-based transformation”.**

These Tech Talks were well attended by multiple organizations. The tag cloud below shows the participant organizations that attended the Tech Talk in January 2023.



**Figure 68. Organizations that attended the Tech Talk on January 24, 2023.**

In addition, the team prepares graphics and flyers to promote the event. The following two images show the banner that the team prepared for one of the events. This material is used in emails newsletters, websites, and social media.





Figure 69. D&D KM-IT Tech Talk banner for the next event on April 25, 2023.

The image below shows the flyer of the Tech Talk on April 25<sup>th</sup>, 2023.



Figure 70. Tech Talk flyer for April 2023.

During the month of April, the team hosted a Tech Talk featuring former DOE Fellow, Dr. Hansell Gonzalez-Raymat, who is now a Senior Scientist working at Savannah River National Laboratory (SRNL). The title of the Tech Talk was “DOE’s ALTEMIS Project: Advanced Long-Term Monitoring of Complex Groundwater Plumes”. This Tech Talk was hosted virtually on the D&D KM-IT framework on April 25, 2023. The image below is a screenshot of the Tech Talk event website which includes the information about the Tech Talk (title, description and speaker’s picture and bio).

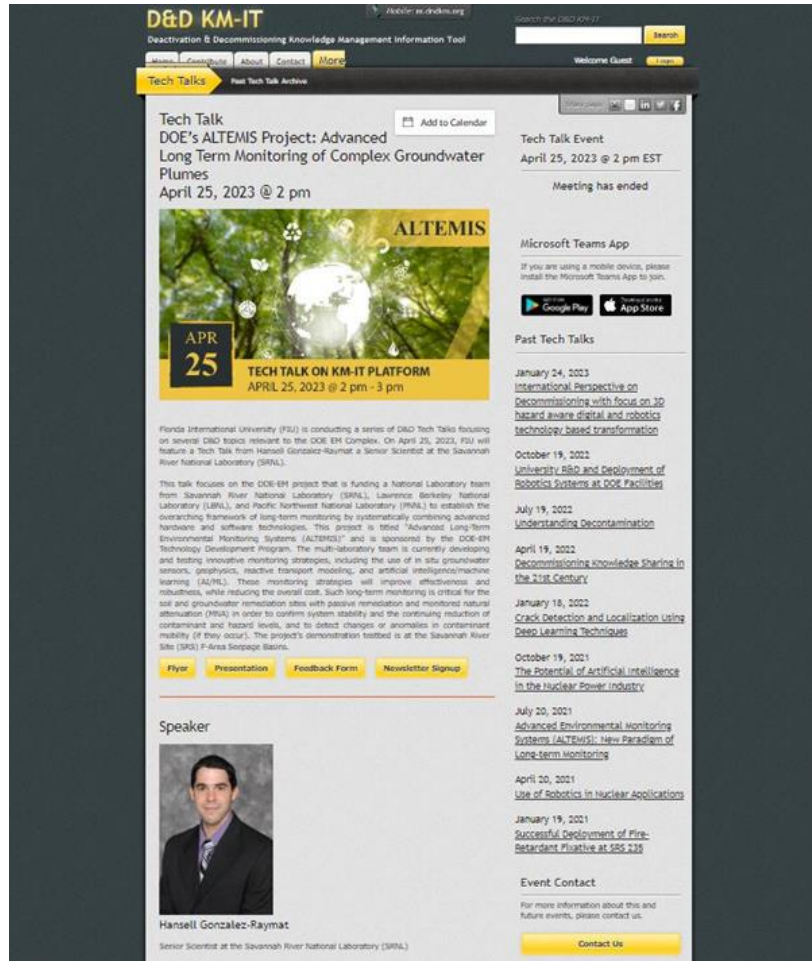
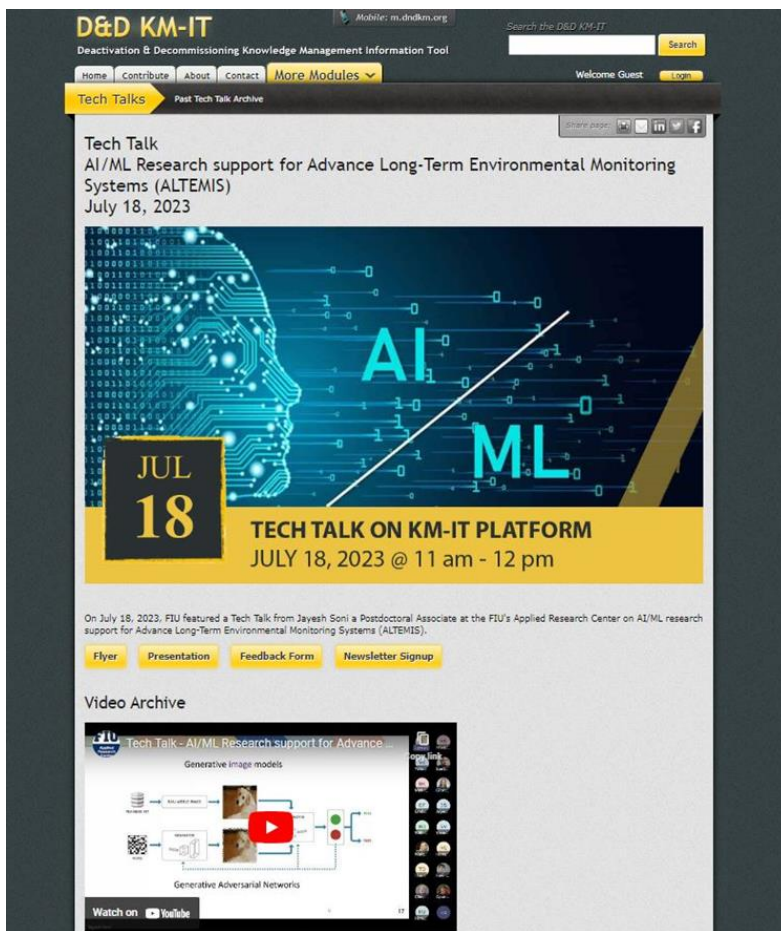


Figure 71. D&D KM-IT Tech Talk event webpage hosted on April 25, 2023.

The Tech Talk was well attended with members from SRNL, OREM, Longenecker and Associates, EM-411 and FIU-ARC.

The final Tech Talk hosted during this period was on July 18, 2023 titled “*AI/ML Research support for Advance Long-Term Environmental Monitoring Systems (ALTEMIS)*” presented by Dr. Jayesh Soni, a Postdoctoral Associate at FIU's Applied Research Center.



**Figure 72. KM-IT Tech Talk webpage conducted on July 18, 2023 titled “AI/ML Research support for Advance Long-Term Environmental Monitoring Systems (ALTEMIS)”.**

In summary, the following Tech Talks were conducted during this period.

- October 19, 2022, University R&D and Deployment of Robotics Systems at DOE Facilities
  - Topic – Deployment of FIU robotics system at DOE Facilities
  - Collaborator – FIU, Washington River Protection Solutions (WRPS)
  - Speaker – Dr. Leonel Lagos, Anthony Abrahao
  - Deliverable - 2022-P3-D1
- January 24, 2023, International Perspective on Decommissioning with focus on 3D hazard aware digital and robotics technology-based transformation
  - Topic – International perspective on decommissioning with focus on 3D hazard aware digital and robotics technology-based transformation
  - Collaborator – Institute for Energy Technology in Norway
  - Speaker – Dr. István Szőke
  - Deliverable - 2022-P3-D3
- April 25, 2023, DOE’s ALTEMIS Project: Advanced Long-Term Monitoring of Complex Groundwater Plumes
  - Topic – This talk focuses on the DOE-EM project that is funding a National Laboratory team from Savannah River National Laboratory (SRNL), Lawrence



Berkeley National Laboratory (LBNL), and Pacific Northwest National Laboratory (PNNL) to establish the overarching framework of long-term monitoring by systematically combining advanced hardware and software technologies

- Collaborator – Savannah River National Laboratory (SRNL)
- Speaker – Dr. Hansell Gonzalez-Raymat
- Deliverable - 2022-P3-D4
- July 18, 2023, AI/ML Research support for Advance Long-Term Environmental Monitoring Systems (ALTEMIS)
  - Topic – AI/ML Research support for Advance Long-Term Environmental Monitoring Systems (ALTEMIS)
  - Collaborator – FIU, Savannah River National Laboratories (SRNL)
  - Speaker – Dr. Jayesh Soni
  - Deliverable - 2022-P3-D7

All Tech Talk recordings are uploaded to YouTube on the FIU-ARC YouTube channel. The image below shows a screenshot of one of the recordings on YouTube. These videos are embedded into the KM-IT Tech Talk website.

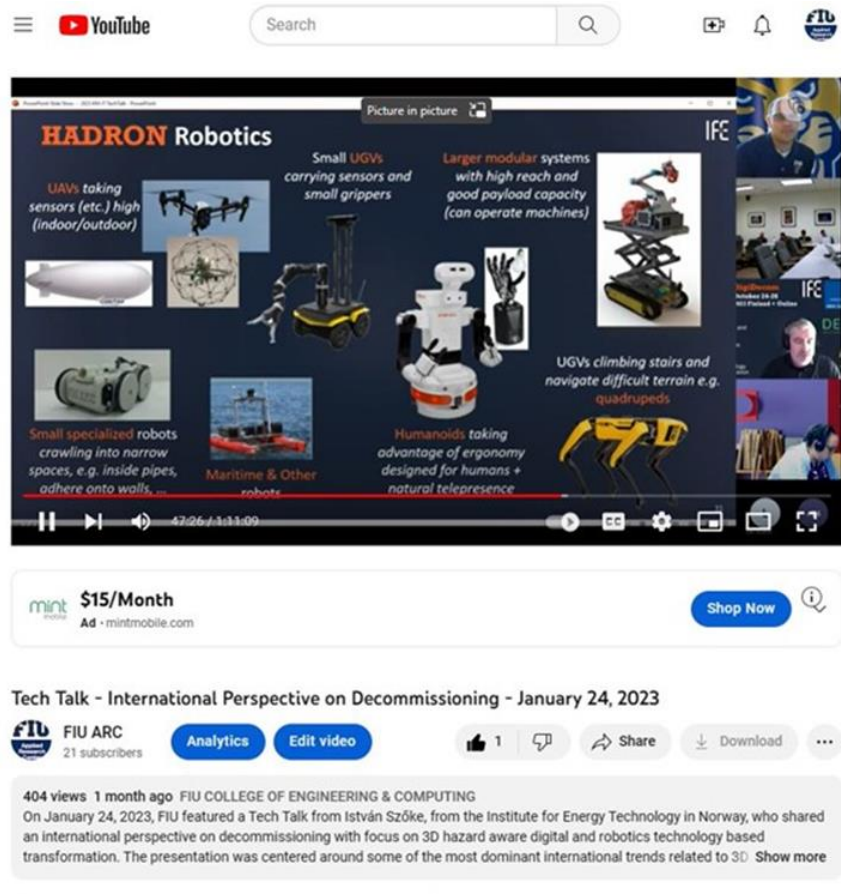


Figure 73. Tech Talk recording from February uploaded to the YouTube platform.



The following screenshot shows the embedded video on the KM-IT website after they are uploaded to YouTube. All the past Tech Talks can be viewed at <https://www.dndkm.org/TechTalk/>.

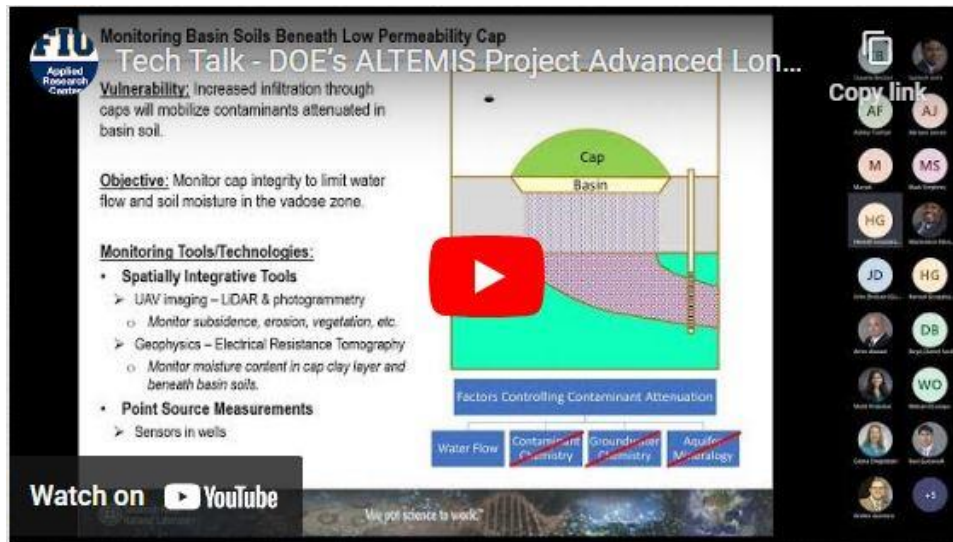


Figure 74. Tech Talk recording uploaded to YouTube and embedded on the KM-IT website.

### Subtask 3.8: Conclusions

These Tech Talk events allowed subject matter experts (SMEs) to share their knowledge and experience with DOE EM sites and stakeholders. These were virtual one-hour events, which included one or two guest speakers on relevant topics of interest to the community. The events were recorded and published on D&D KM-IT (<https://www.dndkm.org/TechTalk/>) along with other associated material such as the agenda, presentation slides and lessons learned for post-event viewing as well.

### Subtask 3.8: References

*Deactivation and Decommissioning Knowledge Management Information Tool (D&D KM-IT)*, <https://www.dndkm.org/>, Applied Research Center, Florida International University.

*Microsoft Forms*, <https://forms.office.com/>, Microsoft Form, Microsoft Corporation.

## **TASK 7: AI FOR EM PROBLEM SET (SOIL AND GROUNDWATER) - EXPLORATORY DATA ANALYSIS AND MACHINE LEARNING MODEL FOR HEXAVALENT CHROMIUM [CR (VI)] CONCENTRATION IN 100-H AREA (PNNL)**

---

The U.S. Department of Energy's (DOE's) Hanford Site 100 Areas contain monitoring data for groundwater wells (in situ sensing, water sampling), Hexavalent Chromium (Cr(VI)) pump and treat (P&T) activities (extraction and injection flow rates, weekly Cr(VI) sampling of influent water, etc.), as well as water table levels and river stage monitoring data. Artificial Intelligence /Machine Learning (AI/ML) algorithms may help in understanding complex hydrogeological processes and interactions among the aquifers and the dynamic river stage in the Columbia River using these legacy datasets. Machine learning and deep learning models can be developed to identify patterns, address knowledge gaps and ultimately predict transport of Cr(VI) in the subsurface of the 100-H Area. The aim of this research is to develop a robust AI/ML-based platform for long-term monitoring, analysis and prediction of Cr(VI) contamination in the subsurface of the U.S. Department of Energy's (DOE's) Hanford Site 100 Areas. AI/ML algorithms can leverage high-performance computing to predict the spatial and temporal distribution of Cr(VI) as well as help in identifying any spatiotemporal relationship in the dataset.

The overarching goal of this research is to couple long-term monitoring data of hexavalent chromium (Cr(VI)) with AI/ML models to identify temporal and spatial relationships of subsurface chromium transport that reduces uncertainties in the conceptual site model (CSM). The objectives for this year involved looking at those relationships and behaviors that change according to time. This analysis allows for inference of daily directionality for a target.

### **Subtask 7.3: Algorithm development for spatiotemporal relationship identification**

#### **Subtask 7.3: Introduction**

In collaboration with PNNL subject-matter experts, FIU has undertaken a comprehensive exploration of machine learning and deep learning algorithms to establish a robust methodology for identifying spatiotemporal relationships in hexavalent chromium [Cr(VI)] content between groundwater wells. This innovative approach, guided by data-driven insights, facilitates the uncovering of hidden trends within the temporal and spatial intricacies of the Cr(VI) dataset. The multifaceted subtask encompasses the research of diverse machine learning and deep learning techniques for AI/ML modeling of time-series data, the application of modern statistical methods and machine learning algorithms for spatial data analysis, exploration of spatiotemporal linkages through information fusion strategies, and the evaluation of directional performance using the nearest groundwater wells and aquifer tubes as targets. In this research, time-series forecasting was used, the function of predicting future values given an amount of historical data, to identify spatiotemporal relationships in Cr(VI) content between groundwater wells [1]. The main models added and analyzed were the AdaBoost regression model for overall spatiotemporal relationship identification, a Long Short-Term memory (LSTM) deep learning neural network for temporal prediction and a Convolutional 1D neural network (CNN) to compare the temporal predictions with the LSTM model. Both LSTM and CNN classify as recurrent neural networks (RNNs) due to their ability to capture time dependencies within data effectively. The first model used, the

AdaBoost regression model, is a sequential technique that assigns weights to all the training points to enhance predictive accuracy [2]. The LSTM model is a popular variant of RNNs, that excels in handling sequential or time series data by using a gated architecture [1]. The final model, CNN, is a model that learns from raw time-series data and uncovers internal representations of the temporal patterns [3].

Most of the well relationship analysis relies on the extraction of feature importance. For neural networks, the extraction of feature importance cannot be achieved in the same manner as it is achieved for previously used machine learning models like AdaBoost or Random Forest. This is due to deep learning models generally being what is considered a “black box”, meaning they are not as easily explainable as typical machine learning models that make their decisions based on trees as in ensemble models or a linear set of weights like in linear regression. However, there is a Python package, SHAP (Shapely Additive exPlanations), that aims to unify an interpretation approach of feature importance [4]. The package contains a Deep-Explainer class based on the concept of layer-wise relevance propagation (LRP). Basically, LRP assigns a relevance score to each input feature, the score being the contribution to final prediction. Contributions are like feature importance; except they refer to a finite amount of added/subtracted unit values a feature has for a given prediction (i.e., Well x contributed .05  $\mu\text{g/L}$  of Cr(VI) to the final prediction of 10  $\mu\text{g/L}$  at a Well y on a given day).

### **Subtask 7.3: Objectives**

The overall goal of this research is to develop a methodology for identifying spatiotemporal relationships in Cr(VI) content between groundwater wells. The goal is to extract temporal features, analyze spatial data, and utilize information fusion techniques to uncover hidden patterns in the dataset, therefore advancing our knowledge of the intricate relationships at play.

### **Subtask 7.3: Methodology**

At the beginning of the year, efforts were focused on utilizing the AdaBoost ensemble algorithm and the feature extraction thereof. Feature (well) importance bar plots were generated specifically for the groundwater wells in the context of the AdaBoost regression models. Additionally, a ground truth vs prediction plot was developed to assess the performance of the AdaBoost model. Finally, a regression plot showing the feature important vs distance for each groundwater well within a 1,000-meter radius of target and all directions (240 degrees to 400 degrees) was created.

To capture the time dependency more effectively, recurrent neural networks were explored and used throughout the rest of the year in the form of LSTMs and CNNs. With further development of time series modeling, focus shifted to determining the relationship between wells as opposed to groundwater vs. aquifer well relationships and thus the entire available dataset of wells within the HR-D area was used instead of just utilizing wells around a specified radius of selected target. Time series analysis starts with taking preprocessed HR-D groundwater data from Subtask 7.2 and removing one well from the available wells within the dataset. This well marks the selected target for which our time series modeling will attempt to predict the Cr(VI) concentration. The two-dimensional data will be transformed into three-dimensional data as sequence samples for each well's Cr(VI) time series is made according to a length of 10-time steps. The sample sequences are then shuffled. The time sequences are given to the LSTM architecture and CNN architecture for training, where the epoch count is decided by an early stopping callback which automatically stops training once validation loss stops improving. The predicted values from the models are used to evaluate them, with the best model being selected for further use after training 10 instances of

the models for the sake of consistent performance. Whichever model performs best with the given target in mind is the one that gets pushed further in the analysis pipeline (which ended up being the LSTM model for most target wells). The model is then passed into SHAP together with a testing set for the generation of feature (or well) contributions for every sample prediction. Contribution daily deltas are calculated (change in contribution from one day to the next), representing our contribution change for each well. The deltas are visualized for every well and are used in a spatial visualization to color the surrounding wells of a selected target according to a gradient. There is also a scaled direction vector that is included in the spatial plot which is the sum of vectors made from the product of a given well's delta value (or contribution value depending on specification) and the coordinate distances between the given well and the target. The spatial plots are generated for each day available in the testing set and put into animation.

The described analysis workflow is performed with only the chromium concentrations of the modeled wells in mind, primarily because the inclusion of extra features in the established workflow results in worse prediction performance. However, the inclusion of more well sensor data can give more insight into the relationship of the wells within groundwater's Cr(VI) when previously mentioned contribution extraction is applied. Of all methods explored for the incorporation of extra features per well, the use of principle component analysis (PCA) on a feature set that groups features to a well by prefixing the well name to the feature name was the only method that resulted in prediction improvement. Since the application of PCA changes the feature set down into principal components, previous contribution extraction using SHAP would only give contributions of the principal components, not the wells (or parts thereof). Yet, loadings can be extracted from principal components to find correlations between a principal component and an original feature. By dividing a feature's correlation to a principal component by the sum of all correlations for a component, a percentage coefficient representing how much an original feature makes up the component can be calculated. When retrieving the contribution values from the principal component set using SHAP, approximations of original feature contributions can be extrapolated by multiplying the contribution by the percentage coefficient a feature has in each principal component. This allows the contributions of the principal components to be tied back to the original features used.

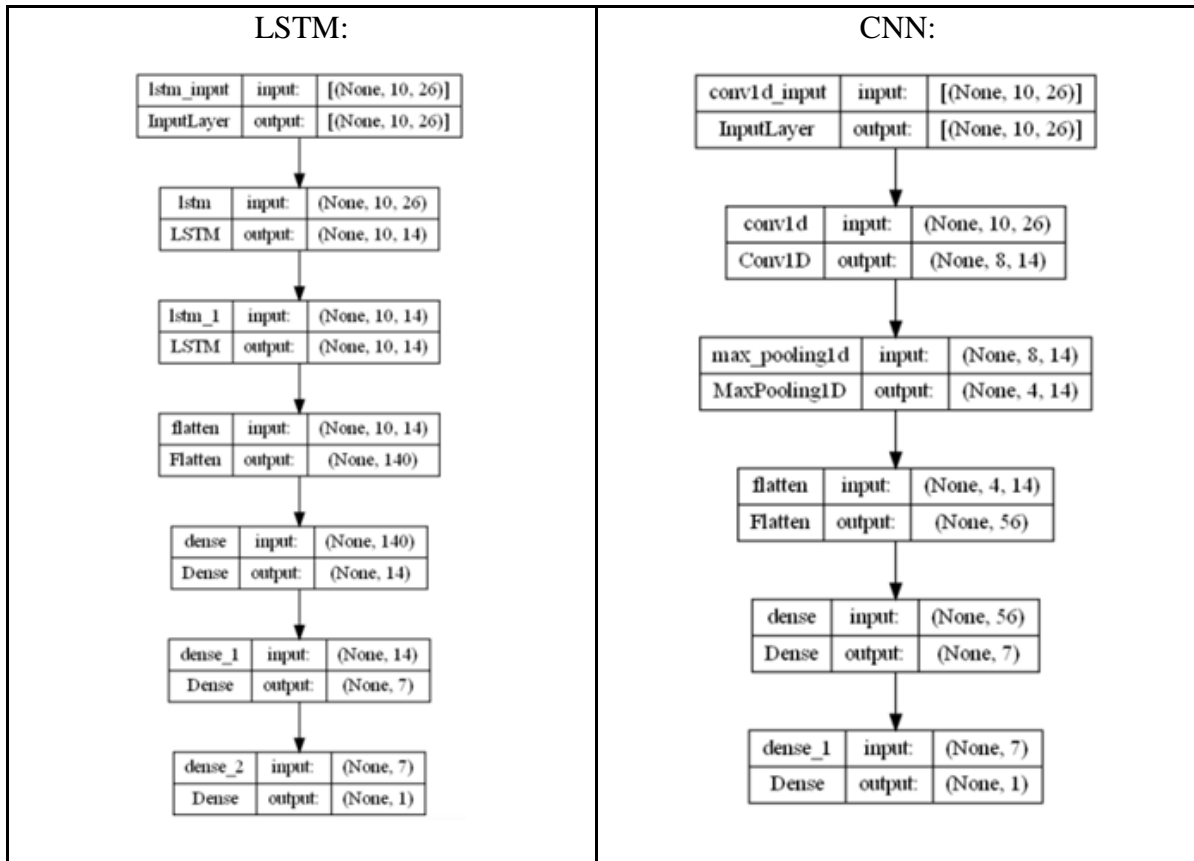


Figure 75. LSTM/CNN model architectures (modeling with 26 wells).

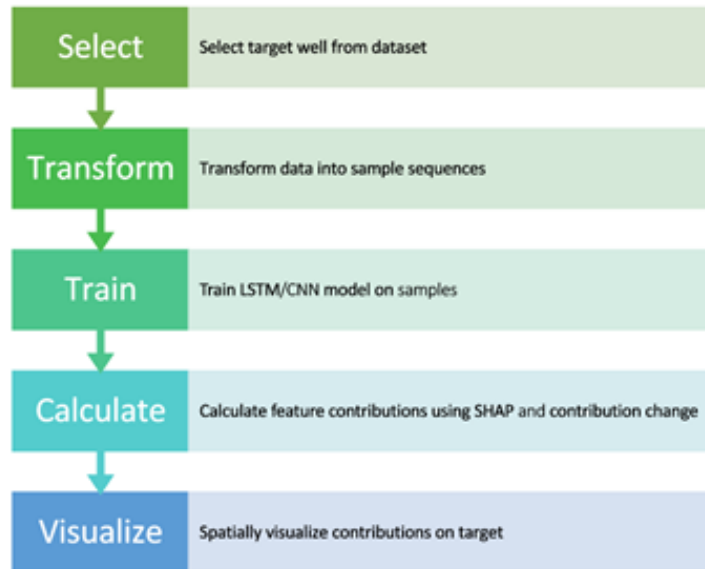


Figure 76. Analysis workflow for Subtask 7.3.

### Subtask 7.3: Results and Discussion

In terms of the AdaBoost model results, feature importance was easily extractable from the ensemble of trees model and is shown below when modeling with target well 199-D8-55 in mind. The performance of the model on target well 199-D4-39 is also shown below. Like the modeling performed in Subtask 7.2, the AdaBoost model was trained on wells a certain distance away from the target (1000 meters), with the relationship of a well’s importance (with respect to target 199-D8-55) and the distance to the nearest shoreline aquifer as determined by the AdaBoost algorithm and other previously used algorithms to compare (those being Random Forest regression, XGBoost regression, GradientBoosting regression, and ExtraTrees regression).

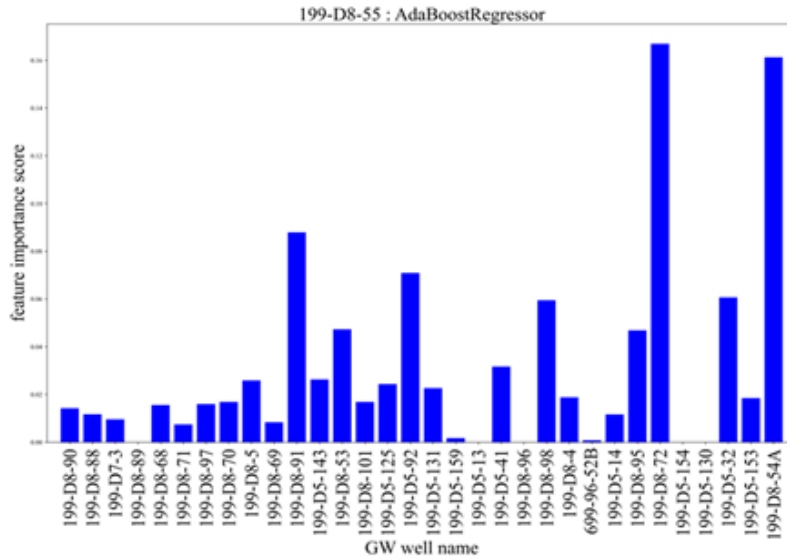


Figure 77. Feature importance bar plot for target groundwater well 199-D8-55. The most influential well in the decision-making process here was 199-D8-72.

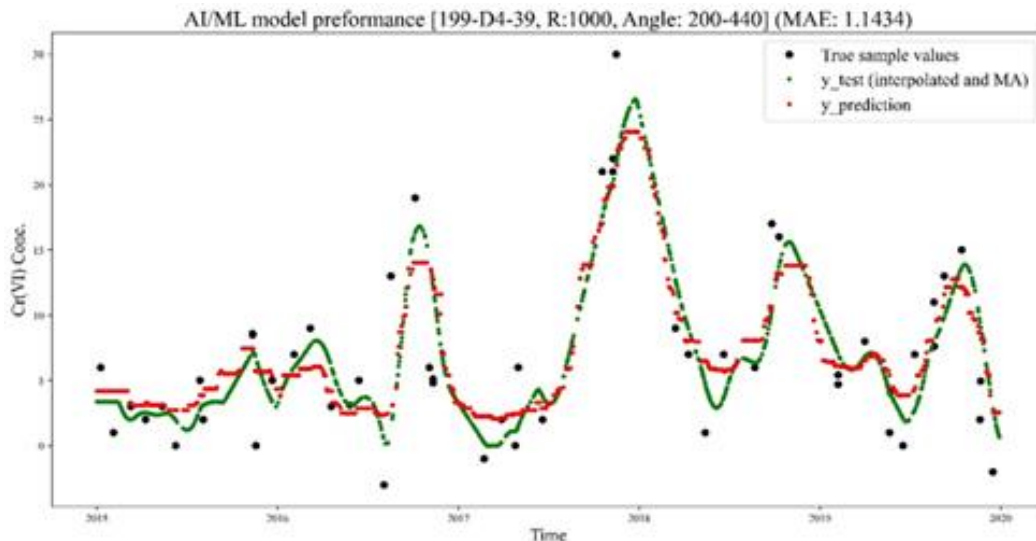
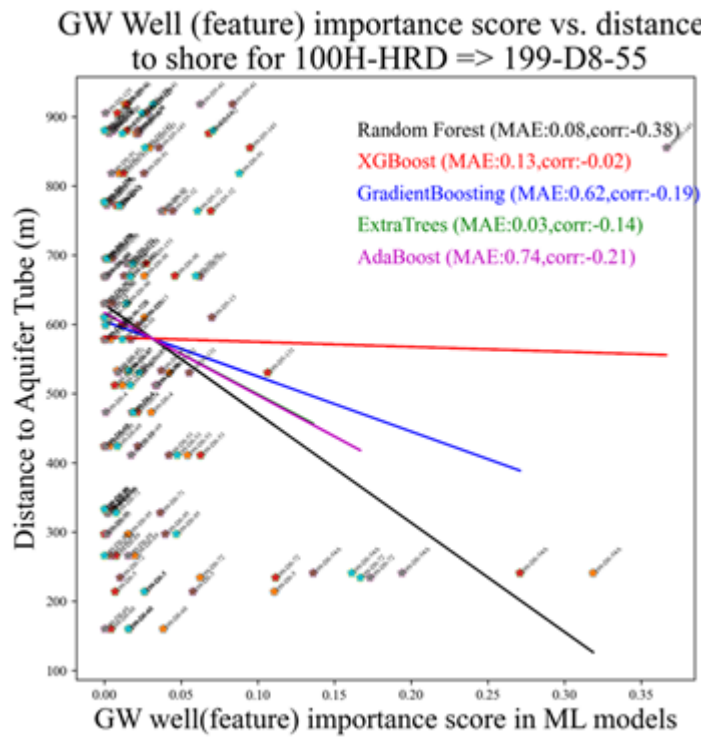


Figure 78. Regression prediction performance of the AdaBoost model predicted chromium concentration values vs actual concentration values for 199-D4-39 for all angles and 1,000-meter radius. MAE was 1.1434.





**Figure 79. Overall feature importance versus distance plot for target well 199-D8-55. MAE error wise, the best performing models were Random Forest and ExtraTrees. Correlation wise, all the algorithms suggest that the relationship between the feature importance score and the distance is negatively correlated.**

In terms of modeling with time dependency capture (modeling with RNNs), the contributions are generated off the testing set split of the data. This testing split contains values across the last year of the 4-year span of data used for this task. The training data consists of values from 2015 to 2018, while the testing data consists of values from the inspected test year of 2019. The contribution change lets us see how surrounding wells behave over time according to target. Below mentioned two Figures show 8 top wells which have exhibited the highest change in contribution throughout the inspected year. Seeing behavior as well for at least some wells vary substantially, snapshots of surrounding contribution throughout the year are visualized as shown below. Results show some wells have a consistent change impact at certain parts of the year. Taking well 699-98-49A as an example, its placement among top wells with negative change to target concentration at months favoring the end of the year (supported in snapshot from 2019-08-05 and 2019-12-06) show that it has highly dynamic behavior within the end of fall to start of winter season as far as the well 199-D4-98 is concerned.

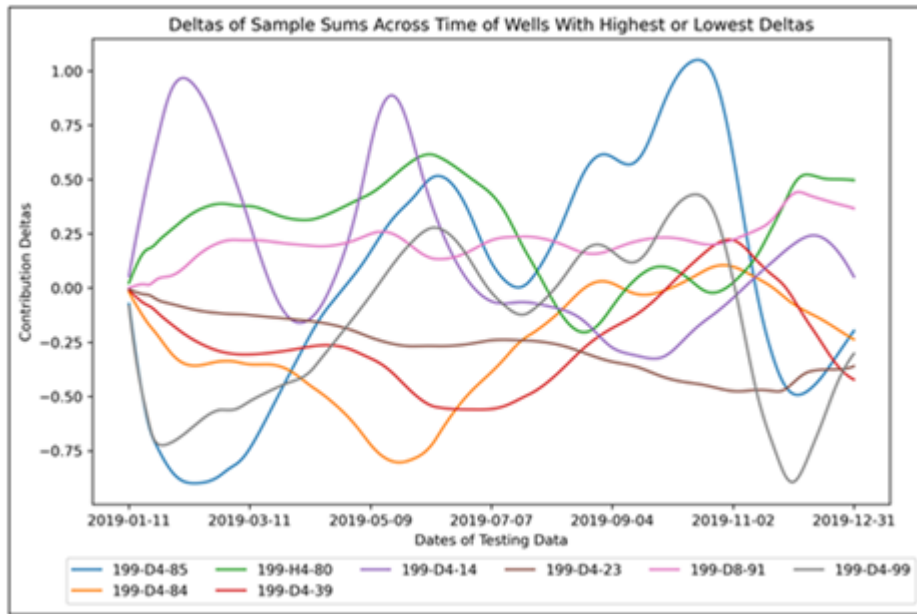
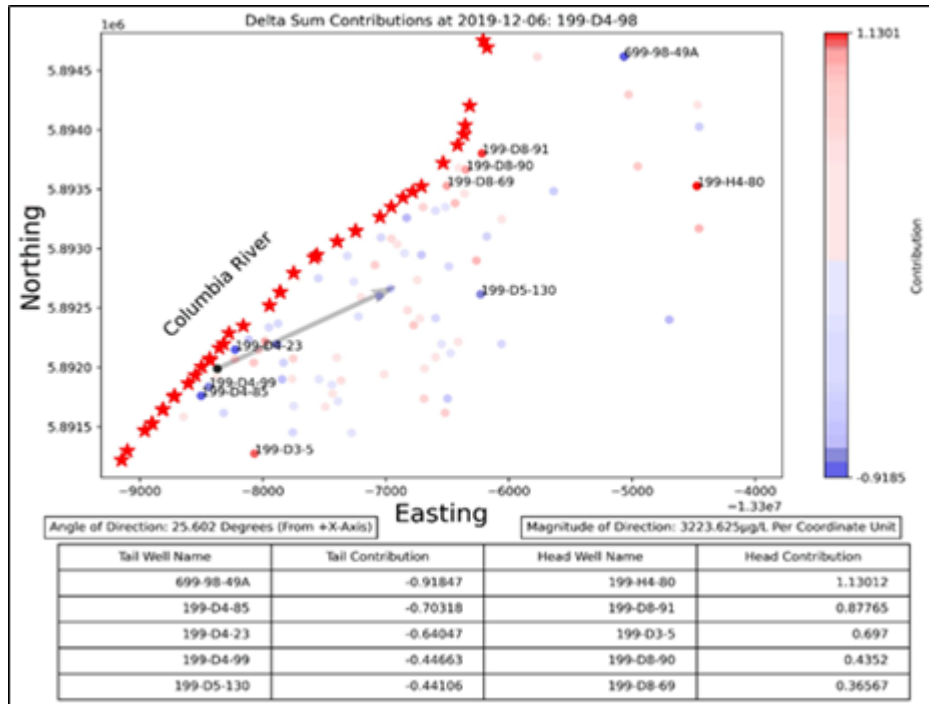
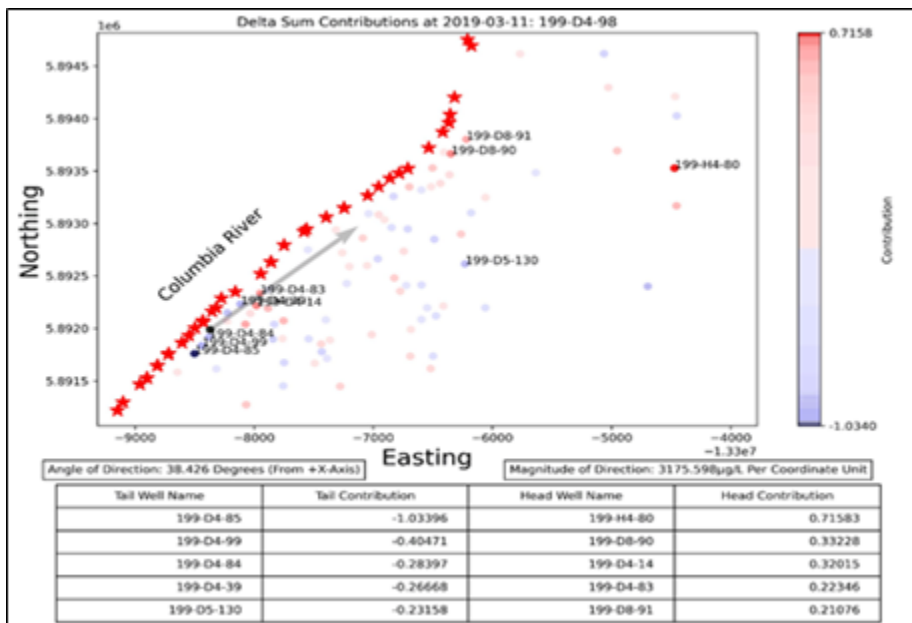


Figure 80. Wells exhibiting the biggest contribution change according to target well 199-D4-98.

(a)



(b)



(c)

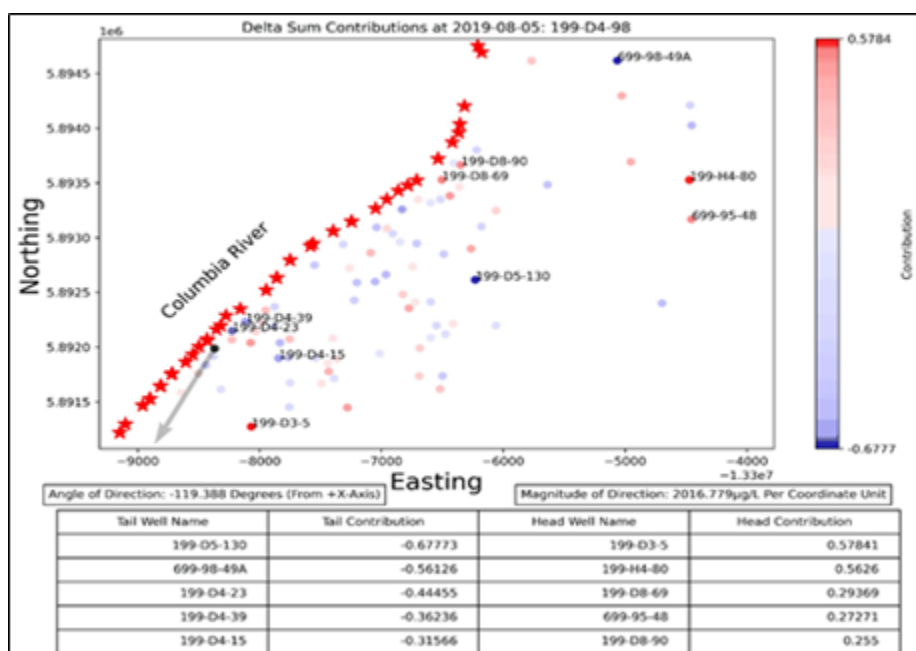
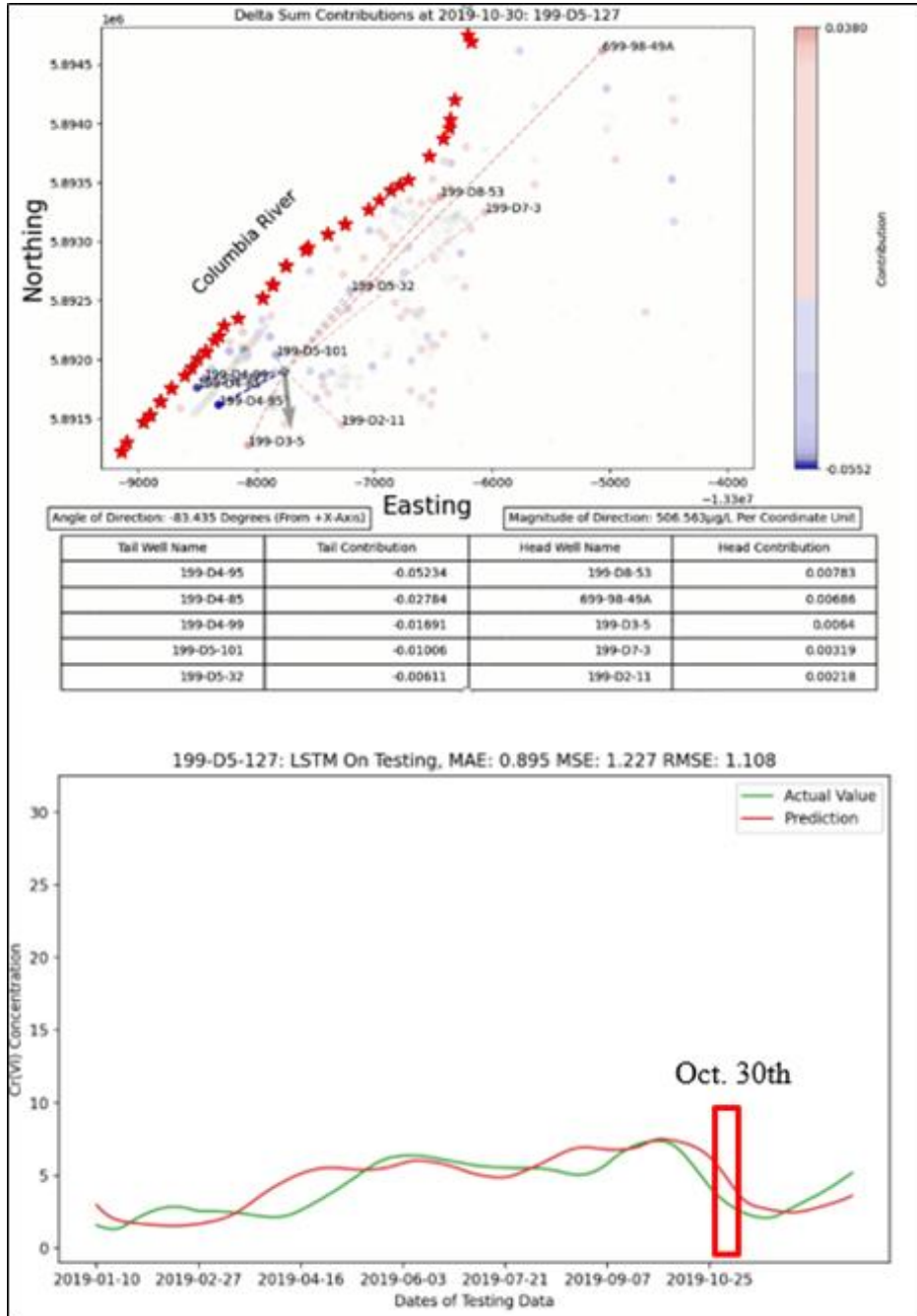


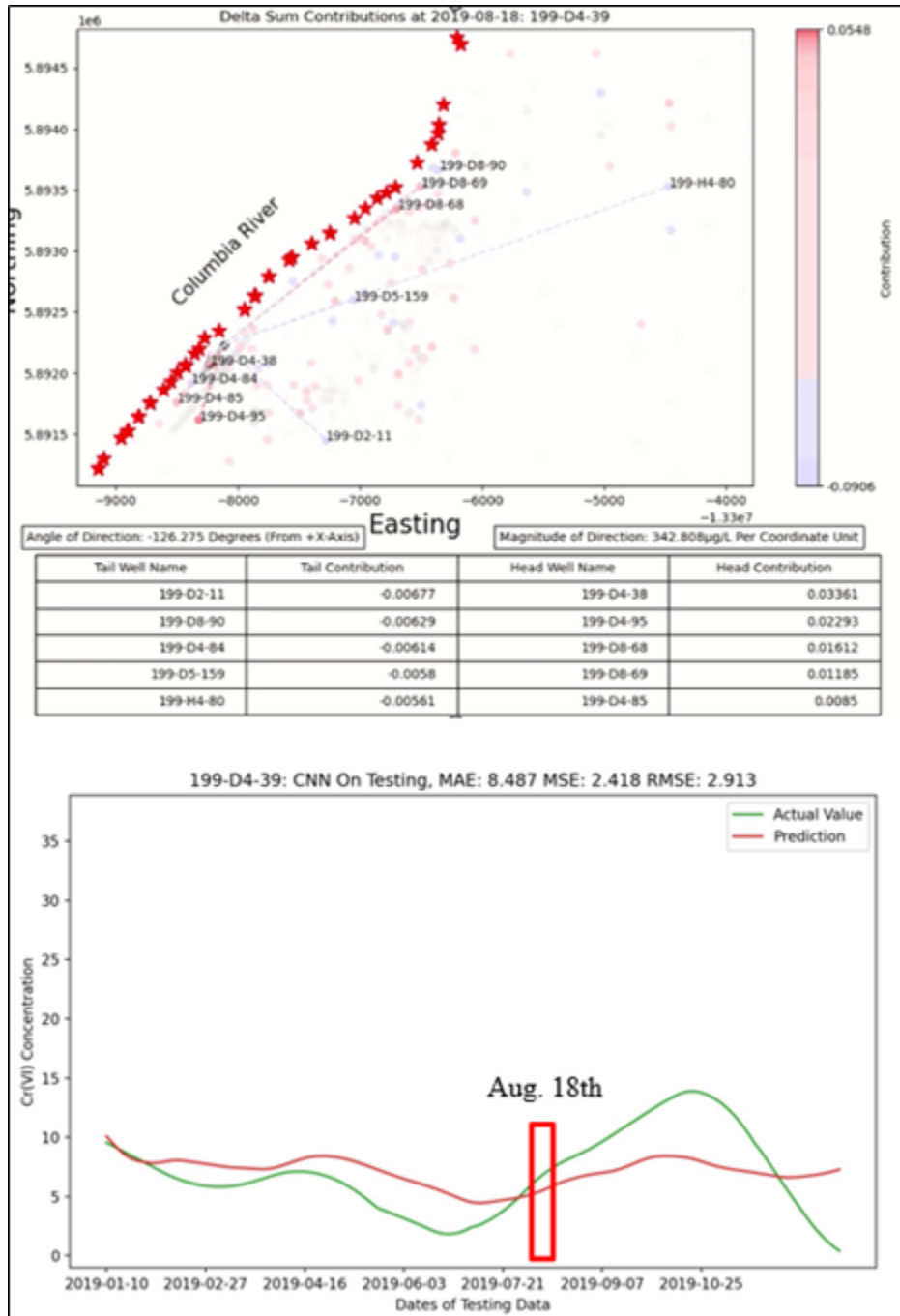
Figure 81. Spatial plots of 199-D4-98 contributions on (a) 2019-12-06, (b) 2019-03-11, and (c) 2019-08-05.

Wells with high deltas (synonymous with contribution/impact change) explain the trend (tangent) of the predicted time series at a given day. This is especially apparent when the delta at a given day represents the peak negative/positive delta exhibited throughout the inspected timeframe. The figure below are the examples of snapshots that show peak deltas having a dominant effect on the trend present in the predicted line. Since contributions explain the predicted line, the closer the predicted line is to the actual line, the more confidence can be placed on the top contributors affecting actual Cr (VI) concentration.

(a)



(b)



(c)

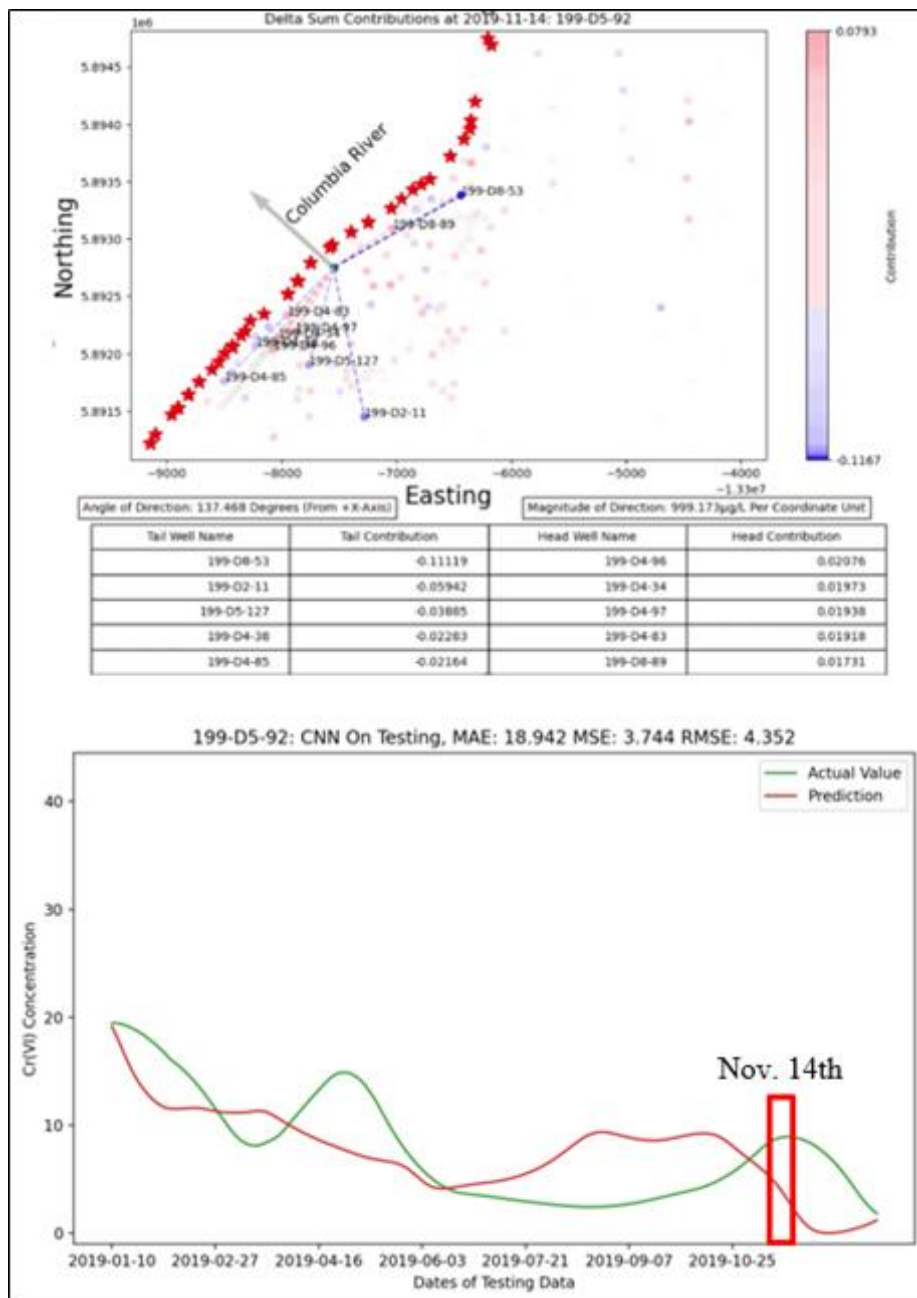


**Figure 82. Instantaneous contribution explanations on prediction. (a) Target well 199-D5-127 had its change in concentration on October 30<sup>th</sup> largely due to wells 199-D4-95, 199-D4-85, and 199-D4-99. (b) Target well 199-D4-39 had its change in concentration on August 18<sup>th</sup> largely due to wells 199-D4-38, 199-D4-95, and 199-D8-68. (c) Target well 199-D5-92 had its change in concentration on November 14<sup>th</sup> largely due to wells 199-D8-53, 199-D2-11, and 199-D5-127.**

So far, results from modeling with just Cr(VI) concentrations have been shown. The following results include each well’s location, pH levels, and specific conductance along with their Cr(VI) values. As mentioned in our methodology, the use of PCA was the only method to show improved prediction performance with the inclusion of extra well sensor data, which is shown below. If modeling with just each well’s Cr(VI) alone gave us 86 features in the feature set when a target is selected, then modeling with the extra sensor data gives us 430 features in the feature set. The



application of PCA boiled down the expanded feature set to 10 principal components which capture 90% of the variance found in the original expanded set. The figure also shows how much each feature contributes to the explained variance of the principal component set. With principal component 1 (PC1) being the component capturing the highest variance.

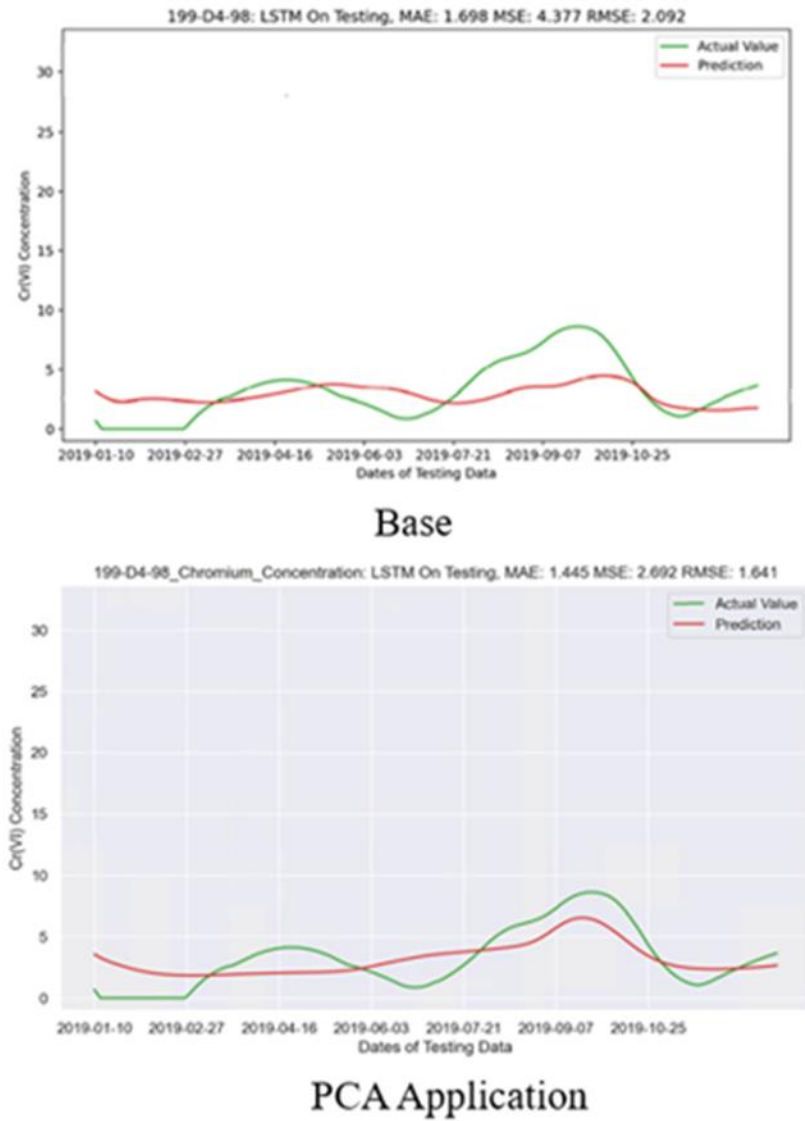


**Figure 83. Base prediction results using established modeling on contaminant concentration versus prediction results using extra sensor data and PCA.**

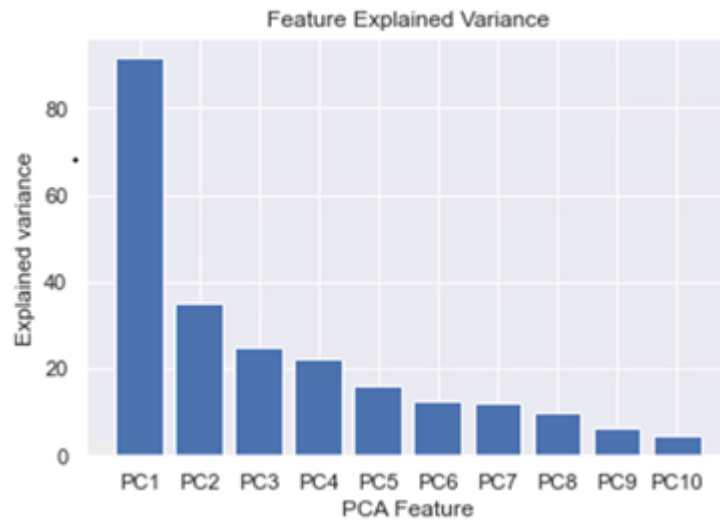


Figure 84. The amount of explained variance from each principal component.

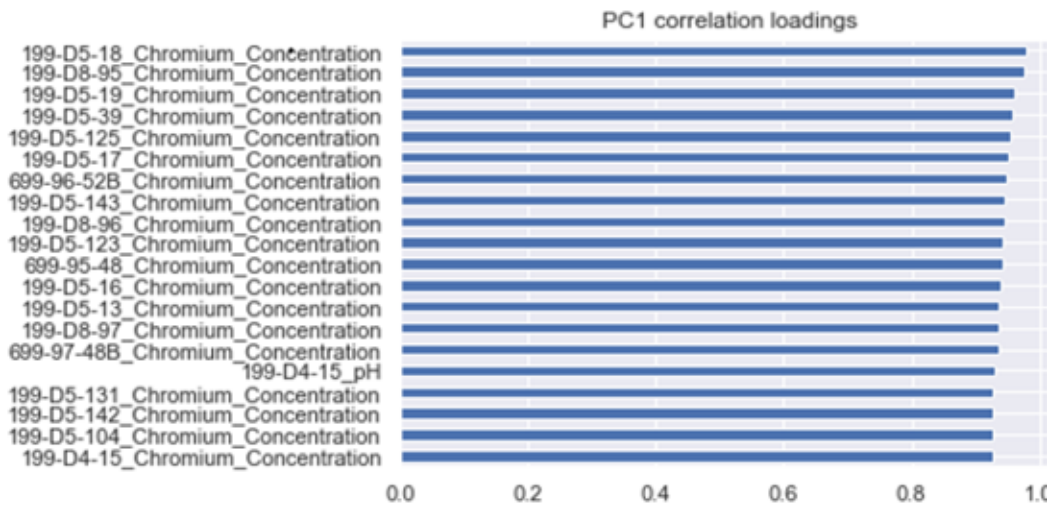
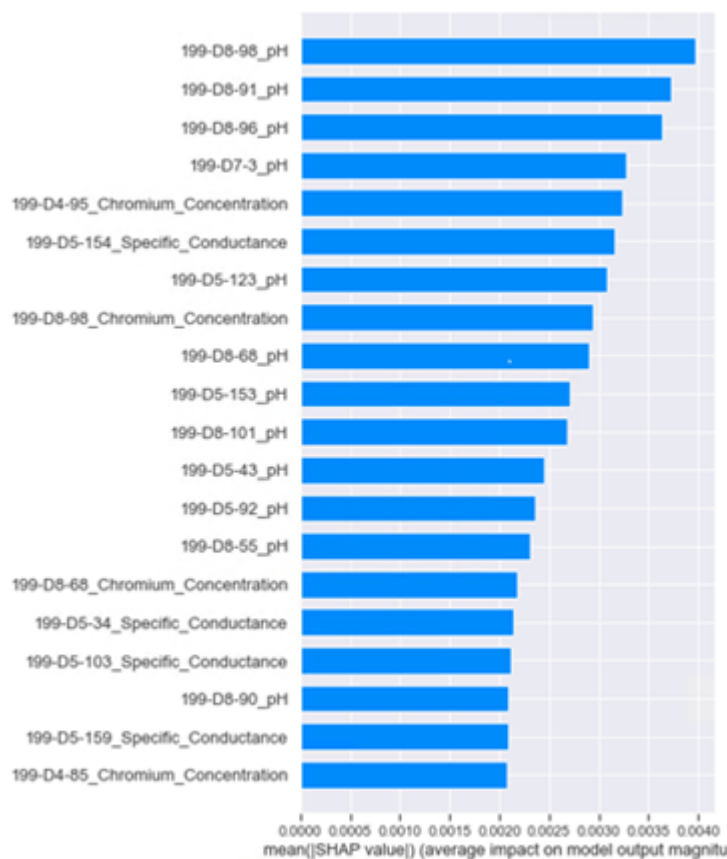


Figure 85. Correlations principal component with the highest explained variance it has with original features.

For the retrieval of SHAP contribution values from the principal components when modeling with respect to target well 199-D4-98, the below Figure shows the original feature contributions after multiplication of the correlation percentages with the principal component contributions on the last sample sequence in the time series (well contributions on the last day). After summing feature contributions back into their well grouping (indicated by feature name prefix), the same spatial

visualizations as shown below can be generated with the inclusion of extra well data taken into account.



**Figure 86. The absolute mean contribution of original features on the last sequence gathered from correlation coefficient approximation.**

### Subtask 7.3: Conclusions

The collaboration between FIU and PNNL has led to a comprehensive exploration of machine learning and deep learning algorithms for identifying spatiotemporal relationships in Cr(VI) content between groundwater wells. Guided by data-driven insights, how groundwater wells impact each other as they change in behavior according to natural factors throughout the year were explained and visualized in spatial plots with the help of feature importance/contribution extraction from our models. Those models being Adaboost, LSTM, and CNN, with the LSTM model being the most capable in providing the best comparative prediction performance and interpretive insight via contribution extraction. The use of PCA and coefficient calculation using correlation loadings allows for the approximation of contributions of well features beyond just Cr(VI), additionally resulting in better prediction performance.

### Subtask 7.3: References

- [1] A. Sagheer and M. Kotb, ‘Time series forecasting of petroleum production using deep LSTM recurrent networks’, *Neurocomputing*, vol. 323, pp. 203–213, 2019.
- [2] G. Shanmugasundar, M. Vanitha, R. Čep, V. Kumar, K. Kalita, and M. Ramachandran, ‘A Comparative Study of Linear, Random Forest and AdaBoost Regressions for Modeling Non-Traditional Machining’, *Processes*, vol. 9, no. 11, 2021.

[3] M. Markova, ‘Convolutional neural networks for forex time series forecasting’, AIP Conference Proceedings, vol. 2459, no. 1, p. 030024, 04 2022.

[4] Scott M. Lundberg, & Su-In Lee (2017). A unified approach to interpreting model predictions. CoRR, abs/1705.07874.

## **Subtask 7.4: Publishing AI/ML models on AAML System**

### **Subtask 7.4: Introduction**

AAMLS (Advanced Automated Machine Learning System) is a system accessible through aamls.org as a website that users can utilize for the sake of creating models and predictions on any dataset, they seem fit to provide, without the need to know the slightest bit of programming [1]. Various options are available to the user in order to customize their modeling, with different modeling tasks separated into different modules. A time series regressive modeling task, like that of Subtask 7.3, would fall into the Regression module of AAMLS, for example. The main algorithm used within Subtask 7.3 was the long, short-term memory (LSTM) model, which is named LSTM-DENSE in AAMLS in reference to the architecture makeup of the algorithm [2].

### **Subtask 7.4: Objectives**

The objective of this subtask is to provide an accessible way to utilize the algorithms developed as part of Task 7 for individual purposes through an automated system via AAMLS.

### **Subtask 7.4: Methodology**

AAMLS already contains multiple algorithms for the handling of data within various problem areas. Hence, the structure is developed for the addition of a new algorithm in the system. Adding the LSTM-DENSE algorithm into AAMLS simply amounted to copying over the LSTM python code utilized in Subtask 7.3 to a block handling supported requests within the AAMLS AI engine and modifying a few database entries to make those engine options available to the user for selection.

### **Subtask 7.4: Results and Discussion**

The Figure below shows the UI of AAMLS with the addition of the LSTM-DENSE architecture used within Subtask 7.4.

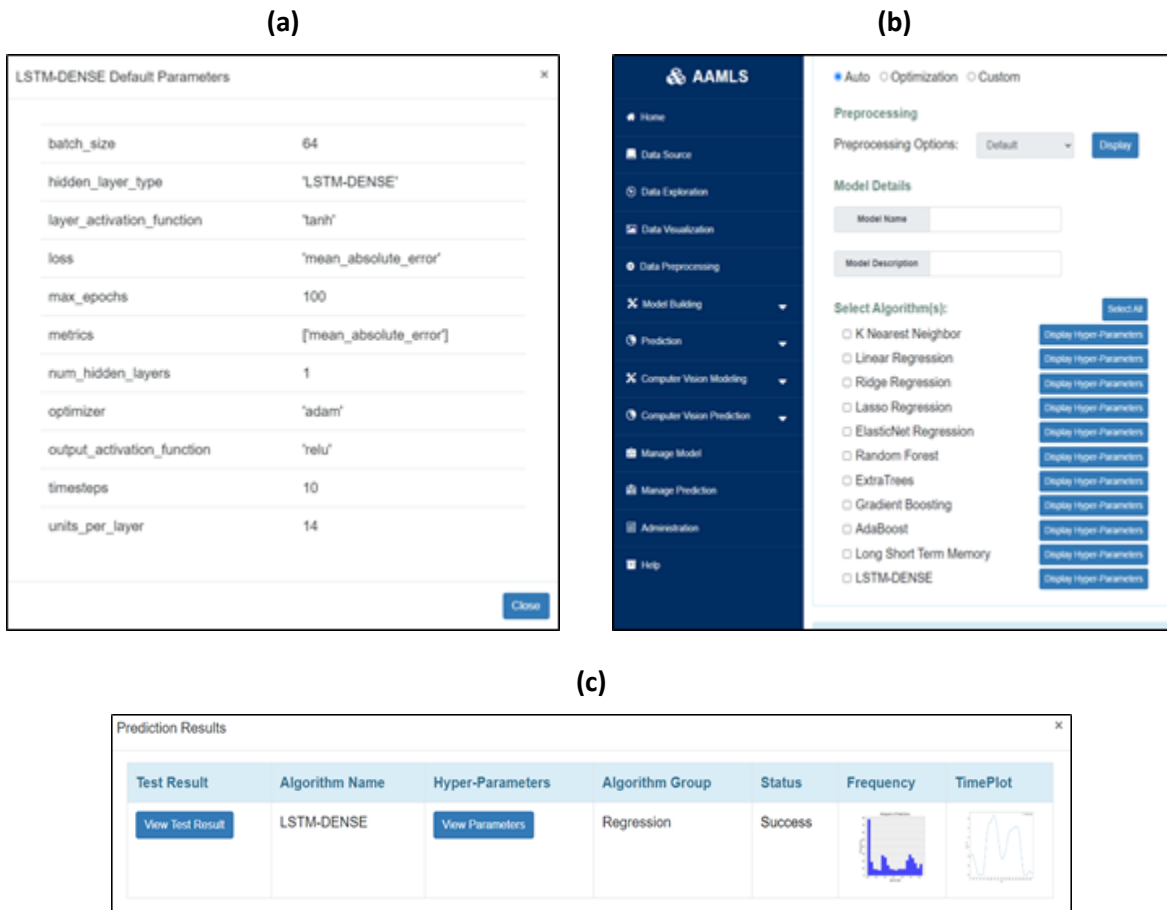


**Figure 87. Deployment of LSTM-DENSE algorithm within AAMLS: (a) has the default hyper parameters to use when building the model; (b) shows LSTM-DENSE as a selectable algorithm in the model building page of AAMLS; and (c) shows how results would look when predicting with the model built using LSTM-DENSE.**

### Subtask 7.4: Conclusions

AAMLS incorporated subtask’s 7.3 LSTM algorithm within the regression module under the name LSTM-DENSE. The implementation has been generalized to work with any time series data.

### Subtask 7.4: References

[1] Upadhyay, H., et al, "Advanced Automated Machine Learning System (AAMLS) -23265", 2023.

[2] A. Sagheer and M. Kotb, ‘Time series forecasting of petroleum production using deep LSTM recurrent networks’, Neurocomputing, vol. 323, pp. 203–213, 2019.

## **TASK 8 AI FOR EM PROBLEM SET (SOIL AND GROUNDWATER) - DATA ANALYSIS AND VISUALIZATION OF SENSOR DATA FROM THE WELLS AT THE SRS F-AREA USING MACHINE LEARNING (LBNL, SRNL)**

---

Task 8 is focused on creating a data interface module for the AI system. This kind of module assists in ingesting the time-series data from the sensors that the ALTEMIS project has deployed. Prior to the raw data from the sensors being used by the AI system, this module comprises of submodules like data exploration, visualization, and anomaly detection. The SRS area will serve as the initial development location for the AI system for pattern identification, prediction, and anomaly detection. SRS is the target site for sensor deployment under the ALTEMIS project. The AI system is fine-tuned and put through its tests using the time-series (Aqua TROLL 500 sensors) datasets made available by the recently deployed sensors. Regarding anomaly identification and time-series analysis. Lastly, these trained models are then deployed onto the Advanced Automated Machine Learning (AAML) System.

### **Subtask 8.6: Subtask 8.6: Publishing AI/ML models on AAML System**

#### **Subtask 8.6: Introduction**

FIU investigates Recurrent Neural Network - Long Short-Term Memory (RNN-LSTM) [1] and Auto Encoder. Other DOE sites with comparable sensor and AI system implementations can use the trained AI system. Successful models will be deployed on the AAML system.

#### **Subtask 8.6: Objectives**

The primary objective is the development and continuous refinement of cutting-edge AI/ML models. These models are specifically designed for accurately predicting contaminant concentrations and determining the most effective sensor placements in groundwater wells. This ambitious endeavor involves a series of iterative improvements to deep learning models. Central to this is the meticulous adjustment of input parameters and the optimization of training methods, tailored to enhance the models' predictive accuracy and reliability. The scope of the project is broad and dynamic, encompassing various aspects of machine learning and data analysis. A significant portion of the team's effort is dedicated to experimenting with Long Short-Term Memory (LSTM) architectures. This is particularly focused on the time series prediction of tritium concentrations, a challenging yet critical aspect of groundwater quality assessment. In parallel, the team is also actively involved in constructing a robust and efficient data pipeline. This pipeline is crucial for harnessing and processing data from the HydroVu sensor network, a key component in real-time groundwater monitoring. Addressing and overcoming challenges related to model accuracy forms a core part of the project. The team at FIU is not only developing different machine learning techniques but also delving into advanced methods like anomaly detection using LSTM models.



### Subtask 8.6: Methodology

FIU team worked on tweaking the Deep learning models for predicting contaminant concentrations. The updated highest performing models were then pushed to the AAML platform. The team experimented on the input parameters passed to the Deep learning models. Previously, the models relied on all 6 input parameters (pH, specific conductance, water temperature, water table, precipitation, and air temperature) to make predictions. Upon further inspection, there was no variance in the precipitation and air temperature data so that did not contribute any value to the model. For that reason, those two variables were removed entirely. There was also interest in exploring the importance of each input variable, along with the impact that a combination of inputs has on the overall output prediction. The four cases listed below were the first to be tested:

1. Train with input = all 4 in-situ variables at all wells
2. Train with input = all 4 in-situ variables at the prediction well
3. Train with input = specific conductance at all wells
4. Train with input = specific conductance at the prediction well

From these 4 tests, Case 2 produced the best result. This case trained all four variables, pH, specific conductance, water temperature, and water table, across all wells to predict each well’s contaminant levels one at a time. This most likely produced the best result due to having more spatial information embedded.

To visualize the individual performance of each model (each model predicts the contaminant concentration at one well), a new function was scripted to plot a spatial map of the site where the color of the dot represents the test set prediction error. This plot generated for Case 2 is shown in Figure 88.

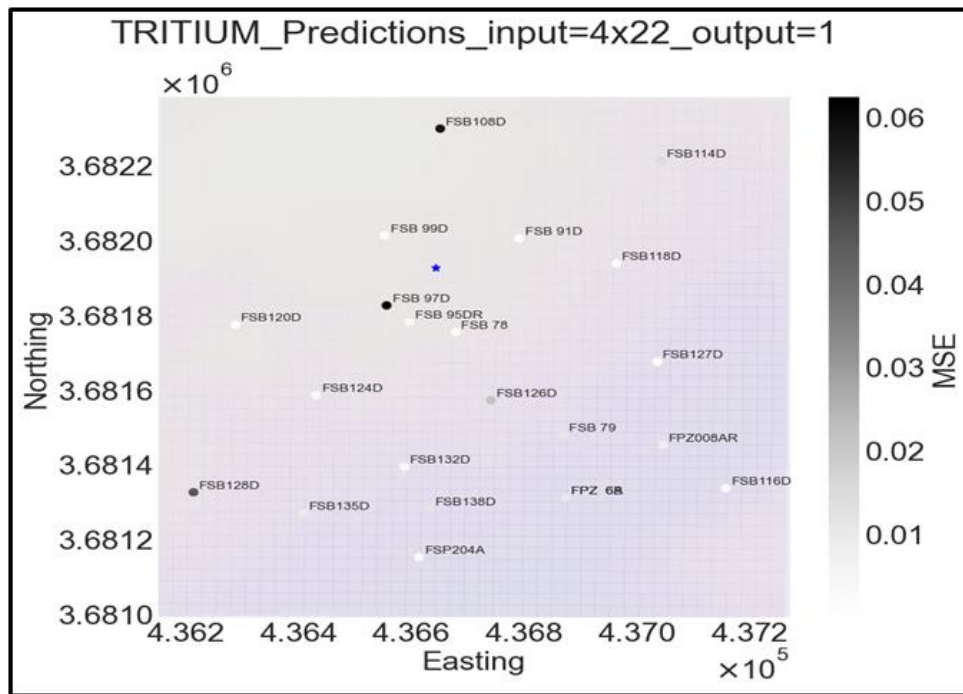
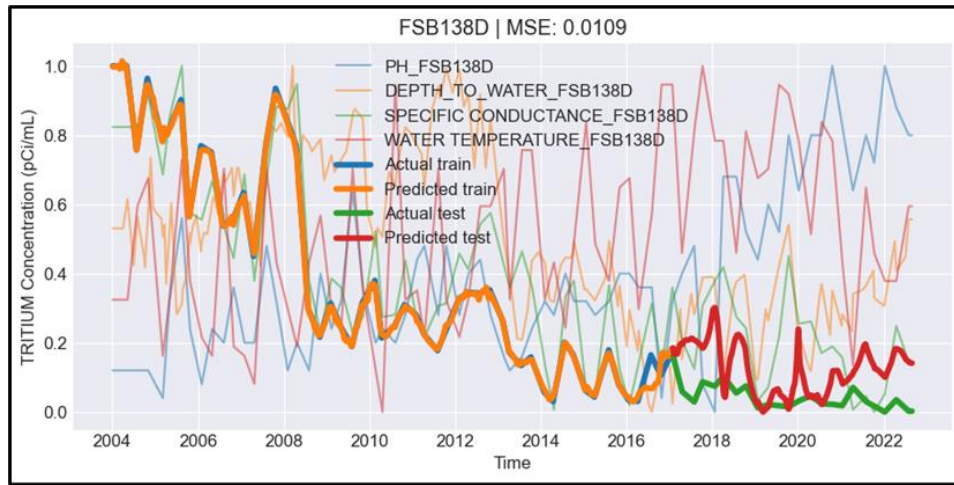


Figure 88. Spatial map of SRS F-Area with individual test prediction errors are shown as a colormap,

To demonstrate the predictive capability of these current models, a time series plot of the inputs (shown as the thin lines) and the target predictor, tritium (shown as the thick line) for well FSB138D, is shown in Figure 89. The plot shows the scaled version of the data, where each time series is individually normalized to values between 0 and 1.



**Figure 89. FSB138D tritium prediction using all 4 input variables at all 22 wells.**

For testing the importance of each input variable on the output prediction, FIU ran the model on the powerset of the 4 input parameters. A powerset is the set that contains all subsets of a given set. This should include  $4^2 - 1 = 15$  experiments. The value 1 was removed from  $4^2$  since this includes the empty set which is no input. To compare the performance of each experiment, the MSE of all 22 well predictions was aggregated using both the average and sum, although these two metrics show the same trend. This comparison is plotted as a bar graph below in Figure 90. From this analysis, specific conductance is shown to be the most important individual input to the model as it appears in the top 7 of the 15 experiments. In addition, the three experiments that overall had a better MSE than the experiment with specific conductance as the only variable, performed only slightly better which is negligible.

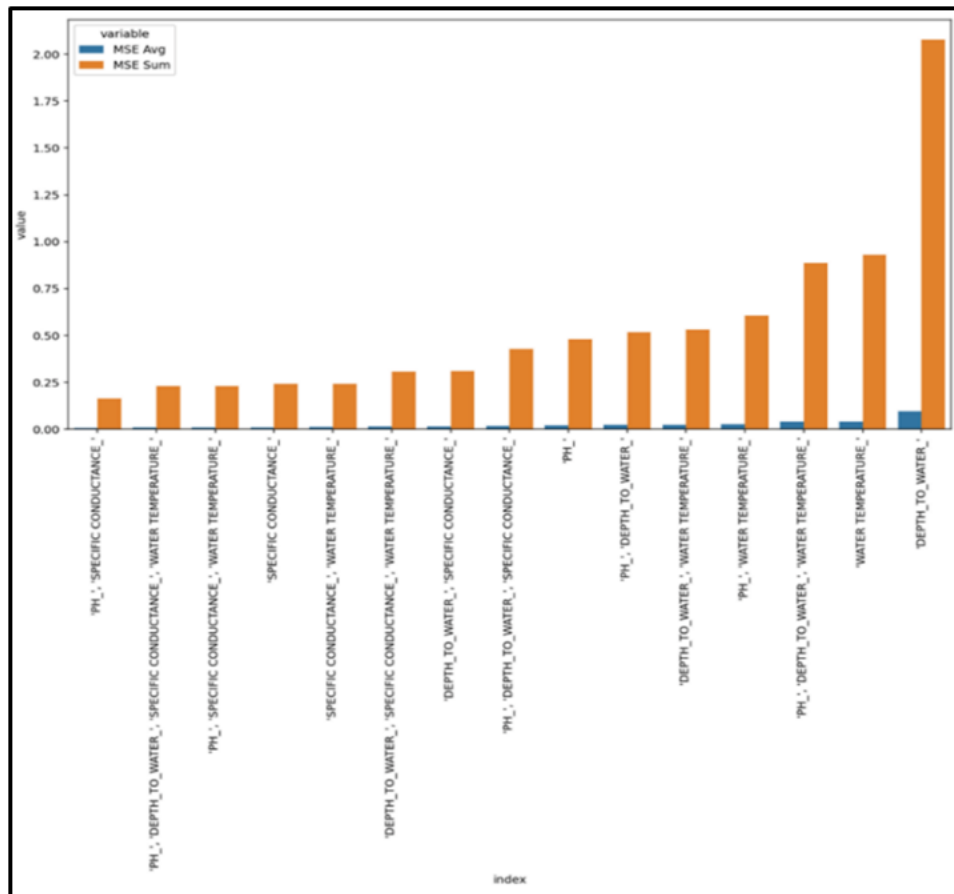


**Figure 90. Comparison of the powerset of inputs on prediction.**

The team also worked on using historical tritium concentration time series to predict future concentrations. The idea behind this research and implementation is to see how well historical information can influence future levels of tritium. To implement this in python, the FIU team started with the same LSTM architecture previously used for predicting tritium using in situ variables, aside from the number of input layers for the time component. This implementation was initiated with an input of 30 days to predict the next 30 days. Previously, the prediction was simply one day in advance, so this is an introduction of multi-timestep prediction. For training purposes, the training time series data was transformed into a series of 30-day inputs and outputs, shifting the time step by one day. By shifting the time step by one day, the number of training samples is maximized. For example, the first sample might be:

$$\text{Input: } \{t-60, t-59, \dots, t-32, t-31\} \quad \text{Output: } \{t-30, t-29, \dots, t-2, t-1\}$$

The second sample might be:

$$\text{Input: } \{t-59, t-58, \dots, t-31, t-30\} \quad \text{Output: } \{t-29, t-28, \dots, t-1, t\}$$

For testing purposes however, our time shift is equal to the number of output time steps. Since the testing case mimics what we would see in reality, we want to make an initial prediction to predict the next 30 days, and then use that same prediction to make an inference on the next 30 days after that, and so on. In other words, our testing case will be structured like this:

$$Y(\{t+1,t+2,\dots t+29,t+30\}) = \mathbf{model}(\{t-29,t-28,\dots,t-1,t\})$$

$$Y(\{t+31,t+32,\dots t+59,t+60\}) = \mathbf{model}(Y(\{t+1,t+2,\dots t+29,t+30\}))$$

As can be seen, the previous prediction was used as input to the subsequent predictions. This strategy was implemented in python and tested on the tritium time series at well FPZ 6A. The results on the training set deviated substantially from the ground truth as can be seen in Figure 91. The predicted line does not remotely follow the ground truth trend.

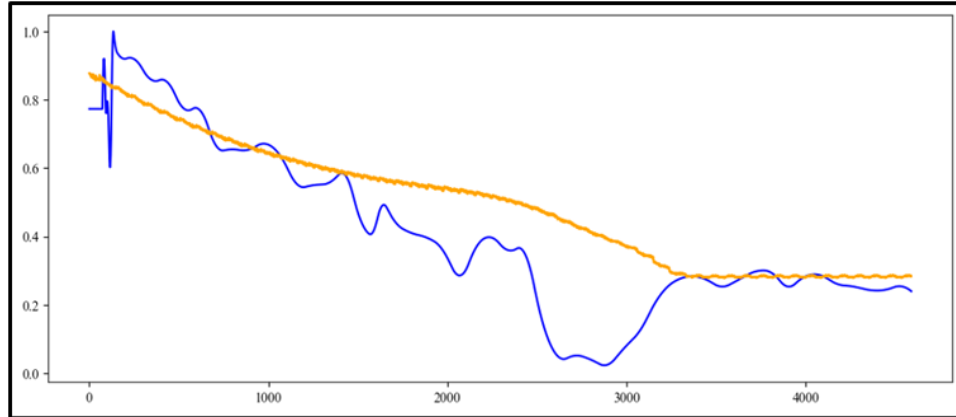


**Figure 91. Tritium prediction using previous architecture (relu activation).**

Next, the team focused on finalizing a Python script that could efficiently extract data from the HydroVu API and store it on an MS SQL server, using test API credentials. The script was designed to handle large amounts of data and to optimize data storage and retrieval. The team plans to request access to the real sensor data in January, which allowed them to further test and improve the script.

In addition, the team also began work on incorporating a time component as an additional feature in their Long Short-Term Memory (LSTM) model. The LSTM model is a type of Recurrent Neural Network (RNN) that is well-suited for timeseries data, such as that generated by the HydroVu sensor network. The team has been utilizing a simple sine wave to ensure that the model is functioning correctly before proceeding with the implementation of real well sensor data. The use of sine wave data allows the team to evaluate the model's ability to predict future values based on historical data, which is a crucial aspect for the successful prediction of water level in the wells. The added feature is depicted in Figure 92.

timestamp	sin_input
0	1.000000
1	1.009601
2	1.019201
3	1.028799
4	1.038394
...	...
9995	1.989790
9996	1.988376
9997	1.986871
9998	1.985275
9999	1.983568

**Figure 92. Added feature to the input of the LSTM model.**

Furthermore, the team has been exploring the use of various techniques to improve the performance of their LSTM model. These techniques include: the use of dropout layers, which are used to prevent overfitting by randomly dropping out a fraction of the neurons during training; regularization, which is used to prevent overfitting by adding a penalty term to the loss function; and increasing the number of hidden layers, which increases the model's capacity to learn. The team has also been experimenting with different optimizers, such as Adam, RMSprop and Adagrad, and learning rates to improve the model's accuracy.

For analyzing the mean difference, a function was written which takes the mean of all the values in a previous year and for a specific well. This mean value is compared with the current year's in-situ data to check the mean difference in the sensor value. This operation is performed for three different analytes namely pH, specific conductance, and depth to water. The team has also written a function to perform linear regression analysis for three different analytes with varied year data. The R-squared value for pH is 0.002, for specific conductance is 0.678 and for depth to water is 0.767, as shown in Figure 93, Figure 94 and Figure 95 respectively.

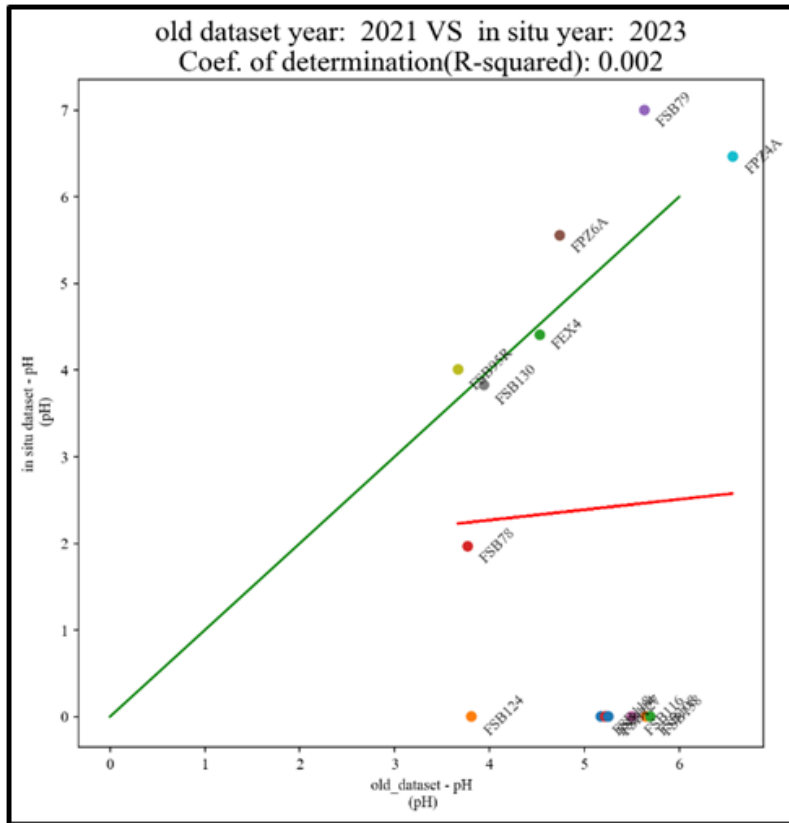


Figure 93. Linear regression model for pH.

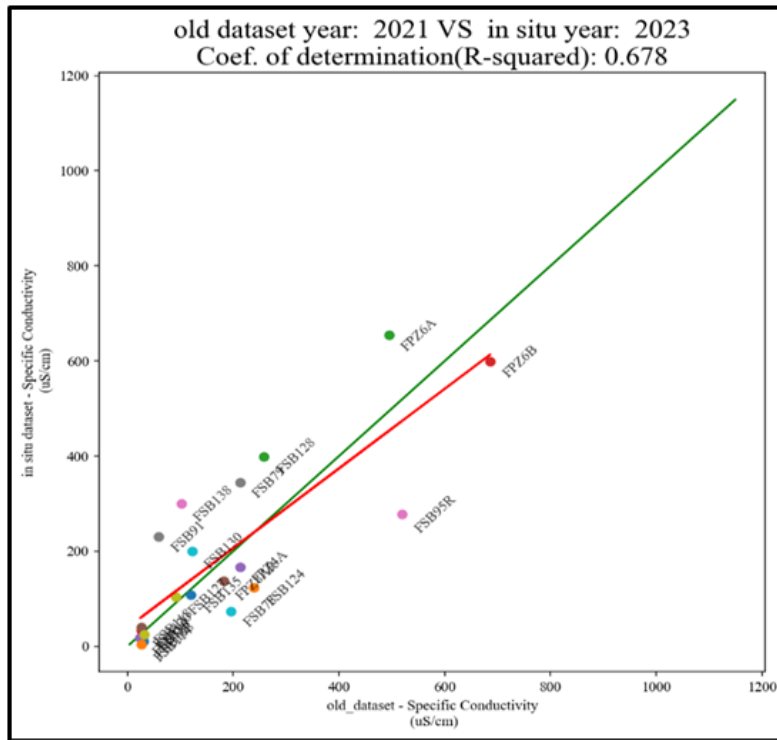


Figure 94. Linear regression model for specific conductivity.

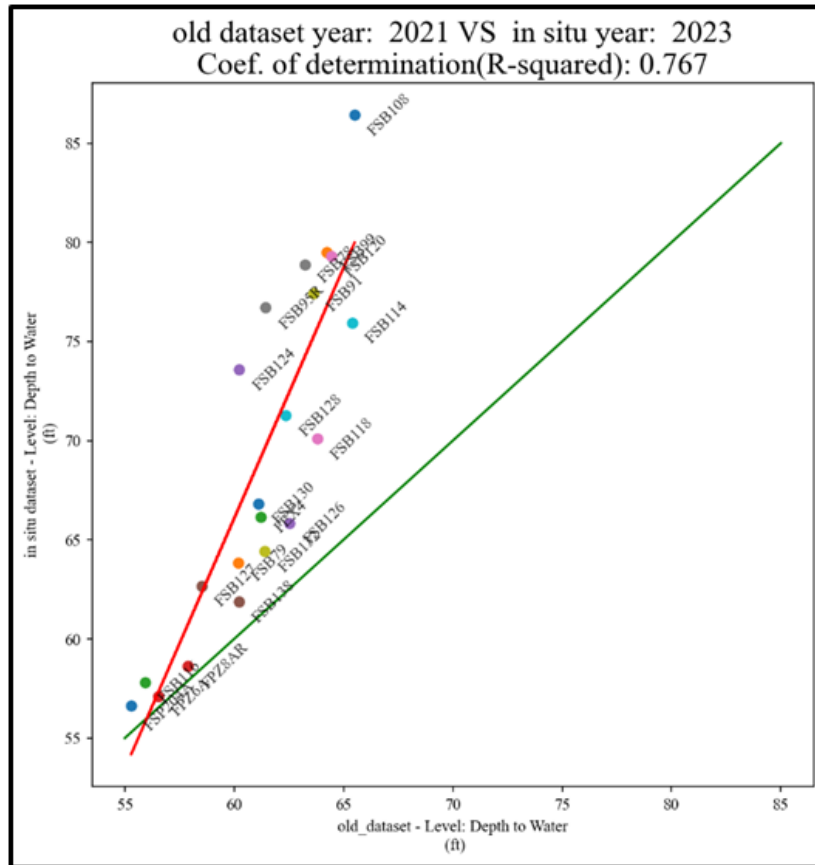


Figure 95. Linear regression model for depth to water.

***Python Script for Downloading In-Situ Data from HydroVu API***

The Python script carries out three primary functions to retrieve data from the HydroVu API and store it in the FIU-ALTEMISAI database. Firstly, the script uses the pyodbc module to establish a connection to the database and retrieve the last recorded time step for each well. Next, the script sends requests to the HydroVu API to retrieve data and saves it to a temporary folder before formatting the data and storing it in the master\_json list. Finally, the script uses a SQL INSERT statement to insert the data into the FIU-ALTEMISAI database and commit the changes.

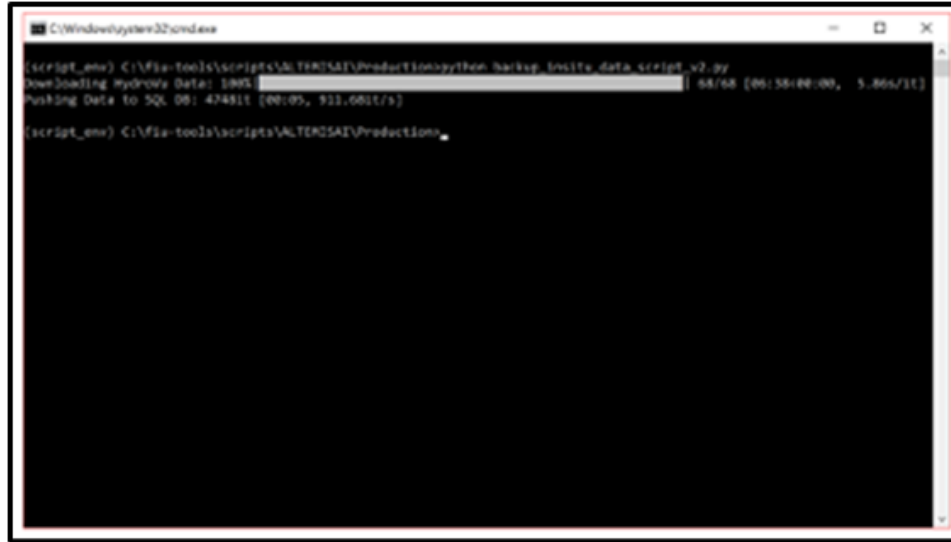
To perform these functions, the script imports various Python modules, such as requests, json, time, pandas, os, pyodbc, and tqdm, and uses the HydroVu API to retrieve the data. The script sets the maximum number of retries, time between retries, and timeout using the MAX\_RETRIES, RETRY\_SLEEP\_SECONDS, and TIMEOUT\_SECONDS variables, respectively.

Before retrieving the data, the script checks whether a 'temp' folder exists in the script directory and creates it if it does not exist. The script then retrieves access tokens and sends requests to the HydroVu API to retrieve friendly names associated with the sensors and a list of locations. If there are multiple pages of data, the script uses a 'while' loop to retrieve data for each page and a 'for' loop to retrieve data for each location ID.

For each location ID, the script sends a GET request to the HydroVu API to retrieve the data and checks if the request is successful. If the request fails, the script retries the request a maximum of MAX\_RETRIES times with a sleep period of RETRY\_SLEEP\_SECONDS seconds between each



retry. The script saves the data to a CSV file in the 'temp' folder, formats the data, and appends it to the master\_json list. Lastly, the script inserts the data into the FIU-ALTEMISAI database using a SQL INSERT statement and commits the changes. The script also uses the tqdm library to provide a progress bar of the status of the downloading process. This can be seen in Figure 96 as the script is running.



```

C:\Windows\system32\cmd.exe
(script_ame) C:\Vfa-tools\scripts\ALTEMISAI\Production\Then backup_0nline_data_script_v2.py
Downloading hydrova data: 1895
Pushing Data to SQL DB: 474811 (00:05, 911.6811/s)
(script_ame) C:\Vfa-tools\scripts\ALTEMISAI\Production\

```

**Figure 96. Screenshot of command line that runs the python script.**

The ALTEMISAI Database was created as an SQL database to store all the information. Three tables were created. The first table, SensorData, is the main table where data is stored, and it contains several columns such as location ID, sensor type, timestamp, and various sensor readings such as temperature, pH, and conductivity. The second table, SensorMetadata, contains information about the sensor locations such as latitude, longitude, and well name. The third table, SensorUnits, stores the units of measurement for each parameter/analyte.

The FIU team continued to work on improving the Python script responsible for downloading the in-situ data provided by the HydroVu API. Version 3 (v3) of the script was developed, which included several changes and updates to the code.

The first significant change was the renaming of all the table names in the ALTEMISAI database. The tables were renamed, adding “SRS\_” in front of each name to improve readability and ease of use. For example, “SensorData” became “SRS\_SensorData”. The variables in the tables were also updated to be in a standard format. A camel case was used, where each variable name (column in the tables) has no spaces and starts with capital letters for each word. For example, “Battery Level” became “BatteryLevel”. Some names were also changed to be more standard. For instance, “% Saturation O<sub>2</sub>” became “PercentSaturationO<sub>2</sub>”, and “Level: Depth to water” became “DepthToWater”.

Another major change was the development of a stored procedure for efficiently accessing and filtering the data in the SQL database as shown in Figure 97. The stored procedure SensorData\_GetSensorDataByDateRangeAndWellNameAndSensorType takes four input parameters: @StartDate, @EndDate, @WellName, and @SensorType. The stored procedure filters data based on these input parameters and returns the results. The stored procedure shown in

Figure 97 minimizes the number of lines of code required to filter data and makes it more efficient to retrieve specific data from the database.

```

USE [ALTEHISAI]
GO
/***** Object: StoredProcedure [dbo].[SensorData_GetSensorDataByDateRangeAndWellNameAndSensorType]  Script Date: 3/14/2023 2:55:06 PM *****/
SET ANSI_NULLS ON
GO
SET QUOTED_IDENTIFIER ON
GO

ALTER PROCEDURE [dbo].[SensorData_GetSensorDataByDateRangeAndWellNameAndSensorType]
    @StartDate datetime = null,
    @EndDate datetime = null,
    @WellName nvarchar(50) = null,
    @SensorType nvarchar(50) = null
AS
BEGIN
    SET NOCOUNT ON;

    SELECT * FROM SensorData
    WHERE (@StartDate IS NULL OR COLLECTION_DATE >= @StartDate)
    AND (@EndDate IS NULL OR COLLECTION_DATE <= @EndDate)
    AND (@WellName IS NULL OR STATION_ID = @WellName)
    AND (@SensorType IS NULL OR sensor_type = @SensorType)
END
    
```

**Figure 97. Screenshot of SQL stored procedure for efficiently accessing and filtering the data in the SQL database.**

The team also conducted several tests on the script and the stored procedure to ensure that they functioned correctly. The tests included checking the validity of the data and the time taken to retrieve data from the database. The tests were successful, and the team is confident in the script and stored procedure's performance.

To standardize the station IDs (well names), a function was written called *remove\_unwanted\_zeros\_and\_spaces* that removes unwanted zeros and spaces from the station ID strings. This function ensures that different sources of data with slightly different station ID formats can be linked together to access the desired information. Figure 98 shows the code for the function.

```

def remove_unwanted_zeros_and_spaces(s):
    s = s.replace(' ', '')
    pattern = r'(?<!\d)0+|\b0+'
    # Explanation of the regular expression pattern:
    # (?<!\d)0+ matches one or more zeros that are not preceded by a digit
    # \b0+ matches one or more zeros that appear at the beginning of the string
    # or after a non-word character (such as a space or punctuation)
    # The | symbol means "or"
    return re.sub(pattern, '', s)
    
```

**Figure 98. Screenshot of the code for the function *remove\_unwanted\_zeros\_and\_spaces*.**

For example, the station IDs "FEX 4" and "FEX004" would be transformed into "FEX4", and "FSB0120D" would become "FSB120D". It is expected that this standardized naming scheme will facilitate data processing and analysis going forward.

In addition to standardizing station IDs, we also started examining ways to deal with the fluctuating nature of sensor data for machine learning. Specifically, we explored different resampling and interpolation combinations that could affect the "smoothness" of time series data for two variables: "Depth to Water" and "Specific Conductance". A code was written to plot four sample time series for "Depth to Water", which can be seen in Figure 99. The same thing for "Specific Conductance" was also plotted, shown in Figure 100.

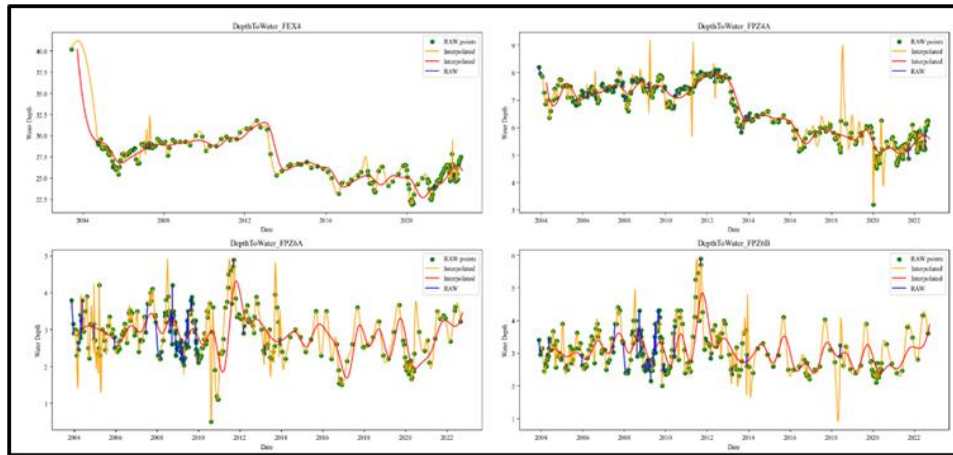


Figure 99. Sample time series for "Depth to Water".

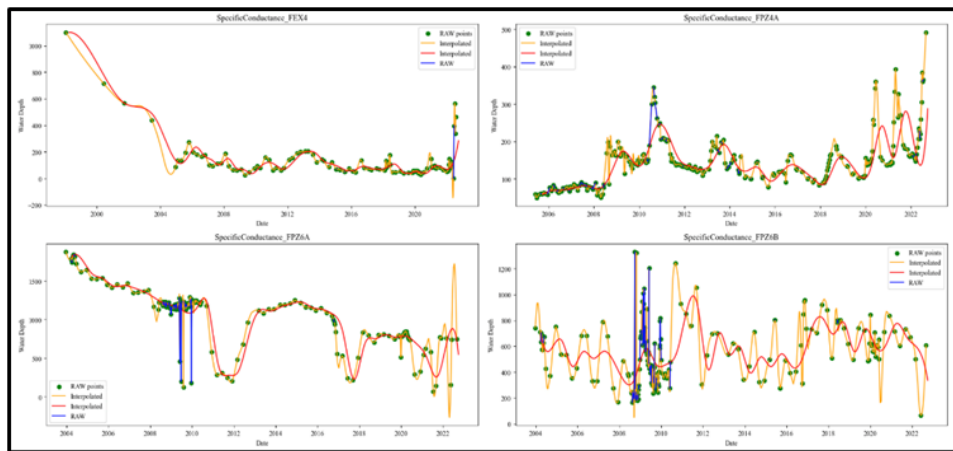


Figure 100. Sample time series for "Specific Conductance".

**Subtask 8.6: Results and Discussion**

**LSTM Model Analysis for Anomaly Detection**

The team started with an LSTM model for anomaly detection specifically for a well named FAI11D. The analysis focused on two different analytes: Specific Conductivity and DepthToWater. These analytes were chosen because they had the highest number of non-null rows, indicating they were the most reliable measurements for anomaly detection.

The LSTM model was configured with the following settings:

Look Back: 7

The look back value determines the number of previous time steps that the LSTM model takes into account when making predictions. In this case, the model considered the past 7 time steps to detect anomalies.

Number of LSTM Layers: 1

The LSTM model consisted of a single layer. Each layer in an LSTM network contains LSTM cells, which are responsible for capturing and remembering long-term dependencies in the data.

Number of LSTM Cells: 10

The LSTM layer had 10 LSTM cells. Each cell processes input data and produces an output based on its internal state and the input from the previous time step.

Activation Function: Rectifier Linear Unit (ReLU)

The ReLU activation function was used within the LSTM cells. ReLU is a commonly used activation function that introduces non-linearity to the model by mapping negative values to zero and leaving positive values unchanged.

Optimizer: Adam

Adam is an optimization algorithm commonly used for training deep neural networks. It combines the advantages of adaptive learning rates and momentum methods to efficiently update the model's weights during training.

Loss: Mean Square Error (MSE)

Mean Square Error was chosen as the loss function for training the LSTM model. It calculates the average squared difference between the predicted values and the actual values, providing a measure of how well the model is performing.

By training this LSTM model with the specified configurations on the data from well FA111D, the aim was to detect anomalies in Specific Conductivity and DepthToWater measurements.

Figure 101 and Figure 102 provide visual representations of the LSTM model's performance during training for Specific Conductivity and DepthToWater, respectively. Each epoch represents a complete pass through the entire training dataset, where the model updates its parameters based on the optimization algorithm (Adam) and the chosen loss function (Mean Square Error).

```

Epoch 1/15
98/98 [=====] - 5s 10ms/step - loss: 43490.4766
Epoch 2/15
98/98 [=====] - 1s 10ms/step - loss: 13388.1348
Epoch 3/15
98/98 [=====] - 1s 9ms/step - loss: 2669.2153
Epoch 4/15
98/98 [=====] - 1s 10ms/step - loss: 333.4617
Epoch 5/15
98/98 [=====] - 1s 9ms/step - loss: 104.1066
Epoch 6/15
98/98 [=====] - 1s 10ms/step - loss: 80.1562
Epoch 7/15
98/98 [=====] - 1s 10ms/step - loss: 67.5764
Epoch 8/15
98/98 [=====] - 1s 10ms/step - loss: 84.5496
Epoch 9/15
98/98 [=====] - 1s 10ms/step - loss: 82.9108
Epoch 10/15
98/98 [=====] - 1s 10ms/step - loss: 81.6736
Epoch 11/15
98/98 [=====] - 1s 10ms/step - loss: 81.2435
Epoch 12/15
98/98 [=====] - 1s 11ms/step - loss: 80.7050
Epoch 13/15
98/98 [=====] - 1s 11ms/step - loss: 80.6323
Epoch 14/15
98/98 [=====] - 1s 11ms/step - loss: 80.5890
Epoch 15/15
98/98 [=====] - 1s 10ms/step - loss: 80.4454
    
```

**Figure 101. LSTM model's performance for Specific Conductivity.**

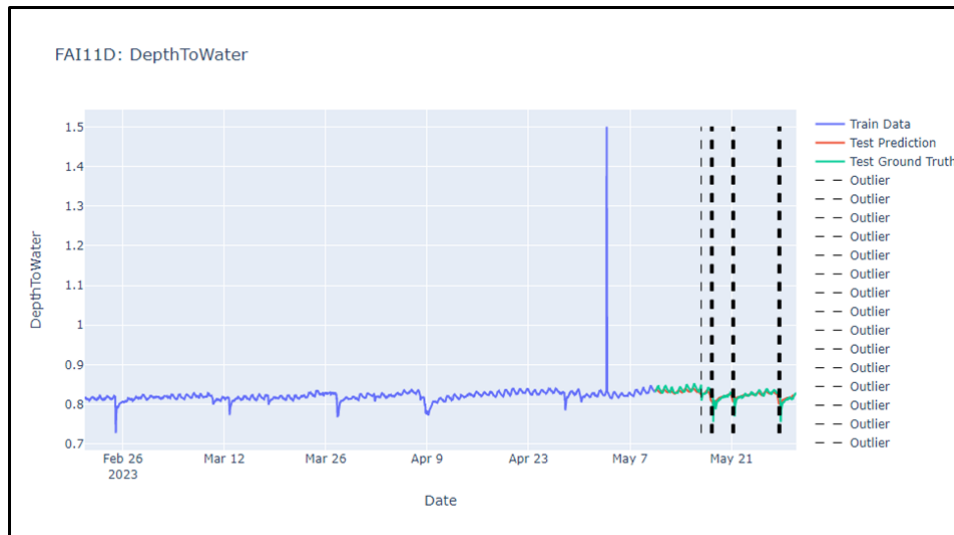
```

Epoch 1/10
98/98 [=====] - 4s 10ms/step - loss: 0.2305
Epoch 2/10
98/98 [=====] - 1s 10ms/step - loss: 3.3540e-04
Epoch 3/10
98/98 [=====] - 1s 10ms/step - loss: 2.8541e-04
Epoch 4/10
98/98 [=====] - 1s 10ms/step - loss: 2.8288e-04
Epoch 5/10
98/98 [=====] - 1s 10ms/step - loss: 2.8437e-04
Epoch 6/10
98/98 [=====] - 1s 10ms/step - loss: 2.8351e-04
Epoch 7/10
98/98 [=====] - 1s 10ms/step - loss: 2.8307e-04
Epoch 8/10
98/98 [=====] - 1s 10ms/step - loss: 2.8222e-04
Epoch 9/10
98/98 [=====] - 1s 10ms/step - loss: 2.8334e-04
Epoch 10/10
98/98 [=====] - 1s 11ms/step - loss: 2.8373e-04
    
```

**Figure 102. LSTM model's performance for DepthToWater.**



**Figure 103. Time Series of Specific Conductivity with LSTM Predictions and Outlier Detection.**



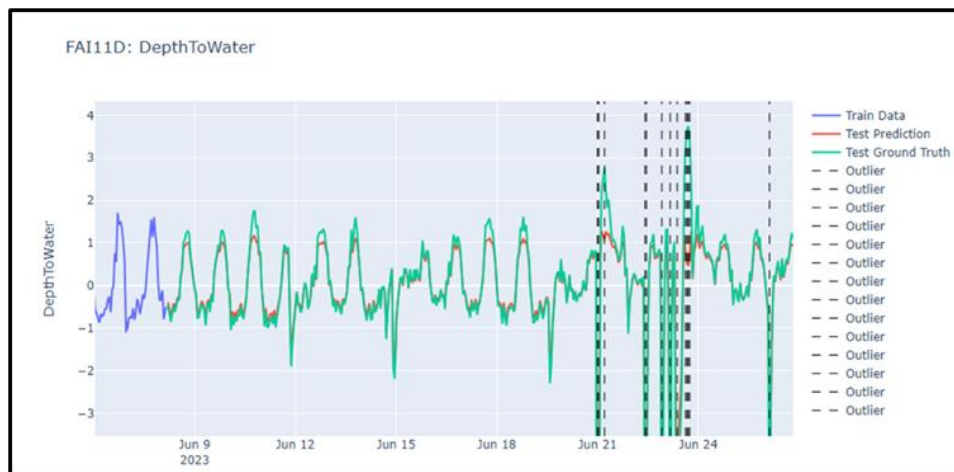
**Figure 104. Time Series of DepthToWater with LSTM Predictions and Outlier Detection.**

Figure 103 and Figure 104 provide a visual representation of the time series data for Specific Conductivity and DepthToWater respectively, along with the LSTM model's predictions and the detection of outliers. It allows for a comparative analysis of the actual values, predicted values, and the presence of anomalies. The green line in the figure represents the actual Specific Conductivity values observed over time. These values are typically obtained through measurements or observations in the real-world setting. The red line represents the LSTM model's predictions for the Specific Conductivity values during the testing phase. These predicted values are generated by the LSTM model based on the learned patterns and relationships in the training data. The black dotted line in the figure represents the outlier threshold. It serves as a reference line to visually identify data points that fall outside the normal range or show unusual behavior. Points above or below this threshold line are considered potential outliers. By comparing the green line (actual values) and the red line (predicted values), one can assess the model's accuracy in capturing the underlying patterns and dynamics of the Specific Conductivity data. If the red line closely follows the green line, it suggests that the LSTM model has successfully learned the patterns and can effectively predict the values. However, significant deviations between the red



and green lines may indicate the presence of anomalies or inaccuracies in the predictions. The presence of outliers can be identified by observing the data points that cross or fall outside the black dotted line. These outliers represent instances where the Specific Conductivity values deviate significantly from the expected or normal range. Detecting these outliers is crucial for identifying unusual or anomalous behavior in the data.

The team worked on an advanced LSTM model specifically tailored to comprehend intricate sensor sequence data pertaining to ‘depth to water’ measurements. A primary challenge in working with sequential data lies in determining the lookback required for the model to comprehend patterns. During the training phase, a vast array of lookback values was explored to ensure the model adeptly captures nuanced temporal patterns. The experiments were systematic, and the chosen values were aimed to enhance the predictive accuracy of the model. FIU’s research team invested significant efforts in preprocessing. Techniques implemented include Smoothing, Differencing and Normalization. Another innovative step was the application of the Interquartile Range (IQR) – a measure of statistical spread between the 25th and 75th percentile. This was pivotal in outlier detection and removal from our training data. By eliminating such outliers, we conferred additional robustness to our model's training, enhancing its generalization capabilities and predictive performance. Figure 105 shows the prediction from the LSTM model with the application of pre-processing techniques.



**Figure 105. LSTM Model Prediction with Pre-Processing.**

Next, the WaterLevel in numerous wells has undergone significant fluctuations. To elucidate these changes, an animated plot was meticulously crafted using data sourced via the Subsurface Insights API Key. This animation provides a day-by-day depiction of WaterLevel in each well, allowing viewers to effortlessly track its daily shifts. The dynamic nature of this animated representation not only captures the nuanced intricacies of WaterLevel variations but also aids in discerning overarching patterns or sudden, drastic shifts that might otherwise go unnoticed in static data sets.

The primary motivation behind this enhancement is to bolster rapid identification of potential concerns, enriching the user's interpretative experience. When anomalies are visually discernible, it empowers stakeholders and decision-makers with the ability to swiftly address issues, ensuring the sustained functionality and safety of the wells. As we forge ahead, it will be pivotal to perpetually update this animation with fresh data from Subsurface Insights. Figure 106 shows the snippet of WaterLevel data for each well on an hourly basis.



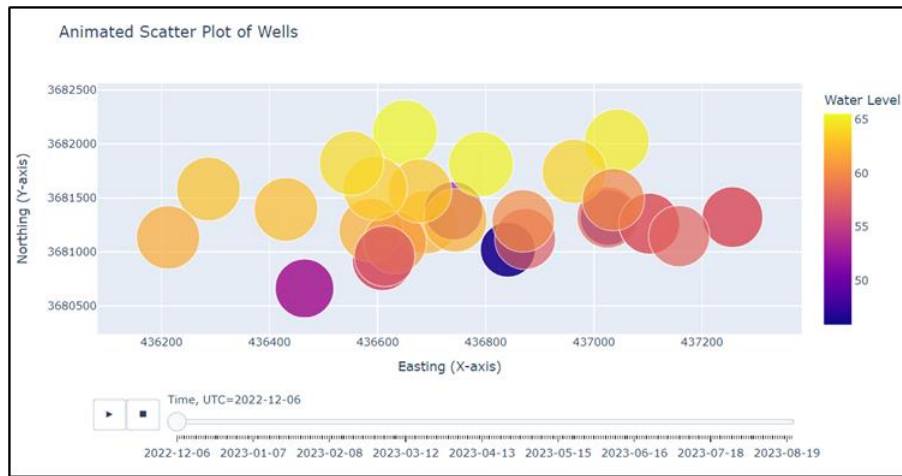


**Figure 106. WaterLevel data for each well.**

At FIU, the team delivered a tech talk on AI/ML research support for Advanced Long-Term Environmental Monitoring Systems (ALTEMIS). This presentation highlighted the crucial intersection of artificial intelligence and machine learning with environmental monitoring, underscoring their potential in enabling long-term, sustainable monitoring solutions. Furthermore, one of the team members was also a key speaker at RemPlex's 2023 Global Summit, held in collaboration with the International Atomic Energy Agency at PNNL. Here, they focused on the application of Long Short-Term Memory (LSTM) networks for anomaly detection in environmental monitoring sensor time series data. Adding to these achievements, their paper was accepted for presentation at the prestigious Waste Management Symposia 2024, marking a significant contribution to the field.

**AAML Deployment:**

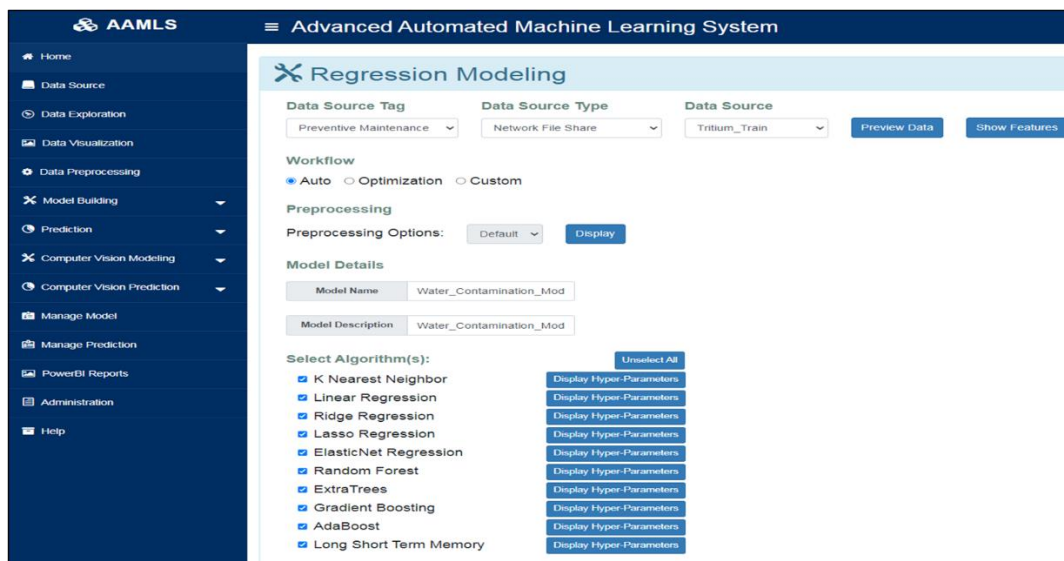


**Figure 107. AAML model development for water contamination dataset**

Validation Result	Algorithm Name	Hyper-Parameters	Algorithm Group	Metrics	Status	R2	TimePlot
<a href="#">View Validation Result</a>	K Nearest Neighbor	<a href="#">View Parameters</a>	Regression	MAE: 0.07 MSE: 0.02 RMSE: 0.15	Success		
<a href="#">View Validation Result</a>	Linear Regression	<a href="#">View Parameters</a>	Regression	MAE: 25.51 MSE: 950.57 RMSE: 30.83	Success		
<a href="#">View Validation Result</a>	Ridge Regression	<a href="#">View Parameters</a>	Regression	MAE: 25.52 MSE: 950.79 RMSE: 30.83	Success		
<a href="#">View Validation Result</a>	Lasso Regression	<a href="#">View Parameters</a>	Regression	MAE: 26.58 MSE: 1041.04 RMSE: 32.26	Success		
<a href="#">View Validation Result</a>	ElasticNet Regression	<a href="#">View Parameters</a>	Regression	MAE: 47.98 MSE: 3266.70 RMSE: 57.15	Success		
<a href="#">View Validation Result</a>	Random Forest	<a href="#">View Parameters</a>	Regression	MAE: 0.17 MSE: 4.37 RMSE: 2.09	Success		

Figure 108. AAML model validation results for water contamination dataset

Figure 109. AAML Prediction development for water contamination dataset

Prediction Results						
Test Result	Algorithm Name	Hyper-Parameters	Algorithm Group	Status	Frequency	TimePlot
<a href="#">View Test Result</a>	K Nearest Neighbor	<a href="#">View Parameters</a>	Regression	Success		
<a href="#">View Test Result</a>	Linear Regression	<a href="#">View Parameters</a>	Regression	Success		
<a href="#">View Test Result</a>	Ridge Regression	<a href="#">View Parameters</a>	Regression	Success		
<a href="#">View Test Result</a>	Lasso Regression	<a href="#">View Parameters</a>	Regression	Success		
<a href="#">View Test Result</a>	ElasticNet Regression	<a href="#">View Parameters</a>	Regression	Success		
<a href="#">View Test Result</a>	Random Forest	<a href="#">View Parameters</a>	Regression	Success		

Figure 110. AAML Prediction results for water contamination dataset

### Subtask 8.6: Conclusions

The team demonstrates significant progress in the development and refinement of AI/ML models for environmental monitoring at the SRS F-Area. They successfully employed advanced LSTM models for predicting contaminant concentrations in groundwater wells and anomaly detection, showing remarkable improvements in predictive accuracy and reliability. Innovations such as the efficient data pipeline from the HydroVu sensor network, the integration of complex machine learning techniques like multi-timestep prediction and preprocessing strategies and training of the LSTM model for anomaly detection have been pivotal in enhancing the model's performance. The project has not only made strides in the technical realm, but also contributed to the broader scientific community through tech talks, collaborations, and paper presentations. Moving forward, the team's focus on leveraging AI-driven methodologies for real-time monitoring promises to bring more accurate, timely, and actionable insights, significantly contributing to the sustainability of environmental management and protection strategies.

### Subtask 8.6: References

[1] A. Sagheer and M. Kotb, ‘Time series forecasting of petroleum production using deep LSTM recurrent networks’, *Neurocomputing*, vol. 323, pp. 203–213, 2019.

## **TASK 9: AI FOR EM PROBLEM SET (WASTE PROCESSING) - NUCLEAR WASTE IDENTIFICATION AND CLASSIFICATION USING DEEP LEARNING**

---

### **Subtask 9.1: Algorithm and Model Development to Identify and Classify Nuclear Waste**

#### **Subtask 9.1: Introduction**

Research was conducted to develop state-of-the-art Artificial Intelligence (AI) algorithms that are suitable for detecting nuclear waste, specifically, low level nuclear waste. The team built many models using recent advancements in Deep Learning (DL) like Vision Transformers and Convolutional Neural Networks among others. Because nuclear waste detection is a task from the real world, it can be represented as different computer vision tasks like object detection, instance segmentation, depth detection, unsupervised semantic segmentation, one shot object detection, among others. As such, each of the models developed represents a specialized approach to nuclear waste detection, where each approach has its own advantages and disadvantages. As such, these models provide an encompassing solution to nuclear waste identification where stakeholders can choose the model that fits their needs best.

#### **Subtask 9.1: Objectives**

The objective of this subtask is to implement algorithms and develop models that can identify the location of nuclear waste as well as determine what kind of object it is. The models developed were given to the FIU-DOE robotic team, so part of this task includes the development of scripts that allow for model predictions that can be integrated with ROS2.

#### **Subtask 9.1: Methodology**

The models researched as part of this task were: YOLOv7, STEGO, SD Mask R-CNN, and OWL-ViT. YOLOv7, STEGO, and OWL-ViT were pretrained on the COCO dataset which contains annotations for 80 classes of common objects. The team further finetuned the models in this dataset to increase their performance.



**Figure 111. Example of an image in the COCO dataset and its corresponding pixel masks.**

SD Mask R-CNN was pretrained on the WISDOM-SIM dataset which contains 50 classes of warehouse objects like flashlights, different types of cans and bottles, among others.

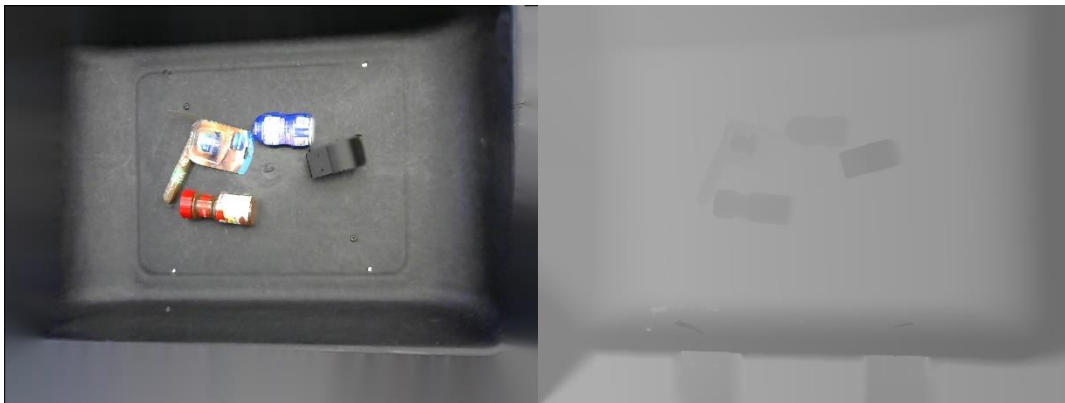


**Figure 112. Example of an image in WISDOM dataset and its corresponding disparity image.**

The projection heads of the models were then finetuned on a custom dataset internal to the FIU team which contains cans and bottles with different positions and arrangements. The goal of this dataset is to assess the model’s ability to detect new waste.





**Figure 113.** Example of an image in the custom dataset from the robotics team.

Since the models were going to be given to the FIU-DOE robotics team to integrate with their robots, the inference speed of the models should be close to real-time or real-time without a GPU. As such, as part of the data preprocessing, the size of the images was reduced to increase the inference speed. This caused a decrease in the performance of the models, but it was not significant enough to outweigh the speedup gains.

The size and variance of the datasets were increased through data augmentations. The team implemented flipping, rotating, cropping, zooming in, zooming out, among other data augmentations that represent realistic variations that the models are likely to encounter in the real world and as such, it would be beneficial for the model to learn to handle them during training.

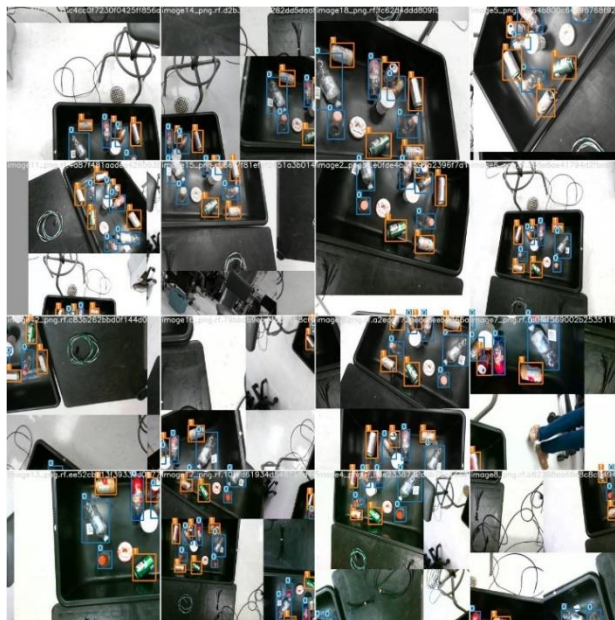


**Figure 114.** Example of augmentations applied to the dataset like mosaic, rotations, cropping, etc.

YOLOv7 was implemented for object detection and instance segmentation. Object detection refers to training the model to predict bounding boxes while instance segmentation refers to training the model to predict a pixel mask for each object in the input image. All YOLO algorithms work by

dividing an input image into equal NxN grid cells, where each cell is responsible for localizing and predicting the class of the object that it covers. Each of the grid predictions are then converted to bounding boxes, and those bounding boxes are filtered using IoU with the ground truth and NMS with other predicted boxes. This ensures that the model predicts bounding boxes that are close to the ground truth bounding boxes in space and quantity. For instance, with segmentation, the main difference lies in the head. The backbone is the same since the feature extraction process is the same, but the instance segmentation head uses ProtoNet to produce prototype masks instead of bounding boxes based on the anchors.

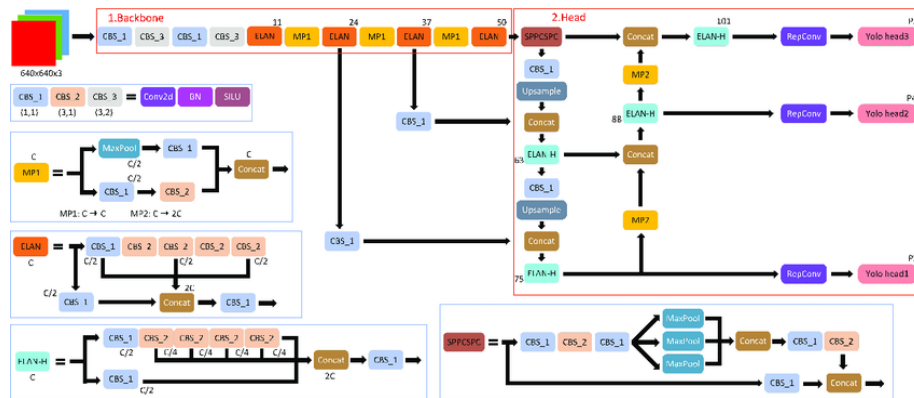


Figure 115. YOLOv7 architecture.

STEGO was implemented for unsupervised semantic segmentation where the model is trained without labels to predict the semantic mask for all objects in the input image that belong to the same class. The main idea of the algorithm is that similar image features placed together approximate the ground truth for instance segmentation without actually knowing the ground truth. During training the model takes two images as input, turns them into features using a Vision Transformer, and the similarity between those features is evaluated using cosine similarity, which results in feature correspondences. The features are also passed as input to the segmentation head that learns to amplify the structure of the features. The model does this procedure for combinations of an image with itself, and image with a similar image (determined using KNN), and an image with a random image to better learn how to amplify the feature correspondences. During prediction, the image and itself are used as an input, passed through the model, and the result is further refined using clustering with a CRF.

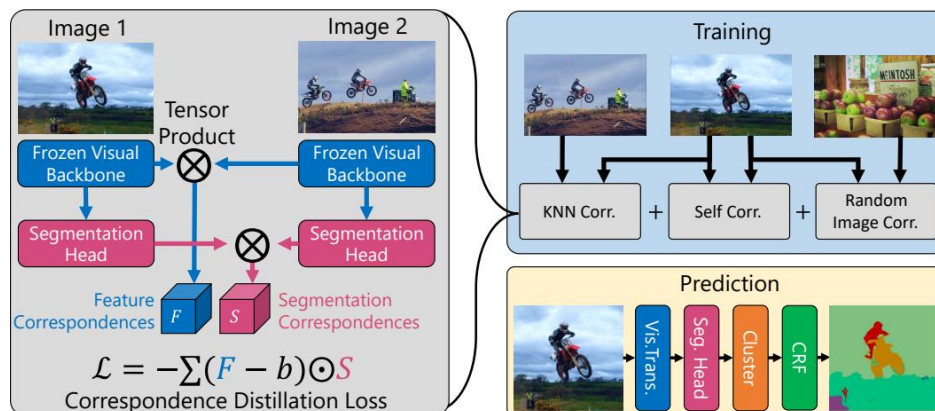


Figure 116. STEGO architecture.



SD Mask R-CNN was implemented for depth-based instance segmentation where the model is trained to predict pixel masks for each object in an input disparity image. The main idea of the algorithm is to leverage the information disparity (depth) images have that color RGB images do not. That is, using the information contained in the disparity image, the model learns how to detect foreground and background objects better than using RGB images. The architecture is not too different from conventional instance segmentation models. It uses Mask R-CNN which proposes regions of interest and then evaluates the regions of interest to find the corresponding masks. The main difference is that the input is a grayscale disparity image on three channels.

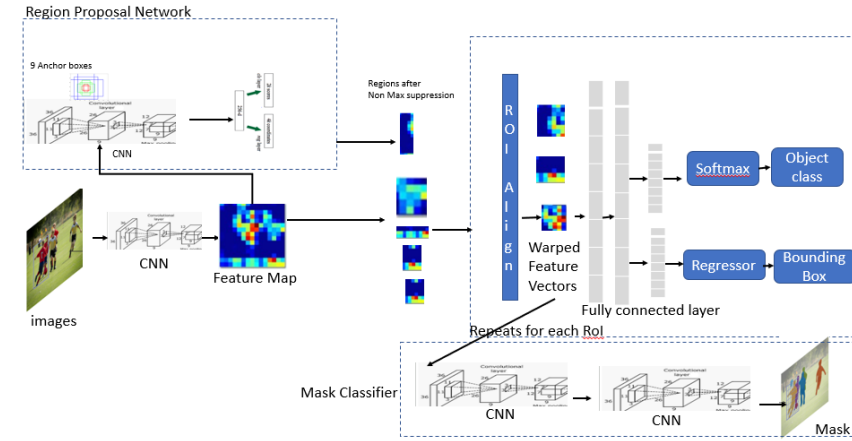


Figure 117. Mask R-CNN architecture.

OWL-ViT was implemented for one shot object detection where the model is not trained but simply takes as input a query image representing the object to be detected in the target input image. The main idea of this algorithm is to use vision transformers to extract embeddings for images. During training, a vision transformer outputs embeddings for images referring to the same objects and uses contrastive loss to adjust the embedding representation of the images such that similar images have similar representations and not similar images have not similar representations. Then, during prediction, these embeddings from the target image are projected using multilayer perceptron to predict bounding boxes. And the embeddings are passed through a separate multilayer perceptron which are then matched to the embeddings from the query image to predict object classes.

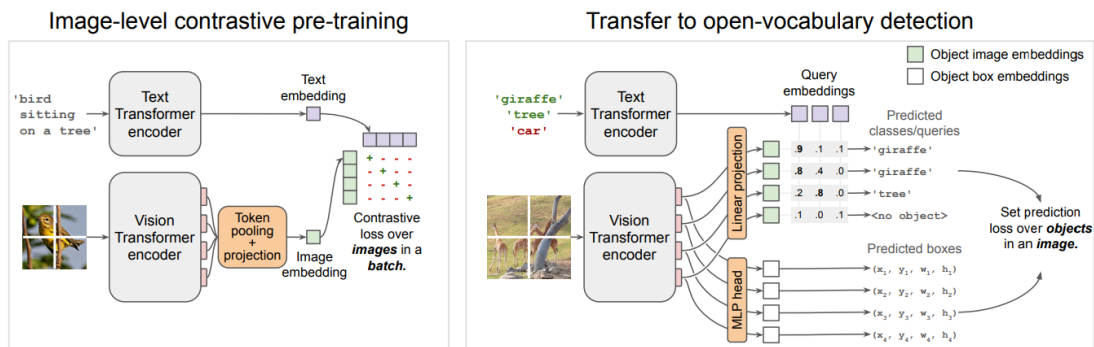
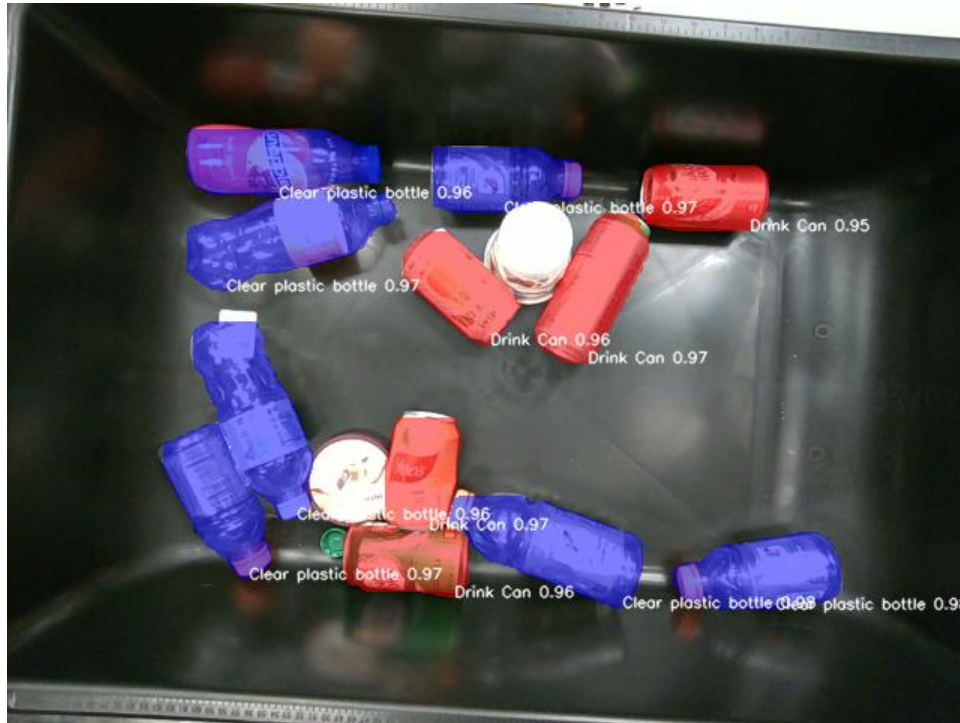


Figure 118. OWL-ViT Architecture for zero-shot object detection where the text transformers were replaced with vision transformers for one shot object detection.

### Subtask 9.1: Results and Discussion

Overall, the best performing model in terms of mean average prediction (mAP) was YOLOv7 for instance segmentation. However, this is not without some caveats.



**Figure 119. Example of the best results from the instance segmentation YOLOv7 model.**

For the instance segmentation of YOLOv7 to achieve this performance, it was trained for 200 epochs with a batch size of 32 on the labeled data with an image size of 640 by 640 pixels.

This means that to add a new object, large amounts of data about the object must be gathered and labeled. Then, the model must be retrained and finetuned and some care must be taken not to decrease the performance on other objects when adding the new object.

This is an issue for the detection of low-level nuclear waste because, by definition, low level nuclear waste is, by definition, not high-level radioactive waste, spent nuclear fuel, or byproduct materials. This means that, at any given point in time, there could be a need to detect a new object. And adapting the instance segmentation version of YOLOv7 to these new objects is a task that requires human resources and time.

Similarly, YOLOv7 for object detection has the same issues of struggling to quickly and easily adapt to the detection of a new object. And it underperforms YOLOv7 for instance segmentation on the custom FIU dataset.

The reason why the object detection version underperforms when compared to the instance segmentation version is due to the nature of the bounding boxes and the objects to be detected. When creating the bounding boxes for the bottles, the area covered by the bounding box includes both the bottle and the dark background. But, because bottles are thin and can be oriented in a diagonal, what happens is that the ground truth bounding box covers more of the background than of the bottle, which is the target object. As such, the model struggles to learn how to detect the

bottles because the information given by the ground truth is mostly background, which is not a good enough signal for the model.

Moving away from supervised learning, the team implemented STEGO, which is an unsupervised learning algorithm for semantic segmentation. STEGO was trained for 130 epochs with a batch size of 38 with 8 nearest neighbors without any labels. The results were quite good, resembling the results of YOLOv7 for instance segmentation.

However, when the objects are placed together, the STEGO model is unable to differentiate between them. This is an inherent flaw in semantic segmentation where all pixels that belong to the same class are given the same label and there is no way to differentiate between multiple objects that belong to the same.

And when the pixel masks are converted to convex polygons to provide the results to the FIU robotics team, this lack of differentiation between objects of the class results in convex polygons that have holes in them.



**Figure 120. Example of the results from STEGO where blue pixels are convex polygons and red pixels are the holes within the convex polygons.**

As such, STEGO can learn to detect new objects without needing large amounts of labeled data, but it still needs the data. And then, STEGO can make detections, but if the objects are clustered together, it will struggle to partition each object correctly, which may or may not be an issue depending on the stakeholders' needs.

To address the clustering issues with STEGO, the team implemented SD Mask R-CNN, which is an instance segmentation model that uses disparity or depth images. SD Mask R-CNN was trained for 150 epochs with a batch size of 64 on simulated and real data. The results were also quite good.

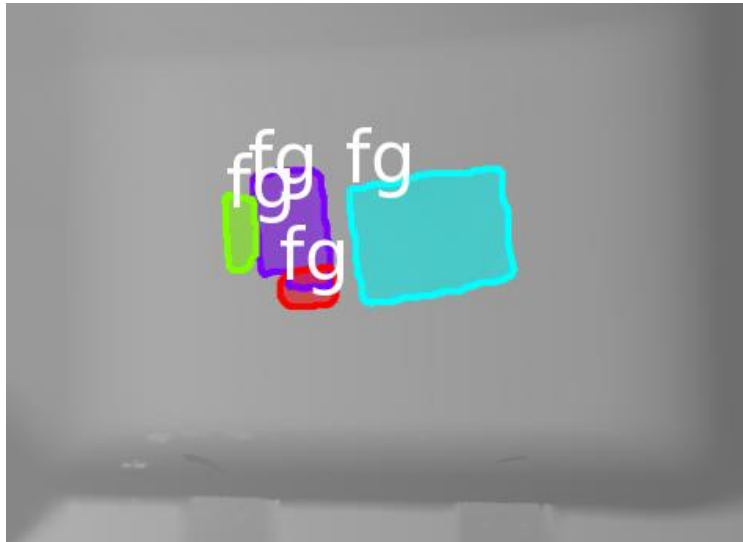


**Figure 121. Example of the results from SD Mask R-CNN.**

An advantage of SD Mask R-CNN is that it uses disparity images, for which data can be more easily simulated than with regular color images. This means that to add a new object, it is only needed to build a 3D mesh of the object. It is then possible to simulate dropping the object from different places and at different orientations into a bin. This can generate large amounts of labeled data without the human effort to gather and label the data.

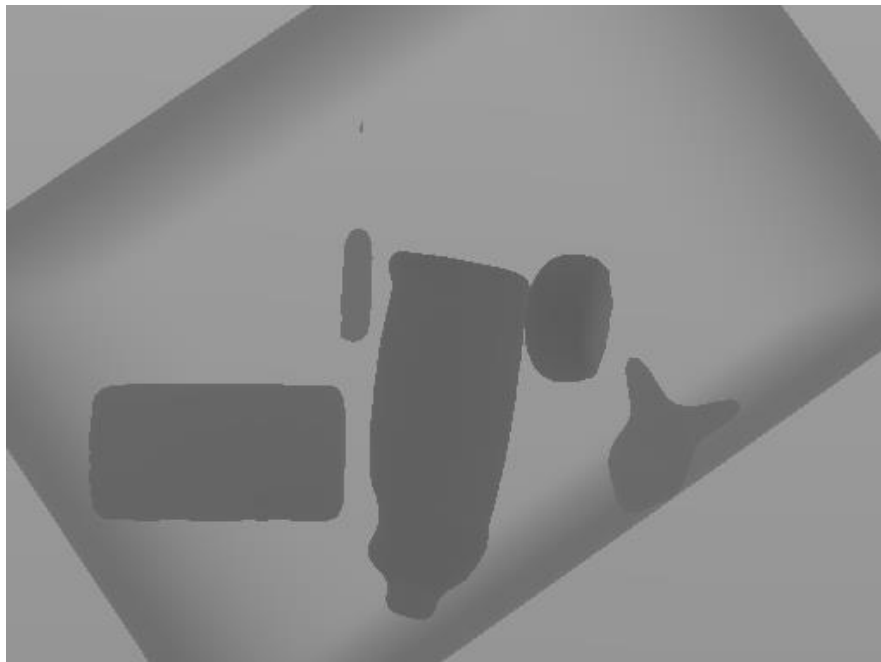


**Figure 122. Example of simulated images that resemble real disparity images.**

However, due to the nature of the disparity image, similarly shaped objects are likely to be thought of as the same by the model. And the model can only detect foreground and background, so stacking objects within each other can lead to issues detecting them. Lastly, since the simulated environment consists of objects within bins, deviations from that environment can also cause a decrease in the performance of the model.

As such, SD Mask R-CNN can learn to detect new objects given its 3D mesh and time to simulate the data and retrain the model. However, it can struggle distinguishing objects with similar shapes or specific environments.

More recently, with the emergence of vision transformers, there has been a rise in one shot object detection and zero shot object detection research. One of these new algorithms is OWL-ViT which can do both object detection given a text or image query. As part of this subtask, the team implemented OWL-ViT as a one-shot object detection algorithm. OWL-ViT was trained for over 1000 epochs on the COCO dataset to further improve its performance. It was then evaluated on the custom FIU robotics dataset. The results were quite lacking in that the predicted bounding boxes encompassed the target object, but the bounding boxes also encompassed other objects and parts of the background.

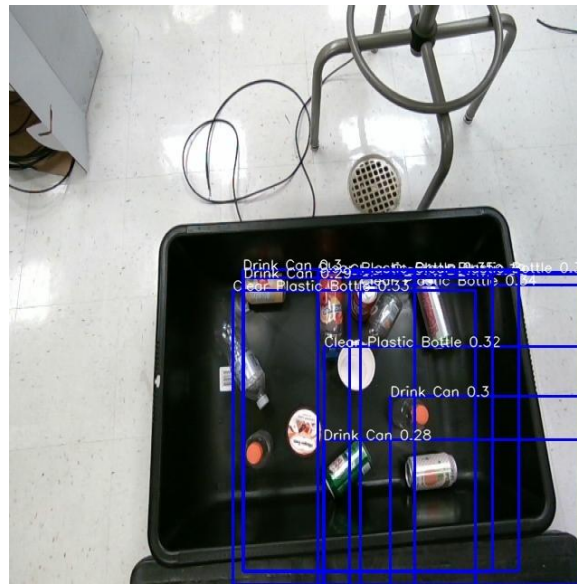


**Figure 123. Example of the results from OWL-ViT where the boxes are too large for the object it is encompassing.**

However, a major advantage of OWL-ViT is that it can detect new objects from a single image. That is, to add a new object, there is no need to gather data or label the data or build a 3D mesh of the object, a single image is enough.

Thus, OWL-ViT is a good algorithm for scenarios where new objects are constantly being added and the loss in mAP when compared to previous algorithms is compensated for by the ability to quickly and effectively adapt to any and all new objects.

### Subtask 9.1: Conclusions

For the detection of nuclear waste, the team researched multiple models with their own advantages and disadvantages. The team researched YOLOv7 for object detection and instance segmentation. The team then researched STEGO for unsupervised semantic segmentation, SD Mask R-CNN for instance segmentation on depth images, and OWL-ViT for one-shot object detection. For each model, prediction scripts were implemented in such a way that they can be integrated with ROS2, and they were given to the robotics team within FIU-ARC.





**Figure 124. Image of the robotic arm which uses the computer vision models to determine what objects to collect and how to collect them (from their shape).**

### **Subtask 9.1: References**

Danielczuk, M., Matl, M., Gupta, S., Li, A., Lee, A., Mahler, J., & Goldberg, K. (2019, March 3). *Segmenting unknown 3D objects from real depth images using mask R-CNN trained on Synthetic Data*. arXiv.org. <https://arxiv.org/abs/1809.05825>

Hamilton, M., Zhang, Z., Hariharan, B., Snavely, N., & Freeman, W. T. (2022, March 16). *Unsupervised semantic segmentation by distilling feature correspondences*. arXiv.org. <https://arxiv.org/abs/2203.08414>

Lin, T.-Y., Maire, M., Belongie, S., Bourdev, L., Girshick, R., Hays, J., Perona, P., Ramanan, D., Zitnick, C. L., & Dollár, P. (2015, February 21). *Microsoft Coco: Common Objects in Context*. arXiv.org. <https://arxiv.org/abs/1405.0312>

Minderer, M., Gritsenko, A., Stone, A., Neumann, M., Weissenborn, D., Dosovitskiy, A., Mahendran, A., Arnab, A., Dehghani, M., Shen, Z., Wang, X., Zhai, X., Kipf, T., & Houlsby, N. (2022, July 20). *Simple open-vocabulary object detection with Vision Transformers*. arXiv.org. <https://arxiv.org/abs/2205.06230>

Wang, C.-Y., Bochkovskiy, A., & Liao, H.-Y. M. (2022, July 6). *Yolov7: Trainable bag-of-freebies sets new state-of-the-art for real-time object detectors*. arXiv.org. <https://arxiv.org/abs/2207.02696>

Zhuang, F., Qi, Z., Duan, K., Xi, D., Zhu, Y., Zhu, H., Xiong, H., & He, Q. (2020, June 23). *A comprehensive survey on Transfer Learning*. arXiv.org. <https://arxiv.org/abs/1911.02685>

## **Subtask 9.2: Transition Previously Trained Deep Learning Models to Advance Automated Machine Learning System (AAMLS)**

### **Subtask 9.2: Introduction**

Previously, FIU researched state-of-the-art Artificial Intelligence (AI) algorithms to identify defects for structural surveillance and monitoring. The team developed these models using Convolutional Neural Networks. However, the capabilities of these algorithms can be extended beyond the datasets that they were trained on and onto similar problems faced in other facilities within the DOE complex. As such, each of the developed models were abstracted to allow the models to train and predict on different kinds of datasets.

### **Subtask 9.2: Objectives**

The objective of this subtask is to take the previously developed models by the FIU team and abstract them within AAMLS such that the models can be used to provide a solution to different kinds of computer vision problems within the DOE facilities.

### **Subtask 9.2: Methodology**

There were three kinds of models previously developed by the FIU team: classification, anomaly detection, and object detection for images. The goal of the classification models is to determine what the object in the image is. This was used to detect if there was a crack or not within the image, but it can be extended to classify corrosion within tools, etc. The goal of the anomaly detection models is to determine any deviation from the normal image data. This was used to detect the presence of cracks within walls, but it can be extended to determine the presence of fire within a room, etc. Lastly, the goal of object detection models is to determine within an image where an object is located and what the class of the objects is. This was also used to detect the presence of cracks within an image, but it can be extended for surveillance to track the movement of people outside or inside a facility.

For image classifications, the models transitioned were VGG16, ResNet50, InceptionNet, EfficientNet, and a custom convolutional neural network architecture.

The idea behind VGG16 is to use a deep convolutional neural network with only 16 layers, but each layer consists of many nodes. This means that little to no information is lost in backward propagation during training and the large size of the layers allows the architecture to learn complex features in images.



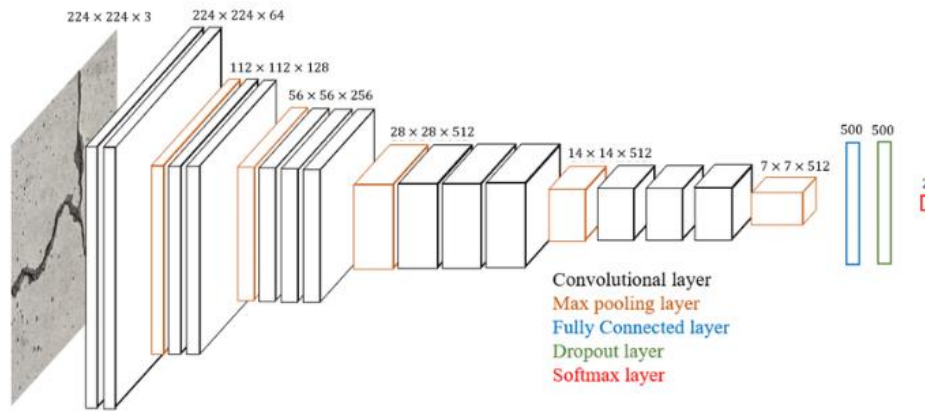


**Figure 125. VGG16 architecture.**

The idea behind ResNet50 is to use deep convolutional neural network architecture with 50 layers, but many layers have skip connections, where their output is passed to both the next layer and the layer that is two connections away from the current layer. This helps alleviate the issue of losing information during backward propagation for deep neural networks, and by passing the lower-level features to higher level layers, it enables the model to learn an identity function, where higher layers cannot do worse than lower layers.

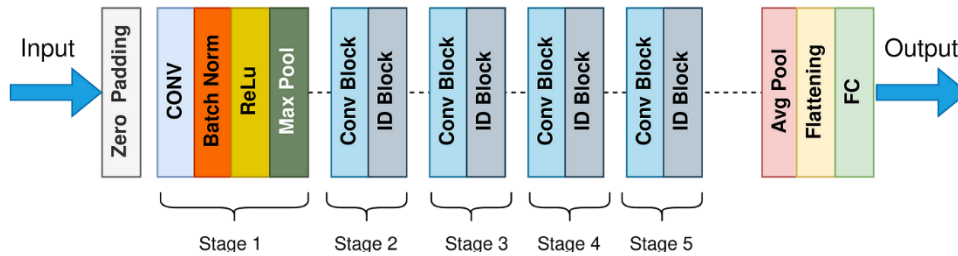


**Figure 126. ResNet50 architecture.**

The idea behind InceptionNet is to use deep convolutional neural network architecture that outputs multiple results, passes them through different size Convolutional Neural Network kernels, and concatenates them into the next layer. This uses the idea that important features in an image come in different sizes, so the use of larger kernels allows the model to learn features that are distributed throughout the image, while the smaller kernels allow the model to learn features that are more local to different parts of the image. InceptionNet-v3 also has auxiliary classifiers, normalization, and smoothing to help improve the results.

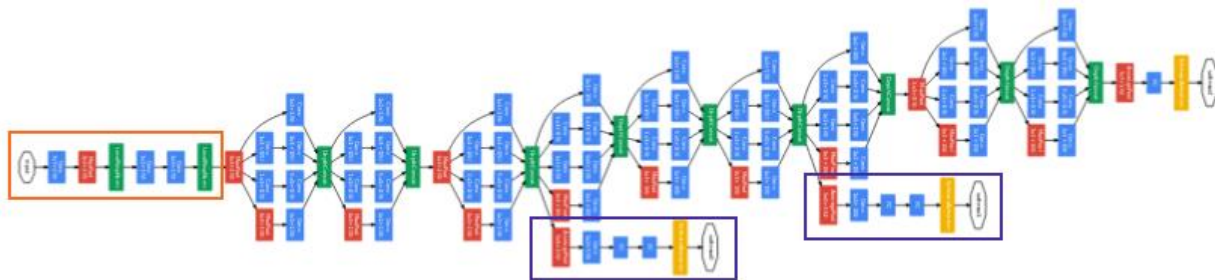


**Figure 127. InceptionNet architecture.**

The idea behind EfficientNet is to use convolutional neural networks and use the concepts of Neural Architecture Search (NAS) to reduce the size of the neural network while maintaining its high accuracy. It also uses regularization to improve the results.

For anomaly detection, the team had previously developed an autoencoder architecture to detect anomalies. Autoencoders are neural network models that aim to reconstruct their input data. They consist of an encoder and a decoder, where the encoder compresses the input data into a lower-dimensional representation, and the decoder reconstructs the data from this representation. Anomaly detection using autoencoders involves training the model on normal data and evaluating the reconstruction error. Instances with high reconstruction errors are considered anomalies. Autoencoders can capture complex patterns and are effective for detecting anomalies in images.

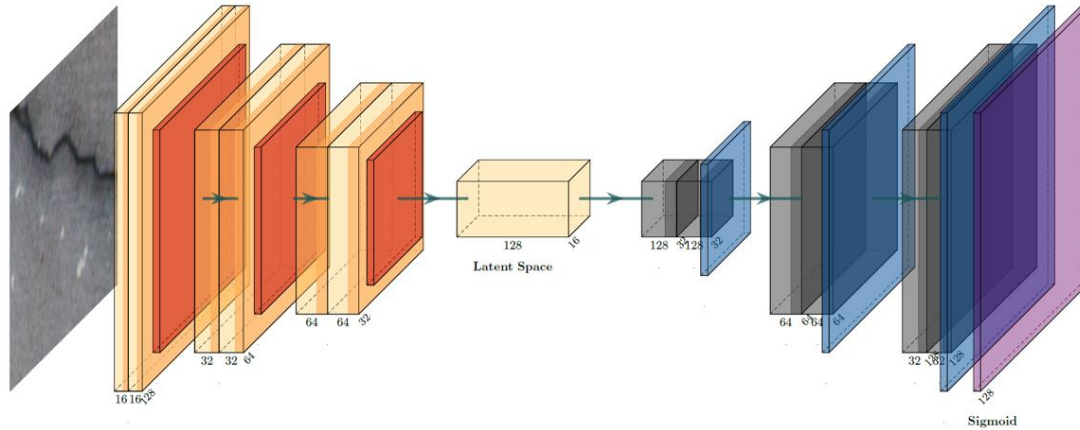


Figure 128. Autoencoder architecture.

For object detection, the team had previously developed a model of YOLOv3. It is a popular real-time object detection algorithm that performs object detection in a single pass. Instead of generating region proposals, YOLOv3 divides the input image into a grid and predicts bounding boxes and class probabilities directly from the grid cells. What made YOLOv3 better than YOLOv2 was the fast inference speeds and performance achieved by leveraging the concept of anchor boxes with different sizes, which helps handle objects of different sizes and aspect ratios.

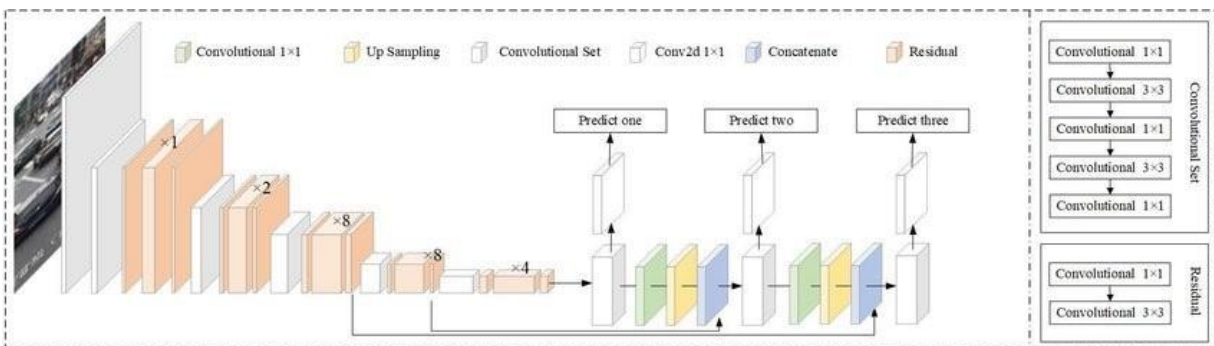


Figure 129. YOLOv3 architecture

Moreover, within AAMLS, as part of this subtask, hyperparameter optimization was implemented. Hyperparameter optimization allows for changes in number in hidden layers, activation functions, loss functions, among others for each algorithm which increases their performance.

### Subtask 9.2: Results and Discussion

The team implemented all the image classification models within AAMLS.

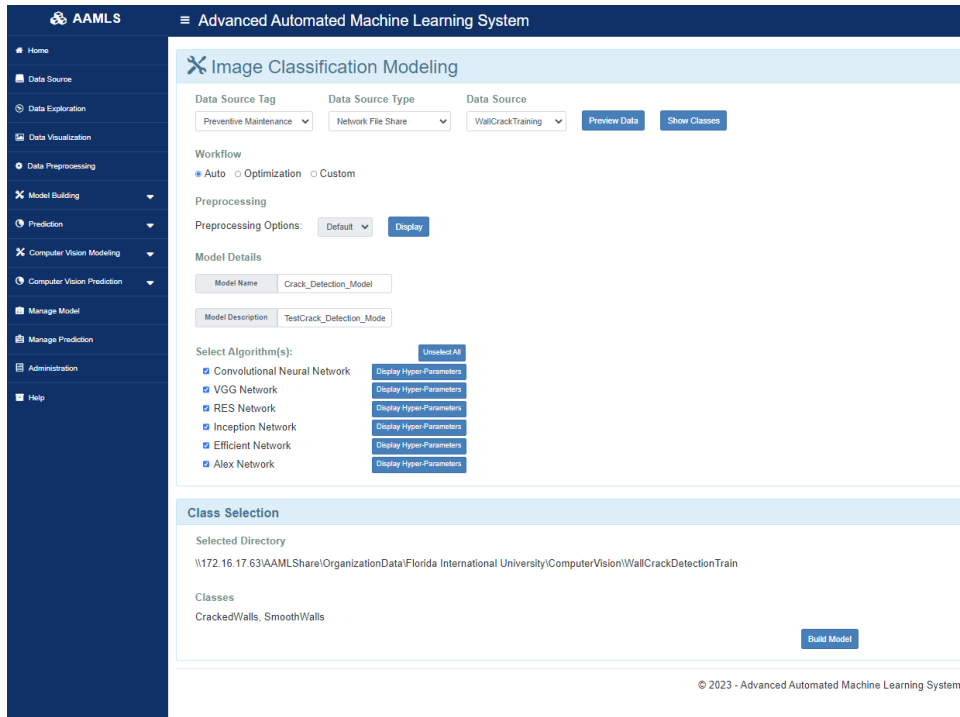


Figure 130. Image Classification page at AAMLS.

Through this page, a user can build a model on their specific dataset and then do validation on the models or predictions.

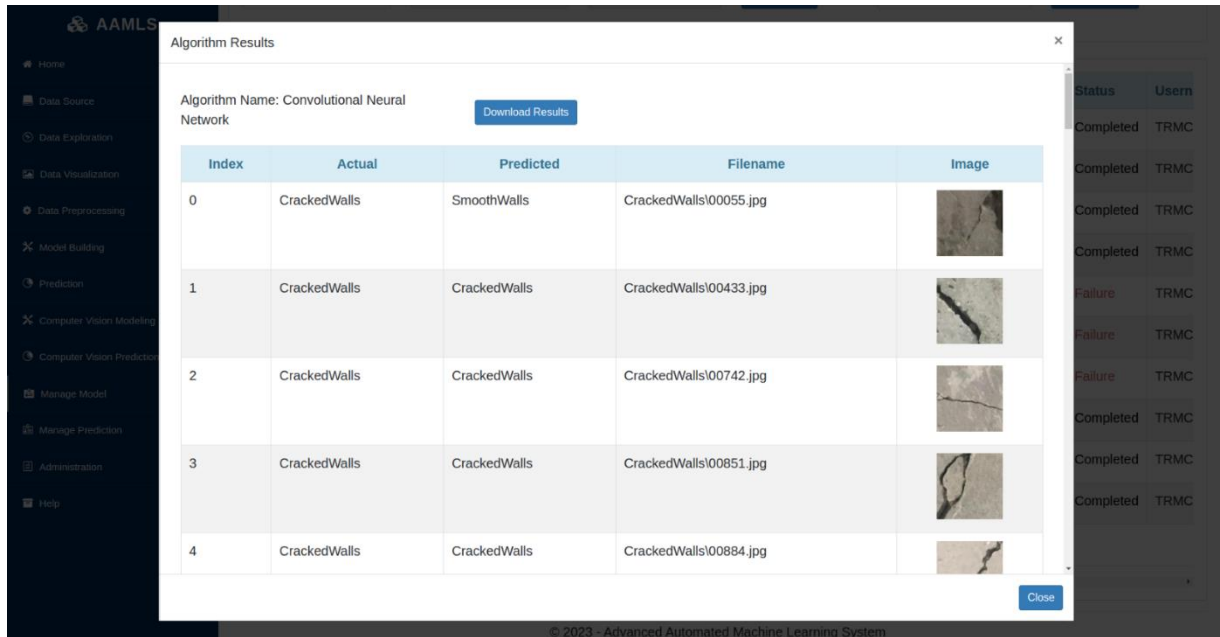
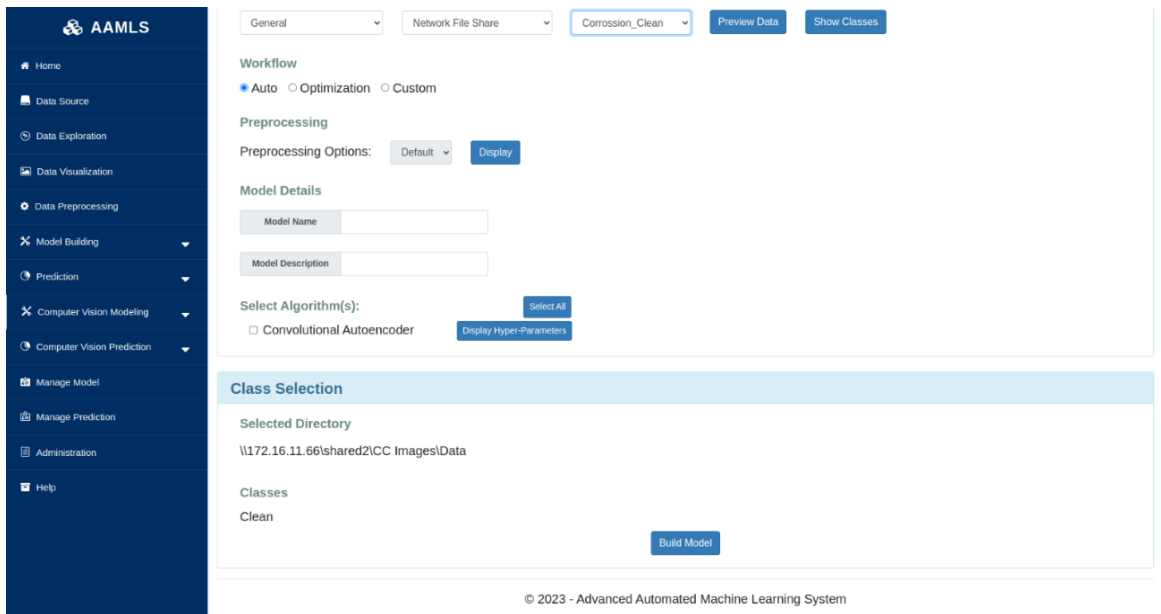


Figure 131. Image Classification Validation Results page at AAMLS.

And then through this page, the user can view and analyze the model predictions. The team then implemented the anomaly detection models into AAMLS:



**Figure 132. Anomaly Detection page at AAMLs.**

Through this page, a user can build a model on their specific dataset and then do validation on the models or predictions. The results on the anomaly detection page are similar to the results on the image classification page.

For object detection, the team then implemented the following pages:

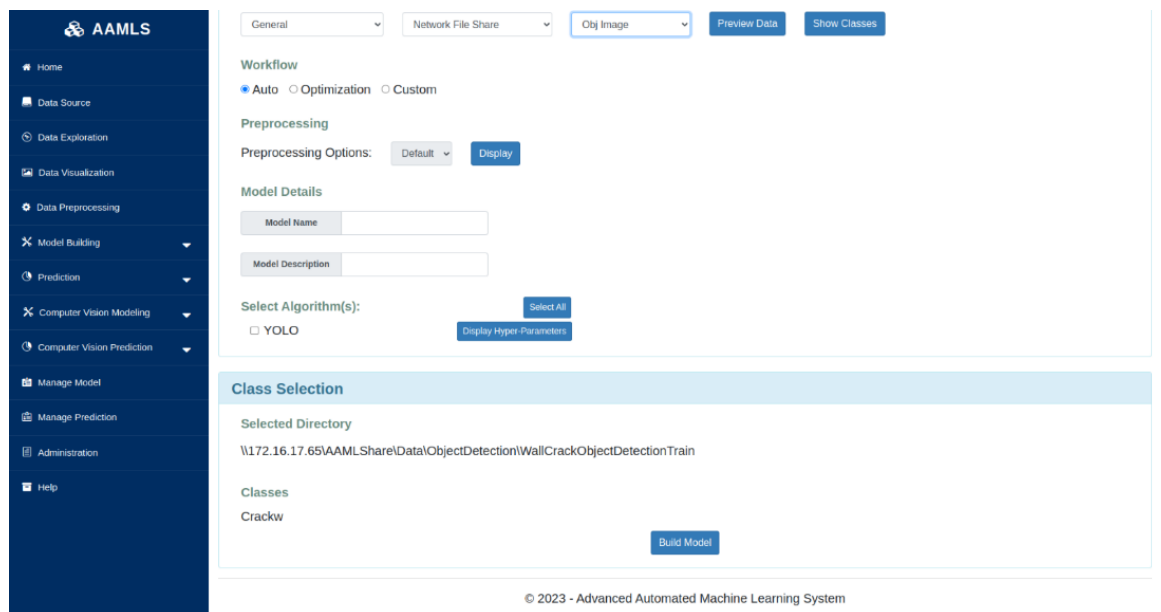


**Figure 133. Object Detection page at AAMLs.**



**Figure 134. Example of object detection pages.**

Through this, a user can use their own dataset source to build their own models and make their predictions which they can access through a user interface.

### Subtask 9.2: Conclusions

In conclusion, FIU had previously developed multiple models for image classification, anomaly detection, and object detection for the purpose of identifying defects for surveillance and maintenance within DOE facilities. These models were abstracted and deployed to AAMLS in such a way that they can be used with other kinds of data for tasks like corrosion detection, fire detection, human surveillance, among others.

### Subtask 9.2: References

- He, K., Zhang, X., Ren, S., & Sun, J. (2015, December 10). *Deep residual learning for image recognition*. arXiv.org. <https://arxiv.org/abs/1512.03385>
- Redmon, J., & Farhadi, A. (2018, April 8). *Yolov3: An incremental improvement*. arXiv.org. <https://arxiv.org/abs/1804.02767>
- Simonyan, K., & Zisserman, A. (2015, April 10). *Very deep convolutional networks for large-scale image recognition*. arXiv.org. <https://arxiv.org/abs/1409.1556>
- Szegedy, C., Liu, W., Jia, Y., Sermanet, P., Reed, S., Anguelov, D., Erhan, D., Vanhoucke, V., & Rabinovich, A. (2014, September 17). *Going deeper with convolutions*. arXiv.org. <https://arxiv.org/abs/1409.4842>
- Tan, M., & Le, Q. V. (2021, June 23). *EFFICIENTNETV2: Smaller models and faster training*. arXiv.org. <https://arxiv.org/abs/2104.00298>

## CONFERENCE PARTICIPATION, PUBLICATIONS, AWARDS & ACADEMIC MILESTONES

---

### Professional Conference Presentations and Proceedings

Himanshu Upadhyay, Walter Quintero, Santosh Joshi, Leonel Lagos, “*D&D KM-IT 2023 Updates*” Poster Presentation at the Waste Management Symposia 2023, Phoenix, AZ, February 26- March 2, 2023.

Himanshu Upadhyay, Walter Quintero, Leonel Lagos, Santosh Joshi. “*Waste Information Management System with 2022-23 Waste Streams*” Proceedings of the Waste Management Symposia 2023, Phoenix, AZ, February 26- March 2, 2023.

Himanshu Upadhyay, Santosh Joshi, Leonel Lagos, Walter Quintero. “*Advanced Automated Machine Learning System*” Proceedings of the Waste Management Symposia 2023, Phoenix, AZ, February 26- March 2, 2023.

Kexin Jiao, Joseph Sinicrope, Mellissa Komninakis, Johnbull Dickson. “*Recyclable, Magnetic Responsive Micro-Ribbon Sorbent Synthesis for Mercury Abatement and Waste Oil Cleaning*” Proceedings of the Waste Management Symposia 2023, Phoenix, AZ, February 26- March 2, 2023.

Mellissa Komninakis, Joseph Sinicrope, Kexin Jiao, James Nicholson, Jennifer Wohlwend. “*Determination of Airborne Release Fractions for Fixative Technologies under Impact Stress for D&D Activities*” Proceedings of the Waste Management Symposia 2023, Phoenix, AZ, February 26- March 2, 2023.

Joseph Sinicrope chaired the ASTM International E10.03 Subcommittee in January and June of 2023.

### Awards:

The Project 3 Information Technology team received the “*Best ASME paper*” award which was accepted by Dr. Himanshu Upadhyay on behalf of the team.

Joseph Sinicrope received an award from ASTM International for his leading the initiative to establish the 1<sup>st</sup> ASTM Student Chapter at a university focused on integrating consensus-based standards and uniform testing practices into university research supporting DOE EM projects.

## ACKNOWLEDGEMENTS

---

Funding for this research was provided by U.S. DOE Cooperative Agreement #DE-EM0005213. FIU’s Applied Research Center would like to acknowledge the commitment of DOE-EM to this Waste and D&D Engineering and Technology Development project and to all the research being conducted as part of the Cooperative Agreement. The partnership between DOE EM and FIU has resulted in the development and training of outstanding minority STEM students that will benefit this country as a whole.

## APPENDIX

---

The following documents are available at the DOE Research website for the Cooperative Agreement between the U.S. Department of Energy Office of Environmental Management and the Applied Research Center at Florida International University:

<https://doeresearch.fiu.edu/SitePages/Welcome.aspx>

FIU Year 3 Annual Research Review Presentations:

1. FIU Research Review - Project 1
2. FIU Research Review - Project 2
3. FIU Research Review - Project 3 - D&D IT ML
4. FIU Research Review - Project 4 & 5
5. FIU Research Review - Project 4 - DOE Fellow Aris Duani Rojas
6. FIU Research Review - Project 4 - DOE Fellow Aubrey Litzinger
7. FIU Research Review - Project 4 - DOE Fellow Brendon Cintas
8. FIU Research Review - Project 4 - DOE Fellow Bryan Torres
9. FIU Research Review - Project 4 - DOE Fellow Carolina Trummer
10. FIU Research Review - Project 4 - DOE Fellow Joel Adams
11. FIU Research Review - Project 4 - DOE Fellow Josue Estrada
12. FIU Research Review - Project 5 - DOE Fellow Shawn Cameron
13. FIU Research Review - Wrap Up - Project 1
14. FIU Research Review - Wrap Up - Project 2
15. FIU Research Review - Wrap Up - Project 3 – D&D IT ML
16. FIU Research Review - Wrap Up - Project 4
17. FIU Research Review - Wrap Up - Project 5